

**DEVELOPMENT OF RADIOACTIVE SOURCES FOR
INDUSTRIAL AND MEDICAL APPLICATIONS THROUGH
DIFFERENT CHEMICAL METHODS**

By

MANOJ KUMAR

CHEM01201204019

Bhabha Atomic Research Centre, Mumbai

A thesis submitted to the

Board of Studies in Chemical Sciences

In partial fulfillment of requirements

for the Degree of

DOCTOR OF PHILOSOPHY

of

HOMI BHABHA NATIONAL INSTITUTE



October, 2017

Homi Bhabha National Institute

Recommendations of the Viva Voce Committee

As members of the Viva Voce Committee, we certify that we have read the dissertation prepared by **Manoj Kumar** entitled “**Development of Radioactive Sources for Industrial and Medical Applications Through Different Chemical Methods**” and recommend that it may be accepted as fulfilling the thesis requirement for the award of Degree of Doctor of Philosophy.

| | |
|---|-------------|
| Chairman –Prof. P.K. Pujari | date |
| Guide/Convener –Prof. A. Dash | date |
| Examiner - Prof. Alok Srivastava | date |
| Member1 - Dr. R.K. Mishra | date |
| Member 2 - Dr. Tapas Das | date |
| Technology Advisor –Dr. A.K. Satpati | date |

Final approval and acceptance of this thesis is contingent upon the candidate’s submission of the final copies of the thesis to HBNI.

I/We hereby certify that I/We have read this thesis prepared under my direction and recommend that it may be accepted as fulfilling the thesis requirement.

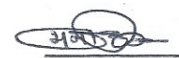
Date:

Place:

Guide/Convener

STATEMENT BY AUTHOR

This dissertation has been submitted in partial fulfillment of requirements for an advanced degree at Homi Bhabha National Institute (HBNI) and is deposited in the Library to be made available to borrowers under the rules of HBNI. Brief quotations from this dissertation are allowable without special permission, provided that accurate acknowledgement of the source is made. Requests for permission for extended quotation from or reproduction of this manuscript in whole or in part may be granted by the Competent Authority of HBNI when in his or her judgment the proposed use of the material is in the interests of scholarship. In all other instances, permission must be obtained from the author.



Manoj Kumar

DECLARATION

I hereby declare that the work presented in the thesis has been carried out by me.
The work is original and has not been submitted earlier as whole or in part for a degree /
diploma at this or any other Institution / University.

A handwritten signature in blue ink, appearing to read 'Manoj Kumar', is written over a horizontal line.

Manoj Kumar


Dedicated to my Wife, Son and Parents.....

ACKNOWLEDGEMENTS

First and foremost, I would like to express my sincere gratitude to my guide Prof. Ashutosh Dash, Head, Radiopharmaceuticals Division, BARC for his unwavering support, motivation and encouragement. His observations and comments helped me to establish the overall direction of the research and to move forward with the experiments in depth. I am thankful to Prof. Dash for sharing his knowledge and scientific understanding during the fruitful discussions with me throughout the work. I consider it a great opportunity to carry out my doctoral programme under his guidance and to learn from his research expertise. It gives me a great pleasure to acknowledge Shri J. Udhayakumar for his help and support in facilitating my work as well as for his inspiring words, encouragement and good wishes throughout my research tenure. I owe a great deal of gratitude to Dr. Usha Pandey, my immediate superior. Her guidance helped me a lot during the preparation of my thesis. I thank Dr. Pandey for her guidance and encouragement as well as for sharing her scientific and experimental knowledge with me. I am grateful to Dr. Rubel Chakravarty for his help and guidance during preparation of sources using electrodeposition techniques. His invaluable constructive criticisms and suggestions on academic level have always been helpful to me. I also thank my colleague Smt. Shyamala S. Gandhi for sharing her work experience with me and for her complete co-operation during the course of this work. I wish to pay my sincere thanks to Dr. Tapas Das for his helpful suggestions and encouragement. My sincere thanks to Prof. A.K. Tyagi, Dean- Chemical Sciences), HBNI, Dr. Rakesh Shukla and Shri Jitendra Nuwad from Chemistry Division for their kind help in carrying out X-ray diffraction, Scanning Electron Microscopy (SEM) and Energy Dispersive X-Ray (EDX) studies of the various samples reported in this thesis. I am also grateful to the doctoral committee Chairman,

Prof. P.K. Pujari, (Head, Radiochemistry, BARC), former Chairman, Prof. A. Goswami (Former Head, Radiochemistry, BARC) and the members Dr. R.K. Mishra (Chemistry Division), Dr. Tapas Das (Radiopharmaceuticals Division) and Dr. A.K. Satpati (Technical Advisor, Analytical Chemistry Division) of the doctoral committee, for their suggestions and constructive criticism during the annual progress reviews and pre-synopsis viva-voce. My sincere thanks are due to all my colleagues, Shri S.K. Saxena, Smt. Akanksha Jain, Shri. Yogendra Kumar, Shri. Naresh Gamre and Smt. Yugandhara Yadav of Therapeutic & Reference Sources Section (T&RSS) and Smt. Kusum Vats from Radiopharmaceutical Chemistry Section for their help and support. I would like to thank Dr. Sudipta Chakraborty of Radiochemical Section for providing access to the radioactivity measurement facilities such as dose calibrator and ion-chamber regularly for the work reported in this thesis. I am also thankful to my Radiochemical Section colleagues, Dr. K.V. Vimalnath Nair, Shri R.N. Ambade, Shri S.N. Shinde, Shri. Ramuram, Shri. Sahiralam Khan, Shri. Sharad Lohar, Ms. Rajeswari and Ms. Priyalata Shetty for their help during radioactivity assay. I am also thankful to Shri. B.G. Avhad and colleagues from the Divisional workshop for their contribution in the fabrication of source matrices. Shri. Pritam Bansode is hereby acknowledged for preparing the diagrams/drawings of the sources and Shri. S. Moorthy for the fabrication of the glassware required during the work. I thankfully acknowledge the help and technical assistance received from Shri. M.S. Tikka, Shri. B.J. Jadhav and Shri Umesh Kumar throughout the course of work. I sincerely acknowledge all my other colleagues from Radiopharmaceuticals Division for their help and support during the course of the work. I would also like to thank Shri. A.S. Tapase and Shri Nilesh Pershetye of IRAD Division, BARC for his help during the autoradiography experiments reported in this thesis. I am

also grateful to the staff of the Health Physics Group, Isotope Wing for their co-operation and help during the course of the thesis. Finally I would like to thank my family and friends for their continued support and encouragement. Most importantly, I would like to pay high regards to my wife Chandra Kala and my parents who encouraged and helped me at every stage of my personal and academic life and longed to see this achievement come true. I salute them for their selfless love, care, pain and sacrifice to shape my life. I would not have made it this far without their help and support. Last but not the least, I want to thank my son Aditya M Kumar and my nephew Dheeraj for their love and affection which provided me the strength and patience to complete this challenging task.



Manoj Kumar

Trombay, Mumbai-85

October, 2017

List of Publications arising from the thesis

Journal:


1. **Kumar Manoj**, Gandhi S S, Udhayakumar J, Satpati A K, Shukla R, Tyagi A K and Dash A: An electrochemical technique to prepare ^{55}Fe source for the calibration of the X-ray detectors, *Radiochimica Acta*, 101, 185-193, 2013.
2. **Kumar Manoj**, Gandhi S S, Nuwad J, Udhayakumar J, Dash A: A novel and facile approach for the preparation of ^{133}Ba source core, encapsulation and quality evaluation, *Radiochimica Acta*, 101, 195-203, 2013.
3. **Kumar Manoj**, Gandhi S S, Chakravarty Rubel, Nuwad J, Udhayakumar J, and Dash A: A novel method for the preparation of large-area $^{90}\text{Sr}/^{90}\text{Y}$ sources for the calibration of hand contamination monitors. *Applied Radiation and Isotopes*, 79, 5–11, 2013.
4. Saxena S K, **Kumar Manoj**, Kumar Yogendra, Udhayakumar J, Pandey Usha, Dash Ashutosh: Preparation of ^{57}Co point sources for the performance evaluation of nuclear imaging instruments. *Applied Radiation and Isotopes*, 79, 12–17, 2013.
5. Udhayakumar J, Gandhi Shyamala S, **Kumar Manoj**, and Dash Ashutosh: A chemical deposition method to prepare circular planar ^{147}Pm sources for the measurement of particulate emission in air. *Applied Radiation and Isotopes*, 79, 80–84, 2013.
6. Gandhi S S, **Kumar M**, Chakravarty R, Nuwad J, Udhayakumar J and Dash A: An electrochemical route to prepare planar ^{204}Tl sources for the calibration of beta surface contamination monitors. *Radiochimica Acta* 101, 427-436, 2013.
7. **Kumar Manoj**, Gandhi Shyamala S, Nuwad J, Udhayakumar J, and Dash A: An electrochemical pathway to prepare circular planar $^{90}\text{Sr}/^{90}\text{Y}$ source for the

List of Publications

calibration of surface contamination monitor. J Radioanalytical & Nuclear Chemistry, 302, 709-719, 2014.

Conferences:

1. Gandhi Shyamala S, **Kumar Manoj**, Udhayakumar J, Dash Ashutosh: Development of multi dimensional $^{90}\text{Sr}/^{90}\text{Y}$ thin film sources, 5th International Symposium on Material Chemistry held at Multipurpose Hall BARC Training School, Mumbai, 334, 9-13 December, 2014.
2. **Kumar Manoj**, Gandhi Shyamala S, Udhayakumar J, Dash Ashutosh: Development of ^{57}Co pen pointer marker source for applications in nuclear medicine procedures, Nuclear and Radiochemistry Symposium (NUCAR), held at Multipurpose Hall TSH, BARC, Mumbai, 462-463, 9-13 February, 2015.



Manoj Kumar

| | <u>Page No.</u> |
|---|------------------------|
| SYNOPSIS | i |
| LIST OF FIGURES | xix |
| LIST OF TABLES | xxv |
| ABBREVIATIONS | xxvii |
| Chapter-1: Introduction | 1 |
| 1 Sealed Radioactive Sources | 2 |
| 1.2 Laboratory Reference Sources | 2 |
| 1.2.1 <i>Classification of Laboratory Reference Sources</i> | 2 |
| 1.2.2 <i>Low Level Laboratory Check Sources</i> | 2 |
| 1.2.3 <i>Custom-made Special Sources</i> | 3 |
| 1.3 Common Terms Used in Radiation Sources | 4 |
| 1.3.1 <i>Sealed Source</i> | 4 |
| 1.3.2 <i>Activity</i> | 4 |
| 1.3.3 <i>Recommended Working Life</i> | 4 |
| 1.3.4 <i>Standard</i> | 5 |
| 1.4 Methodologies for Fabrication of Custom-made Sources | 5 |
| 1.5 Important Factors for the Preparation of Custom-made Sources | 5 |
| 1.5.1 <i>Choice of Matrix/Substrate</i> | 5 |
| 1.5.2 <i>Criteria for the Selection of Source Preparation Methods</i> | 6 |
| 1.6 Evaporation Technique | 7 |
| 1.7 Electrodeposition | 7 |
| 1.7.1 <i>Theory of Electrodeposition</i> | 8 |

Contents

| | | |
|--------|---|----|
| 1.7.2 | <i>Faraday's Law</i> | 9 |
| 1.7.3 | <i>Electrochemical Equivalence</i> | 9 |
| 1.7.4 | <i>Requirements for Electrodeposition</i> | 10 |
| 1.8 | Electrodeposition System | 10 |
| 1.8.1 | <i>Electrodes</i> | 10 |
| 1.8.2 | <i>Choice of Substrate</i> | 10 |
| 1.8.3 | <i>Preparation of Substrate Surface</i> | 11 |
| 1.8.4 | <i>Electrolyte</i> | 13 |
| 1.8.5 | <i>Electrodeposition Bath</i> | 13 |
| 1.8.6 | <i>Types of Electrolytic Solutions</i> | 13 |
| 1.8.7 | <i>Criteria for Electrolytic Bath</i> | 14 |
| 1.8.8 | <i>Factors Influencing Electrodeposition</i> | 16 |
| 1.8.9 | <i>Cathode Efficiency</i> | 16 |
| 1.9 | Electrodeposition Parameters for Preparation of Radioactive Sources | 17 |
| 1.10 | <i>Properties of the Deposited Film</i> | 17 |
| 1.10.1 | <i>Adhesion</i> | 17 |
| 1.10.2 | <i>Mechanical Properties</i> | 17 |
| 1.10.3 | <i>Brightness</i> | 18 |
| 1.11 | Quality of the Electrodeposited Samples | 18 |
| 1.12 | Advantages of Electrodeposition Technique | 19 |
| 1.13 | Anodisation Technique | 20 |
| 1.14 | Solvent Extraction Followed by Polymer Formation | 22 |
| 1.14.1 | <i>Solvent Extraction</i> | 22 |

Contents

| | | |
|--------|--|----|
| 1.14.2 | <i>Liquid-Liquid Extraction</i> | 22 |
| 1.14.3 | <i>Selection of the Solvent</i> | 23 |
| 1.14.4 | <i>Distribution Coefficient (Kd)</i> | 23 |
| 1.14.5 | <i>Liquid-Liquid Extraction of a Metal-Ligand Complex</i> | 23 |
| 1.14.6 | <i>Extraction of Inorganic Species</i> | 24 |
| 1.14.7 | <i>Extraction Procedures</i> | 25 |
| 1.14.8 | <i>Batch Extraction Process</i> | 25 |
| 1.15 | Mixing with the Polymer | 26 |
| 1.15.1 | <i>Choice of Polymer</i> | 27 |
| 1.15.2 | <i>Properties of PMMA</i> | 28 |
| 1.16 | Quality Control | 29 |
| 1.16.1 | <i>Evaluation of Performance of Sealed Radiation Sources</i> | 29 |
| 1.16.2 | <i>Wipe Test "A"</i> | 29 |
| 1.16.3 | <i>Test for Leachability of Radioactivity</i> | 29 |
| 1.16.4 | <i>Measurement of Radioactivity</i> | 31 |
| 1.16.5 | <i>Activity Tolerance</i> | 32 |
| 1.16.6 | <i>Accuracy & Uncertainty in measurement</i> | 32 |
| 1.17 | Performance Investigation of Custom-made Radiation Sources | 32 |
| 1.18 | Scope of the Present Thesis | 32 |
| | Chapter-2: Preparation of ^{55}Fe, ^{57}Co and ^{204}Tl Sources for Multifarious Applications Using Electrodeposition Technique | 33 |
| 2.1 | Use of Electrochemical Technique To Prepare ^{55}Fe Source For Calibration of X-Ray Detectors | 34 |

Contents

| | | |
|---------|---|----|
| 2.1.1 | Introduction | 34 |
| 2.1.2 | Materials | 37 |
| 2.1.3 | Experimental | 38 |
| 2.1.3.1 | <i>Preparation of Electrodes</i> | 38 |
| 2.1.3.2 | <i>Preparation of Electrolyte</i> | 38 |
| 2.1.3.3 | <i>Electrochemical Set-up</i> | 39 |
| 2.1.3.4 | <i>Cyclic Voltammetry and Amperometry</i> | 40 |
| 2.1.3.5 | <i>Optimization of Electrodeposition Parameters</i> | 40 |
| 2.1.3.6 | <i>Characterization by X-ray, SEM and EDS</i> | 40 |
| | <i>Analysis</i> | |
| 2.1.3.7 | <i>Preparation of ^{55}Fe Sources</i> | 41 |
| 2.1.3.8 | <i>Coating of ^{55}Fe Sources with PMMA Polymer</i> | 41 |
| 2.1.3.9 | <i>Measurement of Activity of the Source</i> | 41 |
| 2.1.4 | Quality Control of ^{55}Fe Sources | 42 |
| 2.1.4.1 | <i>Autoradiography</i> | 42 |
| 2.1.4.2 | <i>Determination of Surface Contamination</i> | 43 |
| 2.1.4.3 | <i>Determination of Percentage Activity Leached</i> | 44 |
| | <i>Out</i> | |
| 2.1.4.4 | <i>Immersion Test</i> | 44 |
| 2.1.4.5 | <i>Source Assembly</i> | 44 |
| 2.1.5 | Results and Discussion | 45 |
| 2.1.5.1 | <i>Cyclic Voltammetry Studies</i> | 46 |
| 2.1.5.2 | <i>Amperometric Deposition Studies</i> | 47 |

Contents

| | | |
|---------|---|----|
| 2.1.5.3 | <i>Voltammetry Stripping Studies</i> | 48 |
| 2.1.5.4 | <i>Effect of Electrodeposition Parameters</i> | 48 |
| 2.1.5.5 | <i>Morphology Studies</i> | 50 |
| 2.1.5.6 | <i>Activity Measurement</i> | 53 |
| 2.1.5.7 | <i>Quality Control</i> | 53 |
| 2.1.6 | Conclusion | 57 |
| 2.2 | Preparation of ^{57}Co Point Sources for the Performance Evaluation of Nuclear Imaging Instruments | 57 |
| 2.2.1 | Introduction | 57 |
| 2.2.2 | Materials and Instrumentation | 59 |
| 2.2.2.1 | <i>Materials</i> | 59 |
| 2.2.2.1 | <i>Instrumentation</i> | 59 |
| 2.2.3 | Experimental | 60 |
| 2.2.3.1 | <i>Preparation of ^{57}Co Source</i> | 60 |
| 2.2.3.2 | <i>Source Assembly in a Titanium Capsule</i> | 61 |
| 2.2.3.3 | <i>Laser Encapsulation</i> | 62 |
| 2.2.3.4 | <i>Activity Assay of ^{57}Co Sealed Source</i> | 62 |
| 2.2.3.5 | <i>Quality Control</i> | 63 |
| 2.2.3.6 | <i>Radiological Safety</i> | 63 |
| 2.2.4 | Results | 64 |
| 2.2.4.1 | <i>Source Preparation</i> | 64 |
| 2.2.4.2 | <i>Leachability of Source Core</i> | 64 |
| 2.2.4.3 | <i>Encapsulation</i> | 64 |

Contents

| | | |
|----------|---|----|
| 2.2.4.4 | <i>Measurement of Activity of the Source</i> | 65 |
| 2.2.5 | Quality Control | 67 |
| 2.2.5.1 | <i>Uniformity distribution of ^{57}Co on Source Core</i> | 67 |
| 2.2.6 | Discussion | 70 |
| 2.2.7 | Conclusion and Scope of the Work | 70 |
| 2.3 | An Electrochemical Route to Prepare Planar ^{204}Tl Sources for the Calibration of Beta Surface Contamination Monitors | 71 |
| 2.3.1 | Introduction | 71 |
| 2.3.2 | Materials | 72 |
| 2.3.3 | Experimental | 74 |
| 2.3.3.1 | <i>Production and Processing of ^{204}Tl</i> | 74 |
| 2.3.3.2 | <i>Electrochemical Preparation of ^{204}Tl</i> | 74 |
| 2.3.3.3 | <i>Voltammetric Experiments</i> | 75 |
| 2.3.3.4 | <i>Optimization of Electrodeposition Parameters</i> | 76 |
| 2.3.3.5 | <i>Preparation of Source</i> | 76 |
| 2.3.3.6 | <i>Surface Characterization</i> | 77 |
| 2.3.3.7 | <i>Assay of Activity of the Source Core</i> | 77 |
| 2.3.3.8 | <i>Coating of the Sources with PMMA Polymer</i> | 77 |
| 2.3.3.9 | <i>Quality Control</i> | 78 |
| 2.3.3.10 | <i>Source Assembly in a Circular Holder</i> | 78 |
| 2.3.3.11 | <i>Radiological Safety</i> | 79 |
| 2.3.4. | Results | 80 |
| 2.3.4.1 | <i>Preparation of the Electrolyte</i> | 80 |

Contents

| | | |
|---|--|----|
| 2.3.4.2 | <i>Voltammetric Studies</i> | 80 |
| 2.3.4.3 | <i>Optimization of Electrodeposition Parameters</i> | 81 |
| 2.3.4.4 | <i>Influence of pH of the Electrolyte</i> | 81 |
| 2.3.4.5 | <i>Influence of Current Density</i> | 82 |
| 2.3.4.6 | <i>Influence of Deposition Time</i> | 83 |
| 2.3.4.7 | <i>Influence of Thallium Content in the Electrolyte</i> | 84 |
| 2.3.4.8 | <i>Influence of Bath Temperature</i> | 85 |
| 2.3.5 | SEM Analysis | 86 |
| 2.3.6 | EDS Characterization | 87 |
| 2.3.7 | Atomic Force Microscopy (AFM) | 89 |
| 2.3.8 | Preparation of ^{204}Tl Sources | 90 |
| 2.3.9 | Quality Control | 90 |
| 2.3.9.1 | <i>Activity Measurement</i> | 90 |
| 2.3.9.2 | <i>Autoradiography Examination</i> | 91 |
| 2.3.9.3 | <i>Leachability of Radioactivity</i> | 91 |
| 2.3.9.4 | <i>Swipe Test</i> | 92 |
| 2.3.10 | Discussion | 93 |
| 2.3.11 | Conclusion and Scope of the Work | 94 |
| Chapter-3: A Two-Step Electrochemical Process for the Preparation of ^{133}Ba and $^{90}\text{Sr}/^{90}\text{Y}$ Sources for Calibration of Instruments | | 95 |
| 3.1 | A Novel and Facile Approach for the Preparation of ^{133}Ba Source Core, Encapsulation and Quality Evaluation Towards its Use in Calibration of Instruments | 96 |

Contents

| | | |
|---------|--|-----|
| 3.1.1 | Introduction | 96 |
| 3.1.2 | Materials | 97 |
| 3.1.3 | Experimental | 98 |
| 3.1.3.1 | <i>Pretreatment of Titanium Rods</i> | 98 |
| 3.1.3.2 | <i>Electrochemical Deposition of ^{133}Ba onto Anodized Titanium Rod</i> | 99 |
| 3.1.3.3 | <i>Optimization of Electrodeposition Parameters</i> | 100 |
| 3.1.3.4 | <i>SEM and EDS Analysis</i> | 100 |
| 3.1.3.5 | <i>Preparation of Source Core</i> | 100 |
| 3.1.3.6 | <i>Assay of Activity of the Source Core</i> | 101 |
| 3.1.3.7 | <i>Encapsulation</i> | 102 |
| 3.1.4 | Quality Control | 103 |
| 3.1.4.1 | <i>Testing of the Source Core</i> | 103 |
| 3.1.4.2 | <i>Testing of the Sealed Sources</i> | 104 |
| 3.1.5 | Results | 104 |
| 3.1.5.1 | <i>Optimization of Electrodeposition Parameters</i> | 104 |
| 3.1.5.2 | <i>Influence of pH of the Electro-bath</i> | 104 |
| 3.1.5.3 | <i>Influence of Current Density</i> | 105 |
| 3.1.5.4 | <i>Influence of Deposition Time</i> | 106 |
| 3.1.5.5 | <i>Influence of Temperature</i> | 107 |
| 3.1.6 | Morphology studies | 108 |
| 3.1.6.1 | <i>SEM Analysis</i> | 108 |
| 3.1.6.2 | <i>EDS Characterization</i> | 108 |

Contents

| | | |
|---------|--|-----|
| 3.1.6.3 | <i>Preparation of ^{133}Ba Source Core of Different Strength</i> | 110 |
| 3.1.7 | Quality Evaluation of Source Core | 110 |
| 3.1.7.1 | <i>Leachability</i> | 110 |
| 3.1.7.2 | <i>Autoradiography Examination</i> | 111 |
| 3.1.7.3 | <i>Encapsulation</i> | 112 |
| 3.1.7.4 | <i>Quality control of Sealed Sources</i> | 113 |
| 3.1.8 | Discussion | 114 |
| 3.1.9 | Conclusion | 114 |
| 3.2 | An Electrochemical Pathway to Prepare Circular Planar $^{90}\text{Sr}/^{90}\text{Y}$ Sources for the Calibration of Surface Contamination Monitors | 115 |
| 3.2.1 | Introduction | 115 |
| 3.2.2 | Experimental | 117 |
| 3.2.2.1 | <i>Materials and Equipment</i> | 117 |
| 3.2.2.2 | <i>Preparation of the Anodized Titanium Substrate</i> | 118 |
| 3.2.2.3 | <i>Electrochemical Cell</i> | 118 |
| 3.2.2.4 | <i>Optimization of Electrodeposition Parameters</i> | 120 |
| 3.2.2.5 | <i>Preparation of $^{90}\text{Sr}/^{90}\text{Y}$ Source</i> | 121 |
| 3.2.2.6 | <i>Coating of the Sources with Polystyrene Polymer</i> | 121 |
| 3.2.2.7 | <i>Surface Characterization</i> | 121 |
| 3.2.3 | Quality Evaluation of the $^{90}\text{Sr}/^{90}\text{Y}$ Sources | 122 |
| 3.2.3.1 | <i>Leachability</i> | 122 |
| 3.2.3.2 | <i>Swipe Test</i> | 122 |

Contents

| | | |
|--|--|-----|
| 3.2.3.3 | <i>Autoradiography</i> | 122 |
| 3.2.3.4 | <i>Source Assembly in a Circular Holder</i> | 123 |
| 3.2.3.5 | <i>Radiological Safety</i> | 123 |
| 3.2.4 | Results | 124 |
| 3.2.4.1 | <i>Preparation of the Electrolyte</i> | 124 |
| 3.2.4.2 | <i>Optimization of Electrodeposition Parameters</i> | 124 |
| 3.2.4.3 | <i>Influence of pH</i> | 126 |
| 3.2.4.4 | <i>Influence of Current Density</i> | 127 |
| 3.2.4.5 | <i>Influence of Carrier Concentration</i> | 127 |
| 3.2.4.6 | <i>Influence of Deposition Time</i> | 128 |
| 3.2.4.7 | <i>SEM Analysis</i> | 129 |
| 3.2.4.8 | <i>EDS Characterization</i> | 130 |
| 3.2.4.9 | <i>Measurement of Activity of the $^{90}\text{Sr}/^{90}\text{Y}$ Source</i> | 131 |
| 3.2.5 | Quality Evaluation of $^{90}\text{Sr}/^{90}\text{Y}$ Source | 132 |
| 3.2.5.1 | <i>Leachability</i> | 132 |
| 3.2.5.2 | <i>Autoradiography Examination</i> | 134 |
| 3.2.5.3 | <i>Swipe Test</i> | 134 |
| 3.2.5.4 | <i>Source Assembly in a Circular Holder</i> | 135 |
| 3.2.5.5 | <i>Preparation of $^{90}\text{Sr}/^{90}\text{Y}$ Sources</i> | 135 |
| 3.2.6 | Discussion | 135 |
| 3.2.7 | Conclusion and Scope of the Work | 136 |
| Chapter-4: Preparation of $^{90}\text{Sr}/^{90}\text{Y}$ Sources towards Use in Hand | | 137 |
| Contamination Monitors Using Solvent Extraction and | | |

Contents

| Polymerization Techniques | | |
|---------------------------|--|-----|
| 4.1 | Introduction | 138 |
| 4.2 | Materials | 140 |
| 4.3 | Experimental | 140 |
| 4.3.1 | <i>Studies on the Extraction of ^{90}Sr into the Organic Phase</i> | 140 |
| 4.3.2 | <i>Optimization of Solvent Extraction Parameters</i> | 141 |
| 4.3.2.1 | <i>Dependence of Extraction Yield on the Acidity of the Aqueous Phase</i> | 141 |
| 4.3.2.2 | <i>Dependence of Extraction Yield of ^{90}Sr on the Concentration of DCH18C6</i> | 141 |
| 4.3.2.3 | <i>Dependence of Extraction Yield of ^{90}Sr on Equilibration Time</i> | 141 |
| 4.3.2.4 | <i>Selection of Polymer</i> | 142 |
| 4.3.2.5 | <i>Concentration of PMMA Solution for Preparation of Radioactive Film</i> | 143 |
| 4.3.2.6 | <i>Viscosity of the Polymer Solution</i> | 143 |
| 4.3.2.7 | <i>Preparation of ^{90}Sr Source</i> | 143 |
| 4.3.3 | <i>SEM and EDS Analysis</i> | 146 |
| 4.3.4 | <i>Assay of Activity of the Source Core</i> | 146 |
| 4.4 | Quality Control Tests | 146 |
| 4.4.1 | <i>Test for Leachability</i> | 146 |
| 4.4.2 | <i>Swipe Test</i> | 146 |
| 4.4.3 | <i>Autoradiography</i> | 147 |

Contents

| | | |
|--|--|-----|
| 4.5 | Results | 147 |
| 4.5.1 | <i>Studies on the Extraction of ^{90}Sr into Organic Phase</i> | 147 |
| 4.5.1.1 | <i>Dependence of Extraction Yield of ^{90}Sr on the Acidity of the Aqueous Phase</i> | 147 |
| 4.5.1.2 | <i>Dependence of Extraction Yield of ^{90}Sr on the Concentration of DCH18C6</i> | 148 |
| 4.5.1.3 | <i>Dependence of Extraction Yield of ^{90}Sr on Equilibration Time</i> | 149 |
| 4.5.1.4 | <i>Concentration of PMMA Solution for Preparation of Radioactive Film</i> | 149 |
| 4.5.1.5 | <i>Viscosity of the Polymer Solution</i> | 150 |
| 4.5.2 | <i>SEM and EDS Analysis</i> | 151 |
| 4.5.3 | <i>Extraction of ^{90}Sr into the Organic Phase</i> | 152 |
| 4.5.4 | <i>Autoradiography Examination</i> | 153 |
| 4.6 | Discussion | 155 |
| 4.7 | Conclusion and Scope of the Work | 156 |
| Chapter-5: Preparation of ^{147}Pm Sources for Measurement of Dust in Environment using Chemical Deposition on Ni Coated Copper Substrate | | 157 |
| 5.1 | Introduction | 158 |
| 5.2 | Experimental | 159 |
| 5.2.1 | <i>Materials</i> | 159 |
| 5.2.2 | <i>Instrumentation</i> | 159 |
| 5.2.3 | <i>Preparation of Copper Electrode for Electrodeposition of Ni</i> | 160 |

Contents

| | | |
|--------|---|-----|
| 5.2.4 | <i>Preparation of Electrolyte for Ni Deposition</i> | 160 |
| 5.2.5 | <i>Electrodeposition of Ni</i> | 160 |
| 5.2.6 | <i>Optimization of ^{147}Pm Deposition Parameters</i> | 161 |
| 5.2.7 | <i>Preparation of ^{147}Pm Source</i> | 162 |
| 5.2.8 | <i>Assay of Deposited ^{147}Pm Activity</i> | 163 |
| 5.2.9 | <i>Source Assembly in a Circular Holder</i> | 163 |
| 5.2.10 | <i>X-ray, EDS, SEM and AFM Analysis</i> | 164 |
| 5.2.11 | <i>Quality Control</i> | 165 |
| 5.3 | Results | 165 |
| 5.3.1 | <i>Influence of pH of the Chemical Bath</i> | 166 |
| 5.3.2 | <i>Influence of Contact Time</i> | 167 |
| 5.3.3 | <i>Effect of Reaction Volume</i> | 168 |
| 5.3.4 | <i>X-ray Diffraction Studies</i> | 169 |
| 5.3.5 | <i>Scanning Electron Microscopy (SEM) Analysis</i> | 170 |
| 5.3.6 | <i>EDS Characterization</i> | 172 |
| 5.3.7 | <i>AFM Analysis</i> | 175 |
| 5.3.8 | <i>Source Preparation</i> | 175 |
| 5.3.9 | <i>Activity Assay of Deposited ^{147}Pm Source</i> | 177 |
| 5.3.10 | <i>Quality Control of the Sources</i> | 177 |
| 5.3.11 | <i>Source Assembly</i> | 178 |
| 5.4 | Discussion | 179 |
| 5.5 | Conclusion and Scope of the Work | 180 |

Contents

| | |
|--|-----|
| Chapter-6: Summary, Conclusions and Future Directions | 181 |
| 6.1 Summary of the Thesis | 182 |
| 6.2 Future Scope of the Work | 183 |

SYNOPSIS

Radioisotopes are widely employed in industry and medicine for a wide range of applications either as open sources or as sealed radioactive sources. A sealed radioactive source is a radioactive material that is permanently sealed in a capsule or bonded in a solid material. The design of the capsule is such that it prevents the release of radioactive material during normal use and under possible accident conditions [1]. The sealed radioactive sources are fabricated for applications in nuclear industries, electronics industries, educational institutions, nuclear medicine and Research and Development (R&D) units. In industry, common uses include non-destructive testing, radiation sterilization of health care products, modification of polymeric materials, on-line process control systems, elemental analysis of raw materials, mineral resource evaluation, food irradiation and smoke detection. In medicine, sealed radioactive sources are commonly used in teletherapy and brachytherapy for the treatment of cancer as well as for blood irradiation. Some well known examples of the sealed sources used in medicine are: ^{60}Co sources for teletherapy, brachytherapy, food irradiation and sterilization of health care products. ^{60}Co sources are also employed for the measurement of thickness, density and other properties of materials in industrial processes. The radioactive isotopes employed in the sealed radioactive sources are used in a variety of chemical and physical forms such as the metallic form or oxide, impregnated into ceramics, electroplated onto other support metals as thin films or deposits. These are finally enclosed in various devices that can channel a direct radiation beam at the target material or target tissues while shielding the operating personnel from unwanted exposure [1]. Sealed radioactive sources are prepared by employing diverse chemical methods such as evaporation, electrodeposition,

anodization followed by cathodic electrodeposition, solvent extraction and radioactive polymer film preparation etc. depending upon factors such as the type and geometry of the source matrix required, activity of the source and its final application. Of these different methods mentioned above, electrodeposition, chemical adsorption and solvent extraction followed by polymerization are the most commonly used methods for the preparation of radioactive sources for end use. The activity levels of sealed radioactive sources for various applications can range widely from few micro-curies (laboratory check sources) to curies (teletherapy sources). The sealed radioactive sources are subjected to sealed sources classification performance tests as stipulated by the Atomic Energy Regulatory Board (AERB) regulations [2]. The type of tests carried out on a sealed radioactivity source depends upon the nature of application and the level of radioactivity used. Low level radiation sources (activity of < 1 MBq each) which are used for calibration of counting instruments are exempted from the performance tests due to the low levels of radioactivity in them. However, all the low activity sources undergo tests for surface contamination as per AERB regulations [2]. The chemical methods which are employed for the preparation of sealed radioactive sources described in this thesis are briefly discussed below.

Single-stage electrodeposition: It is a process wherein electrical current is employed to reduce cations of a desired metal from its solution and coat that metal as a thin adherent layer onto a conductive substrate surface [3, 4]. Use of this technique for preparation of sealed radioactive sources of desired specifications depends on the availability of a conducting surface and good adhesion of the desired metal ion on the substrate, uniform current distribution on the substrate surface and compatibility of the plating solution with the substrate material. The experimental parameters on which the efficiency of

electrodeposition depends are current density, nature of the cations and anions in solution, composition of the electrolyte bath and its temperature, concentration of the electrolyte, presence of impurities in the electrolyte bath and the physical and chemical nature of substrate surface. Chapter 2 of the thesis describes the use of electrodeposition technique for the preparation of radioactive sources by optimization of the experimental parameters and their characterization by X-Ray Diffraction (XRD), Scanning Electron Microscopy (SEM) and Energy Dispersive X-ray Spectroscopy (EDS) analysis of the inactive samples and autoradiography of the radioactive sources.

Anodization Followed by Cathodic Electrodeposition: Anodization is the general name applied to methods of treating metals, where the particular metal is made the anode in an electrolytic cell, usually to form oxide coatings for the purpose of increasing the performance of the surface. In case of titanium, the anodization process forms a layer of titanium oxide which is very hard, relatively inert, electrically insulating and can absorb various radionuclides on its surface. The anodic film grows at the titanium/titanium oxide interface by the continuous formation and dissolution of the oxide. This is called barrier layer and its thickness is a function of the applied potential for anodization and the time of anodization. Chapter 3 of the thesis describes the use of anodization followed by electrodeposition for the preparation of sealed radiation sources by a two-step process. The first step involves the anodization of titanium substrate to form a titanium oxide layer. The second step involves the reversing the polarity of the titanium substrate (as a cathode) in an electrolyte bath containing the desired radiometal ion to deposit a stable and adherent layer of the desired radiometal on the titanium oxide layer.

Solvent Extraction Followed by Polymerization: The ability of a solute to distribute itself between an aqueous solution and an immiscible organic solvent can be used for the

separation and purification of solutes either by extraction into organic phase leaving undesirable substances in the aqueous phase, or by extraction of the undesirable substances into the organic phase, leaving the desirable solute in the aqueous phase. Solvent extraction methods use non-polar solvents which are miscible with water to extract the target compound from water by using the greater solubility of the target compound in the solvent than water. This method can be advantageously utilized in the preparation of radioactive sources by extracting the radiometal into a volatile organic solvent using a chelator followed by immobilization of the radionuclide in a polymeric film. In this thesis, the solvent extraction cum polymer film formation method has been utilized in the preparation of large-area $^{90}\text{Sr}/^{90}\text{Y}$ sources as described in chapter 4.

Selective Area Chemical Deposition

Chemical deposition is a simple technique to obtain homogenous films on various metallic substrates. The chemical deposition of desired metal ions (electroless deposition) on electrodeposited metal surfaces could be advantageously utilized in the preparation of radioactive sources. The advantages of such chemical deposition are numerous such as economy, requiring less energy and space and relatively low temperature operating conditions. Moreover, deposit composition, structure and their properties can be tailored by varying bath composition and operating conditions. Based on the reports on chemical deposition of cerium on nickel coated (electrochemically) copper substrates, an attempt was made to prepare radioactive sources of ^{147}Pm by coating the Pm activity (electroless) on a Ni coated Cu matrix which is described in chapter 5 of the thesis.

In this thesis consisting of six chapters, the preparation of sealed radioactive sources for industrial, space and medical applications adopting diverse chemical methods such as single step electrodeposition, two-step electrodeposition, solvent extraction and

polymer formation as well as chemical adsorption is described. The development of these radioactive sources using the different techniques is described in separate chapters in this thesis. Use of non-destructive characterization techniques such as XRD, SEM, EDS and autoradiography to characterize the inactive as well as active samples is also described in each chapter. A brief summary of the contents of each chapter is given below.

Chapter 1: Introduction

The introductory chapter gives an overview of the field of sealed radioactive sources. The categorization of radioisotopes based on their applications and the essential characteristics of each category are described in detail. The classification of sealed radioactive sources as laboratory reference sources and custom-made special radiation sources is also detailed with examples of each category. Different routes for the production of sealed radioactive sources such as simple evaporation, electrodeposition, solvent extraction followed by polymer formation and chemical adsorption are described in detail along with their relative advantages and disadvantages. The importance of quality control tests for the performance evaluation of sealed radioactive sources is emphasized and the quality control tests used are also described. The source classification performance tests as stipulated by AERB Safety Standard are also given. Applications of sealed radioactive sources in different fields such as in industry and medicine are described. Finally, the chapter presents a broad outline of the scope of the work carried out by the author.

Chapter 2: Preparation of ^{55}Fe , ^{57}Co and ^{204}Tl Sources for Multifarious Applications using Electrodeposition Technique

This chapter describes the utilization of electrodeposition technique for the preparation of sealed radioactive sources for diverse applications. The preparation of

electrodeposited ^{55}Fe , ^{57}Co and ^{204}Tl sources for the calibration of X-ray detectors, performance evaluation of nuclear imaging instruments and for calibration of beta surface contamination monitors respectively are described in this chapter.

Chapter 2.1: Use of Electrochemical Technique to Prepare ^{55}Fe Sources for Calibration of X-ray Detectors:

In order to calibrate X-ray detectors, a sealed radioactive source having adequately long shelf-life capable of providing a steady X-ray output is required. ^{55}Fe , a low-energy X-ray emitter [5.9 keV ($\text{Mn } K\alpha$) and 6.5 keV ($\text{Mn } K\beta$)] having a half-life of 2.75 y [5] is one such radionuclide which is well-suited for the calibration of low energy X-ray detectors in the energy range of 2 to 10 KeV. An important feature of ^{55}Fe is the absence of continuum or bremsstrahlung X-rays. ^{55}Fe is also convenient and safe radioisotope to handle as it emits only low energy X-rays. For a ^{55}Fe source to be qualified as an X-ray source for use in X-ray detectors, the amount of ^{55}Fe activity is required to be deposited in a very small circular cross sectional flat surface area of the tip of a long cylindrical copper rod of overall dimensions 3 mm (ϕ) \times 4 mm (l). In recent years, a number of methods for the preparation of radioactive sources have been described [6-9]. Among the various methods which have been reported, electrodeposition is particularly suitable for the preparation of ^{55}Fe containing sources since it is technically simple and reproducible. Hence, electrodeposition technique was chosen for depositing the required amount of ^{55}Fe activity on Cu substrate. Detailed studies were carried out to determine the electrodeposition behaviour of ^{55}Fe at micro molar levels in aqueous solution. The required activity of ^{55}Fe needs to be deposited selectively on the outer surface area of the Cu substrate with negligible leaching of activity from the substrate. No-carrier-added ^{55}Fe solution is required for the preparation of the source as the required ^{55}Fe activity has to be deposited in a very small cross

sectional area at the tip of a cylindrical copper rod. Selection of a suitable electro-bath is of utmost importance for deposition of ^{55}Fe at trace concentrations. Sulphate electro-bath is a good choice as it can be employed at room temperatures at low current density. Various factors that influence the electrodeposition of ^{55}Fe in the sulphate bath were identified and a careful optimization of these factors was carried out in order to ensure optimum deposition of ^{55}Fe activity on the target area of the Cu substrate. In this chapter, details of the laboratory-scale electrodeposition method for the preparation of ^{55}Fe sources by electrodeposition of ^{55}Fe on a precisely defined area of a Cu substrate, covering the radioactive area with a thin layer of organic polymer and quality assurance of this source to meet regulatory requirements, are reported.

Chapter 2.2: Preparation of ^{57}Co Point Sources for the Performance Evaluation of Nuclear Imaging Instruments: The role of Single Photon Emission Computed Tomography (SPECT) in diagnostic nuclear medicine imaging needs hardly to be reiterated. Wide varieties of diagnostic nuclear medicine imaging instruments are used to acquire images and extract quantitative information. Before the instrument is put in to routine use, verification of its performance in terms of sensitivity, constancy and accuracy is essential in order to ensure the performance of a procedure or instrument within an acceptable range. The performance of nuclear medicine instruments is generally evaluated with encapsulated radioactive sources containing long-lived surrogate radionuclides which emits photons of desired energies. In this context, ^{57}Co , which emits gamma-rays of energies 122.1 keV (85.6%) and 136 keV (10.7%) with a half-life of 270 days is considered to be an ideal surrogate for the most commonly used diagnostic radionuclide $^{99\text{m}}\text{Tc}$ ($T_{1/2}=6$ h, $E_{\gamma}=140$ keV) as the γ photon energies of ^{57}Co are close to that of $^{99\text{m}}\text{Tc}$ [10]. Hence, the preparation of sealed ^{57}Co sources for the calibration of

gamma cameras was undertaken. Electrodeposition method was chosen for the work owing to its technical simplicity, cost effectiveness, rapidity and reproducibility [11, 12]. We have earlier reported on the use of the electrochemical technique for the preparation of ^{57}Co sources employed in the radiometric assay of nuclear fuel rods [11] in which various experimental conditions were optimized. As a logical extension, we subsequently used this technique for the preparation of ^{57}Co point sources containing $\sim 1.48 \text{ MBq}$ ($40 \mu\text{Ci}$) of ^{57}Co for the calibration of intra-operative gamma probes [13]. In this chapter, the successful use of electrochemical technique for the deposition of $3.7\text{--}4.81 \text{ MBq}$ ($0.10\text{--}0.13\text{mCi}$) of ^{57}Co from an aqueous solution onto a copper substrate of $0.5 \text{ mm } (\phi) \times 1 \text{ mm}$ (l) towards the preparation of the source is described. The overall design, development and fabrication of titanium capsule and process of encapsulation of ^{57}Co source core are also described in this work. The objective of making sealed ^{57}Co sources commensurate with the user's specifications and compliant with the mandatory regulatory requirements for safe handling during applications has been demonstrated. The mild experimental conditions together with the convenience of electrodeposition technique for depositing the ^{57}Co source core preparation process ensure safe handling of radioactivity.

Chapter 2.3: An Electrochemical Route to Prepare Planar ^{204}Tl Sources for the Calibration of Beta Surface Contamination Monitors: Beta surface contamination monitors are employed in radioactive laboratories to ascertain the beta emitting radionuclide activity levels. Performance as well as sensitivity, constancy and accuracy of these instruments need to be validated before deploying them into service to ensure constancy of response [14]. This objective is achieved through the use of two major types of radioactive reference sources containing appropriate quantities of beta emitting radionuclides. The first type consists of small point sources and the other type comprises

planar sources. Such sources are usually prepared using beta emitting radioisotopes such as ^{14}C , ^{147}Pm , ^{204}Tl , $^{90}\text{Sr}/^{90}\text{Y}$ and $^{106}\text{Ru}/^{106}\text{Rh}$, having E_{β} max of 0.16, 0.24, 0.76, 2.27 and 3.54 MeV, respectively [15]. These sources have reasonably long shelf-life and provide a steady beta radiation flux. In this context, the preparation of ^{204}Tl electrodeposited sources towards use in beta contamination monitors is described in this Section of chapter 2. ^{204}Tl decays by β^- emission to ^{204}Pb (97.4%) and by electron capture (EC) to ^{204}Hg (2.6%) with a half-life of 3.78 years [16]. For use with beta contamination monitors, the source design requires use of a circular disc of Cu having 10 mm (ϕ) on which ~ 3.7 MBq (~ 100 μCi) of ^{204}Tl is required to be deposited homogenously on one of the flat surfaces. The effectiveness of the source preparation technique largely determines the extent to which the radioactive material is uniformly distributed over the source area and adherence to the substrate [17]. A detailed literature survey showed that the electrochemical deposition of Tl and its alloys from aqueous solutions has been the subject of investigations and there have been a few reports depicting its usefulness. Herein, a facile laboratory-scale electrochemical method for the preparation of circular planar ^{204}Tl sources is described. Electrodeposition of ^{204}Tl activity on a precisely defined area of a metallic substrate by optimisation of the various experimental parameters and quality control tests of the source to meet regulatory requirement are reported. Copper was chosen as the basic matrix owing to the attributes such as ready availability in high purity at a reasonable cost, radiation stability, adequate mechanical strength, durability in extreme environments and suitable electro potential for deposition of Tl. The reported process successfully addresses several issues such as preparation of copper substrate of defined geometry and size, electrochemical deposition of ^{204}Tl onto the targeted area of the substrate, coating the radioactive area with a thin layer of polymer, mounting the

source in a holder and quality control of the source to comply with the regulatory norms. It is pertinent to note that the ^{204}Tl sources prepared by the reported procedure were found to be effective in the routine performance evaluation of beta surface contamination monitors. The objective of preparing planar disc source of ^{204}Tl utilizing electrodeposition technique with precise control of radioactivity content, commensurate with user's specifications and compliance with the mandatory regulatory requirement for safe handling during applications could be successfully achieved.

Chapter 3: A Two-step Electrochemical Process for the Preparation of ^{133}Ba and $^{90}\text{Sr}/^{90}\text{Y}$ Sources for Calibration of Instruments

This chapter describes the utilization of two-step electrodeposition technique for the preparation of sealed radioactive sources for diverse applications. The preparation of electrodeposited sources ^{133}Ba and $^{90}\text{Sr}/^{90}\text{Y}$ for the calibration dose calibrators and beta surface contamination monitors respectively are described in this chapter.

Chapter 3.1: A novel and facile approach for the preparation of ^{133}Ba source core, encapsulation and quality evaluation towards its use in calibration of instrument:

Treatment of hyperthyroidism using ^{131}I is one of the oldest and most commonly practiced therapeutic modality [18]. Measurement of ^{131}I activity prior to therapy is usually carried out using well-type dose calibrators. Before the dose calibrator is put into service, verification of its performance in terms of sensitivity, constancy and accuracy is extremely important. In order to evaluate the performance of such dose calibrators, sealed radioactive sources containing long-lived surrogate radionuclides with appropriate photon emissions are employed. ^{133}Ba which emits gamma-rays of 81.0 keV (32.9%), 276.4 keV (7.17%), 302.9 keV (18.3%), 356.0 keV (62.0%) and 383.9 keV (8.93%) energy with a half-life of 10.53 years is considered as an ideal surrogate to ^{131}I as the γ photon energies

of ^{133}Ba are close to that of ^{131}I [19]. Hence, towards evaluating the performance of the well-type dose calibrators which are used for the ^{131}I therapy study, preparation of ^{133}Ba sources of overall dimensions $5.8\text{ mm }(\phi) \times 15\text{ mm } (l)$ containing $\sim 3.7\text{--}11.1\text{ MBq}$ ($0.1\text{--}0.3\text{ mCi}$) of ^{133}Ba activity was undertaken. Towards preparation of the ^{133}Ba source, the possibility of using a titanate substrate to deposit ^{133}Ba from an aqueous solution in the form of barium titanate seemed to be an interesting proposition as there are few reports to support its effectiveness. In order to tap the potential of anodized titanium as an effective substrate, we evaluated the suitability of this substrate for the electrodeposition of ^{133}Ba . In the first Section of this chapter (chapter 3A), an electrochemical technique for the deposition of ^{133}Ba from an aqueous solution onto the surface of an anodized titanium substrate is described. The factors that influence the electrodeposition of ^{133}Ba onto the anodized titanium were identified and careful optimizations of the various experimental parameters were carried out to arrive at the conditions for optimum deposition of ^{133}Ba activity. Evaluation of the quality of the ^{133}Ba source core, design and fabrication of titanium capsule, process of encapsulation and quality evaluation of the ^{133}Ba sources are also described in this chapter.

Chapter 3.2: An Electrochemical Pathway to Prepare Circular Planar $^{90}\text{Sr}/^{90}\text{Y}$ Sources for Calibration of Surface Contamination Monitors: Beta surface contamination monitors are used for routine monitoring and controlling of contamination levels of beta emitting radionuclides in radioactive laboratories. Validation of sensitivity, constancy and accuracy of these instruments needs to be carried out regularly to ensure constancy of the instrument's response to the beta radionuclide contaminants. This objective is primarily achieved through the use of an external radioactive calibration source containing a long lived beta emitting radionuclide [20]. Suitability of the beta emitting radionuclides for

this application depends on their ability to provide traceable beta particle flux of known energy over a longer period of time. Hence, towards evaluating the performance of beta surface contamination monitors, preparation of a circular planar source of $^{90}\text{Sr}/^{90}\text{Y}$ was undertaken. ^{90}Sr , a pure beta emitter, decays into ^{90}Y with maximum beta energy of 0.546 MeV and a half-life of 28.8 years. ^{90}Y too is a pure beta-emitter with a half-life of 64.1 h and has a considerably high maximum beta energy of 2.28 MeV. The source required for this application consists of a flat circular planar disc of 16 mm (ϕ) on which ~ 3.7 MBq (~ 100 μCi) of ^{90}Sr activity is required to be homogenously deposited. In pursuit of a pragmatic approach to undertake the routine preparation of circular planar $^{90}\text{Sr}/^{90}\text{Y}$ sources for the above application, various radioactive source preparation strategies were scrupulously evaluated. Among the various options, the scope of using electrodeposition technique was considered from the viewpoint of technical simplicity, scalability, rapidity and reproducibility. Electrodeposition of ^{90}Sr from ionic state to metallic state from an aqueous solution is precluded owing to the low solution potentials and the difficulty encountered in controlling the electrolytic deposition of ^{90}Sr on a metallic cathode. Although the scope of using anodized titanium substrate holds significant promise, utility of this technique for the preparation of circular planar $^{90}\text{Sr}/^{90}\text{Y}$ sources requires a judicious design of an electrolytic cell, selection of an appropriate electrolyte and a thorough optimization of experimental parameters to arrive at the conditions for optimum deposition of ^{90}Sr on the substrate. It is also essential not only to characterize the deposit in term of their adherence to the substrate but also to qualify for safe handling as well as for regulatory compliances. In this section of chapter 3, the successful use of electrochemical technique for the deposition of ~ 3.7 MBq (~ 100 μCi) of ^{90}Sr from an aqueous solution onto an anodized circular planar titanium substrate of 16 mm (ϕ) is

described. The factors that influence the electrodeposition of ^{90}Sr onto the anodized titanium surface such as pH of the electrochemical bath, applied current density, time of electrodeposition and carrier strontium concentration were systematically investigated for the optimum deposition. The overall design and development of electrochemical cell for electrodeposition of ^{90}Sr , coating the source with a thin layer of polymer and process for nesting the source in a circular holder are described in this chapter. Quality control tests for determination of leachability, uniform distribution of radioactivity and stability of the source performed to ensure compliance with regulatory safety requirements have also been described. The objective of depositing the required quantity of ^{90}Sr activity on the designated area of a circular planar substrate using electrochemical technique could be successfully achieved under the optimized source preparation conditions.

Chapter 4: Preparation of Large Area $^{90}\text{Sr}/^{90}\text{Y}$ Sources Towards use in Hand Contamination Monitors using Solvent Extraction and Polymerization Techniques

Hand contamination monitors are used to check the presence of radioactive contamination on the hands of the working personnel while leaving the radioactive laboratory. For carrying out the routine calibration of hand monitors for β^- radiation, an external radioactive source of large area containing the long-lived β^- emitter ^{90}Sr ($t_{1/2}$ 28.8 years) is required. Hence, work towards the development of a simple method for the fabrication of large area ^{90}Sr sources for calibration of hand monitors was carried out. Preparation of such sources requires judicious selection of a technique, careful preparation of source to adhere to the specifications and evaluation of quality of the sources as per the regulatory requirements. There are two methods reported in the literature for the preparation of $^{90}\text{Sr}/^{90}\text{Y}$ sources [20]. The method reported by Rao et al is based on the deposition of a $^{90}\text{Sr}/^{90}\text{Y}$ solution on polyvinyl chloride-polyvinyl acetate

copolymer (VYNS) films followed by its slow evaporation [20]. This method is suitable for the preparation of small area sources. In the pursuit of a facile approach for the preparation of large-area $^{90}\text{Sr}/^{90}\text{Y}$ sources, the utility of solvent extraction process to extract the required $^{90}\text{Sr}/^{90}\text{Y}$ activity into an organic phase followed by its immobilization with a polymer, thereby making a large area film of the radioactive polymer was considered. For the preparation of a radioactive polymer film of $^{90}\text{Sr}/^{90}\text{Y}$, quantitative extraction of $^{90}\text{Sr}/^{90}\text{Y}$ into an organic phase is desired which requires an effective extractant. There are several literature reports on the use of di-tertiary butyl cyclohexano 18-crown-6 (DCH18C6) for the selective extraction of ^{90}Sr from acidic solutions. In this chapter, the development of a novel process for preparation of a large area $^{90}\text{Sr}/^{90}\text{Y}$ source is reported using DCH18C6 as the extractant. The process consists of solvent extraction using DCH18C6 to extract the required quantity of $^{90}\text{Sr}/^{90}\text{Y}$ activity into an organic phase, addition of a soluble polymer to the organic solvent, spreading of the radioactive polymer solution on a suitable planar surface and evaporation of the solution to form a large area film. The factors that influence the extraction of $^{90}\text{Sr}/^{90}\text{Y}$ into the organic phase were identified and were optimized to arrive at the conditions for optimum extraction. Quality of the radioactive film thus prepared was also evaluated to determine its suitability for the desired application as well as its compliance to the radiation safety aspects.

Chapter 5: Preparation of ^{147}Pm Sources for Measurement of Dust in Environment using Chemical Deposition on Ni Coated Copper Substrate

The technical and economic benefit of β^- gauge dust monitors towards the continuous monitoring of particulate concentration in air is well recognized [21]. Beta emitters provide a steady β^- radiation flux to measure the concentration of suspended particles using β^- -ray attenuation. The most important component of the dust monitors is a

radioactive source which contains a low energy pure β^- emitting radioisotope. In order to tap the potential of β^- emitting radioactive sources for such applications, a rod type ^{147}Pm source was successfully developed previously by our group which consisted of a cylindrical rod in which the activity was deposited on a small surface area at the tip of the rod [22]. Although the basic principle of β^- particle attenuation remains unaltered in the current generation of dust monitors, over the years dust monitor technology has undergone an extensive design overhaul. Consequently, the radioactive source design has also changed and planar circular ^{147}Pm sources are replacing rod-type ^{147}Pm sources for these applications. Therefore an attempt was made to develop a planar circular ^{147}Pm source for use in dust monitors. The radioactive source for this purpose consists of a circular planar ^{147}Pm source with an active area of 17 mm diameter containing ~ 400 kBq of ^{147}Pm activity homogeneously distributed on one side of the Ni coated copper substrate and housed in a 22 mm (Φ) cylindrical aluminium source holder. Among several methodologies available for preparation of radiation sources, in the present case, a two-step process was considered appropriate to deposit the required amount of ^{147}Pm activity homogeneously on the substrate with good adherence owing to its proven effectiveness in making small area source. In this chapter, utilization of chemical deposition technique for the deposition of ^{147}Pm activity on to Ni coated copper substrate (17 mm (Φ)) and quality control of the prepared ^{147}Pm source to ascertain compliance with regulatory norms, is reported. The chapter describes in detail the concept of chemical deposition for source preparation, experimental procedures for preparation and quality control of ^{147}Pm sources for use in dust monitors. The utility of the chemical deposition technique to prepare circular planar ^{147}Pm sources commensurate with product specifications and regulatory requirements could be successfully achieved.

Chapter 6: Summary, Conclusions and Future Directions

This chapter gives a brief summary of the use of various techniques utilized for the preparation of sealed radioactive sources which are employed for different applications. The work reported in this thesis resulted in the preparation of sources which were supplied to users for actual utilization based on the requirement of the user and satisfactory performance of the sources could be demonstrated. The methods reported in this thesis could be utilized for the preparation of novel radioactive sources in the future for various applications in industry and medicine.

References:

1. International atomic energy agency, international catalogue of sealed radioactive sources, IcSRS.
2. AERB safety standard No. AERB/SS/3 (Rev.1)/INDIA (based on ISO 2919).
3. Andricacos P C: Copper on-chip interconnections, a breakthrough in electrodeposition to make better chips, *Electrochem. Soc. Interface*, 8, 32-37, 1999.
4. Schwarzacher W: Metal nanostructures, a new class of electronic devices, *Electrochem. Soc. Interface*, 8, 20-24, 1999.
5. Krishnaswami S, Lal D, Amin B S, Soutar A: Geochronological studies in Santa Barbara Basin: ^{55}Fe as a unique tracer for particulate settling *Limnol. Oceanogr.* 18, 763, 1973.
6. Power W H, Heyd J W: Modified Joliot apparatus for study of electrodeposition of radioactive materials. *Anal. Chem.* 28, 523, 1956.
7. Steeb J, Josowicz M.: Nickel-63 microirradiators, *Anal. Chem.* 81, 1976, 2009.
8. Udhayakumar J, Pardeshi G S, Gandhi S S, Chakravarty R, Kumar M, Dash A, Venkatesh, M: Development of technology for the large scale preparation of ^{60}Co polymer film source. *Applied Radiation & Isotopes.* 66, 1825, 2008.

9. Was B, Koval'ik, A, Novgorodov, A F, Rak J.: A new technique for the preparation of small-size radioactive samples based on the Langmuir–Blodgett method. Nucl. Instrum. Methods 332, 334, 1993.
10. Zanzonico P,: Routine quality control of clinical nuclear medicine instrumentation: a brief review. J.Nucl.Med.49, 1114–1131, 2008.
11. Dash A, Kumar M, Udhayakumar J, Gandhi S S, Satpati A K, Nuwad J, Shukla R, Pillai C G S, Venkatesh M, Venugopal V,: On the application of electrochemical techniques for the preparation of ^{57}Co source core, encapsulation and quality evaluation for radiometric assay of nuclear fuel rods. Radiochimica Acta.99, 103–111, 2011.
12. Dash A, Udhayakumar J, Kumar M, Shukla R, Gandhi S S, Tyagi A K, Venkatesh M: Development of a micro electrochemical cell for in situ deposition of ^{63}Ni for use in electron capture detector (ECD) in gas chromatography. Radiochimica Acta 99,733–741, 2011.
13. Udhayakumar J, Kumar M, Gandhi S S, Tomar B S, Venkatesh M, Dash A: Preparation of spherical ^{57}Co source for the calibration of intra-operative gamma probe. App.Radiat.Isot.70, 167–170, 2012.
14. American National Standard Institute: performance testing of extremity dosimeters, ANSI/HPS N13.32-1995, Health Physics Society, McLean, VA, 8, 1995.
15. International Organization for Standardization, nuclear energy, reference beta-particle radiation – Part 3: Calibration of area and personal dose meters and the determination of their response as a function of beta radiation energy and angle of incidence ISO 6980-3, Geneva, 2006.

16. Lagoutine F, Coursol N, Legrand J: Table de radionuclide's. commissariat a 'Energie Atomique, Bureau National de Metrologie, Laboratoire de Metrologie des Rayonnements Ionisants, Gif sur Yvette, France ,1985.
17. Lowenthal G C, Wyllie H A: Special methods of source preparation, Nucl. Instrum. Methods 112, 353, 1973.
18. Franklyn J A.: The management of hyperthyroidism. N. Engl. J. Med. 330, 1731, 1994.
19. Dantas B M, Dantas A L A, Santos, D S, Cruz-Su'arez R: IAEA regional intercomparison of *in vivo* measurements of ^{131}I in the thyroid the Latin American and Caribbean experience. Radiat. Prot. Dosim. 144 , 291,2011.
20. Sundara Rao, I S, Vadiwala R, Ram N: Preparation and standardization of β -surface sources for calibration of contamination monitors. Int. J. Appl. Radiat. Isot. 34, 1398–1399, 1983.
21. Jaklevic J.M, Gatti R C, Golding F S, and Loo B W A, β -gauge method applied to aerosol samples. Environ. Sci. Technol. 15, 680–686, 1980.
22. Kumar M, Shukla R, Gandhi SS, Udhayakumar J, Tyagi A.K, Dash, A: Selective area chemical deposition process: an innovative and facile route to prepare ^{147}Pm sources for dust monitors. Ind. Eng. Chem. Res. 51, 11147–11156, 2012.

LIST OF FIGURES

| | | <u>Page No.</u> |
|------------|---|------------------------|
| Figure 1.1 | A simple electrodeposition set-up for the deposition of copper | 8 |
| Figure 2.1 | Electrodeposition cell set-up of ^{55}Fe | 39 |
| Figure 2.2 | Auto-radiography device (a) Circular disc base (b) Nut attached to metallic cap (c) Tubular source holder for positioning the radioactive source (d) Metallic cap sited at the top of the tubular source holder (e) ^{55}Fe electrodeposited source (f) Assembled device | 43 |
| Figure 2.3 | Schematic diagram of the ^{55}Fe source assembly | 45 |
| Figure 2.4 | Cyclic voltammetric plot | 47 |
| Figure 2.5 | Amperometric deposition and voltammetry stripping of Fe (a) Amperometric deposition studies, (b) Voltammetry stripping studies | 48 |
| Figure 2.6 | Influence of experimental parameters on the electrodeposition of ^{55}Fe (a) pH of the electrolyte (b) Current density (c) Electrodeposition time (d) Bath temperature | 50 |
| Figure 2.7 | SEM micrograph of the electrodeposited surface | 51 |
| Figure 2.8 | Energy Dispersive X-ray (EDX) spectrum (a) Cu substrate (b) Fe electrodeposited on Cu substrate | 52 |
| Figure 2.9 | X-ray diffraction pattern of substrate, (a) Copper substrate | 53 |

| | | |
|-------------|--|----|
| | (b) Electrodeposited sample (c) Electrodeposited Fe stripped from the Cu base | |
| Figure 2.10 | Electrodeposition assembly for preparation of ^{57}Co point source | 60 |
| Figure 2.11 | Schematic of ^{57}Co source in titanium capsule | 61 |
| Figure 2.12 | Variation of the efficiency of the HPGe detector for ^{152}Eu gamma rays. | 67 |
| Figure 2.13 | Autoradiograph of ^{57}Co point source. | 68 |
| Figure 2.14 | Schematic diagram of the electrochemical cell. | 75 |
| Figure 2.15 | Source assembly in a circular holder. (a) Source holder base is threaded on the inside edge to accommodate a matching threaded cap, (b) Electrodeposited ^{204}Tl disc source is fitted inside the base with its radioactive end facing down towards the open end, (c) Source cap is threaded on the outside edge to enclose the source, (d) Source assembly. | 79 |
| Figure 2.16 | Cyclic voltammetric plot of $1 \times 10^{-4} \text{ M Tl (I)}$ solution in 0.1M boric acid medium at varying scan rates: (1) 100mVs^{-1} (2) 200mVs^{-1} (3) 300mVs^{-1} (4) 400mVs^{-1} | 81 |
| Figure 2.17 | Influence of pH of the electrolyte | 82 |
| Figure 2.18 | Influence of current density | 83 |
| Figure 2.19 | Influence of deposition time | 84 |

| | | |
|---------------|---|-----|
| Figure 2.20 | Influence of thallium content in the electrolyte | 85 |
| Figure 2.21 | Influence of bath temperature | 86 |
| Figure 2.22 | Scanning Electron Microscope (SEM) images of Tl deposited surface at different magnification (a) $\times 5.0K$ (b) $\times 10.0K$ (c) $\times 20.0K$ | 86 |
| Figure 2.23 | Scanning Electron Microscope (SEM) images of Tl deposited polymer coated surface at different magnification (a) $\times 5.0K$ (b) $\times 10.0K$ (c) $\times 20.0K$ | 87 |
| Figure 2.24 | Energy Dispersive X-ray (EDS) spectrum of (a) Tl deposited surface (b) Tl deposited polymer coated surface | 88 |
| Figure 2.25 | Atomic Force Microscopy (AFM) images of Tl deposited on Cu substrate (a) 2D image (b) 3D image | 90 |
| Figure 3.1 | Schematic diagram of the electrochemical cell set-up for ^{133}Ba deposition | 99 |
| Figure 3.2 | Welding set up for the encapsulation of ^{133}Ba sources | 103 |
| Figure 3.3(a) | Influence of pH of the electrolyte | 105 |
| Figure 3.3(b) | Influence of current density | 105 |
| Figure 3.3(c) | Influence of deposition time | 106 |
| Figure 3.3(d) | Influence of bath temperature | 107 |
| Figure 3.4 | SEM micrograph of (a) Anodized titanium rod, (b) Barium | 108 |

| | | |
|-------------|--|-----|
| | deposited anodized titanium rod | |
| Figure 3.5 | EDS spectrum of anodized titanium rod | 109 |
| Figure 3.6 | EDS spectrum of barium deposited titanium rod | 109 |
| Figure 3.7 | Barium-133 source core assembly in a cylindrical titanium capsule (a) Loading of source core in the capsule (b) Assembled source (c) Photograph of the capsule and source. | 113 |
| Figure 3.8 | Schematic diagram of ^{90}Sr electrodeposition set-up | 120 |
| Figure 3.9 | Source assembly in a circular holder | 125 |
| | (a) Source holder base is threaded on the inside edge to accommodate a matching threaded cap | |
| | (b) Electrodeposited $^{90}\text{Sr}/^{90}\text{Y}$ circular planar source is fitted inside the base with its radioactive end facing down towards the open end | |
| | (c) Source cap is threaded on the outside edge to enclose the source | |
| | (d) Source assembly | |
| Figure 3.10 | Effect of pH of the electrolyte on electrodeposition of $^{90}\text{Sr}/^{90}\text{Y}$ | 126 |
| Figure 3.11 | Influence of applied current density on the deposition of ^{90}Sr | 127 |
| Figure 3.12 | Influence of strontium carrier on the deposition of ^{90}Sr | 128 |
| Figure 3.13 | Influence of deposition time | 129 |
| Figure 3.14 | Scanning electron microscopy (SEM) images anodized Ti | 129 |

| | | |
|-------------|---|-----|
| | substrate at different magnification | |
| Figure 3.15 | Scanning electron microscopy (SEM) images of Sr deposited anodized Ti substrate at different magnification | 130 |
| Figure 3.16 | EDS spectrum of (a) Anodized Ti surface (b) Sr deposited anodized Ti substrate | 130 |
| Figure 3.17 | Image of the exposed radiographic film | 134 |
| Figure 4.1 | (a) Schematic diagram of the gadget used for the preparation of large area rectangular $^{90}\text{Sr}/^{90}\text{Y}$ sources and (b) Actual photograph | 144 |
| Figure 4.2 | Dependence of percentage extraction of ^{90}Sr on the acidity of aqueous phase | 148 |
| Figure 4.3 | Dependence of extraction yield of ^{90}Sr on concentration of DCH18C6 of the organic phase | 148 |
| Figure 4.4 | Variation of ^{90}Sr extraction yield with time | 149 |
| Figure 4.5 | Variation of viscosity (η) with concentrations of PMMA in chloroform | 150 |
| Figure 4.6 | SEM micrograph of the polymeric film at different magnifications(a) 5 K (b) 10K (c) 40K | 151 |
| Figure 4.7 | Energy Dispersive X-ray (EDS) spectrum of the polymeric film | 151 |
| Figure 5.1 | Schematic of set-up for the electrodeposition of Ni on the circular Cu substrate | 161 |

| | | |
|---------------|---|-----|
| Figure 5.2 | Schematic diagram of (a) Circular threaded source holder cap, (b) Circular planar ^{147}Pm source (c) Circular source holder base (d) Source assembly. | 164 |
| Figure 5.3 | Influence of pH of the feed solution on the chemical deposition of ^{147}Pm | 166 |
| Figure 5.4 | Influence of contact time on the chemical deposition of ^{147}Pm | 167 |
| Figure 5.5 | Influence of reaction volume on the chemical deposition of ^{147}Pm | 168 |
| Figure 5.6 | XRD pattern of (a) Copper substrate (b) Electrodeposited Ni sample and (c) Chemical deposited Sm sample | 169 |
| Figure 5.7 | SEM micrograph of (a) Copper substrate (b) Electrodeposited Ni surface (c) Chemically deposited Sm sample | 170 |
| Figure 5.8 | SEM micrograph of chemical deposited Sm samples at different concentrations of Sm feed concentration (a) 500 \times magnification (b) 1K \times magnification (c) 3K \times magnification | 172 |
| Figure 5.9(a) | Electrodeposited Ni surface | 173 |
| Figure 5.9(b) | Chemically deposited Sm surface | 173 |
| Figure 5.10 | AFM images of the (a) Electrodeposited Ni surface (b) Chemical deposited Sm surface | 175 |
| Figure 5.11 | Dose rate vs. activity relationship | 177 |

LIST OF TABLES

| | <u>Page No.</u> |
|--|-----------------|
| Table 1.1 Low level Laboratory check sources | 3 |
| Table 1.2 Custom-made special sources | 4 |
| Table 1.3 De-lamination characteristics of polymers | 28 |
| Table 1.4 Typical physical properties of Poly(methyl methacrylate) | 28 |
| Table 1.5 Classification of sealed source performance tests | 30 |
| Table 1.6 Performance requirements for sealed radiation sources | 31 |
| Table 2.1 Elemental mapping of Fe deposited on Cu substrate | 52 |
| Table 2.2 Leachability of ^{55}Fe source | 54 |
| Table 2.3 Quality control of ^{55}Fe source | 56 |
| Table 2.4 Optical density distribution of ^{57}Co source | 69 |
| Table 2.5 Quality assessment of sealed ^{57}Co source | 69 |
| Table 2.6 Elemental composition of electrolytic deposit | 89 |
| Table 2.7 Elemental composition of the Tl electrodeposited substrate coated with PMMA | 89 |
| Table 2.8 Optical densities of the exposed radiographic film at different position | 92 |
| Table 3.1 Amount of cold barium carrier used for the preparation of different source strength | 101 |
| Table 3.2 Chemical deposition of Ba deposited Titanium rod | 110 |
| Table 3.3 ^{133}Ba deposition efficiency in the preparation of ^{133}Ba sources of different strengths | 110 |

| | | |
|-----------|--|-----|
| Table 3.4 | Optical density variations | 110 |
| Table 3.5 | Elemental composition of the Sr electrodeposited anodized Ti substrate | 131 |
| Table 3.6 | Preparation of $^{90}\text{Sr}/^{90}\text{Y}$ sources of different strengths | 132 |
| Table 3.7 | Leachability of $^{90}\text{Sr}/^{90}\text{Y}$ from the electrodeposited surface | 133 |
| Table 4.1 | De-lamination characteristics of polymer for making radioactive film | 142 |
| Table 4.2 | Optimization of the concentration of PMMA solution | 150 |
| Table 4.3 | Elemental composition of the Sr PMMA film | 152 |
| Table 4.4 | Extraction of $^{90}\text{Sr}/^{90}\text{Y}$ into the organic phase containing ligand | 152 |
| Table 4.5 | Optical densities of the exposed radiographic film at different position of the $^{90}\text{Sr}/^{90}\text{Y}$ sources | 154 |
| Table 5.1 | Effect of concentration of Sm in the feed solution on the Sm content of the deposited surface obtained from EDS measurements | 174 |
| Table 5.2 | Efficiency of the chemical deposition process | 176 |
| Table 5.3 | Quality evaluation of ^{147}Pm sources | 178 |

ABBREVIATIONS

| | |
|----------------|--|
| AERB | Atomic Energy Regulatory Board |
| AFM | Atomic Force Microscopy |
| ALARA | As Low As Reasonably Achievable |
| BDL | Below the Detection Limit |
| CD | Current Density |
| CDM | Centre for Design and Manufacturing |
| CV | Cyclic Voltammetry |
| DC | Direct Current |
| DCH18C6 | 18-Crown-6 |
| EC | Electron Capture |
| ECD | Electron Capture Detector |
| EDX | Energy Dispersive X-Ray |
| GM | Geiger Muller Counter |
| HPGe | High Purity Germanium Detector |
| IR | Infra Red |
| K _D | Distribution Coefficient |
| LSC | Liquid Scintillation Counter |
| NCA | No Carrier Added |
| NIST | National Institute of Standards and Technology |
| OD | Optical Density |
| PET | Positron Emission Tomography |
| PMMA | Poly Methyl Methacrylate |

| | |
|-------|--|
| POPOP | 1,4 bis-[2-(5-phenyloxazolyl)]-Benzene |
| PPO | 2,5diphenyl Oxazole |
| PVA | Polyvinyl acetate |
| QC | Quality Control |
| RWL | Recommended Working Life |
| SCE | Saturated Calomel Electrode |
| SD | Standard Deviation |
| SEM | Scanning Electron Microscopy |
| SPECT | Single Photon Emission Computed Tomography |
| TLD | Thermo Luminescence Dosimeter |
| VYNS | Polyvinyl chloride-Polyvinyl acetate Copolymer |
| XRD | X-ray Diffractometer |

CHAPTER-1

INTRODUCTION

“Wisdom is not a product of schooling but of the lifelong attempt to acquire it”.

-Albert Einstein

1. Sealed Radioactive Sources

A sealed radioactive source contains the radioactive material which is permanently sealed inside a capsule or is bonded in a solid form. Sealed radioactive sources are designed and fabricated such that their encapsulation prevents the release of radioactivity during normal use as well as under accidental conditions [1].

1.2. Laboratory Reference Sources:

A radioactive source in liquid or solid form that serves as a reference standard in terms of the energy and types of radiations emitted and which has a reasonably long half life and chemical stability during its use.

1.2.1. Classification of Laboratory Reference Sources

The laboratory reference sources are classified into two categories namely,

- Low Level Laboratory Check Sources
- Custom-made Special Sources

1.2.2. Low Level Laboratory Check Sources

Laboratory check sources are prepared by normal evaporation method wherein a small aliquot of the radiochemical solution is placed at the centre of a standard color coded plastic source holder (disc and rod type shape) and the solvent is allowed to evaporate leaving behind the radioactivity firmly adhered to the source holder. These sources are fabricated using up to ~1 MBq with an overall uncertainty of estimation of $\pm 10\%$. The low level Laboratory check sources are of following types:

- Alpha (incorporated on a stainless steel planchette)
- Beta (Disc)
- Gamma (Disc and rod)
- Conversion electrons (Disc)

- Positron sources (Disc)
- X-ray & low energy gamma (Disc)

The following Table (Table-1.1) gives a list of the low level laboratory check sources

Table-1.1: Low level laboratory check sources

| Category of Radiation Sources | Radioisotopes |
|----------------------------------|--|
| Gamma sources | ^{137}Cs , ^{60}Co , ^{133}Ba , ^{22}Na , ^{57}Co , ^{54}Mn , ^{131}I and ^{152}Eu |
| Beta sources | $^{90}\text{Sr}/^{90}\text{Y}$, ^{204}Tl , ^{45}Ca , ^{32}P and ^{147}Pm |
| Conversion electron sources | ^{141}Ce , ^{137}Cs , ^{57}Co and ^{113}Sn |
| Positron sources | ^{58}Co and ^{22}Na |
| X-ray & low energy gamma sources | ^{57}Co , ^{55}Fe , ^{109}Cd , ^{125}I and ^{113}Sn |
| Alpha sources | ^{241}Am and ^{239}Pu |

1.2.3. Custom-made Special Sources

Sealed radioactive sources are also custom-made adhering to the stringent requirements for various applications using different methodologies. These sources are employed for various purposes including environmental monitoring in petro-chemical industries, oil and gas exploration work, space applications, defence applications, quality control of nuclear medicine imaging instruments such as SPECT and PET cameras etc. Custom-made special sources are prepared by employing different techniques such as electrodeposition, anodization-cum-adsorption, radioactive polymer film preparation etc. depending upon factors such as the type and geometry of the source matrix required, chemical properties of the radioisotope, radioactivity of the source and its final application. Table-1.2 gives information about the various custom-made source preparation techniques and the radioisotopes which are employed for the purpose.

Table-1.2: Custom-made special sources

| Method of preparation | Radioisotopes |
|--|---|
| Electrodeposited sources | ^{57}Co , ^{54}Mn , ^{55}Fe , ^{63}Ni and ^{204}Tl |
| Radioactive polymer film sources | $^{90}\text{Sr}/^{90}\text{Y}$ and ^{60}Co |
| Anodization cum adsorption sources | ^{133}Ba and ^{147}Pm |
| Chemically deposited radioactive sources | ^{109}Cd and ^{147}Pm |

1.3. Common Terms Used in Radiation Sources

1.3.1 Sealed Source

Radioactive material sealed in a capsule that is strong enough to prevent dispersion of the radioactive material under the conditions of use for which it was designed. It can also be an assembly of sealed sources in an array utilized in an irradiator.

1.3.2. Activity

Activity of the radiation source is expressed as "equivalent activity" defined as the activity equal to the activity of a point source of the same radionuclide that gives the same exposure rate at the same distance from the center of the source. Activity tolerance: $\pm 10\%$ [2-6].

1.3.3. Recommended Working Life

The "Recommended Working Life" (RWL) is the duration up to which the radiation source can be safely and effectively used for the intended purpose. Each radiation source is associated with an individual RWL period based on factors such as total activity of the source at the time of fabrication, half-life of the radionuclide, source construction (capsule design, source insert type, etc.), toxicity of the radionuclide, typical application environment, operational experience and adherence to quality control

parameters including leakage of radioactivity, source capsule integrity etc. [7, 8]. The source should preferably be replaced after the RWL.

1.3.4 Standard

Measurement of a variable is determined by comparison with a primary standard, which has the highest metrological qualities, and whose value is established without reference to other standards for the same variable. All measurements with respect to the manufacturing or monitoring of the sealed radiation sources are carried out by comparison with the primary standard.

1.4. Methodologies for Fabrication of Custom-made Sources

The methodologies adopted towards the fabrication of sealed radioactive sources include

- Coating of the radioisotopes in metallic form or in oxide form on suitable substrates
- Impregnation of radioactivity into ceramics
- Electroplating the metals onto other support metallic substrates as thin films or deposits
- Anodization cum adsorption on to aluminium substrate
- Complexation and formation of radioactive polymer

These radiation sources are finally housed in various devices that can be used safely in various fields. Care is taken to provide sufficient shielding to the working personnel from unwanted radiation exposure [1]. Towards safe handling, the radioactive source material is (a) permanently sealed in a capsule or is (b) bounded in a solid form.

1.5. Important Factors for the Preparation of Custom-made Sources

1.5.1. Choice of Matrix/Substrate

The choice of the matrix on which the radioactivity needs to be deposited is based on the following criteria:

- Chemical nature of the matrix which dictates the stability and adherence of the radioactive deposit on it
- Chemical properties of the radioisotope and its compatibility with the matrix
- Geometry and dimensions of the substrate wherein the radioactivity is to be deposited
- Types of radiations (beta, gamma, electron capture (EC) etc.) emitted by the radioisotope. For beta source the radioactive area should be covered with a thin window to minimize the attenuation as well as for safe handling. Gamma radiation sources can be encapsulated or can be housed in a holder with suitable metallic covering.
- Maximum radioactivity to be incorporated
- Half life of the radioisotope
- Intended use

1.5.2. Criteria for Selection of Source Preparation Methods

Selection of methodology of source preparation is based on the following criteria:

- The process should be reproducible, efficient and should be amenable to be executed in minimum time. This would avoid the radiation exposure to the personnel involved in the fabrication of the source
- The process of source fabrication should be simple and require inexpensive equipment. This would not only reduce the capital investment but would also make the source inexpensive
- The fabrication process should generate minimum amount of radioactive waste. Wherever possible, in situ deposition of radionuclide should be performed

- Should be amenable for translation from small scale laboratory experiments to large scale source production
- High temperature operations should be avoided in order to preclude the generation of hazardous air borne radioactivity

1.6. Evaporation Technique

This is the simplest and the quickest source preparation method which is usually employed for the preparation of low activity radiation sources. In this method, a suitable concentration of radiochemical stock solution is identified. The concentration of the identified radiochemical stock is calculated to the current date of use by applying the radioactivity decay equation $A=A_0.e^{-\lambda t}$. The radioactivity concentration per unit volume of the radiochemical is also calculated. The calculated volume of the radiochemical is dispensed at the centre of a suitable source holder using a micropipette. The source is placed under an Infra red lamp clamped at about one foot distance from the source sample. After drying, the sample is counted on a NaI (Tl) counter or a Geiger Muller (GM) counter. The source is finally sealed using an ultrasonic sealing machine.

1.7. Electrodeposition

Electrodeposition is a surface coating technique wherein an adherent layer of one metal is formed on another [9-13]. Electroplating of metals and metallic alloys has been in practice for nearly a century and electro-deposition has been utilized as a means of obtaining films of a wide variety of materials including semiconductors, superconductors, polymer films, materials for specific electronic device application etc. Electrodeposition is also carried out to achieve the desired electrical and corrosion resistance, reduce wear and friction, improve heat tolerance as well as for decorative purposes.

1.7.1. Theory of Electrodeposition

"Electrodeposition", a short version of "electrolytic deposition" is also referred to as "electroplating" and the two terms are used interchangeably. It is a process wherein electrical current is employed to reduce cations of a desired metal from a solution and coat that metal as a thin film onto a conductive surface. Figure-1.1 shows a simple electrodeposition set-up for the deposition of copper from copper sulphate solution.

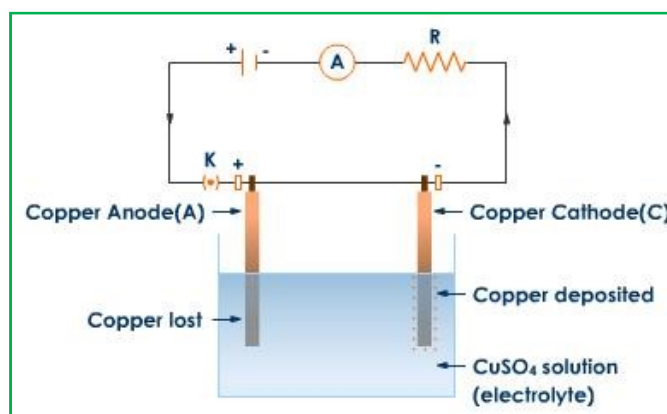
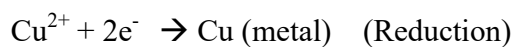
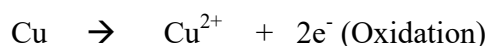


Fig.1.1: A simple electrodeposition set-up for the deposition of copper

The electrolytic solution contains positively charged copper ions (cations) and negatively charged sulphate ions (anions). Under the applied external electric field, the cations migrate to the cathode where they are discharged and deposited as metallic copper.



Copper from the anode dissolves into the solution to maintain the electrical neutrality.



The overall process is known as electrolysis. If a noble metal such as platinum is used as the anode, the overall reaction at the anode is the oxidation of water.



The sulphate ions remain unchanged in quantity during the electrolysis. However, if a noble metal is used as the anode, the concentration of Cu^{2+} ions will decrease and that of H^+ ions will increase with time. Under this situation, extra copper sulphate must be added into the solution from time to time and the hydrogen ions must be removed by neutralization with an alkali or by using a buffering solution.

1.7.2. Faraday's Law

The extent of electrochemical reaction that occurs at an electrode is proportional to the quantity of electric charge (Q) passed through the cell [13]. The weight of a product of electrolysis is W, then

$$W = ZQ \quad (Z \text{ is the electrochemical equivalent})$$

Since $Q = It$, it follows that

$$W = ZIt$$

Production of one gram equivalent of a product at the electrode (W_{eq}) in a cell needs 96487 Coulombs.

1.7.3. Electrochemical Equivalence

The electrochemical equivalent of a metal Z (M) is the weight in grams produced or consumed by one coulomb of charge

$$W_{eq} = A/n$$

$$W_{eq} = 96487 Z$$

$$Z = W_{eq}/96487 = W_{eq}/F$$

$$Z = A/nF \quad W = ZQ = AQ/nF$$

$$\text{When } Q = 1, W (Q=1) = Z$$

1.7.4. Requirements for Electrodeposition

- Availability of a conducting surface
- Pure substrates, solutions and containers as even low impurity levels would result in poor-quality deposition
- Good adhesion of deposit on the substrate The plating solution must be compatible with the substrate
- Uniform current distribution on the substrate surface

1.8. Electrodeposition System

A simple electrodeposition system consists of the following components

1.8.1. Electrodes

There are two electrodes (cathode and anode) required for electrodeposition. An applied electric field across these electrodes provides the main driving force for the mobility of the ions. The positive and negative ions deposit at the cathode and anode respectively. Cathodic deposition is more popular in electroplating because

- Most metal ions are positive ions
- Anodic deposition has been found to give poor stoichiometry and adhesion

1.8.2. Choice of Substrate

Substrate plays an important role in electro-deposition [14-16]. Therefore, in choosing a suitable substrate, in addition to considering the need to provide mechanical support to the electrodeposits, due consideration must be given to the possible influence of the substrate on the properties of the deposit. The following criteria should be applied for the selection of the substrate.

- It should have good conductivity. Good conductivity of the substrate is also beneficial in improving the carrier collection efficiency

- The thermal expansion of the substrate should match well with that of the electrodeposit. Occasionally, in electrodeposition, applied temperatures may be fairly high to improve the grain size or stoichiometry or to fabricate junctions. A mismatch in the thermal expansion often leads to strains that result in cracking or peeling of the deposit film
- The substrate should have good mechanical strength
- For epitaxial films, it is necessary to match the lattice parameters between the single crystal substrate and the growing film
- The substrate should be stable in the electrolyte bath
- The substrate surface should be smooth. Surfaces having waviness, porosity, voids, and other irregularities may be avoided as these factors influence the local current distribution

1.8.3. Preparation of Substrate Surface

Preparation of a smooth and scratch-free substrate surface is extremely important in electrodeposition as surface inhomogeneities tend to amplify during electrodeposition [17-19]. On the atomic scale, surface defects may be point defects, dislocations etc., while on the macroscopic scale they can be scratches left from polishing operations, grain boundaries etc. Substrate preparation consists of three major steps, grinding, polishing, cleaning and testing the surface cleanliness. Emery paper can be used for grinding. After grinding, the surface is either polished mechanically or electrochemically. Electro-polishing yields a scratch-free, deformation-free surface. The surface quality and finish obtained by a prior polishing operation also determine the final finish resulting from electro-polishing.

a) Cleaning

Surface cleaning is an important step prior to electrodeposition. It is necessary to remove the contaminants that would otherwise affect the properties of the films. The properties that can be affected by the presence of the contaminants include adhesion, morphology, nucleation, electronic properties of the film and the substrate film interface. Choice of the cleaning procedure is governed by the substrate as well as by the type of contaminants that are likely to be present. The cleaning process should be chosen to avoid any undesirable damage to the substrate surface and yet result in the complete removal of the contaminant. It is easier to select the cleaning procedure when the nature and origin of the contaminants are known. Some common contaminants encountered are finger tip grease, glue, dust, leftovers of abrasives, etc.

b) Cleaning by Solvents

Solvent cleaning is employed to eliminate or remove the surface contamination of the substrate. Detergent cleaning is useful for metals. Acid cleaning is often employed to remove oxides and oil from inert glass or metal substrates. The contaminants are first converted into water soluble compounds that are subsequently removed in a water rinse. Alkaline cleaners along with some surface active agents are often employed after detergent cleaning to remove oil smuts and oxides. Ultrasonic cleaning is also a useful technique for this purpose.

c) Cleaning by Heating

Heating the substrate may remove the volatile impurities. The heating temperature should be chosen according to the melting point and/or surface reactivity of the substrate.

d) Cleaning by Etching

Solutions of acids such as sulphuric acid and hydrofluoric acid can also be used as etchants for cleaning the surface of the substrate.

1.8.4. Electrolyte

The electrolyte or bath provides the ions to be electrodeposited. It has to be electrically conductive. The electrolyte can be aqueous, non-aqueous or molten, and it must contain suitable metal salts. Sometimes an additive is included to improve the quality of the deposits. An ideal additive should not become incorporated in the film but should lead to improvement of its adhesion, surface finish, uniformity etc.

1.8.5. Electrodeposition Bath

The electrolytic bath is the medium that supplies the ions that migrate upon application of an electric field. In general, ionic transport is facilitated in aqueous solutions, non aqueous solutions or in a molten salt bath [20-23].

1.8.6. Type of Electrolytic Solutions

The choice of the solvent depends on primary factors such as solubility and non-reactivity.

- **Aqueous solvents:** These solvents are suitable for a large number of salts, complexing agents and other compounds. Except for a few hydrolysis reactions, water is generally a non-reactive solvent. However, an aqueous solution contains H^+ and OH^- ions which complicate the electrodeposition process by resulting in the evolution of hydrogen and/or oxygen at the electrodes.
- **Non-aqueous solvents:** These can be further be classified as protic and aprotic solvents.

❖ **Protic Solvents:** These solvents are generally strong hydrogen donors and can exchange protons rapidly. Such solvents also lead to hydrogen evolution.

❖ **Aprotic Solvents:** They contain hydrogen bonded only with the carbon (propylene carbonate, DMF, DMSO, acetonitrile, tetrahydrofuran etc.)

The aqueous solvents have attracted attention for metallic electrodeposition due to facile metal reduction, low current requirement and adherent thin film deposit.

1.8.7. Criteria for Electrolytic Bath

A. Selection of Solvent:

The first step is to choose the appropriate solvent depending upon the material to be deposited. Electrodeposition solvents are stable only in a limited potential range, beyond which reduction-oxidation reactions take place. This potential range is called the working potential range. The potential at which the electrodeposition is to be carried out should be within this range. The morphology and rate of growth depends upon the temperature at which electrodeposition is being carried out. The solvent should remain liquid at the desired temperature. High vapour pressure solvents are preferred because the electrolytic concentration remains more constant. This is particularly true when the solvent is being purged with nitrogen or an inert gas to drive out the dissolved oxygen. Solvents with low viscosity are always preferred because of the better conductivity and diffusion.

B. Selection of Supporting Electrolyte

The supporting electrolyte performs several functions in the electrochemical process.

- It increases the conductivity of the electrolyte
- It reduces the electrode double layer thickness and also influences ion pairing and adsorption

- It effectively eliminates the effect of migration in the mass transport

The criteria for selection of a supporting electrolyte are its solubility in the solvent and a dissociation constant sufficiently high to yield good conductivity and the electrochemical oxidation of anions and electro-reduction of cations at more anionic or cationic potentials, respectively in the electrochemical process under investigation. In aqueous media, KCl and HCl have been commonly used as supporting electrolytes.

C. Additives in Electrolytes

Additives are often added to the plating bath to obtain a brighter and smoother deposit, controllable reaction rate, better adhesion as well as better texture. Additives are used in the electrodeposition process to control the rate of electrodeposition process. Eg: boric acid. Additives also influence the deposit quality and morphology.

D. Purity of Solvent

Impurities in the solvent interfere with the electrochemical processes. In many cases, electrodeposition may not be possible or the deposit morphologies may be affected by the impurities. It is therefore essential to use pure solvent. In some cases, an inert gas is flushed through the solvent to remove oxygen. A common impurity in non-aqueous solvent is oxygen which can be removed by purging with nitrogen.

E. Electroplating

- Place the electrolyte solution containing the metal ion to be deposited (desired radiochemical such as ^{57}Co , ^{55}Fe , ^{133}Ba , $^{90}\text{Sr}/^{90}\text{Y}$, ^{63}Ni etc.) on a hot plate with magnetic stirrer
- Place the cleaned metallic substrate into the plating solution and connect it to the cathode of the power supply.

- Place a platinum strip of similar dimensions into plating solution and connect it to the anode

1.8.8. Factors influencing electrodeposition

The morphology and composition of the electro-deposits vary considerably and depend on a number of experimental parameters such as:

- Current density
- Nature of the anions and cations in solution
- Composition of the electrolyte bath
- Temperature
- Concentration of the electrolyte
- Power Variation
- Presence of impurities in the electrolyte bath
- Physical & chemical nature of substrate surface

1.8.9. Cathode Efficiency

The ratio of the weight of metal actually deposited to the weight that would have resulted if all the current had been used for depositing it is called the cathode efficiency.

Cathode efficiency in plating depends on:

- Electrolyte or bath
- Concentration of chemical components
- pH and agitation
- Current density

The current efficiency in Ni, Co, Fe plating is close to 100%.

1.9. Electrodeposition Parameters for Preparation of Radioactive Sources

- *Electrolyte*: Boric acid 30 mg.mL⁻¹ solution ~10 to 20 mL
- *Radioactive content*: As per requirement (⁵⁷Co, ⁵⁵Fe, ¹³³Ba, ⁹⁰Sr/⁹⁰Y etc.) in order to fabricate custom-made radiation sources containing these radioisotopes
- *Electrolyte pH*: between 2 to 4
- *Temperature range of plating solution*: 15°C to 50°C
- *Applied Voltage*: 2-4 volts
- *Current density used*: 10 mA.cm⁻² to 100 mA.cm⁻²
- *Plating duration*: 4 to 5 hours

While standardizing the electroplating procedure for a desired metal ion, experiments to optimize the electro-deposition parameters such as the composition of the electrolyte bath and its pH, applied voltage, current density, temperature and time of electro-deposition need to be carried out.

1.10. Properties of the Deposited Film

1.10.1. Adhesion

Adhesion is mostly dependent upon the substrate. For proper adhesion, the substrate must be thoroughly cleaned and should be free of any surface films. Alloy formation by the inter-diffusion of the substrate and the deposited metals provides good adhesion. However, an inter-metallic compound is undesirable since it behaves like an inorganic salt and results in poor adhesion.

1.10.2. Mechanical Properties

Mechanical properties of the electrodeposited film depend to a large extent on the types and amounts of growth inhibiting substances at the cathode surfaces. The purpose of using a growth inhibiting substance is to obtain fine grain structure of the deposited

film in which the grain boundaries act as the main obstacles to dislocation motion, leading to higher yield and hard surface. Hardness of the deposited film can also be increased by introducing lattice strain wherein impurities are introduced during the film-growth process. Electroplating processes frequently result in the development of internal stresses. The reasons for internal stresses relate to coalescence of three-dimensional, epitaxial crystallites, dislocation configurations, hydrogen incorporated into the crystal lattice or other factors. Tensile stress is more detrimental than compressive stresses since it easily causes cracks in the deposited film, reducing the fracture strength and ductility. Certain agents for some electroplating solutions have been developed to reduce tensile stress [24-29].

1.10.3. Brightness

The brightness of thin deposited films depends on the surface finish of the substrate. Thicker bright deposited films are produced by additional agents in the plating solution [25-27]. Brightening agents are foreign inclusions in the deposited film. However, over-usage of additives can cause brittleness and lead to cracks and peeling off of the deposited film from the substrate.

1.11. Quality of the Electrodeposited Samples

The quality of the deposited films is depends on the magnitude of the applied electric field across the electrolysis and as well as the nature of the electrolyte used.

A. Grain Size

The grain size depends upon the over-potential which in turn determines whether the deposition is controlled by diffusion, activation or both. At low over-potentials, initially a small number of nuclei grow independently. It is therefore expected that a large

grained deposit will be obtained under these conditions. As the over-potential is increased, a large number of nuclei may be formed leading to a decrease in grain size.

B. Surface Roughness

At an ideal surface, the value of the diffusion layer thickness and the limiting current are constant throughout which leads to a uniform growth. The rate of deposition at the elevations may be higher due to shorter diffusional path between the outer plane of the diffusion layer and the elevations. At the tips of the elevations the diffusion conditions may approach those of spherical diffusion. Spherical diffusion is faster than the linear diffusion because of wider diffusional field in the former case. As a result, surface roughness gets amplified during electrodeposition.

C. Formation of Powdery or Spongy Deposit

Formation of powdery or spongy growth is due to an inter-play of many factors such as viscosity and temperature apart from over-potential. Powdery deposits are classified by their small particle size and poor adhesion to the electrode surface. They are generally obtained when the deposition is carried out under diffusion limited current conditions or close to transition time. The amorphous nature of the powdery deposit is due to the high nucleation rate. Powder formation is enhanced when the concentration of the depositing species is decreased, the supporting electrolyte concentration is increased, solution viscosity is decreased, the temperature is decreased or the stirring rate is decreased.

1.12. Advantages of Electrodeposition Technique

- Simple and reproducible
- Good adhesion properties
- Good radiation and thermal stabilities

- It is possible to grow films over large surface areas as well as on odd-shaped surfaces
- Compositionally modulated structures or non-equilibrium alloys can be electroplated
- It is especially advantageous in terms of cost, high throughput and scalability

1.13. Anodization Technique

A. Anodization

Anodization is the general name applied to methods of treating metals wherein the metal is made as the anode in an electrolytic cell in order to form oxide coatings for the purpose of increasing the performance of the surface. In case of aluminium, the anodizing process forms a layer of aluminium oxide (Al_2O_3) or corundum, which is very hard, relatively inert, electrically insulating and can absorb various radionuclides on the surface. The anodic film itself grows at the aluminium/aluminium oxide interface by the continuous formation and dissolution of a layer of oxide. This is the so-called barrier layer and its thickness is a function of the process-starting voltage. A porous, more structured layer forms on top of the barrier layer making up the rest of the coating [30-31]. The thickness of the film formed during the anodization process is usually determined by a relationship between the current per unit area and process time. With most aluminium alloys, as the anodic film grows, its electrical resistance increases requiring the process voltage to be increased. This is especially significant in case of alloys containing certain elements such as silicon. The electrolyte used is based on sulphuric acid. However, other acids such as chromic, phosphoric, boric or organic acids like oxalic acids are also employed to achieve different properties. As all anodized coatings are derived from oxidation of the metal surface, the alloy composition and heat

treatment conditions have a large impact upon the resultant coating. The anodic film has excellent adhesion to the substrate, as it is an integral part of the structure, in contrast to a painted or electroplated component. Anodized coatings provide enhancement in properties over the base material particularly with respect to wear, corrosion, temperature resistance and electrical insulation. The surface finish of the original work piece is reproduced with slight roughening. Any defects such as corrosion or polishing 'burns' would be enhanced rather than hidden.

B. Anodization in Sulphuric Acid

Includes applications varying from heavy duty black dyed coatings for high-tech instruments to cheap coloured ash trays. It also includes architectural anodizing primarily for protecting aluminium window frames etc. The natural colours of these films is light grey, other colours are achieved by dyeing the film.

C. Hard Anodizing

This is a branch of sulphuric acid anodizing where process conditions have been optimized to achieve significantly harder, thicker, denser films. The coatings thus obtained exhibit resistance to wear, corrosion, temperature effects etc.

D. Chromic Acid Anodizing

Chromic Acid anodizing is an electrochemical process that creates a thin aluminum oxide film by rapidly controlling the oxidation of an aluminum surface [30].

Features of Chromic Acid Anodization:

- Good for tight tolerance parts: will not change dimensions
- Can be black dyed - other colors not practical
- Good for bonding
- Non-conductive

- Good for welded parts and assemblies

1.14.Solvent Extraction followed by Polymer Formation

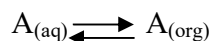
1.14.1. Solvent Extraction

The ability of a solute (inorganic or organic) to distribute itself between an aqueous solution and an immiscible organic solvent has long been applied to separation and purification of solutes either by extraction into the organic phase leaving undesirable substances in the aqueous phase or by extraction of the undesirable substances into the organic phase leaving the desirable solute in the aqueous phase.

1.14.2. Liquid -Liquid Extraction

Solvent extraction methods use non-polar solvents which are miscible with water to extract the target compound from water taking advantage of the greater solubility of the target compound in the solvent than water. Ideally, one selectively extracts the target compound employing a solvent whose polarity is close to that of the target compound. Volatile solvents such as hexane, benzene, ether, ethyl acetate and dichloromethane are commonly used for the extraction of semi-volatile compounds from water. Hexane is suitable for extraction of non-polar compounds such as aliphatic hydrocarbons, benzene is suitable for aromatic compounds, and ether and ethyl acetate are suitable for relatively polar compounds containing oxygen. Dichloromethane has high extraction efficiency for a wide range of non-polar to polar compounds. Solvent extraction is a popular technique for

- Non - semi volatile organic compounds.
- Partitioning the sample between two immiscible phases
- Aqueous phase: Sample matrix
- Organic phase: Organic solvent Like dissolves like



1.14.3. Selection of the Solvent

The solvent used for extraction needs to conform to the following criteria.

- High selectivity for the desired compound
- High capacity
- Miscibility with the primary solvent should be low
- After extraction, the two phases have to be well-separated. The solvent has to be removed from the extracted phase readily to produce solvent-free active agents.
- Low price
- Low toxicity
- To prevent loss by evaporation, a solvent with low vapour pressure at the operating temperature is required
- A low viscosity solvent leads to low pressure drop and good heat and mass transfer.
- It should be chemically and thermally stable

1.14.4. Distribution Coefficient (K_D)

The ratio of the amounts of solute dissolved in two immiscible liquids at equilibrium is given as

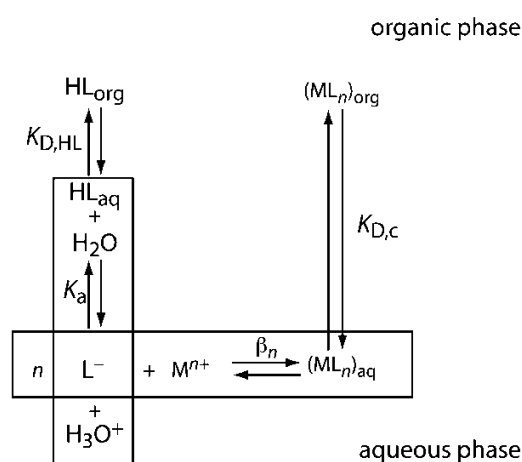
$$K_D = [S]_o / [S]_a$$

where K_D is the distribution coefficient. Large values of K_D would result in the quantitative distribution of the solute in organic solvent.

1.14.5. Liquid–Liquid Extraction of a Metal–Ligand Complex

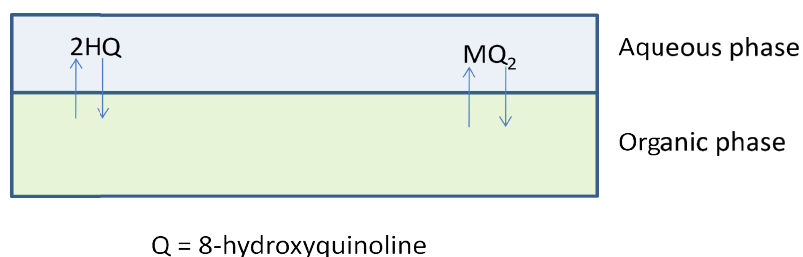
One important application of liquid–liquid extractions is the selective extraction of metal ions using a ligand. Many ligands are not very soluble in water or undergo

hydrolysis or oxidation in aqueous solutions. For these reasons the ligand is added to the organic solvent instead of the aqueous phase. The following Figure shows the relevant equilibria (and equilibrium constants) for the extraction of M^{n+} by the ligand HL including the ligand's extraction into the aqueous phase ($K_{D,HL}$), the ligand's acid dissociation reaction (K_a), formation of the metal–ligand complex (β_n), and the complex's extraction into the organic phase ($K_{D,c}$).



1.14.6. Extraction of inorganic species

Organic chelating agents react with metal ions to form uncharged complexes that are highly soluble in organic solvents.



Overall equilibrium



$$K' = \frac{[\text{MQ}_2]_{\text{org}} [\text{H}^+]_{\text{aq}}^2}{[\text{HQ}]_{\text{org}}^2 [\text{M}^{2+}]_{\text{aq}}}$$

$[\text{HQ}]_{\text{org}}$ is present in large excess with respect to $[\text{M}^{2+}]_{\text{aq}}$

$$K'[\text{HQ}]_{\text{org}}^2 = K = \frac{[\text{MQ}_2]_{\text{org}} [\text{H}^+]_{\text{aq}}^2}{[\text{M}^{2+}]_{\text{aq}}}$$

$$\frac{[\text{MQ}_2]_{\text{org}}}{[\text{M}^{2+}]_{\text{aq}}} = \frac{K}{[\text{H}^+]_{\text{aq}}^2}$$

1.14.7. Extraction Procedures

Shaking: Establish equilibrium concentration of solute between the two immiscible solvents

Venting: Release pressure build-up.

Separating layers: Always remove bottom layer through the bottom

Allow time to separate

Drain some, repeat to get all of the solvent

Drying: Remove traces of water from organic solvent

Remove solvent

Isolate extracted compound.

1.14.8. Batch Extraction Process

The most important application of the distribution law is in the process of extraction, in the laboratory as well as in industry. In the laboratory, it is frequently used for the removal of a dissolved substance from aqueous solution with solvents such as benzene, ether, chloroform, carbon tetrachloride etc. Here, advantage is taken of the fact that the distribution ratio of most of the organic compounds is largely in favour of organic

solvents. It is evident that the process of extraction is more efficient if it is carried out in parts. It is possible to derive a general formula which enables the calculation of the amount that is left unextracted after a given number of operations. Let V mL of a solution containing W gram of a solute be repeatedly extracted with v mL of another solvent which is immiscible with the first. Let w_1 be the weight of the solute that remains unextracted at the end of the first operation. Then, the distribution coefficient K will be given by

$$\frac{w_1/V}{W-w_1/V} = K \quad \text{or} \quad w_1 = W \frac{KV}{KV+v}$$

Similarly, at the end of the second extraction, the amount w_2 that remains unextracted is given by

$$\begin{aligned} w_2 &= w_1 \frac{KV}{KV+v} \\ &= w \left(\frac{KV}{KV+v} \right)^2 \end{aligned}$$

In general, the amount that remains unextracted at the end of n operations, w_n , will be given by

$$w_n = w \left(\frac{KV}{KV+v} \right)^n$$

1.15. Mixing with the Polymer

Sealed radiation sources can be fabricated by extraction of the desired radioisotope into the organic solvent (most commonly chloroform), followed by mixing with a polymer solution and subsequent formation of a thin radioactive polymer. The most commonly employed polymer for the source preparations is polymethyl methacrylate (PMMA). PMMA is a polymer of the esters of methacrylic acids. Poly

(methyl methacrylate) or poly (methyl 2-methyl propionate) is the polymer of methyl methacrylate with chemical formula $(C_5H_8O_2)_n$. It is a clear, colourless polymer available in both pellet and sheet form under the names Plexiglas, Acrylite, Perspex, Plazcyl, Acrylplast, Altuglas, Lucite etc. It is commonly called acrylic glass or simply acrylic. Another polymer, poly(methyl acrylate) (PMA) is a rubbery material, similar to poly(methyl methacrylate), but softer than PMMA, because its long polymer chains are thinner and smoother and can more easily slide past each other.

1.15.1. Choice of Polymer

Choice of a polymeric compound for making a composite film depends on the ability to peel-off the source from the base (with which it remains in close contact) with ease and is the key step for successful realization of this approach for the fabrication of radioactive sources. However, in order to achieve this objective, selection of a suitable polymeric compound is required. A number of polymers such as poly (vinyl acetate), PMMA and polystyrene were evaluated for the preparation of composite films and their de-lamination characteristics were tested. The results obtained are depicted in Table-1.3. The delamination characteristics of PMMA and polystyrene polymers were nearly identical and hence both can be used for preparation of ^{90}Sr source. However, PMMA was chosen for the preparation of radioactive sources as the radioactive film because it has soft and flexible nature and can be easily cut in to require dimensions.

Table-1.3: De-lamination characteristics of polymers

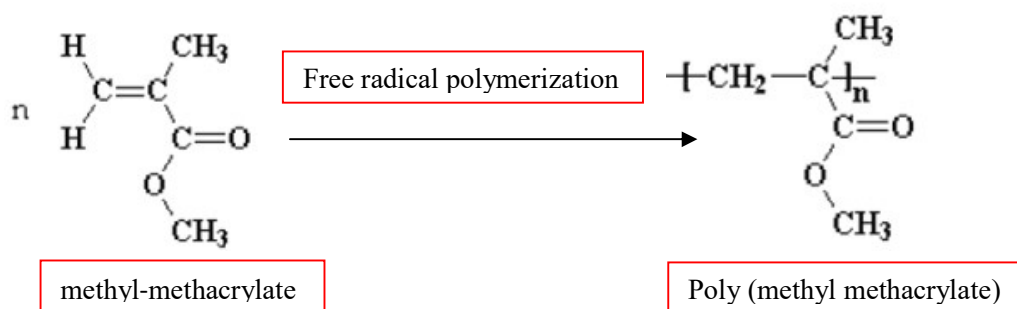
| Polymer used for making radioactive film | Characteristics |
|--|--|
| Polyvinyl acetate (PVA) | Strongly attached to the substrate surface and therefore difficult to peel-off. During peeling, the film teared. |
| Polymethyl methacrylate (PMMA) | Forms poor coating on the substrate surface and can be peeled-off easily (spontaneously comes out on drying under IR lamp) |
| Polystyrene | Forms poor coating on the substrate surface and can be peeled off (spontaneously comes out on drying under IR lamp). |

1.15.2. Properties of PMMA

PMMA is a linear thermoplastic polymer. PMMA lacks methyl groups on the backbone carbon chain and its long polymer chains are thinner and smoother and can slide past each other more easily, so the material becomes softer.

Table -1.4: Typical physical properties of Polymethyl methacrylate

| Physical Properties | Value |
|------------------------------------|-----------------------------|
| Density | 1.15-1.19 g/cm ³ |
| Water Absorption | 0.3-2 % |
| Moisture Absorption at Equilibrium | 0.3-0.33 % |



1.16. Quality Control

1.16.1. Evaluation of Performance of Sealed Radiation Sources

The quality of the sealed radiation sources needs to be evaluated as per the sealed sources classification performance tests stipulated by Atomic Energy Regulatory Board (AERB) Safety Standard. Due to the low radioactivity content in the Laboratory Reference Sources (< 1MBq), they are exempt from the sealed sources classification performance tests. However, they undergo the tests for leakage and surface contamination as per AERB regulations [33]. Other sealed radiation sources with activity levels greater than 1 MBq undergo the sealed sources classification performance tests as detailed in the AERB Safety Standard. The type of tests carried out on a sealed radiation source depends upon the type of intended application and the level of activity used as given in the table-1.5 and table-1.6. Special sources (activity exceeding 1 MBq) undergo the following tests depending upon their use.

1.16.2. Wipe Test "A"

The source is wiped with a swab moistened with water and the swab is counted on a GM counter. The swab counts must not exceed: 185 Bq (5 nCi).

1.16.3. Test for Leachability of Radioactivity

Towards determination of the extent of leaching of radioactivity from the source, the individual source is placed in a glass beaker containing 100 mL of distilled water at

normal temperature and atmospheric pressure for 48 hours. Subsequently, the source is removed from the beaker and the water is concentrated to 100 μ L. The concentrated sample is counted on a suitable counter (NaI (TI) counter or GM counter).

Table-1.5: Classification of sealed source performance tests

| Test | Class | | | | | | |
|-------------------|---------|---|---|---|---|---|--------------|
| | 1 | 2 | 3 | 4 | 5 | 6 | X |
| Temperature | No Test | -40°C (20 min.) +80°C (1h) | -40°C (20 min.) +180°C (1h) | -40°C (20 min.) +400°C (1h) and thermal shock 400°C to 20°C | -40°C (20 min.) +600°C (1h) and thermal shock 600°C to 20°C | -40°C (20 min.) +800°C (1h) and thermal shock 800°C to 20°C | Special test |
| External Pressure | No Test | 25 kpa absolute to atmospheric | 25 kpa absolute to 2Mpa Absolute | 25 kpa absolute to 7Mpa absolute | 25 kpa absolute to 70Mpa absolute | 25 kpa absolute to 170Mpa Absolute | Special test |
| Impact | No Test | 50g from 1m | 200g from 1m | 2kg from 1m | 5kg from 1m | 20kg from 1m | Special test |
| Vibration | No Test | 3 times 10 min 25 to 500 Hz at 49 m/s^2 (5g)* | 3 times 10 min 25 to 500 Hz at 0.635mm amplitude peak-to-peak and 90 to 500 Hz at 98 m/s^2 (10g)* | 3 times 30 min 25 to 80 Hz at 1.5mm amplitude peak-to-peak and 80 to 2000 Hz at 196 m/s^2 (20 g)* | | | Special test |
| Puncture | No Test | 1 gram from 1m | 10 gram from 1m | 50 gram from 1m | 300 gram from 1m | 1kg gram from 1m | Special test |

Table-1.6: Performance requirements for sealed radiation sources

| Sealed source usage | | Sealed source test and class | | | | |
|---|--|------------------------------|----------|--------|-----------|----------|
| | | Temperature | Pressure | Impact | Vibration | Puncture |
| Radiography Industrial | Unprotected source | 4 | 3 | 5 | 1 | 5 |
| | Source in device | 4 | 3 | 3 | 1 | 3 |
| Medical | Radiography | 3 | 2 | 3 | 1 | 2 |
| | Gamma teletherapy | 5 | 3 | 5 | 2 | 4 |
| | Interstitial and Intracavitary appliances ¹ | 5 | 3 | 2 | 1 | 1 |
| | Surface applicators | 4 | 3 | 3 | 1 | 2 |
| Gamma gauge (medium and high energy) | Unprotected source | 4 | 3 | 3 | 3 | 3 |
| | Source in device | 4 | 3 | 2 | 3 | 2 |
| Beta gauges and sources for low energy gamma gauges or for X-ray fluorescence analysis (excluding gas filled sources) | | 3 | 3 | 2 | 2 | 2 |
| Oil well logging | | 5 | 6 | 5 | 2 | 2 |
| Portable moisture and density gauge (including dolly transported) | | 4 | 3 | 3 | 3 | 3 |
| General neutron source application (excluding reactor start-up) | | 4 | 3 | 3 | 2 | 3 |
| Calibration sources Activity greater than 1 MBq | | 2 | 2 | 2 | 1 | 2 |
| Gamma Irradiation sources | Unprotected | 4 | 3 | 4 | 2 | 4 |
| | Source in device | 4 | 3 | 3 | 2 | 3 |
| Ion generators ² | Chromatography | 3 | 2 | 2 | 1 | 1 |
| | Static eliminators | 2 | 2 | 2 | 2 | 2 |
| | Smoke detectors | 3 | 2 | 2 | 2 | 2 |

1.16.4. Measurement of Radioactivity

Radioactivity of both unsealed and sealed radioactive sources is measured using different radiation measurement equipments depending upon the radioactivity strength and the nature of radiations emitted. The activity contained in the source is expressed in kilo Becquerel (μCi), Mega Becquerel (MBq) or disintegrations per minute (dpm). The

sources are assayed using pre-calibrated Ionization Chambers, Gieger Muller counters, NaI (Tl) scintillation counters and liquid scintillation counters (LSC).

1.16.5. Activity Tolerance

After fabrication, the activity content of the source is stated with a maximum value and the associated standard deviation at the date/time of source preparation.

1.16.6. Accuracy & Uncertainty in Measurement

After fabrication, the sealed radiation sources are counted in an appropriate counter (NaI (Tl) for gamma emitting radionuclides and GM counter for beta emitters) and compared with the standards maintaining the similar conditions of source holder configurations, covering material, distance between the detectors and the sources, etc. The radioactivity of the sources thus quoted are normally within overall uncertainties of $\pm 10\%$.

1.17. Performance Investigation of Custom-made Radiation Sources

- Measure the thickness of the deposited film using a thickness gauging instrument
- X-ray diffraction on deposited sample to check the crystallinity
- Using Scanning Electron Microscopy (SEM) to Evaluation of the surface, cross-section, and microstructure of the deposited film using SEM analysis

1.18. Scope of the Present Thesis

The work described in this thesis pertains to the development of methodologies for the preparation of custom-made radiation sources for industrial, space and medical applications, adopting the approaches described in this chapter. The development of each of these radioactive reference sources is described as separate chapters in this thesis (Chapters 2-5) each of which includes the aim of the work, details of the source preparation and characterization techniques as well as the results obtained.

CHAPTER-2

Preparation of ^{55}Fe , ^{57}Co and ^{204}Tl Sources for Multifarious Applications Using Electrodeposition Technique

“Progress is made by trial and failure; the failures are generally a hundred times more numerous than the successes, yet they are usually left unchronicled.”

-William Ramsay

Scope and Objectives of the Present Work

This chapter describes in detail the preparation of electrodeposited ^{55}Fe , ^{57}Co and ^{204}Tl sources for the calibration of X-Ray detectors, performance evaluation of nuclear imaging instruments and calibration of beta surface contamination monitors respectively. Preparation of the ^{55}Fe source based on the selective electrodeposition of ^{55}Fe from an electrolyte solution containing ^{55}Fe by controlled application of electrode potential on a Cu rod of specific dimensions in the form of a point source forms the first Section of chapter-2. In the second section of the chapter, preparation of a ^{57}Co source using electrodeposition technique is described. The third and the last section of the chapter describe in detail the preparation and evaluation of a ^{204}Tl electrodeposited source. In this chapter, the scientific basis of the work, experimental details, process validation and the results obtained during the preparation of the sources using the electrodeposition technique are discussed.

2.1. Use of Electrochemical Technique To Prepare ^{55}Fe Sources for Calibration of X-Ray Detectors

2.1.1. Introduction

Characterization and measurement of X-rays emitted from astrophysical X-ray sources (astronomical objects with physical properties which result in the emission of X-rays) requires the use of well calibrated X-ray detectors. In order to calibrate the X-ray detectors for such applications, an external radioactive source having adequately long shelf life capable of providing a steady X-ray output is required. Iron-55 (^{55}Fe), a low-energy X-ray emitter [5.9 keV (Mn $K\alpha$) and 6.5 keV (Mn $K\beta$)] having a half-life of 2.75 y [34] is one such radioisotope which is well-suited for the calibration of low energy X-ray detectors in the energy range of 2 to 10 keV. An important feature of the decay of ^{55}Fe is

the absence of continuum or bremsstrahlung X-rays. From the perspective of radiation safety and protection also, ^{55}Fe is a convenient radioisotope to handle as it emits only low energy X-rays. For a ^{55}Fe source to be qualified as an X-ray source for use in X-ray detectors, the required ^{55}Fe activity is required to be deposited in a very small circular cross sectional flat surface area ($\sim 0.07 \text{ cm}^2$) of the tip of a long cylindrical copper rod of overall dimension $3 \text{ mm } (\varnothing) \times 4 \text{ mm } (l)$. In recent years, a number of methods such as electrospraying, freeze drying, polymer formation etc. for preparation of radioactive sources have been reported [35–44]. Although, the electrospraying method is reported for the preparation of alpha sources up to 1 mg/cm^2 thickness [36], this method is more common for the fabrication of non-radioactive samples such as polymer micro-particles. The principle of electrospraying is based on the ability of an electric field to deform the interface of a liquid drop. Although electrospraying is a promising technique, the number of parameters which need to be optimized can render development highly complex. Electrospraying technique requires high voltage whereas simple electro-deposition method (used in our studies) requires low voltage which is safe to handle. Moreover, electro-deposition method for radioactive sample preparation is simple, fast & reproducible without the possibility of spreading contamination. An important advantage of electro-deposition is that radioactive sources can be custom-made in any source design such as flat, curved, annular surfaces etc., while it may not be possible in case of electrospraying method for which substrate with a flat surface may be preferred. Electro-deposition is particularly suitable for the preparation of ^{55}Fe containing sources since it is technically simple and is reproducible. Although there are literature reports on the electrochemical deposition of iron from aqueous solutions on metallic substrate, [45–49] as well as the preparation of Mossbauer sources in which ^{57}Fe is diffused throughout the

metallic substrate to obtain a uniform distribution of radioactive iron [50–52], deposition of micromolar quantities of radioactive iron on a metallic substrate has not been reported to the best of our knowledge. Some investigators have carried out cathodic deposition of ^{55}Fe from an aqueous solution [53–61] essentially for its pre-concentration and measurement of radioactivity. However, to our knowledge, detailed technical information about the ^{55}Fe source preparation process and their characterization are limited. Hence, in order to prepare ^{55}Fe sources for calibration of X-ray detectors, detailed studies were carried out to determine the electrodeposition behavior ^{55}Fe at micro molar levels in aqueous solution. For the intended application here, the required activity of ^{55}Fe needs to be deposited selectively on the outer surface area of the Cu substrate with negligible leaching of activity from the substrate. No carrier added ^{55}Fe solution is required for the preparation of the source as the required ^{55}Fe activity has to be deposited in a very small cross sectional area at the tip of a cylindrical copper rod. Selection of a suitable electro-bath is of utmost importance for deposition of ^{55}Fe at trace concentrations. Sulphate electro-bath is a good choice as it can be used at room temperatures at low current density. As the feed concentration is very low, it is extremely difficult for Fe to be cathodically deposited on the substrate as trace metal impurities may interfere in the electrodeposition process, reducing the current efficiency by many orders of magnitude. The resulting high cathodic over-potentials hinder the Fe deposition process. Hence, taking these factors into consideration, only the deposition efficiency of ^{55}Fe was considered and not current efficiency. Various factors that influence the electrodeposition of ^{55}Fe in the sulphate bath were identified and a careful optimization of these factors was carried out in order to ensure optimum deposition of ^{55}Fe activity on the target area of the Cu substrate. In this chapter, details of the laboratory-scale electrodeposition method for

the preparation of ^{55}Fe sources by electrodeposition of ^{55}Fe on a precisely defined area of a metallic substrate covering the radioactive area with a thin layer of organic polymer and quality assurance of this source to meet regulatory requirement, are reported.

2.1.2. Materials

Iron-55 as $^{55}\text{FeCl}_3$ of specific activity $\sim 100 \text{ MBq.mg}^{-1}$ of Fe and radionuclidic purity $> 99\%$ was procured from M/s Polatom, Poland. Reagents such as sulphuric acid, and ammonium hydroxide were of spectroscopic grade and procured from M/s. Sigma, USA. HPLC grade water was purchased from Merck, India. Methyl methacrylate polymer (PMMA) was of analytical grade and was procured from BDH (India). Copper rod and platinum metal foil of high purity (99.99% purity) were procured from M/s. Hindustan Platinum Ltd, Mumbai, India. Deposition and stripping experiments were carried out using “Eco chemie” potentiostat, AUTOLAB-100 run by GPES software using three electrode geometry. A DC power supply with 100 V compliance, a maximum current of 2 A, 1.2 nA current resolution and $> 10^{13}$ Ohms input impedance was used for preparation of ^{55}Fe source. The XRD patterns were recorded on a Philips X-ray diffractometer (Model PW 1710) with Ni-filtered Cu K_α radiation using silicon as an external standard. The XRD patterns were analyzed by comparing with the reported ones. The microstructural features of the anodized samples were analyzed using a Scanning Electron Microscope (SERON, Model AIS-2100). Energy Dispersive X-ray microanalysis technique (Oxford, Model INCA E350) was used to identify the elemental constituents of the sample. Radiation dose rate meter (Teletector 6112M) from M/s Automess, Ladenberg, Germany was used to measure the radiation dose on the surface of the source. A liquid scintillation counter (425-034) from Triathler, Turku, Finland was used for the radioactivity measurement. Liquid scintillation cocktail (w scintillation grade) from M/s. Sisco

Research Lab. Pvt. Ltd., Mumbai, India suitable for measuring low to medium ionic strength aqueous samples was used. AGFA film grade-G-7 was used for autoradiography. Optical density measurements were carried out using an OPTEL Transmission densitometer (B/W transmission densitometer).

2.1.3. Experimental

2.1.3.1. Preparation of the Electrodes

Annealed cylindrical copper rod of dimensions 3 mm (\varnothing) \times 4 mm (l) was used as cathode. Prior to electrodeposition, the targeted circular tip area of the Cu rod was manually polished with emery paper and washed successively with acetone and deionized water. The cathode surface where ^{55}Fe is not intended to be deposited was coated with a polymeric film, leaving the circular cross sectional area free for ^{55}Fe deposition. A Platinum plate of the same surface area was used as anode.

2.1.3.2. Preparation of Electrolyte

The required activity of ^{55}Fe ($\sim 185\text{MBq}$) as $^{55}\text{FeCl}_3$ was pipetted out into a 50 mL capacity quartz beaker to which 1 mL of concentrated nitric acid was added and then slowly evaporated to dryness in a heating mantle. Addition of nitric acid was necessary to destroy the chloride ions which can corrode the platinum electrode. The resulting solution was made up to 1 mL with concentrated sulphuric acid. Subsequently, 1 mL of concentrated hydroxyl amine solution (NH_2OH) was added and evaporated to dryness. Addition of NH_2OH , a reducing agent, was necessary to prevent oxidation of Fe^{2+} to Fe^{3+} . Subsequently, 3 mL of 30% w/vol boric acid in 0.01 N H_2SO_4 solution was added and the solution was transferred into the electrodeposition cell. The final volume of the ^{55}Fe electrolyte bath was adjusted to 10 mL by further addition of the boric acid solution. The

final pH of the solution was adjusted to 2-2.5 by the addition of 0.1 M ammonium hydroxide solution.

2.1.3.3. Electrochemical Set-up

The electrochemical reaction was carried out in a 50 mL capacity Pyrex glass beaker immersed in a temperature controlled water bath. The electrodes were adjusted parallel to each other and fitted 10 mm apart on the acrylic cap. The electrodes were connected to the power supply using small screws, embedded into the acrylic cap. A provision was made for passing Ar gas (at the rate of 0.05 cc.s^{-1}) through a glass tube ($\varnothing = 1 \text{ mm}$) into the electrolyte and a small outlet of $\sim 2.5 \text{ mm}$ (\varnothing) was provided through acrylic cap for venting the gases liberated during electrolysis. Direct current was obtained from a DC power supply for electrolysis and the potential across the electrode was maintained at 1.5 V. Schematic diagram of the electrochemical set up is depicted in Fig. 2.1.

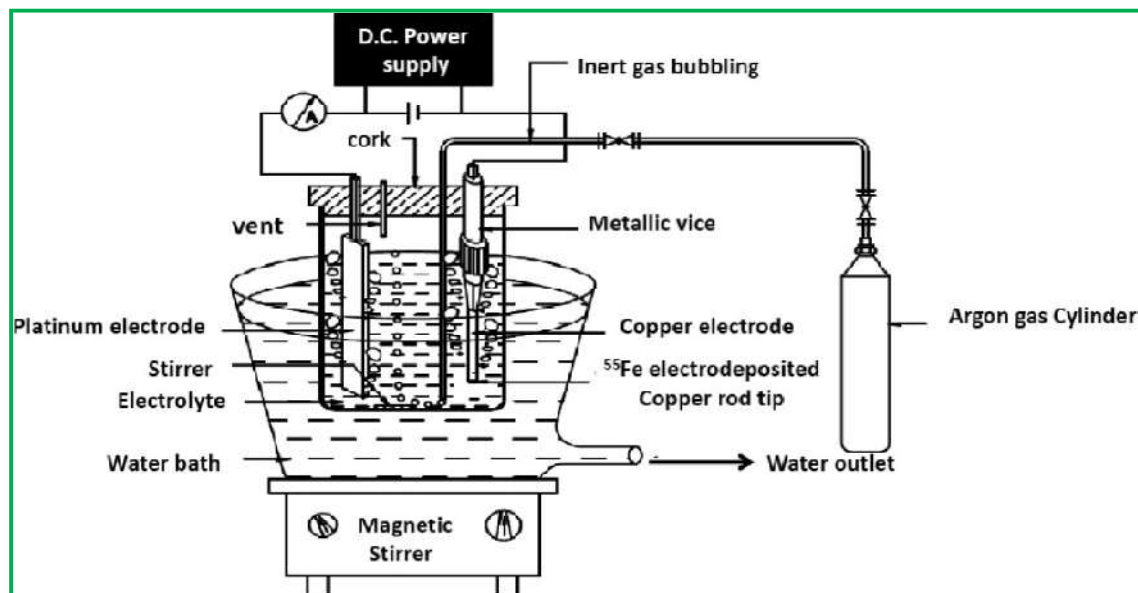


Fig. 2.1: Electrodeposition set-up of ^{55}Fe .

2.1.3.4. Cyclic Voltammetry and Amperometry

Cyclic voltammetric experiments were carried out using three electrodes wherein copper rod was used as the working electrode, platinum rod as the counter electrode and saturated calomel Electrode (SCE) as the reference electrodes. All potentials in this study were applied, measured and reported with respect to the SCE reference electrode. All experiments were performed at room temperature. The amperometric deposition experiments were also carried out at the optimized current density. At the current density of 1 mA.cm^{-2} the deposition potential was stabilized at around -1.4 V . With increase in the current density from 10 to 100 mA.cm^{-2} the deposition potential increase drastically. At a higher cathodic potential hydrogen evolution process would predominate. In order to investigate the electrochemical quality of the deposits, their dissolution pattern was studied. Stability of the Fe film on Cu substrate decreased with increase in current density during deposition.

2.1.3.5. Optimization of the Electrodeposition Parameters

Several experiments were carried out for the optimization of the electrodeposition parameters to obtain the best possible deposition yield of ^{55}Fe . Electrodeposition experiments were carried out by varying experimental parameters such as current density ($5\text{-}100 \text{ mA.cm}^{-2}$), pH of the electrolyte (1-5), temperature of the electrolyte bath ($5\text{-}50^\circ\text{C}$) and time of deposition (0.5-4 h). The amount of ^{55}Fe deposited was estimated in terms of the difference in activity of the solution before and after electrodeposition, as measured by liquid scintillation counting (LSC) [62].

2.1.3.6. Characterization by X-ray, SEM and EDS Analysis

X-ray diffraction and SEM analysis were carried out using a non-radioactive source prepared in an identical manner as the one used for source fabrication, using Fe.

The electrodeposited Fe samples were subjected to SEM examination for surface morphology. Assessment of the presence of iron along the surface of the substrate was achieved from the Energy Dispersive X-ray Spectra (EDS) of the deposited Fe layer.

2.1.3.7. Preparation of ^{55}Fe Sources

Based on the results of the optimization experiments, electrodeposition of ^{55}Fe was carried out at a current density of 20 mA.cm^{-2} for 4 h at 18°C . After electrodeposition, the samples were rinsed in doubled distilled water and were dried under an Infra Red (IR) lamp.

2.1.3.8. Coating of the ^{55}Fe Sources with PMMA Polymer

The sources ^{55}Fe were coated with PMMA polymer to prevent spread of any contamination and safe handling. The active area of the sources was coated with PMMA polymer by the dip-pull method. The ^{55}Fe deposited end of the Cu rod was immersed into a solution of PMMA in chloroform (50 mg.mL^{-1}), stirred using a magnetic stirrer for 3 minutes and taken out. The polymer coated samples were placed onto a perforated tray where the excess of the uncoated PMMA reagent drained out and air-dried.

2.1.3.9. Measurement of Activity of the Source

The amount of ^{55}Fe deposited on the copper substrate was measured by liquid scintillation counting (LSC) as described elsewhere [62]. In liquid scintillation counting (LSC), a small aliquot of the solution containing the radioisotope (beta, alpha, low energy X rays) is mixed with the scintillation cocktail. Scintillation cocktail primarily consists of a solvent such as 1,4-dioxane, xylene or toluene and a solute such as 2,5-diphenyl Oxazole (PPO) or 1,4 bis-[2-(5-phenyloxazolyl)-Benzene (POPOP) along with other optional materials such as solubilisers. The decay energy of the radioisotope will be transferred to the cocktail, the excited molecules can transfer energy to one another

and rise to a state of excitation. The excited molecules return to the ground state and light photons are emitted, the light photons are then passed on to the cathode of the photomultiplier tube, a number of primary electrons are produced which are multiplied to form an electrical pulse for further spectral analysis. In this work, activity measurement of low energy ^{55}Fe X-ray sources was carried out with LSC by drawing suitable aliquots of the feed solution containing ^{55}Fe before and after the electro-deposition. The samples were prepared by taking a known aliquot of the feed solution containing ^{55}Fe in 10 mL of the liquid scintillation cocktail (Aquasafe 300 Plus) in a 22 mL plastic scintillation vial which was then counted by LSC. The ^{55}Fe samples were counted in the settings of ^3H .

1.4. Quality Control of ^{55}Fe the Sources

2.1.4.1. Autoradiography

The ^{55}Fe source was subjected to autoradiography examination to assess the uniformity of activity deposition along the circular cross-sectional area. Owing to the small active area of the source, a special autoradiography gadget made of brass was used. The autoradiography gadget assembly, as shown in Fig. 2.2, consisted of a circular disc base [40 mm (l) \times 18 mm (\varnothing)], tubular source holder for positioning the radioactive source [39 mm (l) \times 8mm (\varnothing)], a threaded S.S. nut [6 mm (l) \times 14 mm (\varnothing)], and a metallic cap [14 mm (l) \times 8mm (\varnothing)] fitted at the top of the tubular source holder. In this method, radiation flux emanating from the ^{55}Fe source diverged to cover an increasingly larger circular area as the distance from the source increases. Towards the determination of uniformity of activity distribution, the ^{55}Fe source was first inserted smoothly through the top opening of tubular source holder, with the radioactive side facing downwards and was closed at the top by metallic cap to position it securely. The source holder was subsequently screwed into the brass disc base and its position was adjusted to the desired

distance using the metallic nut which was used for locking the distance position. Autoradiography was performed by keeping a strip of photographic film at the bottom of the disc. The optical density distribution of the exposed film was measured by B/W transmission densitometer, at various locations of the film.

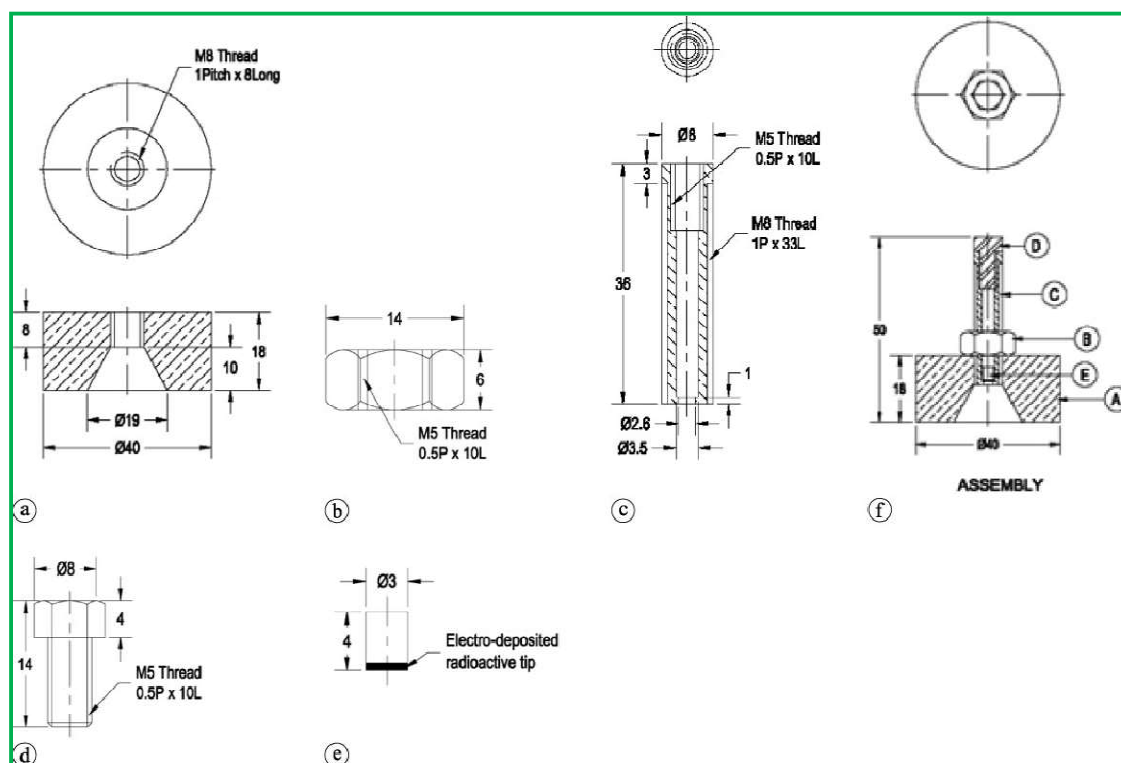


Fig. 2.2: Auto-radiography device (a) Circular disc base, (b) Nut attached to metallic cap, (c) Tubular source holder for positioning the radioactive source, (d) Metallic cap sited at the top of the tubular source holder, (e) ^{55}Fe electrodeposited source, (f) Assembled device

2.1.4.2. Determination of Surface Contamination

The ^{55}Fe sources prepared by the above method were tested for absence of loose activity (surface contamination) by swiping the surface of the source with a cotton wool immersed with alcohol using forceps. The radioactivity content on the cotton wool was estimated by counting in a pre-calibrated GM Counter.

2.1.4.3. Determination of Percentage Activity Leached Out

The amount of ^{55}Fe activity leaching out of the source was determined before and after organic coating as per the method prescribed by the Atomic Energy Regulatory Board, India [63]. In brief, five numbers of ^{55}Fe sources were randomly selected each of which was placed individually in a beaker containing 100 mL water at room temperature for 48 h, at the end of which the sources were removed. The radioactivity in the water was concentrated to 0.1 mL by heating which was counted in a liquid scintillation counter to estimate the ^{55}Fe content.

2.1.4.4. Immersion Test

One PMMA coated source was immersed in 20 mL of water in a glass beaker which was heated to 90-95°C for 4 h. The source was removed, the water was concentrated to 1 mL and the activity released was estimated in a LSC. Activity measuring up to 185 Bq/source in the water sample was considered to be the limit for acceptance [63].

2.1.4.5. Source Assembly

A cylindrical source holder of dimensions 7.1 mm (l) \times 6.55 mm (\varnothing) with a closed top end and an open flat end with screw thread finish made up of brass was designed to hold the ^{55}Fe source. The cap was rounded, open, screw closures made up of brass. The cylindrical cap was appropriately sized to fit in the open screw end of the cylindrical base. Schematic diagram of the source capsule is shown in Fig. 2.3.

The ^{55}Fe source was placed with the help of a tweezer to fit inside the base with the radioactive end facing down towards the open end, and the holder was subsequently closed by winding the screwed cap tightly in position. This design secures the source in the holder during application.

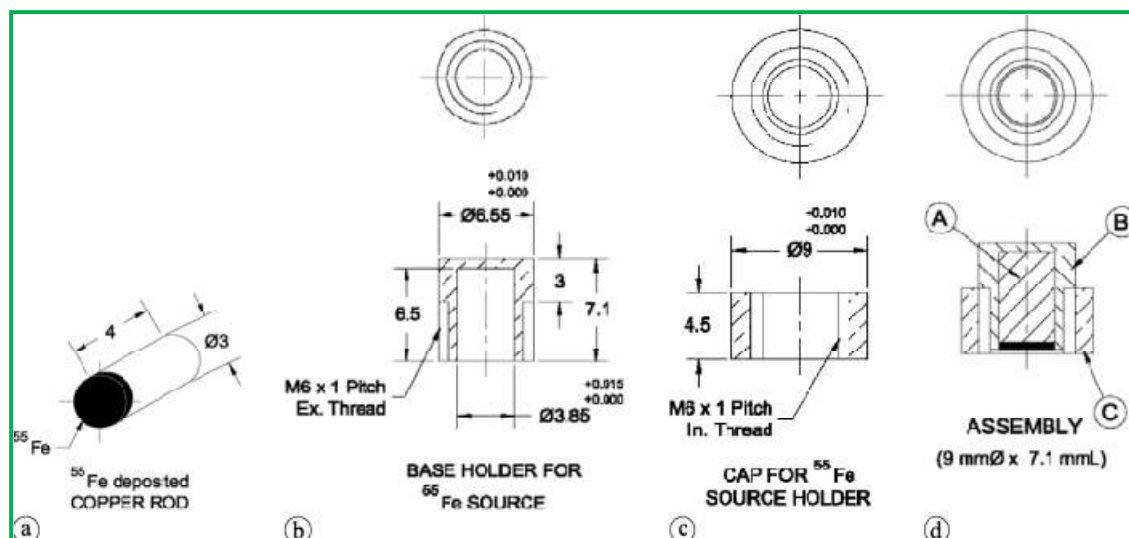


Fig. 2.3: Schematic diagram of the ^{55}Fe source assembly

2.1.5. Results and Discussion

The aim of this work was to optimize the electrochemical procedure to deposit ^{55}Fe activity onto a precisely selected region of a cylindrical copper substrate. In order to reduce the thickness of the deposited ^{55}Fe layer as well as to quantitatively deposit the ^{55}Fe activity in a small area, high specific activity (no carrier added) ^{55}Fe was used. Platinum was chosen as the anode as it is inert, stable and does not passivate easily. Copper was chosen as the basic matrix for source preparation owing to its attributes such as ready availability in high purity at a reasonable cost, radiation stability, adequate mechanical strength and suitable electrode potential for deposition of iron. Standard reduction potential of Fe^{2+} and copper are -0.44 V and $+0.34\text{ V}$, respectively. Use of copper as cathode will drive the hydrogen over potential higher, and would thus favor ^{55}Fe deposition. It could be ascertained that an acidic electrolyte solution was the best medium to achieve the electrodeposition of micro quantities of ^{55}Fe . In an alkaline solution, it is very difficult to electrodeposit Fe because of its precipitation in the hydroxide form. Sulphate electro-bath (Watts's bath) was chosen for this work based on

the literature reports on its use in the electrodeposition of nickel, and because of the similar properties of iron and nickel. The sulphate bath was also considered owing to its high solubility, solution stability, and non-toxic nature. Additionally, it does not evolve chlorine (as in the chloride bath) or dissolve glassware (as in the perfluoroborate system), and the radioactivity deposition is easier to control. Hydroxylamine was used as a reducing agent to reduce Fe (III) to Fe (II) prior to deposition and to avert the oxidation of Fe (II) during electrodeposition. In order to understand the deposition process and to determine the usable potential range for ^{55}Fe deposition, voltammetric studies were carried out.

2.1.5.1. Cyclic Voltammetric Studies

Cyclic voltammetric plots of the Fe (II)/Fe reduction process in 1 mM ferrous ammonium sulfate solution with varying scan rates are shown in Fig. 2.4. The scan rates studied were 0.05, 0.1, 0.2, 0.3, 0.4, 0.5 Vs^{-1} . There are two peaks (denoted as “peak 1” and “peak 2”) seen in the reduction cycle of the cyclic voltammetric scan. “Peak 1” (at -1.5V at 50mVs^{-1}) was found to be sharper in comparison to “peak 2” (at -1.63 V at 50 mVs^{-1}). Further, the peak current values of “peak 1” were plotted verses the square root of the scan rates and the corresponding plot is shown in the inset of Fig. 2.4. Peak current corresponding to “peak 1” was found to increase with increase in the scan rates. Increase in the peak current corresponding to “peak 2” was not prominently observed due to the change in the base line of the peak at higher scan rates. Scan-rate studies revealed that peak current was found to increase with increasing scan rate. A parabolic correlation of the peak current to the square root of the scan rates was observed. This is indicative of additional mass transfer process other than the diffusion controlled mass transfer. The nature of the reduction peak was indicative of the catalytic hydrogen evolution process

along with the reductive deposition of Fe from Fe (II). The fresh Fe metallic deposits acted as a catalyst for hydrogen evolution process. Thus, the reduction peak current increased sharply producing the catalytic peak at the “peak 1” position. The reduction of Fe (II)/Fe continued till the “peak 2” position although the catalytic effect ceases due to the poisoning effect hydrogen evolution of the deposits. On the Cu surface Fe was observed to be deposited at -1.3 V or more cathodic potentials.

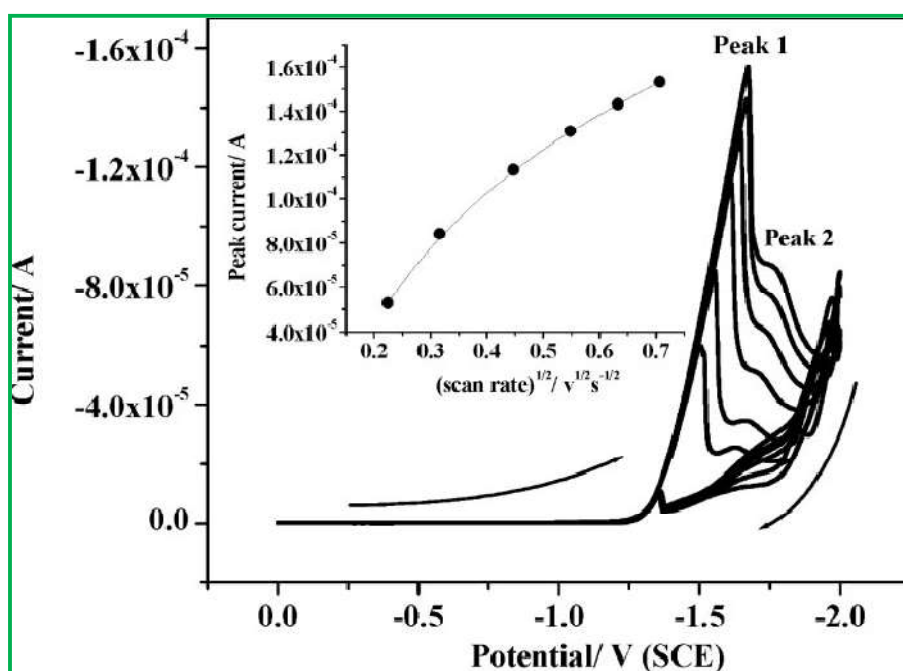


Fig. 2.4: Cyclic voltammetric plot

2.1.5.2. Amperometric Deposition Studies

The amperometric deposition results are shown in Fig. 2.5(a). At the current density of 1 mAcm^{-2} the deposition potential was stabilized at around -1.4 V. With increase in the current density from 10 to 100 mA.cm^{-2} the deposition potential increased drastically indicating unsustainability of the process at 1mM Fe (II) concentration. At a higher cathodic potential, hydrogen evolution process would predominate.

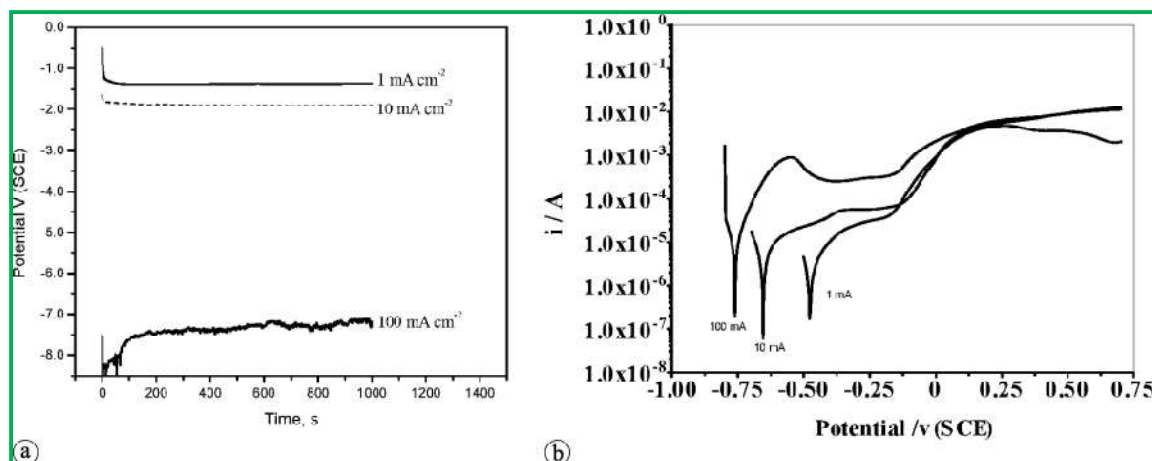


Fig. 2.5: Amperometric deposition and voltammetry stripping of Fe

(a) Amperometric deposition studies (b) Voltammetry stripping studies

2.1.5.3. Voltammetry Stripping Studies

In order to investigate the electrochemical quality of the deposits, their dissolution pattern was studied and the result is shown in Fig. 2.5(b). The dissolution pattern was indicative of iron deposits only. Stability of the Fe film on Cu substrate decreased with increase in current density during deposition.

2.1.5.4. Effect of Electrodeposition Parameters

The influence of pH on the electrodeposition of ^{55}Fe was examined and the result is shown in the Fig. 2.6(a). It was observed that the ^{55}Fe deposition increased with increasing the pH and reached a maximum of $\sim 95\%$ at pH 2, which then dropped gradually with further increase in pH. As Fe^{2+} tends to form hydroxide at alkaline pH, experiments were not conducted at alkaline pH range. The pH of the electrolytic bath was therefore maintained at 2 for further studies. The effect of current density on ^{55}Fe deposition for duration of 4 h at pH ~ 2 was studied and the result is shown in Fig. 2.6 (b). Percentage of ^{55}Fe deposition was found to increase initially with increase in current density up to $20 \text{ mA}\cdot\text{cm}^{-2}$ and decreased thereafter. About $\sim 96\%$ of ^{55}Fe deposition was

observed at 20 mA.cm^{-2} current density. Thus, an applied current of 20 mA.cm^{-2} resulted in optimum deposition of ^{55}Fe . Fig. 2.6(c) is the graphical representation of the influence of deposition time on the electrodeposition of ^{55}Fe at a constant current density of 20 mA.cm^{-2} at $\text{pH} \sim 2$ on the substrate. It is evident that within the range of deposition time investigated, the percentage of ^{55}Fe deposition increased with increasing deposition time and at least 4 h were required to obtain optimum deposition of activity on the substrate. The influence of bath temperature on the deposition of ^{55}Fe at a constant current density of 20 mA.cm^{-2} at $\text{pH} \sim 2$ in 4 h was studied and the results are depicted in Fig. 2.6(d). Initially, percentage deposition of ^{55}Fe was found to increase with increase in temperature up to 20°C and decreased thereafter with further increase in temperature. About 96% of ^{55}Fe deposition was observed when the temperature of the bath was maintained at 20°C . Hence, the bath temperature was maintained at 20°C for subsequent experiments. Thus, use of electro bath prepared at $\text{pH} 2$, maintained at 20°C and application of current density of 20 mA.cm^{-2} for 4 h resulted in optimum deposition of ^{55}Fe . These experimental conditions were therefore chosen for the preparation of the radioactive source subsequently.

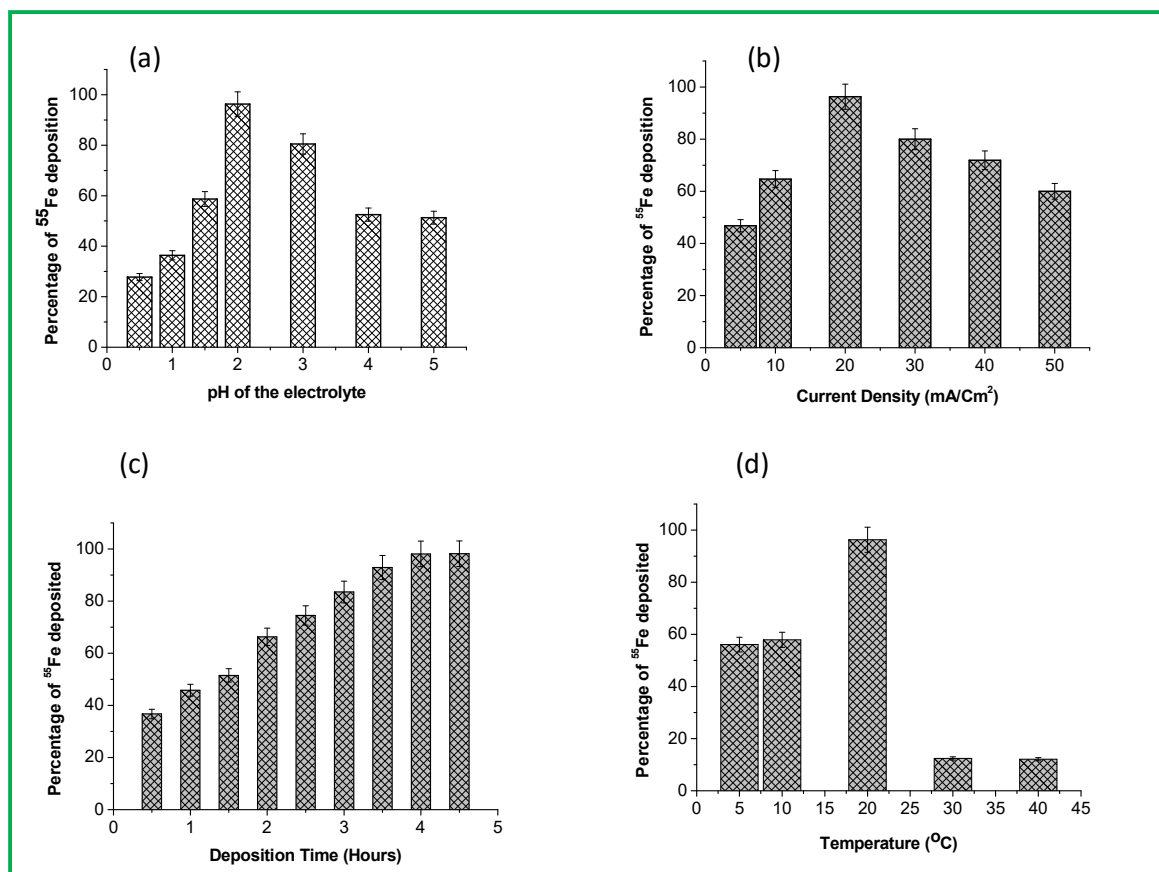


Fig. 2.6: Influence of experimental parameters on the electrodeposition of ^{55}Fe

(a) pH of the electrolyte (b) Current density (c) Electrodeposition time

(d) Bath temperature

2.1.5.5. Morphology Studies

(a) SEM Analysis

Scanning electron microscopy technique was used to study the surface morphology of the electrodeposited surface. Fig. 2.7 depicts the SEM image of the electrodeposited surface. It was seen that dense, smooth and homogeneous electrodeposited film was formed which covered the surface of the substrate without any visible cracks or holes. Electrodeposited particles were distributed regularly over the surface of the substrate in the form of a film.

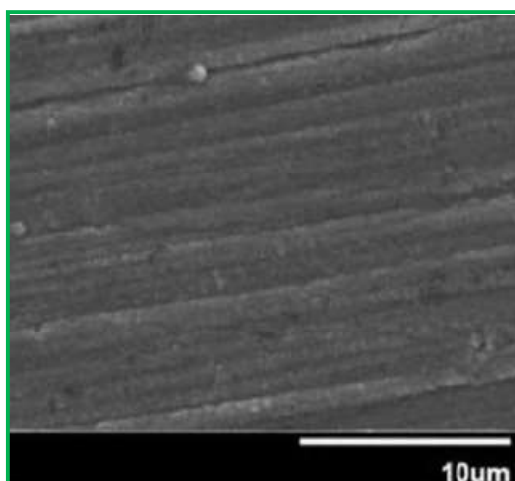
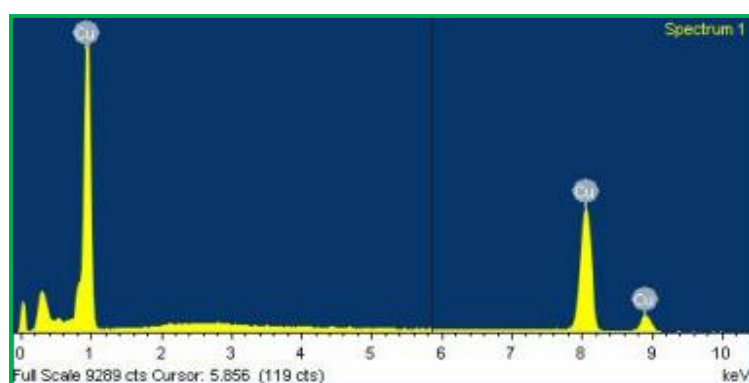


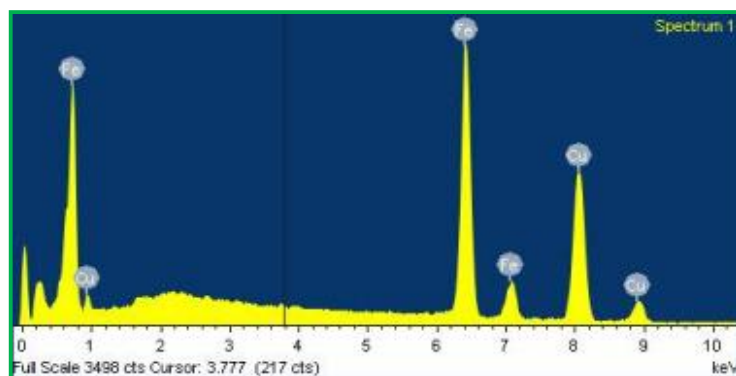
Fig. 2.7: SEM micrograph of the electrodeposited surface

(b) EDS Characterization

Fig. 2.8(a) depicts the typical EDS spectrum of the Cu substrate and Fig. 2.8(b) shows the Fe deposited on the Cu substrate. It was seen that the deposited layers contain only Fe. Element mappings of Fe were made by EDS analysis of the surface at different points of electrodeposited sample. The concentration of Fe as weight percentage derived from the intensity of spectra of Fig. 2.8(b) at different positions is shown in Table-2.1. It was observed that the variation in distribution of iron along the surface of the substrate is within $\pm 1.02\%$ from the mean.



(a)



(b)

Fig. 2.8: Energy dispersive X-ray (EDX) spectrum
(a) Cu substrate (b) Fe electrodeposited on Cu substrate

Table-2.1: Elemental mapping of Fe deposited on Cu substrate

| Position | Fe (weight %) |
|---------------|------------------|
| 1. | 46.52 |
| 2. | 46.68 |
| 3. | 47.13 |
| 4. | 49.03 |
| 5. | 47.81 |
| Mean \pm SD | 47.43 \pm 1.02 |

(c) X-ray Diffraction Analysis

Fig. 2.9 depicts the XRD pattern of the Cu substrate before and after electrodeposition of Fe. Fig. 2.9(a) shows all the peaks of copper metal when compared with the standard PCPDF data (Card no-04-0836). It was observed that the data showed peaks of Fe metal (card no-06-0696) for the sample deposited at room temperature. The deposited material was stripped from the base and the XRD of the stripped powdered sample was recorded which further confirmed the deposition of highly crystalline iron metal over the Cu substrate.

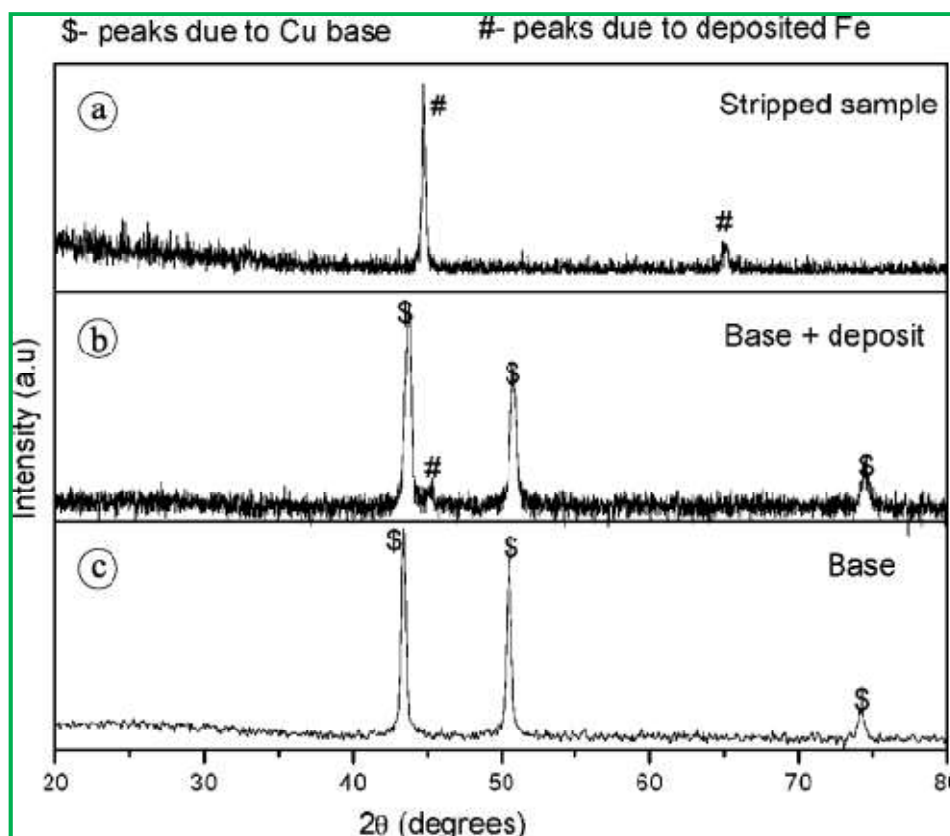


Fig. 2.9: X-ray diffraction pattern of substrate

(a) Copper substrate (b) Electrodeposited sample (c) Electrodeposited Fe stripped from the Cu base

2.1.5.6. Activity Measurement

Liquid scintillation counting (LSC) of the electrolyte was used to follow the progress of electrodeposition process. The measurement of ^{55}Fe activity of the final source by Gun Monitor was used for quoting the total amount of activity deposited on the substrate.

2.1.5.7. Quality Control

In order to comply with the regulatory requirements and to assure safe handling of sources during applications, ^{55}Fe sources were subjected to different quality control tests. Autoradiography was carried out for determining the distribution of ^{55}Fe . The optical density of the photographic film was taken as a measure of the local concentration of ^{55}Fe .

on the substrate. The image obtained was circular in shape without any visible breakage and deletion indicating that ^{55}Fe was well covered to the circular surface of the substrate. The Optical Density (OD) of the exposed radiographic film was measured at various locations and the OD values varied with a mean value of 4.76 ± 0.12 . It is important that the ^{55}Fe deposited is adherent and does not leach out. Table-2.2 shows the results of the leach tests conducted on 5 randomly selected sources before and after polymer coating.

Table-2.2: Leachability of ^{55}Fe source

| Sr. No | Activity of ^{55}Fe source MBq (mCi) | % Radioactivity leached out before PMMA coating | % Radioactivity leached out after PMMA coating |
|-----------------|---|---|--|
| 1 | 173.9 (4.7) | 0.7 | Below Detection Limit |
| 2 | 173.9 (4.7) | 0.7 | Below Detection Limit |
| 3 | 166.5 (4.5) | 0.7 | Below Detection Limit |
| 4 | 177.6 (4.8) | 0.69 | Below Detection Limit |
| 5 | 185.0 (5.0) | 0.7 | Below Detection Limit |
| Mean \pm S.D. | | 0.7 ± 0.01 | Below Detection Limit |

It is evident that 0.7 ± 0.01 % of the original activity leached out from the ^{55}Fe sources which were not coated with the polymer, which was about 70 times higher than the AERB stipulated limits for release of radioactivity from sealed radioactive sources (limit = 0.01%) [63]. Incorporation of a PMMA barrier layer on the ^{55}Fe deposited surface could result in preventing the leaching of radioactivity from the source. In order to have a thin and uniform coating of PMMA on the source, 50 mg of PMMA polymer per mL of chloroform was used. The polymer formed a continuous protective film on the surface of

the ^{55}Fe source. The dimensions of the substrate remained practically unchanged even after coating owing to the low concentration of polymeric solution. It is evident that after PMMA coating, the release of radioactivity from the source could be reduced to very low levels which complied with the specifications (0.01%) prescribed as per the regulatory agency [63]. The radioactivity deposited on the substrate was kept 10 % more than the required radioactivity based on the experimental results, in order to compensate for the attenuation of the low energy X rays by PMMA as well as by the aluminized Mylar film which is used for covering the source. The dip pull method employed here was able to form a very thin layer of organic coating on a small area. Swipe test and immersion test were performed on 5 numbers of randomly selected PMMA coated sources having 166.5MBq (~ 4.5 mCi) to 185 MBq (5 mCi) of activity. The results are depicted in Table 2.3. The result of immersion tests carried out on the sources revealed that they comply with the regulatory limits (185 Bq). The result of the swipe test showed that the counts in the swipe was below detectable limits [63]. Electrodeposits obtained in this process were adherent on account of the nature of the electro bath [64]. Although this method of LSC measurement [62] undoubtedly gives the fraction deposited in the course of electrolysis, it does not necessarily give the fraction remaining on the substrate owing to the dissolution of a metallic deposit after electrodeposition or loss of radioactivity during washing. Therefore, activity deposited on the substrate was estimated using a exposure rate meter. Several sources of strength in the range of 166.5 – 185 MBq (4.5–5.0 mCi) were prepared by above method, extensively tested and mounted in a brass holder for proper positioning in the detector during application. The source strengths were adequate to calibrate the X-ray detectors. The important features of the ^{55}Fe source for the intended application are (a) quantifiable activity should adhere to the substrate and sheathed with a protective film

(b) radioactive deposit should be stable and resist loss of the radioactivity during normal use and handling (c) emerging X-ray flux density from the source should be adequate for satisfactory performance of the instrument and (d) the source should comply with the regulatory norms. The ^{55}Fe Sources prepared by the optimized electrodeposition method were supplied to users for calibration of low energy X-ray detectors. The performances and stability of these sources were evaluated by the users and were found to be satisfactory for the intended application.

Table-2.3: Quality control of ^{55}Fe source

| S. No. | Source activity MBq (mCi) | Leachability | Immersion test Bq (nCi) | Surface contamination Bq (nCi) |
|---------------|------------------------------|-----------------------|----------------------------|--------------------------------------|
| 1. | 173.9(4.7) | Below detection limit | 104.0(2.8) | 79(2.1) |
| 2. | 173.9(4.7) | Below detection limit | 106.5(2.9) | 77(2.1) |
| 3. | 166.5(4.5) | Below detection limit | 107.1(2.9) | 75(2.0) |
| 4. | 177.6(4.8) | Below detection limit | 105.5(2.8) | 76(2.1) |
| 5. | 185.0(5.0) | Below detection limit | 106.0(2.9) | 78(2.1) |
| Mean± S.D. | | Below detection Limit | 105.82±1.2 | 77.0±1.6 |

2.1.6. Conclusion

A one-step electrochemical method to deposit ^{55}Fe on a Cu matrix from an aqueous acidic sulphate bath could be optimized. The electrolysis parameters for optimum ^{55}Fe deposition were judiciously optimized. The optimized method resulted in the formation of a very thin, uniform deposit of ^{55}Fe with good adherence to the copper surface. The ^{55}Fe sources prepared by this method were stable, intact and complied with the standard safety requirements for radioactive sources laid down by the Atomic Energy Regulatory Board, India. Although the present approach has been used for the preparation of ^{55}Fe source, it is anticipated that this strategy will find potential applications in the preparation of solid sources of many other radioisotopes.

2.2 Preparation of ^{57}Co Point Sources for the Performance Evaluation of Nuclear Imaging Instruments

2.2.1 Introduction

The role of Single Photon Emission Computed Tomography (SPECT) in diagnostic nuclear medicine imaging needs hardly to be reiterated. It has been at the forefront of diagnostic nuclear medicine imaging for several decades. A wide variety of diagnostic nuclear medicine imaging instruments are being used to acquire images and extract quantitative information. Before the instrument is put into routine use, verification of its performance in terms of sensitivity, constancy and accuracy is important to ensure that the performance of a procedure or instrument within an acceptable range. Technetium-99m is the most commonly utilized radionuclide for SPECT imaging. The performance of nuclear medicine instruments is generally evaluated not using the radionuclides that are used clinically but with encapsulated radioactive sources containing longer-lived surrogate radionuclides with emission of photons with desired energies. In

this context, ^{57}Co , which emits gamma-rays of energies 122.1 keV (85.6%) and 136 keV (10.7%) with a half-life of 270 days is considered to be an ideal surrogate for the diagnostic radionuclide $^{99\text{m}}\text{Tc}$ ($T_{1/2}=6$ h, $E_{\gamma}=140\text{keV}$) as the γ photon energies of ^{57}Co are close to that of $^{99\text{m}}\text{Tc}$ [65]. With an aim to develop ^{57}Co sources which can be employed to evaluate the performance of nuclear imaging instruments used in the nuclear medicine centres of the country, preparation of sealed ^{57}Co sources of overall dimensions 0.8 mm (\varnothing) \times 4.75 mm (l) containing $\sim 3.7\text{--}4.32$ MBq (0.1–0.16 mCi) was initiated. Previously, several need-based methods have been developed in our laboratory for the preparation of a variety of radioactive sources [66-77]. Among them, electrodeposition was considered to be a favorable pathway and has attracted tremendous attention owing to its technical simplicity, cost effectiveness and reproducibility [66-68]. In order to tap the potential of electro-deposition technique in the preparation of radioactive sources, we have earlier reported on the use of the electrochemical technique for the preparation of ^{57}Co sources employed in the radiometric assay of nuclear fuel rods [67] in which various experimental conditions for the optimum electrodeposition of ^{57}Co were studied and optimized. We subsequently used this technique for the preparation of ^{57}Co point source of ~ 1.48 MBq (40 μCi) for the calibration of intra-operative gamma probes [78]. In this endeavor towards the preparation of ^{57}Co sources for quality control of nuclear medicine imaging instruments, the electrochemical technique was optimized to deposit a known quantity of ^{57}Co onto a metallic substrate of predefined shape and size. In this chapter, the successful use of electrochemical technique for the deposition of 3.7–4.81 MBq (0.10–0.13 mCi) of ^{57}Co from an aqueous solution onto a copper substrate of 0.5 mm (\varnothing) \times 1 mm (l) is reported. The overall design and fabrication of titanium capsule for the encapsulation of ^{57}Co source core is also described in this work.

2.2.2. Materials and Instrumentation

2.2.2.1. Materials

Cobalt-57 as cobalt (II) chloride [specific activity 148–222 MBq (4–6mCi)/mg] was procured from M/s POLATOM, Poland. Reagents such as boric acid and sulphuric acid were of analytical grade and were procured from M/s. BDH (India), Mumbai, India. Copper electrodes of high purity were procured from M/s. Jugal Udyog Ltd., Mumbai, India. Platinum metal of high purity was procured from M/s. Hindustan Platinum Ltd, Mumbai, India. The electrolytic solutions were prepared using ultra pure water (Millipore Milli Q system). Miniature titanium capsules of dimensions 0.8 mm (\varnothing) \times 4.75 mm (l) were fabricated by the Centre for Design and Manufacturing (CDM) of our institution.

2.2.2.2. Instrumentation

A regulated power supply (Model No. L1282, working range: 1– 28 V, 0–2.5 A) from M/s. Aplab Ltd., India was used for electro-deposition experiments. An HPGe detector coupled to a 4096 Channel analyzer (Canberra Eurisys, France) was used for estimation of gamma activity. A 50W Nd: YAG laser welding system M/s Quanta Systems, Italy was used for welding the sources. Optical density measurements of exposed X-ray films (Kodak-400; Industrial Grade) were carried out using OPTTEL — B&W transmission densitometer. Cotton wool samples of swipe test and water samples of immersion test were counted in a NaI (Tl) scintillation detector [Model PNS2, Electronic Enterprises (I) Pvt.Ltd, Mumbai, India]. Well type re-entrant ion chamber [Model-1008] procured from M/s Sun Nuclear Corporation; USA was used for source activity measurement.

2.2.3. Experimental

2.2.3.1. Preparation of ^{57}Co Source

Cobalt-57 chloride [3.7–5.18 MBq (~ 100 – $140 \mu\text{Ci}$)] of specific activity 185 MBq/ μg was pipetted out from the stock solution into a 5 mL capacity glass beaker and the solution was slowly evaporated to dryness under an infrared lamp. The resulting solution was reconstituted in 5 mL of 0.01 N H_2SO_4 containing boric acid at a concentration of $30 \text{ mg}\cdot\text{mL}^{-1}$. The pH of the bath was adjusted to 4.5–5.0 by the addition of 0.1 M NH_4OH . Prior to each experiment, the solutions were purged with argon gas to remove the dissolved gases. The cathode consisted of a cylindrical copper rod at the top edge of which the copper substrate [$0.5 \text{ mm } (\varnothing) \times 1 \text{ mm } (l)$] was welded while a platinum rod of similar dimensions was the anode. Only the tip of the copper rod of dimensions $0.5 \text{ mm } (\varnothing) \times 1 \text{ mm } (l)$ was exposed to the electrolyte and the remaining length of the copper rod was masked with a thick insulating layer of an adhesive to prevent any electrodeposition of ^{57}Co beyond the desired area. The electrodes were positioned face to face, separated 10 mm apart, immersed in the electrolyte and were connected to the power supply using small screws, embedded at the top end. As schematic diagram of the electrodeposition assembly is shown in Fig. 2.10.

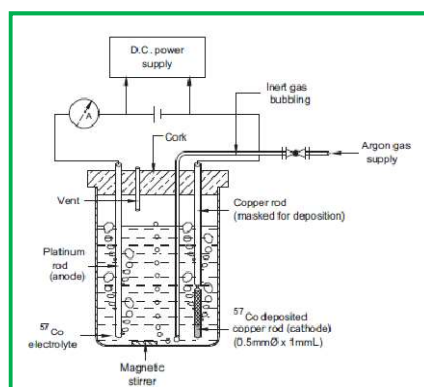


Fig. 2.10: Electrodeposition assembly for preparation of ^{57}Co point source

Subsequently, electrodeposition of ^{57}Co was carried out at a current density of about 40 mA.cm^{-2} for 3 h at 60°C . The ^{57}Co electrodeposited copper rod was then taken out, rinsed with double distilled water, and dried under an infrared lamp. The tip of the copper rod $[0.5 \text{ mm } (\varnothing) \times 1 \text{ mm } (l)]$ comprising the active area was cut for use. A single copper rod was electrodeposited with ^{57}Co in each batch of experiment.

2.2.3.2. Source Assembly in a Titanium Capsule

Titanium capsules of dimensions $0.8 \text{ mm } (\varnothing \times 4.75 \text{ mm } (l))$, comprising of a cylinder with one end closed and a cap to fit at the open end was designed to accommodate the ^{57}Co source core in the cavity. The cap was rounded and could be fixed on the cylindrical body. The schematic diagram of the source capsule along with the source core is shown in Fig. 2.11. Prior to encapsulation, the strength of each ^{57}Co sources was measured by an ionization chamber. Sources in the activity range of ~ 110 – $130 \text{ } \mu\text{Ci}$ were segregated and encapsulated by laser welding. The radioactive ^{57}Co sources were inserted individually into titanium capsules with the help of tweezers to fit inside the capsule. A cylindrical copper spacer of dimensions $0.5 \text{ mm } (\varnothing) \times 2 \text{ mm } (l)$ was placed above the ^{57}Co source to shield the source from thermal degradation during laser welding.

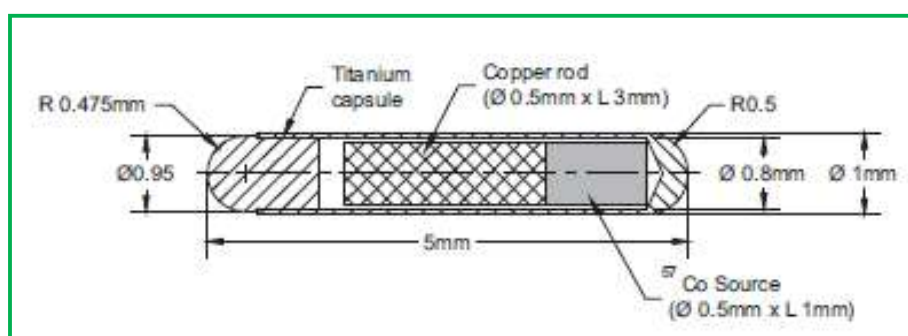


Fig. 2.11: Schematic of ^{57}Co source in titanium capsule

2.2.3.3. Laser Encapsulation

Inactive dummy sources were encapsulated using a laser beam from 50 W Nd: YAG laser welding unit. Laser beam was focused to the joint horizontally by an optic fiber based delivery system and parameters such as capacitor bank discharge voltage, pulse width, frequency, rotational speed etc., were optimized to obtain quality welds. All the parameters for laser welding along with rotation of the capsule including inert gas supply for shielding were controlled through PC. Inactive welded sources were imaged to ascertain the quality of the weld using an optical microscope. The frequency of laser pulse was kept as 1 Hz, the pulse duration was optimized as 4 ms and rotational speed of sample to be welded was kept $\sim 3^\circ/\text{min}$. In the final assembly of radioactive source, hermetic sealing was achieved by welding the cap with the capsule body using laser welding beam using optimized parameters. The sealed sources were ultrasonically cleaned with ethyl alcohol to remove any traces of contamination.

2.2.3.4. Activity Assay of ^{57}Co Sealed Source

The activity assay procedure adopted for each ^{57}Co source consisted of two stages. Gamma spectrometric measurement of the source was carried out in High Purity Germanium (HPGe) detector. In the first step, the source was placed at 30 cm from the front end of the HPGe detector assembly and counted for 300s. The detection efficiency of the detector at this geometry at different photon energies was derived by counting a standard ^{152}Eu point source at the same distance. The absolute activity of the ^{57}Co source was calculated from the measured count rate at $E_\gamma=122.06$ keV as well as $E_\gamma=36.47$ keV and dividing it with the average efficiency corresponding to the measured energy obtained from the efficiency curve obtained with ^{152}Eu . The activity calculated was taken as the average of the values obtained from 122 keV and 136 keV gamma rays [78]. In the

second step, each source was individually measured for its ionization current using a pre-calibrated ionization chamber by comparison method. The ion current ‘I’ was measured and the activity ‘A’ was calculated by the relation

$$A = I/\epsilon \text{ MBq}$$

Where ‘ ϵ ’ is the ionization factor of the ionization chamber in pA.MBq^{-1} and was calibrated periodically with standard ^{57}Co source of known activity.

2.2.3.5. Quality Control

The sealed ^{57}Co source was tested for leachable activity as per the reported procedures [66-78]. The distribution of ^{57}Co activity on the substrate was examined by autoradiography using a specially designed brass circular disc with a central hole of 3 mm diameter and 8 mm depth. Six equidistant radial tunnels (60° angles between consecutive tunnels) of uniform aperture (3.3 mm diameter) were drilled through the central cavity. The source was placed in the central hole and autoradiographed by wrapping a strip of photographic film along the side of brass disc as per the reported procedure. Swipe test and leakage test of the prepared ^{57}Co sources were performed as per the reported method [66-78].

2.2.3.6. Radiological Safety

Due to the radioactive nature of ^{57}Co , safe and appropriate radioactive procedures were adopted during the source preparation process. All the experiments were carried out after thorough planning in order to achieve ‘As Low as Reasonably Achievable (ALARA)’. The personnel involved in this work were monitored for radiation exposure levels by Thermo Luminescence Dosimeters (TLD).

2.2.4. Results

The aim of this work was to develop a procedure to prepare radioactive source cores of ^{57}Co containing 3.7–4.81 MBq (0.10– 0.13 mCi) of activity and encapsulation of source cores in titanium capsules by laser welding in such a way that it behaves as a point source.

2.2.4.1. Source Preparation

Electrodeposition of ^{57}Co on the Cu substrate was carried out using the experimental parameters optimized earlier [66-68]. The amount of ^{57}Co activity that could be deposited on the substrate could be controlled by adjusting the concentration of the electrolyte. Give the optimized conditions here following the procedure described above, several ^{57}Co source cores in the dimensions of 0.5mm (\varnothing) \times 1 mm (l) were prepared. Results of deposition experiments carried out in 5 batches showed that the efficiency of ^{57}Co electrodeposition did not differ significantly from batch to batch and the mean ^{57}Co deposition yield was $93.3 \pm 2.6\%$.

2.2.4.2. Leachability of Source Core

Leach tests were conducted with five randomly selected source of ^{57}Co after thermal treatment at a temperature of 300–350°C for a period of 20 min showed that there was no release of radioactivity in 48 h, which complies with the AERB specifications [63].

2.2.4.3. Encapsulation

In order to prevent the accidental dispersion of radioactivity during end application, the ^{57}Co source core needs to be encapsulated in a capsule. A cylindrical capsule design was chosen owing to the convenience of source core loading with minimum manipulation. The choice of titanium as capsule material was due to high

strength to weight ratio, radiation stability, excellent corrosion resistance, good thermal conductivity, adequate mechanical strength and amenability for welding. The wall thickness of the titanium capsule was configured to provide adequate mechanical strength as well as minimum radiation attenuation. In view of the extremely small wall thickness of the capsule, assessing the potential of laser welding technique was considered as a necessary one. The laser encapsulation process described above allows hermetic sealing of titanium capsules with minimal radioactive contamination. A schematic diagram of the laser welded source is shown in Fig. 2.11.

2.2.4.4. Measurement of Activity of the Source

The efficiency curve for the measurement of ^{152}Eu gamma rays in the gamma energy range of 100–350 keV is given in Fig. 2.12. The efficiencies for measurement of the gamma energies of ^{57}Co were obtained by interpolation of the measured efficiency data. As expected the efficiency of the detector decreases with energy as seen from the results. Experimentally, it was found that the maximum observed percentage differences between the activity measurement values obtained by gamma spectrometric and by ion current measurement techniques was $\pm 1.5\%$. The activity of the sealed ^{57}Co sources as determined using well type ionization chamber was therefore used for quoting the activity owing to operational simplicity. Ion chamber measurement is also an acceptable method for routine determination of activity of sealed radioactive sources [79]. Source strength of each encapsulated ^{57}Co source was estimated in a well type re-entrant ionization chamber pre-calibrated with a standard reference source. Standardization of the reference source was performed by the Radiation Safety System Division of our institute using two 4π β - γ coincidence systems in which a 4π (PC) counter was coupled to a pair of 76 mm \times 76 mm NaI (Tl) scintillators and a HPGe spectrometer. The measurements were performed by

selecting a gamma-ray window comprising the (122 keV+136 keV) total absorption energy peaks in the NaI (Tl) counter and selecting the total absorption peak of 122 keV in the HPGe detector. In order to preclude the geometrical variability on the measurement, the references sources as well as the prepared sources were inserted into the ion chamber centered in the maximum response position of the measuring volume. In order to ascertain the reproducibility of the measurement which is a measure of the percentage deviation of a series of measurements from the sample mean, 10 measurements of a standard ^{57}Co source [3.7 MBq (~ 100 μCi)] were made in the source holder in the measurement position which were then averaged together. The values were within $\pm 1\%$ of the average measured activity for that source. On measurement of standard ^{57}Co sources of different activities [1.85–3.7 MBq (50–150 μCi)], the maximum relative deviation between the measured values and the quoted values were within $\pm 2.1\%$. The experimental uncertainty in the activity measurement of the sources is thus better than the acceptable maximum uncertainty ($\pm 10\%$). Experimental measurement of activities of bare sources (source cores) and sealed sources revealed that 10–13% of the activity is attenuated by the titanium capsules. The ^{57}Co activity electrodeposited on the copper wire was therefore kept 15 % more than the required activity in order to compensate the attenuation effects of the titanium capsule material.

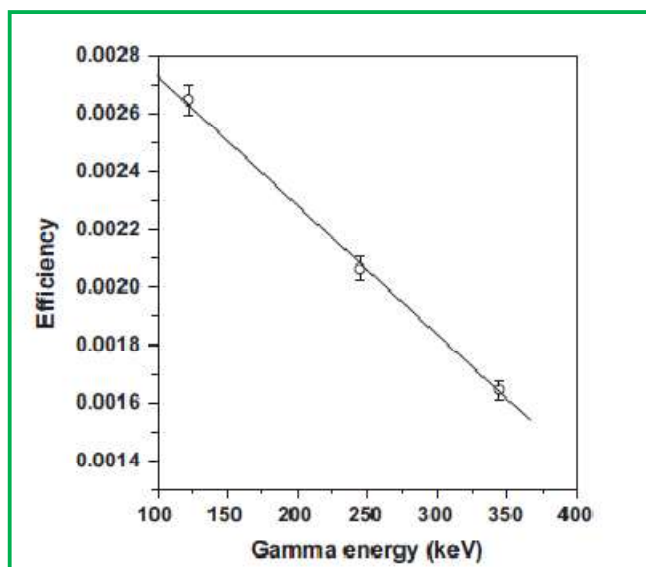


Fig. 2.12: Variation of the efficiency of the HPGe detector for ^{152}Eu gamma rays

2.2.5. Quality Control

The encapsulated ^{57}Co sources were subjected to numerous quality assurance tests in order to ensure their compliance with the stipulations of Atomic Energy Regulatory Board, India AERB/SS/3 (Rev.1, 2001).

2.2.5.1. Uniformity distribution of ^{57}Co on Source Core

The uniform distribution of ^{57}Co activity on the source core was ascertained following the reported procedure [66, 75]. Fig. 2.13 shows the autoradiography image of one of the prepared ^{57}Co point source. Table-2.4 shows the variation of optical densities of the radiographic film after different exposure times in different positions. It is seen that the radiation flux was nearly homogenous along the different directions with deviations within $\pm 3.5\%$ from the mean, confirming the uniform distribution of radioactivity on the source core. Results of leach test, swipe and immersion tests carried out using five different sources are depicted in Table-2.5. Leachability studies conducted on five sources indicated that the leaching of activity from the sealed sources was below the detection limit of the counter, which complies with the specifications laid down by

AERB/SS/3 (Rev.1, 2001), India [63]. In order to ensure the absence of removable activity from the source, swipe test and immersion tests were performed on five numbers of sources of 3.96–4.32MBq (107–116 μCi) strength. The results are depicted in Table 2.5, indicating that the removable counts were less than 185 Bq per source in the solution as well as the swipe, which comply with the specifications laid by the AERB/SS/3(Rev.1, 2001). Each sealed ^{57}Co point source that passed the quality control tests was then mounted on a perspex block used in a nuclear medicine department for ascertaining the performance of the imaging equipment.

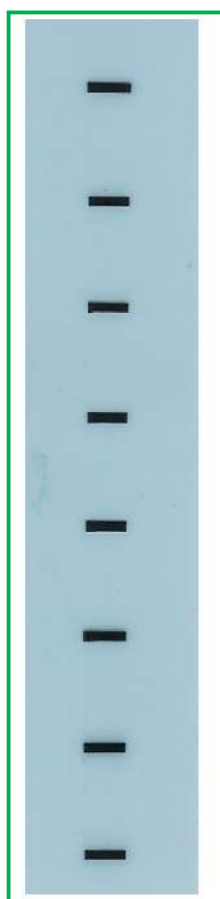


Fig. 2.13: Autoradiograph of ^{57}Co point source

Table-2.4: Optical density distribution of ^{57}Co source

| Position number | Optical density | | |
|-----------------|-----------------|-----------------|-----------------|
| | Source number | | |
| | 1 | 2 | 3 |
| 1 | 0.85 | 0.89 | 0.87 |
| 2 | 0.84 | 0.87 | 0.85 |
| 3 | 0.85 | 0.89 | 0.85 |
| 4 | 0.83 | 0.85 | 0.83 |
| 5 | 0.84 | 0.87 | 0.84 |
| 6 | 0.85 | 0.88 | 0.87 |
| 7 | 0.83 | 0.87 | 0.85 |
| 8 | 0.85 | 0.91 | 0.85 |
| Mean \pm SD | 0.84 \pm 0.01 | 0.88 \pm 0.02 | 0.85 \pm 0.01 |

Table-2.5: Quality assessment of sealed ^{57}Co source

| Batch no. | Activity MBq (μCi) | Leachability (%total activity) | Immersion test (total activity release in 5h) Bq (nCi) | Surface contamination Bq (nCi) |
|---------------|---------------------------------|--------------------------------|--|--------------------------------|
| 1 | 4.18(113) | BDL | 28(0.75) | 10 (0.27) |
| 2 | 4.36(118) | BDL | 41(1.1) | 21(0.56) |
| 3 | 4.25(115) | BDL | 36(0.97) | 12(0.32) |
| 4 | 3.96(107) | BDL | 39(1.05) | 18(0.86) |
| 5 | 4.07(110) | BDL | 46(1.24) | 32(0.86) |
| Mean \pm SD | 4.16 \pm 0.14(113 \pm 3) | BDL | 38 \pm 6 (1.02 \pm 0.16) | 19 \pm 8 (0.49 \pm 20) |

* BDL= below the detection limit

2.2.6. Discussion

Preparation of sealed ^{57}Co sources of desired attributes requires judicious selection of a deposition technique, careful preparation of source, adherence to radioactivity limit of the source within acceptable activity tolerances, encapsulation of the source and evaluation of quality of the source to meet regulatory requirement. Given the simplicity of depositing the required quantity of ^{57}Co on a metallic substrate of predefined geometry and dimensions and the ability to obtain adherent as well as uniform deposition of ^{57}Co on a suitable substrate, the scope of using electrodeposition technique was promising. The salient features of the ^{57}Co sources developed by the aforesaid procedure are (i) amount of ^{57}Co activity electrodeposited on to the copper substrate can be easily controlled by adjusting the radioactive concentration of the electrolyte (ii) sources can be prepared at ambient temperature without the release of radioactivity (iii) radioactive ^{57}Co deposit adhered firmly to the substrate (iv) uniform distribution of ^{57}Co on the substrate for homogeneous delivery of radiation output and (v) compliance with the regulatory norms. Encapsulated ^{57}Co sources prepared by the standardized procedure were found to be effective in the routine performance evaluation of nuclear medicine instruments and have proven their utility for the desired purpose.

2.2.7. Conclusion and scope of the work

The objective of making sealed ^{57}Co sources commensurate with the user's specifications and compliant with the mandatory regulatory requirements for safe handling during applications has been achieved. The mild experimental conditions together with the convenience of electrodeposition technique for depositing the ^{57}Co source core preparation process ensures safe handling of radioactivity. The capsule design and encapsulation technique used in this investigation is satisfactory to achieve hermetic

seal in order to keep the ^{57}Co activity intact under the intended conditions of use, and also under foreseeable accidental conditions. While the techniques described in this chapter have been developed specifically for preparation of ^{57}Co source, they might also be of value in the preparation of radiation sources containing other radionuclides.

2.3. An Electrochemical Route to Prepare Planar ^{204}Tl Sources for the Calibration of Beta Surface Contamination Monitors

2.3.1. Introduction

Beta surface contamination monitors are used to determine the beta emitting radionuclide activity levels in radioactive laboratories. Performance as well as sensitivity, constancy and accuracy of these equipments need to be validated before deploying them into service to ensure constancy of response [81]. This objective is achieved through the use of two major types of radioactive reference sources containing appropriate quantities of beta emitting radionuclides. The first type consists of small point sources and the other type comprises planar sources. Such sources are usually prepared using beta emitting radioisotopes such as ^{14}C , ^{147}Pm , ^{204}Tl , $^{90}\text{Sr}/^{90}\text{Y}$ and $^{106}\text{Ru}/^{106}\text{Rh}$, having E_{β} max of approximately 0.16, 0.24, 0.76, 2.27 and 3.54 MeV respectively [82]. These sources have reasonably long shelf life and provide a steady beta radiation flux. In this respect, planar circular sources of ^{204}Tl can be used effectively for the assessment of the response of beta radiation surface contamination monitors. Thallium-204 decays by a β^- -transition to ^{204}Pb (97.4%) and by electron capture (EC) to ^{204}Hg (2.6%) with a half-life of 3.78 years [83]. The source required for this application consists of a circular disc of 10 mm (\varnothing) on which ~ 3.7 MBq (~ 100 μCi) of ^{204}Tl is required to be deposited homogeneously on one of the flat surfaces. The effectiveness of the source fabrication technique used largely determines the extent to which the radioactive material is uniformly distributed over the

source area and adherence to the substrate [84]. In the quest for an effective approach for the preparation of ^{204}Tl sources, various need-based technical options were explored in our laboratory [40, 44, 66, 67, 70-78] were evaluated. A detailed literature search indicated that the electrochemical deposition of Tl and its alloys from aqueous solutions has been the subject of many investigations [86-94] Although studies about the deposition of micro gram quantities of thallium have seldom been reported, the findings from those reported procedures [86-94] be exploited to realize the objective of preparing a planar ^{204}Tl source. Herein, a facile laboratory scale electrochemical method for the preparation of circular planar ^{204}Tl sources is optimized. In brief, electro-deposition of ^{204}Tl activity on a precisely defined area of a metallic substrate, covering the radioactive area with a thin layer of organic polymer, mounting in a brass holder and quality assurance of this source to meet regulatory requirement is reported. The advantage of the reported technique is that the amount of ^{204}Tl deposition can be controlled with relative ease and accuracy by controlling the electro-deposition parameters, thus making the process attractive.

2.3.2. Materials

All chemicals used during the work were of AR grade and were procured from BDH (India), Mumbai, “Specpure” high-purity thallium metal procured from Johnson Matthey, Mumbai, India, was used as the target for the production of ^{204}Tl . All aqueous solutions were prepared using water from a Millipore Milli-Q water purification system (18.2M Ω cm). Platinum metal foil of high purity (99.99% purity) with material testing certificates was procured from M/s Hindustan Platinum Ltd, Mumbai, India. High purity (99.99%) argon gas was procured from M/s Kolhapur Oxygen & Acetylene Private Limited, Kolhapur, India. Methyl methacrylate polymer (PMMA) was of analytical grade

and was procured from BDH (India). The copper disc used in this work was of high purity metal (99.99%) fabricated in house. Prior to electro-deposition, the surface of the copper disc was polished with emery paper to a rough finish, washed in an ultrasonic bath of acetone, rinsed with deionized water and then air-dried. A D.C. power supply with 100 V compliance, a maximum current of 2 A, 1.2 nA current resolution and $> 10^{13}$ Ohms input impedance was used for electrodeposition experiments. Voltammetric measurements were performed using a computer-controlled potentiostat (CH Instruments, Model CHI 760 C) in a standard three electrode cell. Copper electrode was used as the working electrode, a platinum wire as the counter electrode, and an Ag/AgCl (3M KCl filled) electrode as the reference electrode. A liquid scintillation counter (425-034) from Triathler, Turku, Finland was used for the radioactivity measurement. Liquid scintillation cocktail (w scintillation grade) from M/s Sisco Research Lab. Pvt. Ltd., Mumbai, India suitable for measuring low to medium ionic strength aqueous samples was used. The microstructural features of the anodized samples were analyzed using a Scanning Electron Microscope (SERON, Model AIS-2100). Energy Dispersive X-ray microanalysis technique (Oxford, Model INCA E350) was used to identify the elemental constituents on the sample. Atomic Force Microscopic (AFM) measurements were performed using a model Nanosurf Easy Scan 2 AFM System (Nanosurf AG, Switzerland). Beta Radiation Survey Meter (PRM131A) of PLA Electro Appliance Pvt Ltd, India was used to measure the radiation dose on the surface of the source. Cotton wool samples of Wipe test and water samples of Immersion test were counted in a G M counter (Model ACS 101 P, Electronic Enterprises (I) Pvt. Ltd, Mumbai, India). Radioactivity measurements of the sealed sources were carried out using a well type pre-calibrated ionization chamber (Centronic IG12/A20, Centronic Ltd., New Addington,

UK). AGFA film grade-G-7 was used for autoradiography. Optical density measurements were carried out using an OPTEL Transmission densitometer.

2.3.3. Experimental

2.3.3.1. Production and Processing of ^{204}Tl

Natural thallium metal (1 g) was irradiated in the Dhruva reactor of our Institute at a flux of $\sim 9 \times 10^{13} \text{ n.cm}^{-2}.\text{s}^{-1}$ for 3 years. The irradiated sample was allowed to cool for 20 days, transferred to a 250 mL dissolution flask, followed by addition of 30 mL of 1 N H_2SO_4 and 5 mL 30% v/v H_2O_2 . The solution was refluxed for 30 minutes till all of the metal was dissolved. The resultant solution was evaporated to near dryness to remove H_2O_2 and then reconstituted with 25 mL of 1 N H_2SO_4 solution. Thallium-204 as Tl_2SO_4 in 1 N H_2SO_4 of specific activity 48 GBq (1.3 Ci)/g was obtained.

2.3.3.2. Electrochemical Preparation of ^{204}Tl

The electrochemical cell consisted of a quartz cylinder of 25 mL capacity and an acrylic lid. The cathode used was a circular copper sheet of 25 mm diameter (working area 20 mm \varnothing) and thickness 0.3 mm. For electrical connection, a copper rod was welded at the top edge of the circular sheet. A platinum foil of equal shape and area was used as the anode. One side of the disc area and 1.25 mm from the periphery of other side of the disc were blocked by coating it with an insulating layer of adhesive. The working area of the cathode was 314 mm². In all experiments one anode and one cathode were taken. The electrodes were positioned face to face, separated 10 mm apart, immersed in the electrolyte and were connected to the power supply using small screws, embedded on the top end. A provision was made for passing Ar gas (at the rate of 0.05 cc/s) through a glass tube ($\varnothing = 1\text{mm}$) into the electrolyte and a small outlet of $\sim 2.5 \text{ mm}$ (\varnothing) was provided through the acrylic cap for venting the gases liberated during electrolysis. The schematic

diagram of the arrangement is shown in Fig. 2.14. Prior to electro-deposition, the cell was rinsed thoroughly in deionized water. The cell complete with electrodes was filled with electrolyte followed by deaeration with a rapid stream of argon nitrogen for about 30 min. Electro-deposition of ^{204}Tl was carried out at 60°C using 10.0 mL of electrolyte containing an aqueous solution of 0.04 mM Tl_2SO_4 , 0.1 M $(\text{NH}_4)_2\text{SO}_4$, 0.1 M Na_2SO_4 and 0.1 M H_3BO_3 at a potential of 1 V.

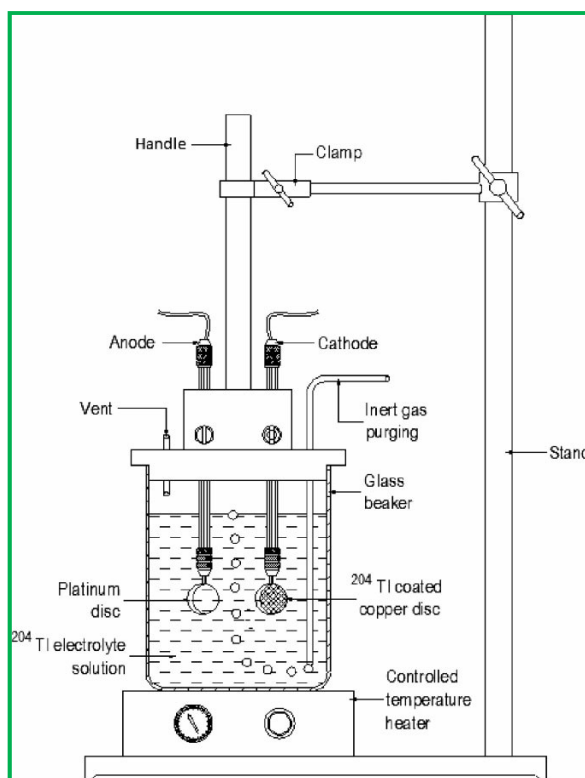


Fig. 2.14: Schematic diagram of the electrochemical cell.

2.3.3.3. Voltammetric Experiments

Voltammetric experiments were carried out using three electrodes geometry in which copper was used as the working electrode, platinum rod as the counter electrode and saturated calomel (SCE) as the reference electrode.

2.3.3.4. Optimization of Electrodeposition Parameters

In order to optimize the experimental conditions, non-radioactive Tl_2SO_4 solution was prepared which was spiked with 370 kBq (10 μCi) of radioactive ^{204}Tl . The cell was placed in a constant temperature water bath and experiments were carried out when the solution in the bath attained the required temperature. In order to obtain the optimum reproducible deposition yield, several deposition experiments were performed using the following ranges of the operational parameters: pH of the electrolytic bath 1–6, cathode current density 1–25 mA.cm^{-2} , time of deposition 1–5 h, thallium concentration in the bath 5 to 50 $\mu\text{g.mL}^{-1}$ and bath temperature 15–70°C. The percent deposition (%) was calculated using the relationship

$$\text{Percentage deposition} = \frac{A_i - A_f}{A_i} \times 100$$

Where A_i and A_f are the initial and final radioactivity of ^{204}Tl , respectively

2.3.3.5. Preparation of Source

The Required quantity of ^{204}Tl activity as Tl_2SO_4 of specific activity 48 GBq.g^{-1} (1.3 Ci.g^{-1}) was pipetted out from the stock solution and taken in a 100 mL capacity beaker. To this, 10 mL of 0.1 M $(\text{NH}_4)_2\text{SO}_4$, 10 mL of 0.07M Na_2SO_4 , 10 mL of 0.1 H_3BO_3 and appropriate amount of non-radioactive (cold) thallium as Tl_2SO_4 as carrier were added so that total concentration of Tl in the final solution remains 5×10^{-5} M (247 μg of Tl_2SO_4) followed by the addition of 1 mL of conc H_2SO_4 . The resulting solution was evaporated to dryness and made up in 10 mL of water. The pH of the electrolyte was brought to ~ 1 by the drop-wise addition of 0.1 M H_2SO_4 . The resulting solution was then transferred into the electrochemical cell. The electrolyte was purged with pure argon (Ar) gas to remove the dissolved gases. Electrodeposition of ^{204}Tl was carried out at a potential of 1 V maintaining a current density of about 15 mA.cm^{-2} for 4 h at 60°C. The electrolyte

was stirred by a magnetic stirrer during the deposition at a constant speed of ~ 200 rpm. A single copper disc was electrodeposited with ^{204}Tl in each batch of experiments. After electrodeposition, the samples were rinsed in doubly distilled water and dried under an IR lamp.

2.3.3.6. Surface Characterization

Scanning Electron Microscopy (SEM), Energy Dispersive X-ray spectra (EDS) and Atomic Force Microscope (AFM) analysis were carried out for both Tl electrodeposited and polymer coated surfaces using a dummy source prepared in an identical manner used for source fabrication (using inactive/cold Tl). EDS microanalysis technique was used to identify the elemental constituents of the electro-deposited samples.

2.3.3.7. Activity Assay of the Source Core

The activity of ^{204}Tl deposited on the copper matrix was determined by measuring the activity in small aliquots of the electrolyte before and after electrodeposition, using a liquid scintillation counter (LSC). The amount of ^{204}Tl activity deposited on the source was calculated from the difference of activity in the bath before and after electrodeposition. Owing to the possibility of surface adsorption of ^{204}Tl on the walls of the beaker, this method was utilized to follow the progress of ^{204}Tl deposition on the substrate. For the purpose of quoting the activity in the source, accurate assaying of the activity on the sources was carried out using an ion chamber calibrated with standard ^{204}Tl sources.

2.3.3.8. Coating of the Sources with PMMA Polymer

The active area of the source was coated with PMMA by the dip-pull method. The ^{204}Tl deposited source was immersed into a solution of PMMA in chloroform solution

(150 mg.mL⁻¹), stirred using magnetic stirrer, for 3 min and taken out with a tweezers. The polymer coated samples were placed onto a perforated tray where the excess of the uncoated PMMA reagent drained out and air-dried [70, 78, 83].

2.3.3.9. Quality Control

The ^{204}Tl source was tested for leachable activity as per the reported procedures. The distribution of ^{204}Tl activity on the source was examined by autoradiography following the reported method [77, 78]. Swipe test and leakage test of prepared ^{204}Tl sources were performed as per the reported method [44, 78].

2.3.3.10. Source Assembly in a Circular Holder

Each circular source holder consisted of an aluminum “cylinder” of 35 mm diameter (OD) and 32 mm (ID) with a flat bottom. The flat bottom had a hole in it to accommodate the source. There was a machined ~ 1.25 mm depression in the metal bottom to hold the source in place. The holder was threaded on the inside edge to accommodate a matching threaded cap. The ^{204}Tl source was placed with the help of a tweezer to fit inside the base with its radioactive end facing down towards the open end. A matching cylindrical aluminum cap of 32 mm \varnothing threaded around the outside edge was used to enclose the source. The cap could be used to turn in either direction. The cap could be rotated in a clockwise direction to fit into the holder and closed by winding the screwed cap tightly in position. The details of the source holder and assembled source are depicted in Fig. 2.15. This design secures the source in the holder during application. Once the useful life of the source is over, the cap can be removed by turning it in a counter clockwise direction; the source can be retrieved and disposed off following the standard practice of radioactive waste disposal protocol adapted by our institution (BARC).

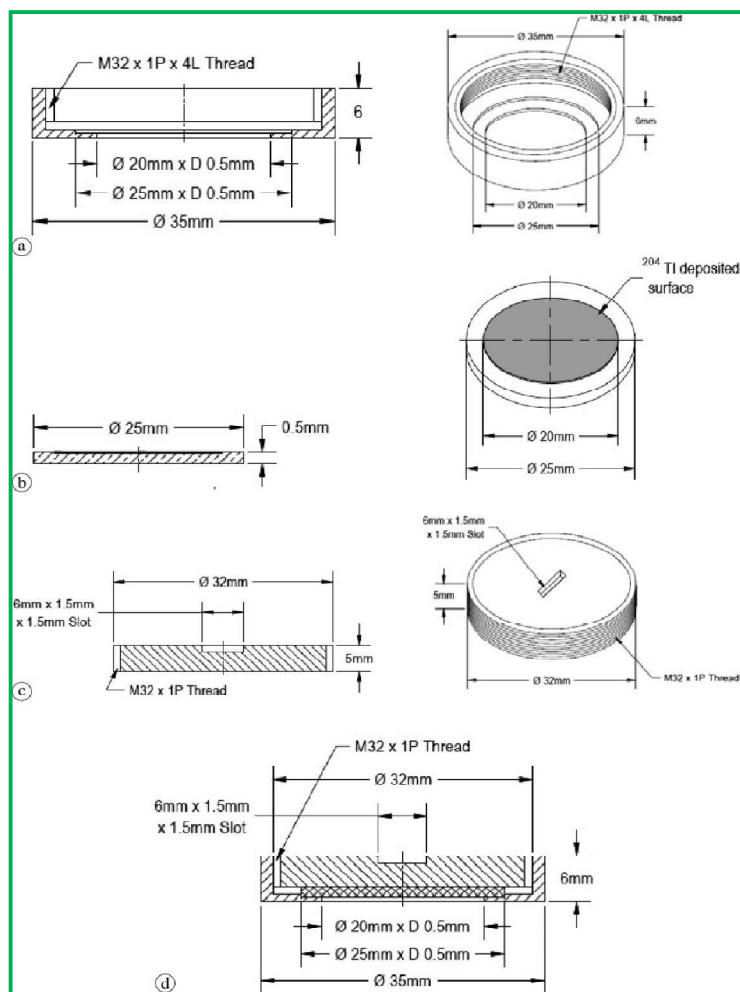


Fig. 2.15: Source assembly in a circular holder. (a) Source holder base is threaded on the inside edge to accommodate a matching threaded cap (b) Electrodeposited ^{204}Tl disc source is fitted inside the base with its radioactive end facing down towards the open end (c) Source cap is threaded on the outside edge to enclose the source (d) Source assembly

2.3.3.11. Radiological Safety

In view of radioactive nature of ^{204}Tl , safe and appropriate radioactive procedures were adopted during the source preparation. All the experiments were carried out after thorough planning in order to achieve “ALARA”. The personnel involved in this work were monitored for radiation exposure levels by TLD dosimeters.

2.3.4. Results

In this work, it was aimed to explore the potential of electrodeposition technique to produce a homogeneous deposition of ^{204}Tl on one side of a circular substrate towards use as a radioactive source with beta contamination monitors.

2.3.4.1. Preparation of the Electrolyte

The selection of an electro-bath is very important for the deposition of ^{204}Tl . While the thallium salts such as the nitrate, sulphate, perchlorate, carbonates have sufficient solubility in water to permit their use for the preparation of electrolyte, sulphate salt was chosen because it behaves in a relatively straight forward manner. Acidic bath is used as it is simpler to handle than basic solutions. Tl(I) salt is preferred to Tl(III) owing to its favorable electrochemical characteristics [76]. The composition of the electro-bath is based on the information derived from the reported procedure [44].

2.3.4.2. Voltammetric Studies

Cyclic voltammetric plots of Tl(I) in boric acid medium with varying scan rates (corrected for background) are shown in Fig. 2.16. The reduction peak observed at ~ -0.8 V was due to reduction of Tl^+ into Tl metallic form. This was further corroborated by the differential pulse voltammetric plot (Fig. 2.16, inset) which shows a distinct reduction peak at -0.78 V. When deposition potential was fixed at -1.00 V, near quantitative deposition of Tl(I) on the electrode surface of Cu was observed. Therefore, this potential was chosen as the optimum electrodeposition potential in all further experiments.

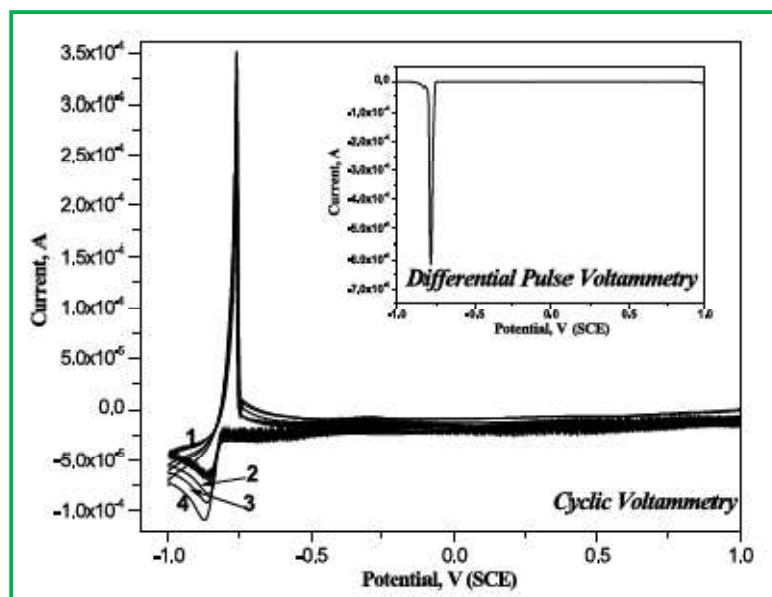


Fig. 2.16: Cyclic voltammetric plot of 1×10^{-4} M Tl (I) solution in 0.1M boric acid medium at varying scan rates: (1) 100 mVs^{-1} (2) 200 mVs^{-1} (3) 300 mVs^{-1} (4) 400 mVs^{-1}

2.3.4.3. Optimization of Electrodeposition Parameters

In order to determine the optimal experimental conditions for the electrodeposition of ^{204}Tl on copper substrates, influence of experimental parameters such as pH of the electrolyte, applied current density, deposition time, bath temperature and thallium content in the electrolyte were systematically investigated. Considering the microgram amount of ^{204}Tl used in this work, only the deposition efficiency is discussed and not current efficiency.

2.3.4.4. Influence of pH of the Electrolyte

The effect of pH of the electro bath on the electrodeposition of ^{204}Tl was studied within the pH range of 1–6 with an aim to determine the optimum conditions for ^{204}Tl deposition. The result is presented in Fig. 2.17. It can be seen that the percentage of ^{204}Tl deposition is maximum at pH 1–2. Thereafter further increase in pH resulted in decrease

of deposited activity. Herein the electrodeposition process is mainly dominated by three factors: (i) the dissolution of the freshly deposited ^{204}Tl atoms on the substrate because of the acid condition in the electrolyte (ii) formation of ^{204}Tl layer on the electrode surface and (iii) the anomalous electrodeposition of ^{204}Tl . At low pH value, the process is predominated by the second factor which favors the electrodeposition of ^{204}Tl layer and depresses the dissolution of the freshly deposited ^{204}Tl .

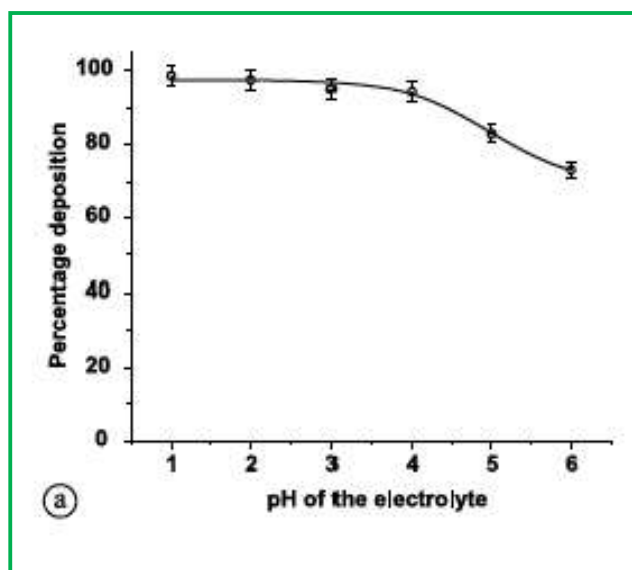


Fig. 2.17: Influence of pH of the electrolyte

2.3.4.5. Influence of Current Density

In order to study the impact of applied current density on the ^{204}Tl deposition, a series of electrodeposition experiments were performed in the current density range of 1–25 $\text{mA}\cdot\text{cm}^{-2}$. The percentage of ^{204}Tl deposition as a function of applied current density is shown in Fig. 2.18. It is evident that within the range of current density investigated, the percentage deposition increased with increasing current density up to 15 $\text{mA}\cdot\text{cm}^{-2}$ and thereafter it remained constant. The best operating current density was therefore found to be 15 $\text{mA}\cdot\text{cm}^{-2}$. At low current density, or lower overpotential, the percentage deposition

decreased due to competitive reaction or proton reduction. Increase in current density usually increases over-potential leading to increase in deposition.

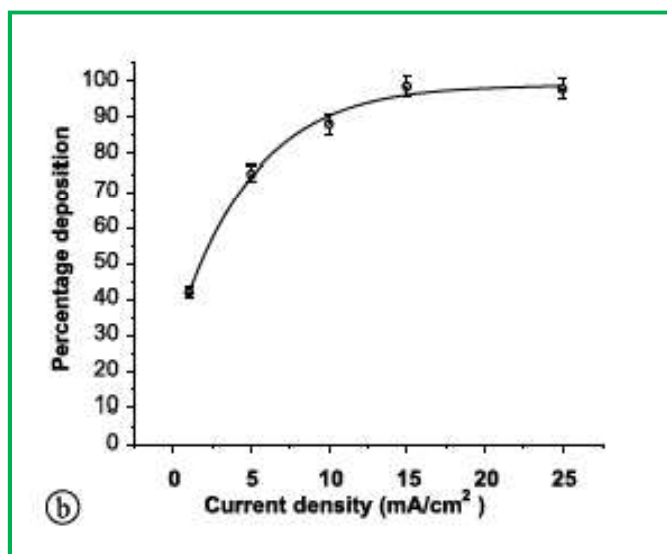


Fig. 2.18: Influence of current density

2.3.4.6. Influence of Deposition Time

In order to determine the optimum deposition time required obtaining quantitative deposition of ^{204}Tl , experiments were performed at different time interval and the results are depicted in Fig. 2.19. It is seen that, within the range of deposition time investigated, the percentage ^{204}Tl deposition increased with increasing contact time and almost a quantitative deposition of activity was obtained after 4 h of electrolysis. As is known, electrodeposition of ^{204}Tl takes place by reduction of Tl^+ . As the deposition time increases, more and more Tl^+ ions get reduced, leading to the increase of the deposition rate. The maximum of deposition rate may be due to complete reduction of Tl^+ ions.

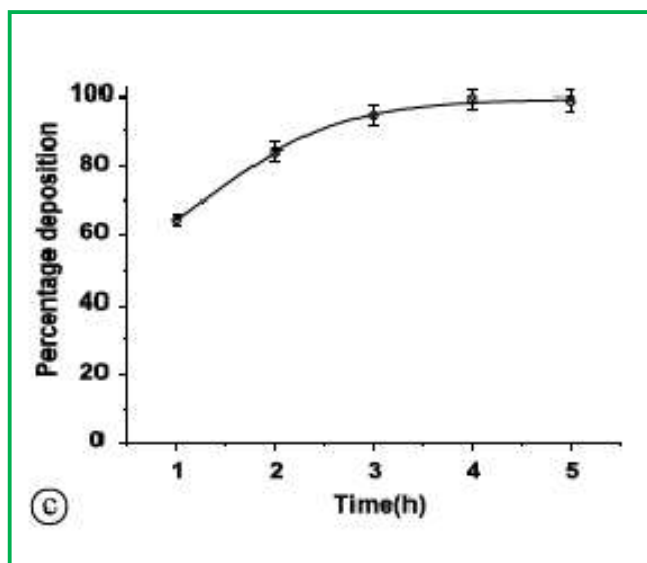


Fig.2.19: Influence of deposition time

2.3.4.7. Influence of Thallium Content in the Electrolyte

In order to reduce the deposited film thickness, it is essential to keep ^{204}Tl concentration as low as possible. In this context, optimization of ^{204}Tl concentration in the bath was considered essential and hence was pursued. Fig. 2.20 depicts the dependence of the ^{204}Tl deposition efficiency on the Tl concentration in the electro bath. The deposition of ^{204}Tl is not significantly changed with increase in Tl content up to 500 μg which is evident from the graph. The deposition efficiency varies from about 95 % at 50 μg of Tl carrier and slightly increases to 97 % at 200 μg beyond which there is a slight decrease to 95 % at 500 μg . Hence, it can be inferred that the deposition efficiency of ^{204}Tl is more or less constant at about 95 % from 50 μg to 500 μg of Tl. The experimental results have been plotted and shown in the Fig.2.20.

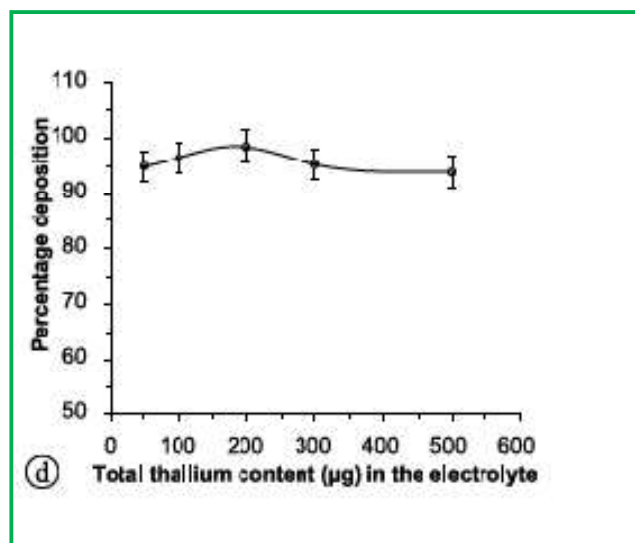


Fig. 2.20: Influence of thallium content in the electrolyte

2.3.4.8. Influence of Bath Temperature

The temperature of electro-bath is one of the crucial operating variables, which needs to be optimized. The effect of temperature on percentage ^{204}Tl deposition was investigated in the range 15–70°C and the result is depicted in Fig. 2.21. At low temperatures, the process is very slow. The deposition rate increases with increasing temperature. It can be seen from the results that maximum percentage deposition was achieved at 60°C. Beyond this temperature, there was no gain in deposition rate. Increasing the temperature of the solution increases the mobility of the Tl^+ ions, reduces the viscosity of the electrolyte, decreases polarization, increases concentration of metal in the cathode diffusion, all of which lead to the increase in deposition.

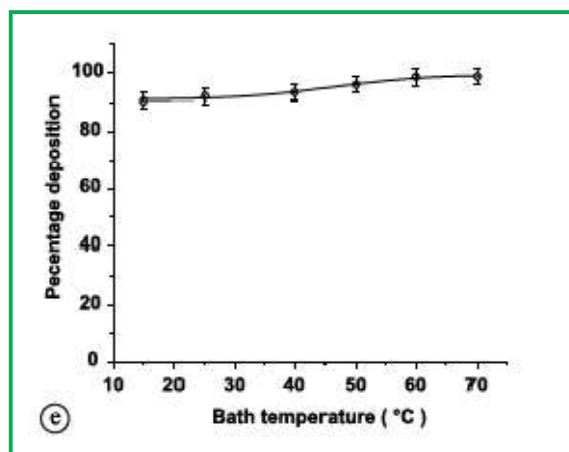


Fig. 2.21: Influence of bath temperature

2.3.5. SEM Analysis

SEM images of Tl-deposited surface and Tl-deposited surface coated with polymer at different magnification are shown in Fig. 2.22. The SEM image of Tl-deposited surface showed a uniform deposition with small granular crystals of Tl metal on the surface of the Cu substrate, indicating good adhesion with the copper backing. The sample at 5.0K magnification (Fig. 2.22(a)) showed various distinct areas, which could be due to Tl in agglomerated form.

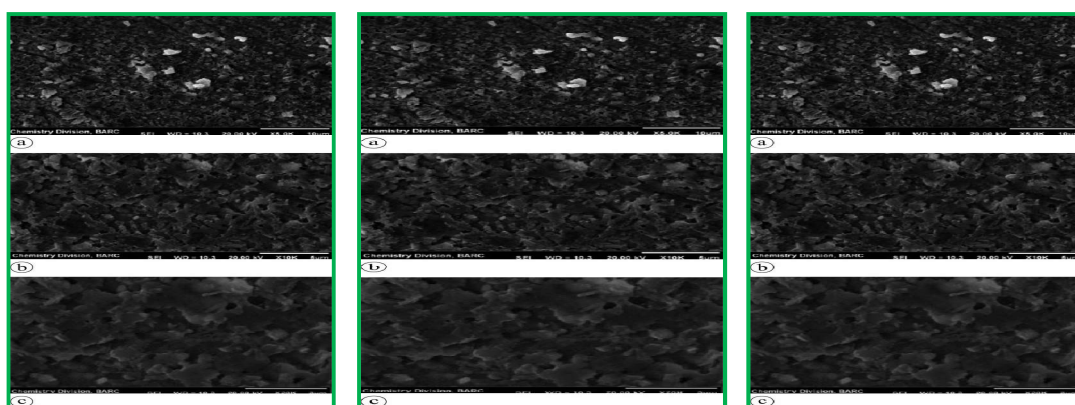


Fig.2.22: Scanning electron microscopy (SEM) images of Tl-deposited surface at different magnification (a) $\times 5.0\text{K}$ (b) $\times 10.0\text{K}$ (c) $\times 20.0\text{K}$

The surface morphology of the Tl- electrodeposited surface coated with polymer as seen through different magnification is depicted in Fig. 2.23. Compared with Fig. 2.22, the polymer coated Tl deposited surface exhibits a different morphology and surface feature. The coated particles are heavily agglomerated because of the polymer coating which acts as a binder. During the precipitation of the polymer, the entanglement of polymer chains between neighboring Tl particles binds them together, forming agglomerates as shown in Fig. 2.23. The polymer coated surface is composed of Tl grains of spherical to sub-spherical morphologies of discrete sizes and grains are grouped in an irregular fashion. During the process of agglomeration, the deposited particles combine together with each other on the substrate surface and form grains. Some of the smaller grains can combine together to form larger grains. The degree of agglomeration was known to be affected by several factors including the polymer weight fraction, polymer concentration, coating temperature etc.

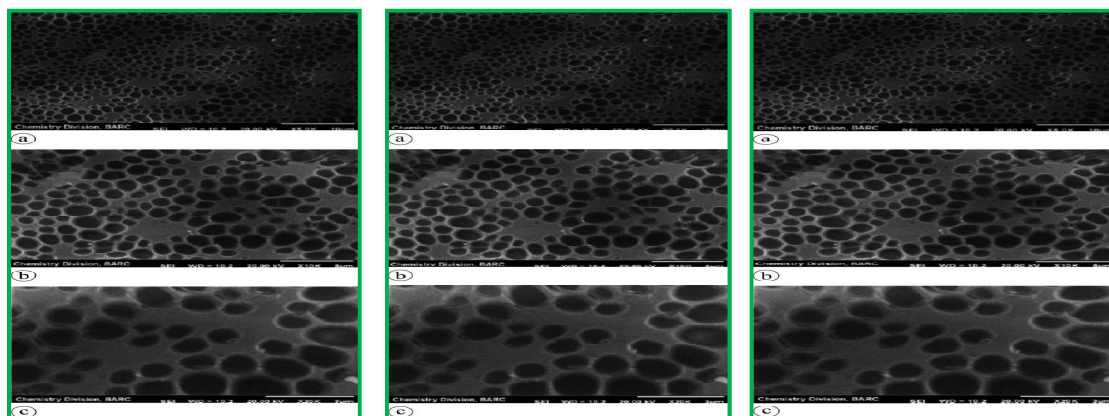
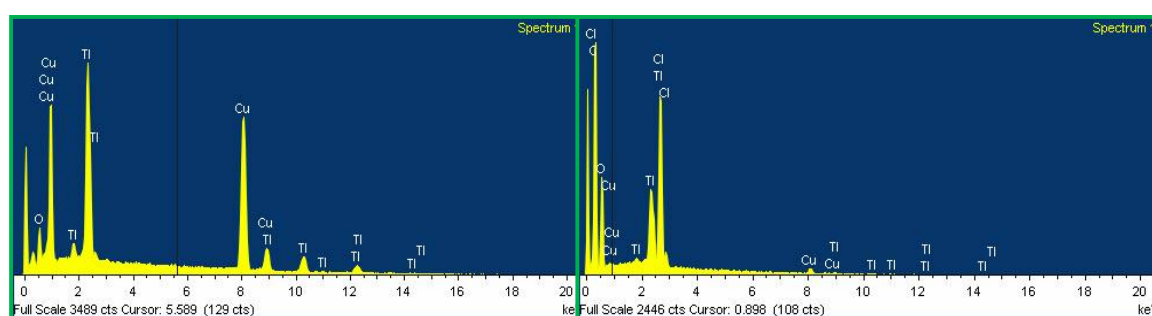


Fig. 2.23: Scanning electron microscopy (SEM) images of Tl-deposited polymer coated surface at different magnification (a) $\times 5.0\text{K}$ (b) $\times 10.0\text{K}$ (c) $\times 20.0\text{K}$

2.3.6. EDS characterization

Fig. 2.24(a) depicts the EDS spectrum of the electrodeposited Tl on the Cu substrate and Fig. 2.24(b) of the Tl deposited polymer coated sample. Fig.2.24(a) shows

peaks pertaining to Tl and Cu only which indicates coverage of Cu surface with Tl and the deposited surface is free from other chemical impurities. In order to ascertain the homogeneity of Tl deposited on the substrate surface, the EDS spectra were recorded at various locations and the quantification of results as weight percentage is given in Table-2.6. The results revealed that about 50% of the substrate surface is covered with Tl and the variation in distribution of Tl along the surface of the substrate is within $\pm 2\%$. It is seen from Fig. 2.24(b) that the deposited surface contains carbon, copper, oxygen and thallium. Table-2.7 depicts the elemental composition of the Tl electrodeposited substrate coated with polymer which indicates the presence of C in addition to O, Cu and Tl. The decrease in weight percentage of Cu compared to Tl electrodeposited substrate is attributed to the coverage of polymer.



(a)

(b)

Fig. 2.24: Energy dispersive X-ray (EDS) spectrum of
(a) Tl deposited surface (b) Tl deposited polymer coated surface

Table-2.6: Elemental composition of electrolytic deposit

| Position | Element (weight %) | | |
|-------------------------------|--------------------|------------------|------------------|
| | O | Cu | Tl |
| 1 | 10.00 | 50.66 | 39.35 |
| 2 | 11.51 | 48.33 | 40.16 |
| 3 | 10.8 | 49.54 | 39.66 |
| 4 | 9.76 | 51.52 | 38.72 |
| 5 | 11.57 | 48.03 | 40.4 |
| Mean \pm SD | 10.72 \pm 0.83 | 49.61 \pm 1.49 | 39.65 \pm 0.66 |
| Coefficient of variation (CV) | 7.78 | 3.0 | 1.68 |

CV = Standard deviation (SD)/Mean

Table-2.7: Elemental composition of the Tl electrodeposited substrate coated with PMMA

| Element | Weight % |
|---------|------------------|
| C | 62.61 \pm 1.02 |
| O | 29.57 \pm 0.60 |
| Cu | 1.04 \pm 0.02 |
| Tl | 6.78 \pm 0.13 |

2.3.7. Atomic Force Microscopy (AFM)

The surface roughness of Ni films was analyzed using atomic force microscopy (AFM) (2D and 3D images). Fig. 2.25 shows AFM image of the representative Tl electrodeposited sample on Cu substrate over a scan area of $12.5\ \mu\text{m} \times 12.5\ \mu\text{m}$. The AFM image

indicates that the Tl electrodeposited film surface is homogenous which is in corroboration with SEM findings. The deposited Tl layer is smooth with average roughness value of 107 ± 1 nm with mean square roughness (Rms) value of 171 ± 2 nm. The AFM images also reveal a layered deposition of Tl on Cu, which is desirable for imparting additional stability to the thin film on the substrate

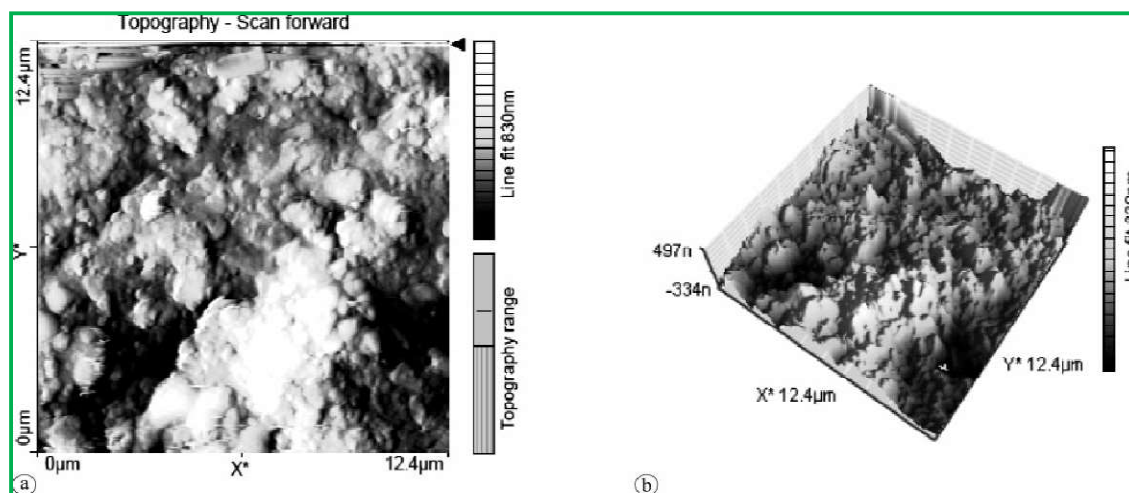


**Fig. 2.25: Atomic force microscopy (AFM) images of Tl deposited on Cu substrate
(a) 2D image (b) 3D image**

2.3.8. Preparation of ^{204}Tl Sources

Under the optimum conditions of electrolysis, several sources of activity content in the range of 3.7–4.44 MBq (0.1–0.12 mCi) were prepared and subjected to quality control tests as described below.

2.3.9. Quality Control

2.3.9.1. Activity Measurement

The indirect methods of measurement of ^{204}Tl activity by liquid scintillation counting (LSC) was adopted for calculating the total amount of activity deposited on the source matrix. Although LSC measurement undoubtedly gives the fraction of ^{204}Tl deposited in the course of electrolysis, it does not necessarily give the fraction remaining

on the substrate owing to the loss during washing or attenuation of radioactivity after polymer coating. The measurement of ^{204}Tl activity of the final source by ion chamber was used for quoting the total amount of activity deposited on the substrate.

2.3.9.2. Autoradiography Examination

In order to evaluate the distribution of ^{204}Tl deposited on the surface, autoradiography examination of three different sources was carried out. The blackening of the image on the photographic film was measured in terms of optical density and the optical density was taken as a measure of the local concentration of ^{204}Tl on the surface. The radiographic image obtained was circular in shape without any visible breakage and deletion indicating that ^{204}Tl was well covered to the circular surface of the substrate. The uniformity of the ^{204}Tl deposition was monitored by measuring the optical density at different positions of the film. The results obtained with three different sources are depicted in Table-2.8. The variation in distribution of ^{204}Tl along the surface of the substrate was within $\pm 3\%$ which corroborated the value obtained by the EDS technique. As values less than $\pm 5\%$ are acceptable, the source prepared by the above method meet the specification.

2.3.9.3. Leachability of Radioactivity

It is important that the ^{204}Tl deposited is firm and does not leach out. The results of leachability tests conducted on 5 randomly selected non-annealed source cores of ^{204}Tl indicated that $0.31 \pm 0.05\%$ of the original activity leached out in 48 h which was ~ 30 times more than the Atomic Energy Regulatory Board, India (AERB) norms [63]. One of the successful ways to avoid leaching was to incorporate a polymer barrier layer that minimizes the access of the leach solution to the ^{204}Tl deposited surface [76-78]. Polymer coating of the source was found to be effective in retarding the leachability to below

detection limit, which is within the limit prescribed by AERB, India. Such coating also protects the radioactive layer against mechanical abrasion or damage during application; hence it provides longer shelf-life to the source.

Table-2.8: Optical densities of the exposed radiographic film at different positions

| Position | Source 1 | Source 2 | Source 3 |
|-------------------------------|-----------------|-----------------|-----------------|
| 1 | 3.10 | 3.08 | 2.94 |
| 2 | 3.12 | 3.10 | 2.93 |
| 3 | 3.08 | 3.16 | 2.98 |
| 4 | 3.18 | 3.12 | 2.99 |
| 5 | 3.16 | 3.19 | 3.09 |
| 6 | 3.11 | 3.08 | 3.09 |
| 7 | 3.17 | 2.99 | 3.06 |
| 8 | 2.95 | 2.98 | 2.95 |
| 9 | 2.92 | 3.00 | 3.13 |
| 10 | 3.15 | 3.09 | 3.15 |
| Mean \pm SD | 3.09 \pm 0.09 | 3.07 \pm 0.07 | 3.03 \pm 0.08 |
| Coefficient of variation (CV) | 2.9 | 2.29 | 2.71 |

2.3.9.4. Swipe Test

Swipe test was performed on 5 randomly selected polymer coated sources containing 3.7–4.44 MBq (0.1–0.12 mCi) of activity. The result of the swipe test showed that 89 ± 18 Bq were found in the swipe, which is well within the specifications of 185 Bq laid by AERB [63]. Following the described procedure, several sources were prepared. The sources that qualified all the QC tests were finally supplied to the user's laboratory.

2.3.10. Discussion

Use of planar ^{204}Tl source for assessing the performance of beta surface contamination monitors is well known. Towards the preparation of an electrodeposited ^{204}Tl source, copper was chosen as the basic matrix owing to the attributes such as ready availability in high purity at a reasonable cost, radiation stability, adequate mechanical strength, durability in extreme environments and suitable electro potential for deposition of Tl. The thickness of the copper substrate should be sufficient to retain its shape in the source holder without distortion but at the same time it should not be too thick to make the source bulky. Standard reduction potential for thallium and copper are -0.34 V and $+0.34\text{ V}$ [92]. Tl has a high hydrogen overpotential, which means that it can be deposited electrolytically from acidic solutions. Use of copper cathode material will drive the hydrogen over potential higher and thus favoring ^{204}Tl deposition. Platinum was used as the anode material as it is inert, stable and does not passivate easily. Acid based electrolyte was preferred as it possesses high solution conductivity. The use of sulphate bath was logical as the SO_4^{2-} anion is neither reduced at the cathode nor oxidized at the anode and at the same time permits operation at low current density. In the electrolyte, the SO_4^{2-} anion provides strength and H_3BO_3 inhibits hydrogen evolution at far negative potentials [94, 95]. The optimized process successfully addresses several issues such as preparation of copper substrate of defined geometry and size, electrochemical deposition of ^{204}Tl onto the targeted area of the substrate, coating the radioactive area with a thin layer of polymer, mounting the source in a holder and quality control of the source to comply with the regulatory norm. The convenience of depositing homogeneously required quantities of ^{204}Tl activity on a metallic substrate of defined geometry coupled with the ease of use and simplicity of electrochemical approach constitute the novelty of

the reported technique. It is pertinent to note that the ^{204}Tl sources prepared by the reported procedure were found to be effective in the routine performance evaluation of beta surface contamination monitors.

2.3.11. Conclusion and Scope of the Work

The objective of preparing planar disc source of ^{204}Tl utilizing electrodeposition technique with precise control of radioactivity content, commensurate with the specifications and compliant with the mandatory requirement for safe handling during applications could be successfully achieved. The efficiency of the process and product quality could be amply demonstrated. The reported method represents a novel method for the preparation of ^{204}Tl source for use with beta contamination monitors.

CHAPTER-3

A Two-Step Electrochemical Process for the Preparation of ^{133}Ba and $^{90}\text{Sr}/^{90}\text{Y}$ Sources for Calibration of Instruments

“If your experiment needs statistics, you ought to have done a better experiment.”

-Ernest Rutherford

3.1. A Novel and Facile Approach for the Preparation of ^{133}Ba Source Core, Encapsulation and Quality Evaluation towards its Use in Calibration of Instruments

This chapter describes the utilization of two-step electrodeposition technique for the preparation of electrodeposited sources of ^{133}Ba and $^{90}\text{Sr}/^{90}\text{Y}$ for the calibration of dose calibrators and beta surface contamination monitors respectively.

3.1.1. Introduction

Treatment of hyperthyroidism using ^{131}I is one of the oldest and most commonly practiced therapeutic modality [96–98]. Measurement of ^{131}I activity prior to therapy is generally carried out using well-type dose calibrators. Before the dose calibrator is put into service, verification of its performance in terms of sensitivity, constancy and accuracy is extremely important. In order to evaluate the performance of the dose calibrators, sealed radioactive sources containing long-lived surrogate radionuclides with appropriate photon emission are required. In this context, ^{133}Ba which emits gamma-rays of 81.0 keV (32.9%), 276.4 keV (7.17%), 302.9 keV (18.3%), 356.0 keV (62.0%) and 383.9 keV (8.93%) with a half-life of 10.53 years is considered as an ideal surrogate to ^{131}I as the γ photon energies of ^{133}Ba are close to that of ^{131}I [99–102]. Hence, towards use in the calibration of the dose calibrators preparation of sealed ^{133}Ba source of overall dimensions 5.8 mm (\varnothing) \times 15 mm (l) containing $\sim 3.7\text{--}11.1$ MBq (0.1–0.3 mCi) of ^{133}Ba activity was undertaken. Over the past few years, several need-based strategies have been developed in our laboratory for the preparation of a variety of radioactive sources for different applications [40, 44, 67–71, 76, 78]. Amongst the various methods used, electrodeposition was considered as the suitable pathway for the present work. Barium, an alkaline earth metal, is a powerful reducing agent and is unstable in aqueous solutions of

any pH. The low solution potentials and the difficulty encountered in controlling the electrolytic-deposition on a metallic cathode have been the major impediments to realize the electrodeposition of ^{133}Ba from an aqueous solution. In order to circumvent such drawbacks, a different methodology is to be pursued in which Ba could be deposited on a reactive substrate. In this context, the possibility of using a titanate substrate to deposit ^{133}Ba from an aqueous solution in the form of barium titanate seemed to be an interesting proposition as there are a few reports to support its effectiveness [103-107]. In the quest for an effective method to prepare the titanate anodization technique was chosen owing to its simplicity, efficacy and rapidity. While the use of anodized titanium substrate to incorporate hydroxyapatite (HA) for its utility as implants in dental and in orthopedic surgical treatments have been extensively reported [108-110], the utility of this substrate in the electrodeposition of Ba from an aqueous solution has not yet been explored. In order to tap the potential of anodized titanium as an effective substrate, we evaluated the suitability of this substrate for the electrodeposition of ^{133}Ba . In the first section of this chapter, an electrochemical technique for the deposition of ^{133}Ba from an aqueous solution onto the surface of an anodized titanium substrate is reported. The factors that influence the electrodeposition of ^{133}Ba onto the anodized titanium were identified and careful controls of the experimental parameters were exercised to arrive at the conditions for optimum deposition of ^{133}Ba activity. Evaluation of the quality of the ^{133}Ba source core, design and fabrication of titanium capsule, process of encapsulation and quality evaluation of sealed sources are also described in this chapter.

3.1.2. Materials

Barium-133 as $^{133}\text{Ba}(\text{NO}_3)_2$ of specific activity 196 GBq (5.3 Ci)/g was obtained from M/s. Polatom, Poland. Reagents such as H_3PO_4 , HF, NaF and NaNO_3 were of

spectroscopic grade and were procured from BDH (India). Polystyrene granules of analytical grade were procured from BDH (India). Titanium metal rods were obtained from M/s. MIDHANI, Hyderabad, India. Platinum metal foil of high purity (99.99 % purity) with material testing certificates, were procured from M/s. Hindustan Platinum Ltd., Mumbai, India. The source capsules were fabricated from titanium metal rods. High purity (99.99 %) argon gas was procured from M/s. Kolhapur Oxygen & Acetylene Private Limited, Kolhapur, India. A D.C. power supply with 100 V compliance, a maximum current of 2 A, 1.2 nA current resolution and $> 10^{13} \Omega$ input impedance was used for anodization experiments. The microstructural features of the anodized samples were analyzed using a Scanning Electron Microscope (SERON, Model AIS-2100). Energy Dispersive X-ray microanalysis technique (Oxford, Model INCA E350) was used to identify the elemental constituents of the sample. A HPGe detector connected to a multichannel analyzer was used for activity estimation. Radiation dose on the surface of the source core was measured using a dose rate meter (Teletector 6112M, M/s. Automess, Ladenberg, Germany). Optical density measurements were carried out using a transmission densitometer. Cotton wool samples of Wipe test and water samples of Immersion test were counted in a NaI (TI) scintillation counter (Model PNS-2, Electronic Enterprises (I) Pvt. Ltd, Mumbai, India). Radioactivity measurements of the sealed sources were carried out using a well-type pre-calibrated ionization chamber (Centronic IG12/A20, Centronic Ltd., New Addington, UK).

3.1.3. Experimental

3.1.3.1. Pretreatment of Titanium Rods

Titanium rods of dimensions 4.8 mm (\varnothing) \times 10 mm (l) were used to grow the anodic porous layers following the reported procedure [108]. The anodic oxidation was

performed under a constant applied potential of 20 V using a DC power supply employing a platinum foil counter electrode as cathode. The electrolyte solution consisted of a mixture of 10 mL 0.5 M H_3PO_4 and 5 mL of 0.15 M NaF in water. The anodization was carried out for about 60 min at room temperature. The anodized Ti sample was then heated at 500°C for about 2 h. The cleaned titanium rods were used as the cathode during electrodeposition of ^{133}Ba . Platinum foil of the same surface area was used as anode.

3.1.3.2. Electrochemical Deposition of ^{133}Ba onto Anodized Titanium Rod

The electrochemical cell was made from a quartz cylinder of 25 mL capacity. The electrodes were adjusted parallel to each other separated 10 mm apart on the acrylic cap and immersed in the electrolyte. Platinum and titanium electrodes were connected to the power supply using small screws, embedded on the top end. A provision was made for passing Ar gas (at the rate of 0.05 cc/sec) through a glass tube ($\text{Ø} = 1 \text{ mm}$) into the electrolyte and a small outlet of $\sim 2.5 \text{ mm}$ (Ø) was provided through the acrylic cap for venting out the gases liberated during electrolysis. The schematic diagram of the arrangement is shown in Fig. 3.1.

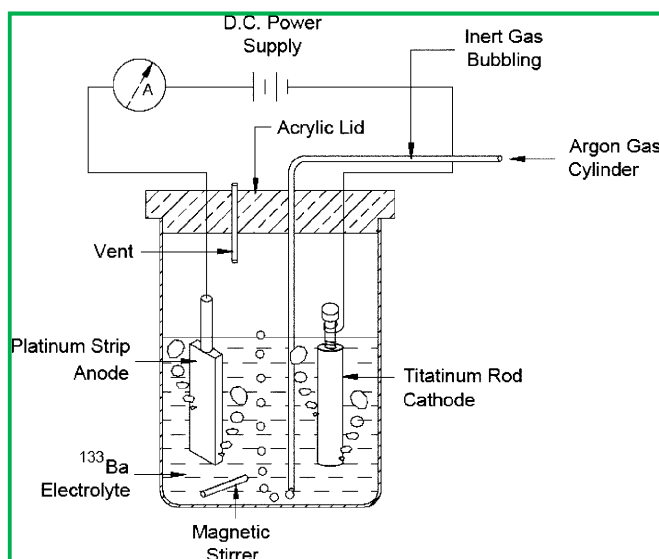


Fig. 3.1: Schematic diagram of the electrochemical cell set-up for ^{133}Ba deposition

Electrodeposition of ^{133}Ba was carried out at room temperature using 15.0 mL of electrolyte with 0.04 M $\text{Ba}(\text{NO}_3)_2$ with required quantities of ^{133}Ba and 0.1 M NaNO_3 at a constant potential of 10–12 V

3.1.3.3. Optimization of Electrodeposition Parameters

In order to obtain the best possible ^{133}Ba deposition yield, the electrodeposition experiments were performed by varying the experimental parameters as follows: pH of the electrolyte bath in the range of 1.0–5.0, current density 10 to 50 $\text{mA}\cdot\text{cm}^{-2}$, temperature of electrolyte from 25°C to 60°C and deposition time 1–5 h. The amount of ^{133}Ba deposited was estimated as the difference in the ratio of the solution before and after deposition. The percent deposition (%) was calculated using the relationship

$$\% \text{ Deposition} = (A_i - A_f) / A_i \times 100$$

Where A_i and A_f are the initial and final radioactivity of ^{133}Ba , respectively.

3.1.3.4. SEM and EDS Analysis

SEM analysis was carried out using a non-radioactive source prepared in an identical manner using inactive barium. Evaluation of the uniformity of distribution of barium along the surface of the substrate was also achieved from the Energy Dispersive X-ray spectra (EDS) of the deposited Ba layer.

3.1.3.5. Preparation of Source Core

The required quantity of ^{133}Ba activity as $\text{Ba}(\text{NO}_3)_2$ of specific activity 196 GBq (5.3 Ci)/g was pipetted out from the original stock solution to prepare the sources. Toward this, 12.75 mg of NaNO_3 and appropriate amount of non-radioactive barium as $\text{Ba}(\text{NO}_3)_2$ as cold carrier was added so that total content of Ba in the final solution remains 200 μg , followed by the addition of 1 mL of Conc. HNO_3 . The amount of barium as cold carrier used in the preparation of electrolyte is given in the Table 3.1.

Table-3.1: Amount of cold barium carrier used for the preparation of different source strength

| Targeted source strength MBq (μCi) | Feed activity ^{133}Ba MBq (μCi) | Amount of ^{133}Ba (μg) | Amount of cold Ba added (μg) | Total Ba Content (μg) |
|---|--|---|---|------------------------------------|
| 3.7(100) | 4.25(115) | 21.69 | 178.31 | 200 |
| 5.55(150) | 6.29(170) | 32.06 | 167.94 | 200 |
| 9.25(250) | 10.36(280) | 52.83 | 147.17 | 200 |
| 11.1(300) | 12.39(335) | 63.19 | 136.81 | 200 |

The resulting solution was evaporated to dryness and made up to 15 mL with water. The pH of the electrolyte was brought to ~ 5 by the drop-wise addition of 0.01 M H_2SO_4 or 0.01 M NaOH . Electrodeposition of ^{133}Ba was carried out at a potential of 10–12 V maintaining a current density of about $50 \text{ mA}\cdot\text{cm}^{-2}$ for 5 h at a temperature of 50°C . After electrodeposition, the samples were rinsed in DD water, dried under an I.R. lamp and heated to $250\text{--}300^\circ\text{C}$ in an oven for 20 min and subsequently cooled to room temperature. A single rod was electrodeposited with ^{133}Ba in each batch of experiment. The Titanium rod containing ^{133}Ba activity was coated with polystyrene as per the reported procedure [102].

3.1.3.6. Assay of Activity of the Source Core

High resolution gamma ray spectrometry using HPGe detector and a ^{152}Eu standard source for energy and efficiency calibration was used for assay of ^{133}Ba activity in the electrolytic bath before and after electrolysis. Aliquots of the electrolyte were measured for appropriate time at a suitable geometry and the counts acquired under the

356 keV photo-peak was used. The amount of ^{133}Ba activity deposited on the cathode was calculated from the difference of activity in the bath before and after electrodeposition. This method was also utilized to follow the progress of ^{133}Ba deposition on the substrate during electrodeposition. Accurate assay of the activity on the sources was carried out using an ion chamber calibrated with standard ^{133}Ba sources.

3.1.3.7. Encapsulation

A cylindrical capsule of dimensions 5.8 mm (\varnothing) \times 15 mm (l) made up of titanium was designed to accommodate the ^{133}Ba source core in the cavity. The capsule assembly contains two pieces, the capsule ‘body’ in the form of a small cylinder closed at one end and the ‘cap’ which fits tightly over the open end of the ‘body’. Each capsule used for making sources is machined from a single piece of titanium metal. Prior to encapsulation, the capsules were cleaned for removal of oxide layer and ultrasonically washed subsequently with acetone to remove micro-debris. The ^{133}Ba source core was placed inside the capsule and closed by placing the cap tightly which needs to be joined together by circular welding from the capsule’s top. The cap and body were assembled together as tightly as possible and fixed on the welding fixture. The cylindrical design allows the source to be sealed by a continuous weld. Micro TIG (argon-arc) welding using a micro torch was used for encapsulation as the thickness of the capsule is sufficient to cause minimal distortion of the capsule and curtails the dispersion of radioactivity. The tungsten electrode and the mating surface of titanium capsule to be welded are connected to a DC power supply in such a manner that the former serves as the cathode and the latter serves as the anode. This is to facilitate cooling the tungsten electrode heating the titanium capsule being welded into which electrons flow. The welding fixture was designed to rotate the capsule during welding. The welding torch was focused to the weld joint

vertically. The welding arrangement for the encapsulation of ^{133}Ba sources is schematically depicted in Fig. 3.2. The welding parameters such as distance between welding torch and the capsule, welding current, arc voltage, welding speed along with rotation of the capsule including inert gas supply etc. were systematically optimized through a series of cold mock-up tests using a set of cold capsules to obtain best possible weld. The welded capsules were subjected to leak test to assess the welding integrity. The welded sources were then ultrasonically cleaned to remove any traces of contamination during welding.

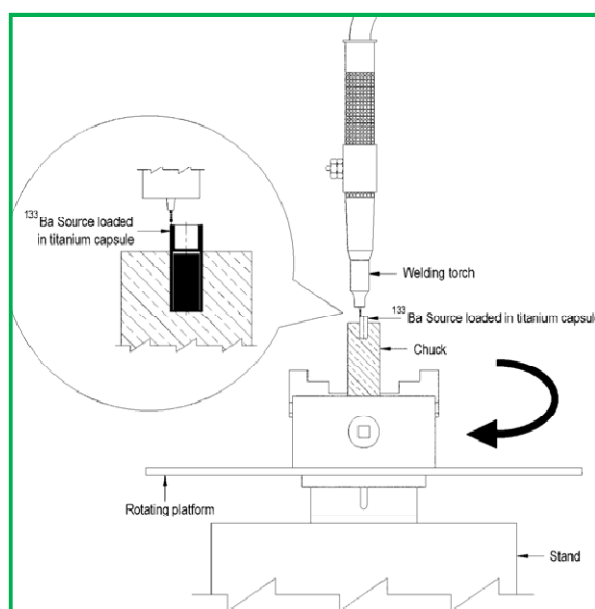


Fig. 3.2: Welding set up for the encapsulation of ^{133}Ba sources.

3.1.4. Quality Control

3.1.4.1. Testing of the Source Core

The ^{133}Ba source core was tested for leachable activity as per the reported procedures [78]. Distribution of ^{133}Ba activity on the surface was examined by autoradiography using a specially designed brass circular disc (4.4 cm dia., 1.4 cm thick)

with a central hole of 5 mm diameter and 12 mm depth and following the reported technique [75].

3.1.4.2. Testing of the Sealed Sources

Swipe test, leakage test and immersion test of the prepared ^{133}Ba sources were performed as per the reported method [78]. Radioactivity content of the sealed sources was measured using a well type ionization chamber calibrated with a standard ^{133}Ba source of known activity.

3.1.5. Results

The primary objective of this study consisted in exploring a viable pathway for the preparation of ^{133}Ba source core of 4.8 mm (\varnothing) \times 10 mm (l) which can be encapsulated in a capsule for their use. The creation of porous reactive surface on the titanium substrate by anodization is necessary to electrodeposit ^{133}Ba from an aqueous solution. The electrolyte composition was formulated based on a reported method [108].

3.1.5.1. Optimization of Electrodeposition Parameters

The influence of experimental parameters such as pH of the electrolyte, applied current density, deposition time, bath temperature and barium content in the electrolyte on the electrodeposition of ^{133}Ba on the anodized titanium rod needed to be systematically investigated in order to arrive at the conditions for the optimum deposition of ^{133}Ba .

3.1.5.2. Influence of pH of the Electro-bath

The effect of pH of the electro-bath on the electrodeposition of ^{133}Ba was studied with an aim to determine the optimum conditions wherein percentage of ^{133}Ba deposition could be maximized. The pH of the bath was varied from 1 to 5 and the influence of pH on the electrodeposition of ^{133}Ba is shown in Fig. 3.3(a).

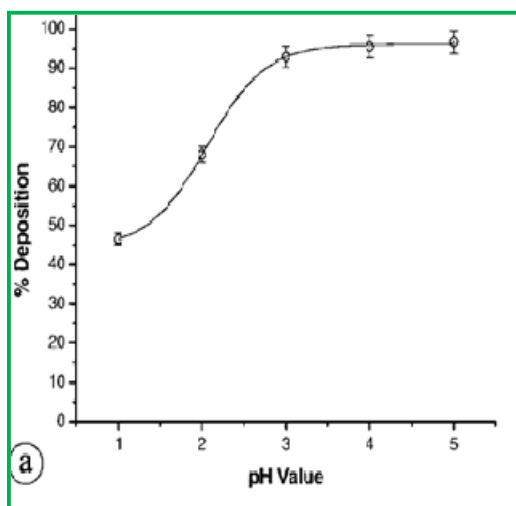


Fig. 3.3(a): Influence of pH of the electrolyte

It can be seen from the Figure that, within the range of pH investigated, the percentage of deposition of ^{133}Ba increased with increasing pH and the deposition was best at pH 4 and 5. Hence pH 5 was selected as the optimum pH for the preparation of sources.

3.1.5.3. Influence of Current Density

Results of the experiments carried out to study the influence of current density on the electro deposition of ^{133}Ba are shown in Fig. 3.3(b).

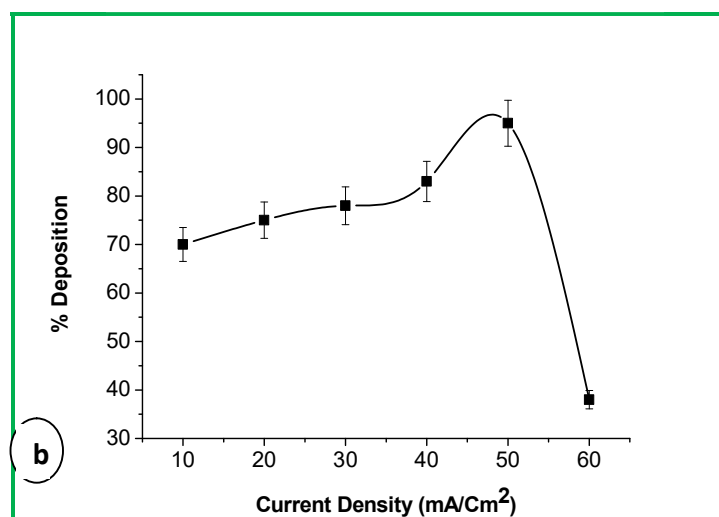


Fig. 3.3(b): Influence of current Density

It can be inferred from the above figure that the percentage of ^{133}Ba deposition increased initially with increasing current density up to 50 mA.cm^{-2} and thereafter decreased with further increase in current density. At low current density or low over-potential, the percentage of ^{133}Ba deposition decreased due to competitive reaction or proton reduction. With the rise in current density the percentage of ^{133}Ba deposition increased and reached a maximum value at 50 mA.cm^{-2} . When the current density was increased beyond 50 mA.cm^{-2} , the percentage of ^{133}Ba deposition was slightly decreased because of hydrogen evolution. The most likely reason for the decrease in the percentage of ^{133}Ba deposition beyond a current density 50 mA.cm^{-2} may be due to the decrease of deposition force and the increase of the cathodic polarization resistance. This indicated the need to maintain the current density at 50 mA.cm^{-2} to obtain nearly quantitative deposition of ^{133}Ba .

3.1.5.4. Influence of Deposition Time

The percentage of ^{133}Ba deposition was also found to be influenced by the deposition time. The effect of deposition time was studied and the results are depicted in Fig. 3.3(c).

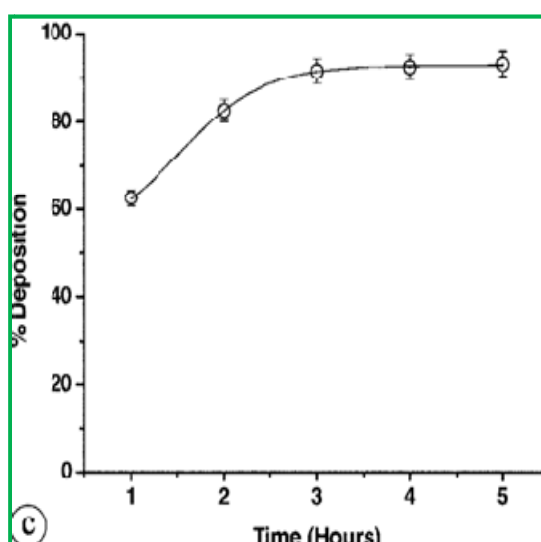


Fig. 3.3(c): Influence of deposition time

It is seen that, within the range of deposition time investigated at a constant current density of 50 mA.cm^{-2} at $\text{pH} \sim 5$, the percentage of ^{133}Ba deposition on the treated surface of the substrate increased with increasing contact time and remain constant after 5 hours.

3.1.5.5. Influence of Temperature

The influence of temperature of the electrolyte bath on the deposition of ^{133}Ba was also investigated and the results are depicted in Fig. 3.3(d). It is apparent from the graph that percentage of ^{133}Ba deposition increased with increase in bath temperature and remained constant at 50°C . From this experiment, the optimum bath temperature was found to be 50°C . It can be concluded that the increase in the temperature of the solution resulted in an increase in the mobility of the Ba ions which in turn enhanced the percentage of ^{133}Ba deposition. The results of these experiments provided the basis for selection of the optimized experimental parameters for preparation of the ^{133}Ba sources.

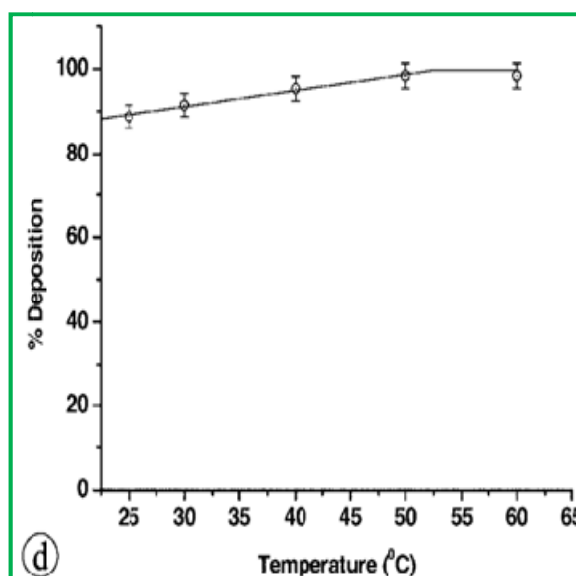


Fig. 3.3(d): Influence of bath temperature

3.1.6. Morphology Studies

3.1.6.1. SEM Analysis

The morphology of the anodized titanium surface as seen through the SEM images is depicted in Fig. 3.4(a). Fig. 3.4(a) shows the development of a coarse porous layer that bonded strongly to the matrix. This reactive surface of the titania promotes adherent deposition of ^{133}Ba ion on the substrate. The micrographs of Ba deposited anodized titanium substrate is shown in Fig. 3.4(b). It was observed that the titania surface is covered with electrodeposited Ba.

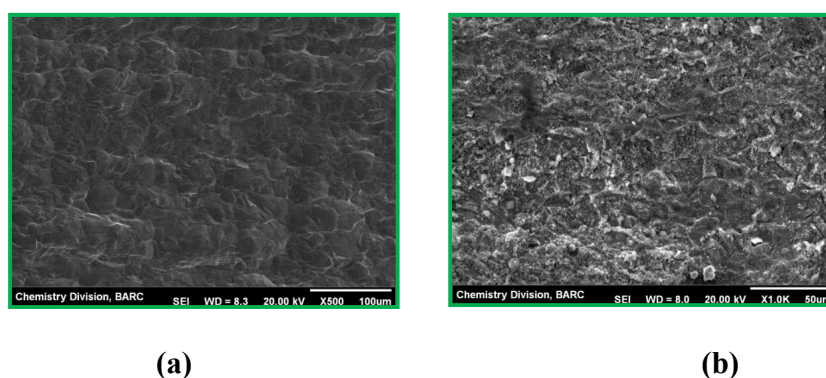


Fig. 3.4: SEM micrograph of (a) Anodized titanium rod (b) Barium deposited anodized titanium rod.

3.1.6.2. EDS Characterization

EDS measurement of the specimens was performed to examine the surface composition of the substrate. The EDS spectrum of anodized titanium as shown in Fig. 3.5 showed peaks of O and Ti on the surface indicating that the surface was titania rather than titanium. The EDS spectrum of electrodeposited anodized titanium substrate as shown in Fig. 3.6 showed peaks of Ba in addition to Ti and O. As EDS analysis is only confined to the top surface of the sample of few microns depth, this result has demonstrated the retention of Ba on the exterior surface rather than in the bulk. The elemental composition of the electrodeposited surface as weight percentage was

calculated from the intensity of the photo peaks of the EDS spectra. The elemental composition of electrodeposited surface in terms of weight percentage was found out to be 10.15 % of Ba, 43.54 % of Ti and 46.31 % of O as shown in Table-3.2 given below. In order to ascertain the homogeneity of Ba in the deposited film, the EDS spectra were recorded at various locations. The result of the element mappings of Ba at different points of electrodeposited sample showed that variation in concentration of Ba along the surface of the substrate was within ± 3.18 % indicating reasonably good uniformity of deposition of Ba on the surface of the titanate substrate.

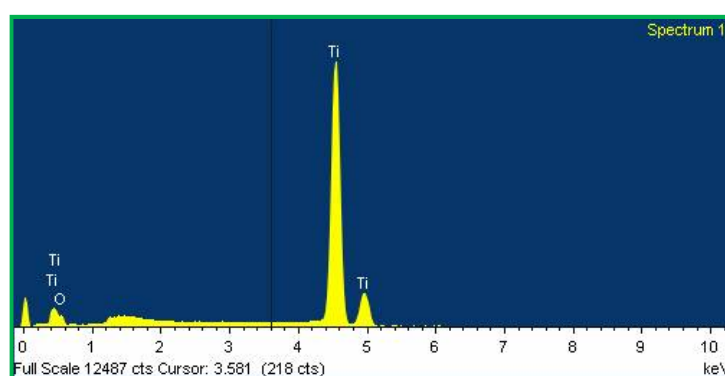


Fig. 3.5: EDS spectrum of anodized titanium rod

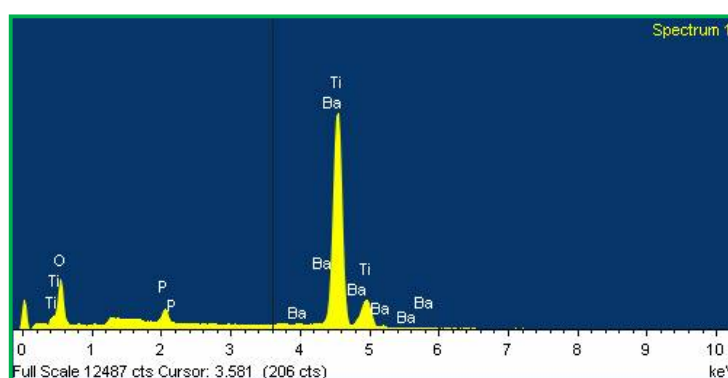


Fig. 3.6: EDS spectrum of barium deposited titanium rod.

Table-3.2: Chemical deposition of Ba deposited Titanium rod

| Sr. No. | Elements | Intensity | Weight % |
|---------|---------------|-----------|----------|
| 1. | Oxygen(O) | 0.3354 | 46.31 |
| 3. | Titanium(Ti) | 0.9086 | 43.54 |
| 3. | Barium(Ba) | 0.9060 | 10.15 |

3.1.6.3. Preparation of ^{133}Ba Source Cores of Different Strengths

Following the optimized conditions, several sources of different strengths were prepared. Results of electrodeposition experiments carried out in 4 batches are presented in Table-3.3. It can be seen that the efficiency of ^{133}Ba electrodeposition did not differ markedly from batch to batch and was always $> 90\%$. The amount of ^{133}Ba activity that can be deposited on the substrate can be therefore tailored as per the need.

Table-3.3: ^{133}Ba deposition efficiency in the preparation of ^{133}Ba sources of different strengths

| ^{133}Ba activity in the feed MBq (μCi) | ^{133}Ba activity deposited on the substrate MBq (μCi) | Deposition Efficiency (%) |
|--|---|------------------------------|
| 4.25(115) | 3.91(105.8) | 92.00 |
| 6.29(170) | 5.69(153.8) | 90.50 |
| 10.36(280) | 9.44(255.4) | 91.12 |
| 12.39(335) | 11.26(304.4) | 90.87 |

3.1.7. Quality Evaluation of Source Core

3.1.7.1. Leachability

The results of leachability tests conducted on 5 randomly selected source cores of ^{133}Ba indicated that $0.2 \pm 0.1\%$ of the original activity leached out in 48 h, which was 17

times more than the norms of AERB [63]. Hence the sources were coated with a polymer such as polystyrene, to retard the leaching. The concentration of polystyrene in benzene was optimized by conducting a series of experiments. In order to have a thin and firm coating of polystyrene on the source, a concentration of 150 mg.mL^{-1} of polystyrene was found to be practically most suitable. Polystyrene coating of the ^{133}Ba electrodeposited sources reduced the leachability to below detection limit, which complied with the specifications laid down by AERB, India [63].

3.1.7.2. Autoradiography Examination

In the autoradiography study, the source core was kept in a specially made gadget [75]. The optical densities (OD) of the exposed radiographic film was measured at various locations and the OD values varied with a mean value of 2.13 ± 0.03 , Table-3.4 indicating good uniformity of radioactivity deposition on the source core.

Table-3.4: Optical density variations

| Sr. No. | Optical Density |
|-----------|-----------------|
| 1. | 2.13 |
| 2. | 2.09 |
| 3. | 2..17 |
| 4. | 2..15 |
| 5. | 2.10 |
| Mean/S. D | 2.13 ± 0.03 |

3.1.7.3. Encapsulation

In order to contain the radioactive source core in a capsule, encapsulation technique was used. It involves the following steps such as (i) design of the capsule, (ii) fabrication of the capsule conforming to the design (iii) assembly of the source core inside the capsule and (iv) hermetic sealing of the capsule by TIG welding. Cylindrical capsule design was conceived as it would offer the convenience of source core assembly with minimum manipulation which in turns reduces time of exposure. Titanium was selected as capsule material owing to its attributes such as high strength to weight ratio, radiation stability, excellent corrosion resistance, good thermal conductivity, adequate mechanical strength and amenability to easy welding. The wall thickness of the titanium capsule was configured to provide adequate mechanical strength as well as the required radiation output. While designing the titanium capsule, attention was given to make the inner cavity of the capsule free from angularities. The design of the titanium capsule offered the convenience of sealing one end by welding. Titanium capsules conforming to the dimension and quality were used for encapsulation. Prior to assembly of the source core inside the capsule, it is very important to remove oxides from the mating parts as the oxide layer melts at a higher temperature than titanium and can enter the molten weld pool to create inclusions that weaken the weld. The process of source core assembly in the capsule is depicted in Fig. 3.7. In order to prevent contamination with oxygen and to avoid degradation of the welded portion the heat affected welding zones were shielded from the external atmosphere until temperatures dropped below 400°C . High purity argon (99.99 %) was used as the shielding gas to preclude the risk of oxygen contamination. The capsule after welding was converted into a single structure as a result of the fusion of titanium metal at the mating zone.

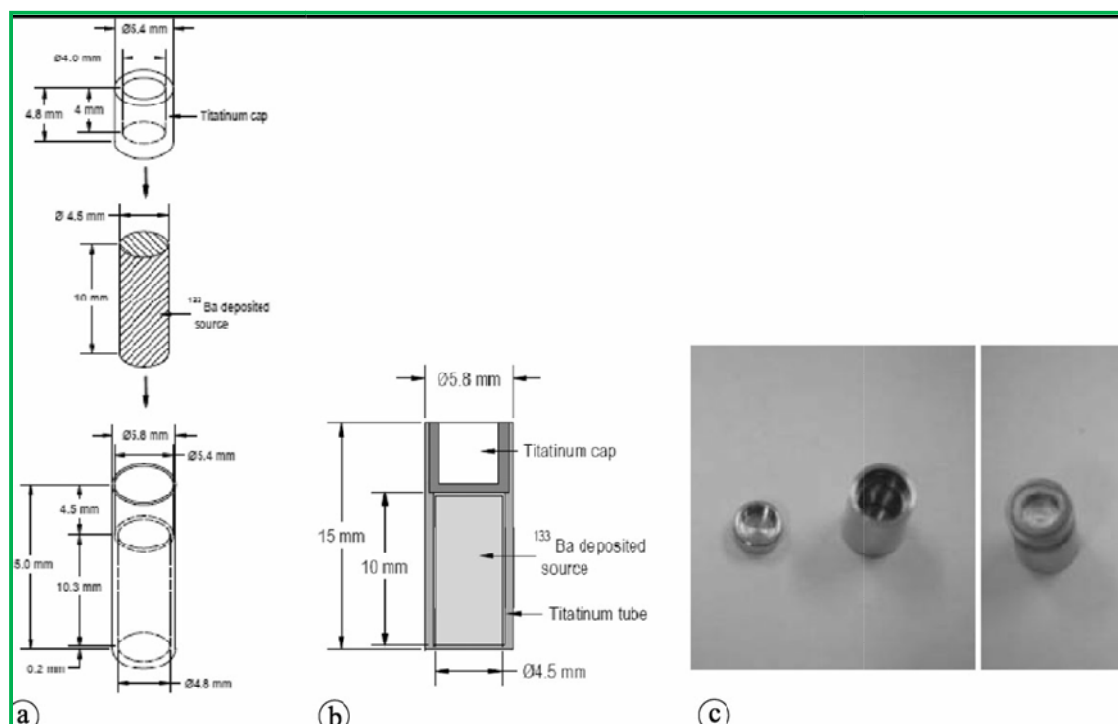


Fig. 3.7: Barium-133 source core assembly in a cylindrical titanium capsule

(a) Loading of source core in the capsule (b) Assembled source (c) Photograph of the capsule and source

3.1.7.4. Quality Control of Sealed Sources

The activity of the sealed ^{133}Ba sources was determined using a well-type ionization chamber [111]. Experimental measurement of activities of source cores and sealed sources revealed that 5-10% of the activity is attenuated by the titanium capsules. All the sources prepared were subjected to quality control tests to ensure their safety as well as to preclude the spread of contamination during the handling of the source. Results of immersion test and surface contamination test revealed that the removable/released radioactivity levels from the encapsulated sources were much below the AERB stipulated permissible levels of 185 Bq (5 nCi) and the sources were also found to be leak-proof. Upon satisfactory compliance with the regulatory requirements of AERB, these sources were supplied to the user's laboratory.

3.1.8. Discussion

The eight day half-life of ^{131}I precludes its use in the preparation of sealed sources required for the regular performance evaluation of dose calibrators. Although the decay properties of ^{133}Ba are not exactly identical to those of ^{131}I , there are some similarities the two radioisotopes that permit the use of ^{133}Ba as a surrogate for ^{131}I . Although the counting efficiency of ^{131}I would be greater than that of ^{133}Ba owing to the higher yield of photons in the region of interest, it could be surmounted by incorporating necessary correction factors amenable for routine performance evaluation of dose calibrators. Anodized titanium substrate was chosen to realize the electrodeposition of ^{133}Ba from aqueous solution. Anodization of titanium substrate facilitates the formation of a thin, porous, reactive, hydrophilic and conductive titanium oxide film over the metallic titanium surface. The capability to deposit the required quantity of ^{133}Ba and to achieve uniform distribution of radioactivity on the substrate are the major advantages of this technique. In view of the long half-life of ^{133}Ba (10.5 y), the shelf-life of the source is quite long and it is desirable to conduct a reliable quality assessment of encapsulated source to permit their safe use during its life time. To the best of our knowledge, this is the first report on the use of anodized titanium substrate for the preparation of a radioactive source.

3.1.9. Conclusion

The objective of preparing sealed ^{133}Ba sources commensurate with the specifications for use and compliant with the mandatory regulatory requirements has been achieved. The potential utility of anodized titanium rod for the preparation of ^{133}Ba source using electrodeposition process could be demonstrated.

3.2. An Electrochemical Pathway to Prepare Circular Planar $^{90}\text{Sr}/^{90}\text{Y}$ Sources for Calibration of Surface Contamination Monitors

3.2.1. Introduction

The role of beta surface contamination monitors for routine monitoring and controlling of contamination levels of beta emitting radionuclides in the working areas of radioactive laboratories needs hardly to be reiterated. While the use of beta surface contamination monitors is essential for monitoring and controlling inadvertent spread of beta radioactive contamination, validation of sensitivity, constancy and accuracy of a measurement needs to be carried out regularly to ensure constancy of the instrument's response to the beta radionuclide contaminants. This objective is primarily achieved through the use of an external radioactive calibration source containing a long lived beta emitting radionuclide [112]. In this context, the scope of using beta emitting radionuclides such as ^{14}C , ^{147}Pm , ^{204}Tl , $^{90}\text{Sr}/^{90}\text{Y}$ and $^{106}\text{Ru}/^{106}\text{Rh}$, having $E_{\beta\text{-max}}$ of 0.16, 0.24, 0.76, 2.27 and 3.54 MeV respectively for the preparation of radioactive calibration sources merits attention [113,114]. The suitability of these beta emitting radionuclides for the application is primarily attributable to their ability to provide traceable beta particle flux of known energy over a longer period of time. Towards evaluation of the performance of beta surface contamination monitors, preparation of a circular planar source of $^{90}\text{Sr}/^{90}\text{Y}$ was undertaken. ^{90}Sr , a pure beta emitter, decays into ^{90}Y with beta energy of maximum 0.546 MeV and a half-life of 28.8 years. ^{90}Y too, is a pure beta-emitter with a shorter half-life of 64.1 h and has considerably higher maximum beta energy of 2.28 MeV. The source required for this application consisted of a flat circular planar disc of 16 mm (\varnothing) on which ~ 3.7 MBq (~ 100 μCi) of ^{90}Sr activity is required to be homogeneously deposited. In pursuit of a practical approach to undertake the routine preparation of circular planar

$^{90}\text{Sr}/^{90}\text{Y}$ sources for the above application. Electrodeposition technique was chosen due to its technical simplicity and reproducibility [44, 66-68, 73, 78]. While the electrodeposition technique has been used for the preparation of a variety of radioactive sources containing different radioisotopes [44, 66-68, 73, 78], electrodeposition of ^{90}Sr from ionic state to metallic state from an aqueous solution is difficult owing to the low solution potentials and the difficulty encountered in controlling the electrolytic-deposition of ^{90}Sr on a metallic cathode. In order to circumvent such limitation, the scope of using a chemically modified conductive electrode containing oxide/hydroxide films similar to that used in the preparation of ^{133}Ba source [115] seemed to be a potential strategy owing to the similar chemical properties of Ba and Sr. Hence, this strategy was evaluated towards the preparation of circular planar $^{90}\text{Sr}/^{90}\text{Y}$ sources using an anodized titanium substrate. Although the scope of using anodized titanium substrate holds significant promise, utility of this technique for the preparation of circular planar $^{90}\text{Sr}/^{90}\text{Y}$ sources requires judicious design of an electrolytic cell, selection of an appropriate electrolyte and thorough optimization of experimental parameters to arrive at the conditions for optimum deposition of ^{90}Sr on the substrate. It is also essential to characterize the deposit in term of its adherence to the substrate and also its quality for safe handling as well as for regulatory compliances. Herein, the successful use of electrochemical technique for the deposition of ~ 3.7 MBq (~ 100 μCi) of ^{90}Sr from an aqueous solution onto an anodized circular planar titanium substrate of 16 mm (\varnothing) is optimized. The factors that influence the electro-deposition of ^{90}Sr onto the anodized titanium surface such as pH of the electrochemical bath, applied current density, time of electrodeposition and carrier strontium concentration were systematically investigated for the optimum deposition of ^{90}Sr . The overall design, development of electrochemical cell for electrodeposition of

^{90}Sr , coating the source with a thin layer of polymer and the process for nesting the source in a circular holder are described in this section of chapter-3. Quality control tests on leachability, distribution of activity and stability of the source performed to ensure compliance with regulatory safety requirements have also been described.

3.2.2. Experimental

3.2.2.1. Materials and Equipment

^{90}Sr in equilibrium with ^{90}Y in nitrate form was available in-house at Radiopharmaceuticals Division (RPhD), BARC. Unless otherwise stated, all other reagents used in this study were of analytical grade and obtained from Merck India Limited, Mumbai, India. Titanium metal foils were obtained from M/s. MIDHANI, Hyderabad, India. Platinum metal foils of high purity (99.99 % purity), with material testing certificates were procured from M/s. Hindustan Platinum Ltd, Mumbai, India. The source holders and electrochemical cell were fabricated at in-house facilities. High purity argon gas (99.99 %) was procured from M/s. Kolhapur Oxygen & Acetylene Pvt. Limited, Kolhapur, India. A D.C. power supply with 100 V compliance, a maximum current of 2 A, 1.2 nA current resolution and $>10^{13} \Omega$ input impedance was used for anodization as well as for electro-deposition experiments. The micro-structural features of the electrodeposited samples were analyzed using a scanning electron microscope (SERON, Model AIS-2100). Energy dispersive X-ray microanalysis technique (Oxford, Model INCA E350) was used to identify the elemental constituents on the sample. Liquid scintillation cocktail (Aqua safe 300 Plus) purchased from M/s. Zinsser Analytic GmbH, suitable for measuring low to medium ionic strength aqueous samples with a high counting efficiency was used. This scintillation cocktail AQUASAFE 300 Plus is capable of holding up to 3 mL of aqueous sample per 10 mL of the cocktail. AGFA film grade-G-

7 was used for autoradiography. Optical density measurements were carried out using an OPTEL transmission densitometer. Cotton wool samples of Wipe test and water samples of immersion test were counted in GM counter made by Electronics Corporation of India ltd (ECIL), Hyderabad, India. The electrolytic solutions were prepared from ultrapure water (Millipore Milli Q system).

3.2.2.2. Preparation of the Anodized Titanium Substrate

Circular planar shaped titanium foils of dimensions 16 mm (\varnothing) 9 0.5 mm (t) were used to prepare anodic porous layers following the reported procedure. Anodic oxidation was performed under a constant applied potential of 20 V using a DC power supply, employing a platinum foil counter electrode as cathode in a solution consisting of 10 mL of 0.5 M H_3PO_4 solution and 0.15 M NaF (7.5 mL 0.5 M H_3PO_4 + 2.5 mL of 0.15 M NaF in water) for about 1 h at room temperature. The anodized Ti sample was then heated to $\sim 500^\circ\text{C}$ for about 2 h.

3.2.2.3. Electrochemical Cell

Design of the electrolytic cell is of crucial importance for realizing the electrodeposition on a circular planar surface because its geometry defines the electric field distribution and uniformity. An electrolytic cell was designed and developed to facilitate deposition of $^{90}\text{Sr}/^{90}\text{Y}$ on the outer surface of the circular planar anodized titanium substrate. The schematic diagram of the electrochemical cell is shown in Fig.-3.8. It consists of a cylindrical housing made up of a non-conductive material such as acrylic having a closure at the bottom end (a cup-shaped housing) for nesting the circular planar anodized titanium substrate. The circular titanium substrate was placed at the bottom of the cylindrical housing with the help of a tweezer with its non-anodized end facing downwards and anodized end facing upward. A neoprene 'O' ring was then placed

on the titanium substrate. A quartz tube of dimensions such that its diameter matches with the internal diameter of the acrylic cup was mounted coaxially in the housing. The quartz tube fitted in the housing and formed a tight annular cylindrical chamber in which the anodized titanium substrate remained at the bottom. The top opening served to fill and evacuate the cell with electrolyte. A downwardly facing thin circular planar platinum electrode of smaller circular dimension than the titanium substrate was suspended vertically from the top. The platinum electrode was positioned concentric with the central axis of the quartz tube. The circular planar platinum electrode and the anodized titanium substrate were used as the anode and cathode respectively. The cell was filled with the electrolyte containing $^{90}\text{Sr}/^{90}\text{Y}$ ensuring that both the electrodes were immersed in the electrolyte. A provision was made for passing Ar gas (at the rate of 0.05 cc/s) through a glass tube ($\text{Ø} = 1 \text{ mm}$) into the electrolyte. Prior to electrodeposition, the cell was rinsed thoroughly with deionized water. The cell was filled with electrolyte and purged with Ar gas for 30 min. The electrodes were connected to a DC current supply as per the arrangement shown in Fig. 3.8. For electrodeposition, the electrodes were positioned face to face, immersed in the electrolyte and reconnected to the DC power supply. Electrodeposition of $^{90}\text{Sr}/^{90}\text{Y}$ was carried out at room temperature using 10.0 mL of electrolyte. After electrodeposition, the sample (titanium substrate) was removed, rinsed in DD water, dried under an I.R. lamp and heated to 250-300°C in an oven for 20 min and subsequently cooled to room temperature. A single substrate was electrodeposited with $^{90}\text{Sr}/^{90}\text{Y}$ in each electro-deposition.

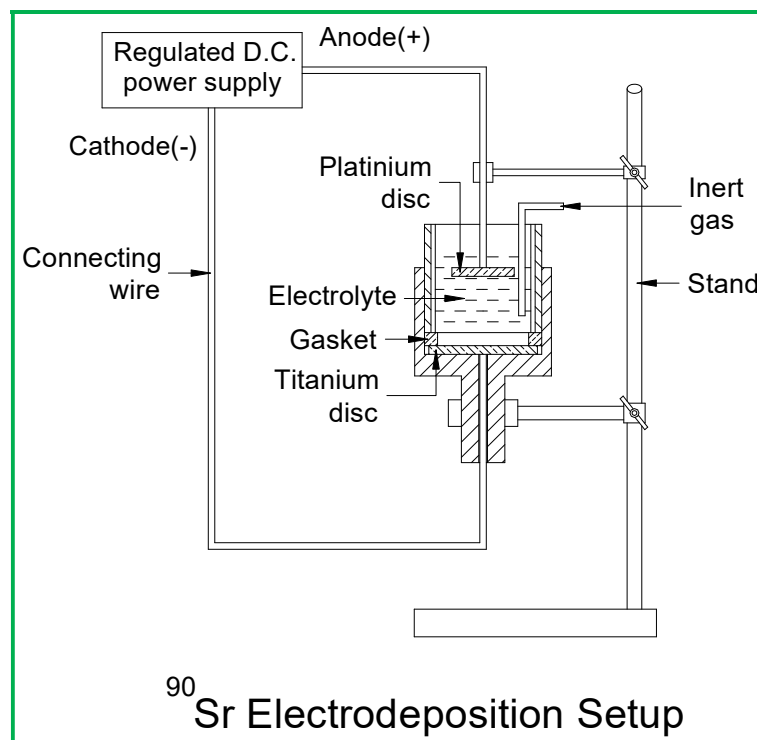


Fig. 3.8: Schematic diagram of ^{90}Sr electrodeposition set-up

3.2.2.4. Optimization of Electrodeposition Parameters

In order to optimize the electrodeposition conditions, a non-radioactive strontium nitrate solution was prepared and spiked with 370 kBq (10 μCi) of radioactive $^{90}\text{Sr}/^{90}\text{Y}$. The pH value of the electrolyte was monitored by a hand held pH meter. With an aim to obtain the optimum reproducible deposition yield, several electrodeposition experiments were performed by varying the following experimental parameters: pH of the electro-bath 1–6, cathode current density 1–25 $\text{mA}\cdot\text{cm}^{-2}$, deposition time 1–5 h, strontium carrier concentration in the bath 5–50 $\mu\text{g}\cdot\text{mL}^{-1}$ and bath temperature 15–70°C. The percent deposition (%) of ^{90}Sr was calculated using the relationship

$$\% \text{ Deposition} = [(A_i - A_f) / A_i] \times 100$$

Where A_i and A_f are the initial and final radioactivity of the ^{90}Sr electrolyte solution respectively.

3.2.2.5. Preparation of $^{90}\text{Sr}/^{90}\text{Y}$ Source

About 4.625 MBq (125 μCi) of no carrier added $^{90}\text{Sr}/^{90}\text{Y}$ solution was pipetted out from the original stock solution and taken in a 25 mL capacity beaker. To this, 12.75 mg of NaNO_3 and 100 μg of non-radioactive $\text{Sr}(\text{NO}_3)_2$ as cold carrier were added. The resulting solution was evaporated to dryness and made to 10 mL with water. The pH of the electrolyte was brought to ~ 1 by the drop wise addition of 0.01 M HNO_3 or 0.01 M NaOH . The resulting solution was then transferred into the electrochemical cell. The electrolyte was then purged with pure argon gas to remove the dissolved gases. Electrodeposition of $^{90}\text{Sr}/^{90}\text{Y}$ was carried out at a potential of ~ 5 V maintaining a current density of $\sim 50 \text{ mA.cm}^{-2}$ for 4 h at room temperature. A single anodized disc was electrodeposited with $^{90}\text{Sr}/^{90}\text{Y}$ in each electrodeposition experiment. After electrodeposition, the samples were rinsed in doubly distilled water, and dried under an I.R. lamp.

3.2.2.6. Coating of the Sources with Polystyrene Polymer

The active area of the source was coated with polystyrene by the dip-pull method following the reported procedure [68, 76-78, 116]. Towards this, the $^{90}\text{Sr}/^{90}\text{Y}$ deposited source was immersed into a solution of polystyrene in benzene (150 mg.mL^{-1}), stirred using magnetic stirrer for 3 min and taken out with tweezers. The polymer coated samples were placed onto a perforated tray where the excess of the uncoated polystyrene reagent drained out and the samples were air-dried.

3.2.2.7. Surface Characterization

SEM and EDS analysis were carried out using a dummy Sr source prepared in an identical manner used for source fabrication (using non radioactive Sr). EDS micro-analysis technique was used to identify the elemental constituents of the electrodeposited samples. Activity content of $^{90}\text{Sr}/^{90}\text{Y}$ in the electrolytic bath was measured by drawing

suitable aliquots of the electrolyte before and after each electrodeposition step and counting using a liquid scintillation counter (LSC). This was used to follow the progress of electrodeposition of ^{90}Sr on the cathode with time. For the purpose of quoting the activity in the source, the radioactivity content was measured in a dose calibrator calibrated with NIST calibrated ^{90}Sr sources. The reference position was chosen ~ 10 mm from the outer detector plane to evoke a 2π geometry.

3.2.3. Quality Evaluation of the $^{90}\text{Sr}/^{90}\text{Y}$ Sources

3.2.3.1. Leachability

Leachability test was carried out following the method prescribed by the AERB, India [63]. In brief, each source was placed for 48 h in a beaker containing 100 mL water at room temperature, at the end of which the source was removed. The water was concentrated to 0.1 mL by heating and radioactivity content was measured in a liquid scintillation counter.

3.2.3.2. Swipe Test

The sources were tested for absence of loose activity (surface contamination) by swiping their surface using cotton wool immersed in alcohol and checking for radioactive contamination on the cotton wool in a G.M. counter.

3.2.3.3. Autoradiography

The uniformity of distribution of $^{90}\text{Sr}/^{90}\text{Y}$ activity in the polymer sources was estimated by autoradiography examination of the randomly selected three sources. A photographic film was wrapped on each of the radioactive source and kept for 5 days in a dark room. The optical density distribution of the exposed film was measured by B/W transmission densitometer.

3.2.3.4. Source Assembly in a Circular Holder

The prepared source was mounted into a disc type circular aluminum holder on which a radioactive titanium foil can be mounted in an extremely simple manner. It consisted of a disc, an opening in the disc and a cap to fit in the disc. The source holder had a precisely sized circular opening and contained a bracket to nest the circular planar $^{90}\text{Sr}/^{90}\text{Y}$ source in position in the disc with its radioactive end facing down towards the open end so that it would radiate through the opening. The holder was threaded inside to accommodate a matching cap. The cap was threaded on the outside edge and matched the internal diameter of the holder. The cap could be turned either in clockwise or counter-clockwise direction for closing and opening. The $^{90}\text{Sr}/^{90}\text{Y}$ source was placed with the help of a tweezer to fit inside the base. The active area of the source was covered by an aluminum foil of 5 mg.cm^{-2} thickness to protect from mechanical abrasion during normal handling and operation. The cap was then rotated in a clockwise direction to screw into the holder. This design secures the source in the holder during application. The process of nesting the $^{90}\text{Sr}/^{90}\text{Y}$ source in a holder is shown in Fig. 3.9.

3.2.3.5. Radiological Safety

Due to the radiotoxic nature of $^{90}\text{Sr}/^{90}\text{Y}$, safe and appropriate radiochemical procedures were employed during the entire electrodeposition process. All the radioactive experiments were carried out after thorough planning in order to achieve ALARA. The personnel involved in this work were monitored for radiation exposure levels by TLD. In order to minimize radiation exposure, electrodeposition was carried out using a portable acrylic “L” shield, mounted in a fume hood. The immediate vicinity of the fume hood area was lined with polyethylene sheets to contain possible radioactive contamination. Continuous radioactivity monitoring of radiation dose in the working area was performed.

3.2.4. Results

In order to obtain a homogeneous deposition of $^{90}\text{Sr}/^{90}\text{Y}$ on one side of a circular planar substrate following an electrochemical pathway, a systematic approach was pursued.

3.2.4.1. Preparation of the Electrolyte

Selection of an electrolyte bath is of utmost importance for the successful deposition of $^{90}\text{Sr}/^{90}\text{Y}$. The electrolyte composition was formulated based on a reported method for Ba deposition due to the similar chemical characteristics of Ba and Sr [115].

3.2.4.2. Optimization of Electrodeposition Parameters

Owing to the no carrier-added (NCA) nature of $^{90}\text{Sr}/^{90}\text{Y}$, the concentration of $^{90}\text{Sr}/^{90}\text{Y}$ used in this investigation was extremely low and the effect of various experimental parameters such as pH of the electrochemical bath, applied current density, time of electrodeposition and carrier strontium concentration was hence considered essential to arrive at the optimum electrodeposition conditions.

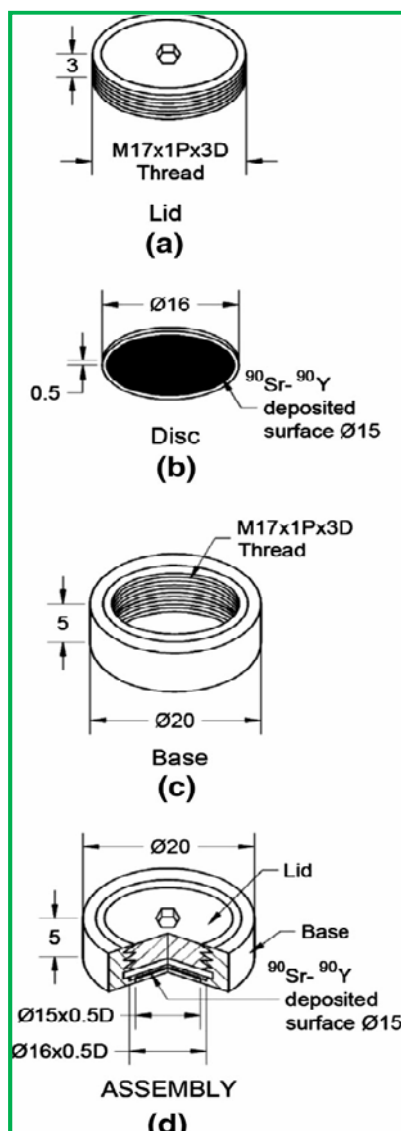


Fig. 3.9: Source assembly in a circular holder (a) Source holder base is threaded on the inside edge to accommodate a matching threaded cap (b) Electrodeposited $^{90}\text{Sr}/^{90}\text{Y}$ circular planar source is fitted inside the base with its radioactive end facing down towards the open end (c) Source cap is threaded on the outside edge to enclose the source (d) Source assembly

3.2.4.3. Influence of pH

The dependence of the deposition of $^{90}\text{Sr}/^{90}\text{Y}$ on the pH of the electrolyte is presented in Fig. 3.10. From the results, it can be inferred that, within the range of pH investigated, optimum deposition of $^{90}\text{Sr}/^{90}\text{Y}$ could be achieved when the pH of the electrolyte was kept at 1. Any further increase of pH resulted in decrease of the deposited activity. Hence, the pH of the electro-bath was kept at 1 for the preparation of sources. The electrodeposition process is considered to be governed by three factors:

- the dissolution of the freshly deposited $^{90}\text{Sr}/^{90}\text{Y}$ atoms on the anodic Ti substrate because of the acidic pH in the electrolyte,
- the formation of SrTiO_3 layer on the electrode surface and
- the anomalous electrodeposition of $^{90}\text{Sr}/^{90}\text{Y}$

At a lower pH value, the process is predominated by the second factor which favors the electrodeposition of $^{90}\text{Sr}/^{90}\text{Y}$ layer and depresses the dissolution of the freshly deposited $^{90}\text{Sr}/^{90}\text{Y}$.

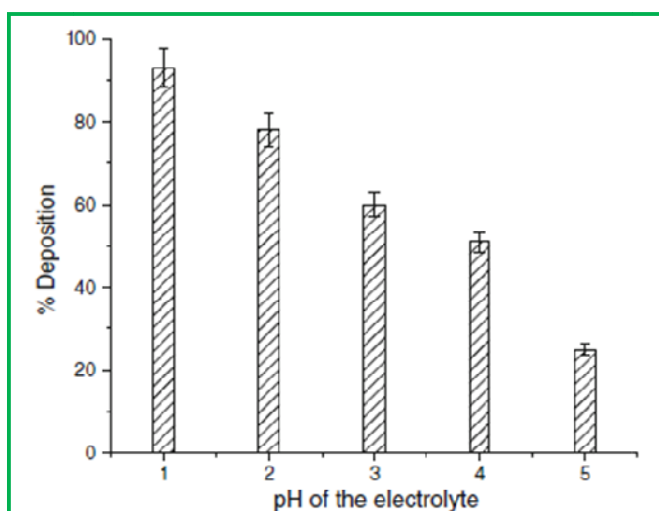


Fig. 3.10: Effect of pH of the electrolyte on electrodeposition of $^{90}\text{Sr}/^{90}\text{Y}$

3.2.4.4. Influence of current density

To study the influence of applied current density on the electrodeposition of $^{90}\text{Sr}/^{90}\text{Y}$, a series of electrodeposition experiments were performed in the range of 1–70 $\text{mA}\cdot\text{cm}^{-2}$ and the results are shown in Fig. 3.11.

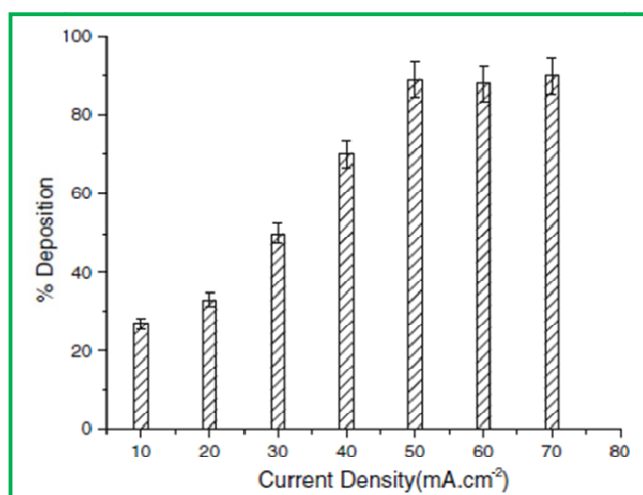


Fig. 3.11: Influence of applied current density on the deposition of ^{90}Sr

It can be seen that the percentage of ^{90}Sr deposition increased with increasing current density up to 50 $\text{mA}\cdot\text{cm}^{-2}$ and thereafter it remained more or less constant. The best operating current density was therefore deduced to be 50 $\text{mA}\cdot\text{cm}^{-2}$. At low current density, or lower over-potential, the percentage deposition is low owing to competitive reaction or proton reduction. Increase in current density usually increases the over-potential, leading to increase in percentage deposition

3.2.4.5. Influence of Carrier Concentration

The results obtained in the investigations carried out to determine the influence of carrier strontium concentration on the $^{90}\text{Sr}/^{90}\text{Y}$ deposition is shown in Fig. 3.12. It is noticeable that the percentage of $^{90}\text{Sr}/^{90}\text{Y}$ deposition increases initially with increasing Sr carrier concentration up to 100 μg and thereafter decreases with further increase in carrier concentration. The decrease in deposition rate at higher carrier concentration may be due

to the attainment of saturation. With a view to realize optimum $^{90}\text{Sr}/^{90}\text{Y}$ deposition onto the substrate, it is essential to keep the carrier concentration of yttrium $\sim 100 \mu\text{g}$ i.e. $10 \mu\text{g.mL}^{-1}$.

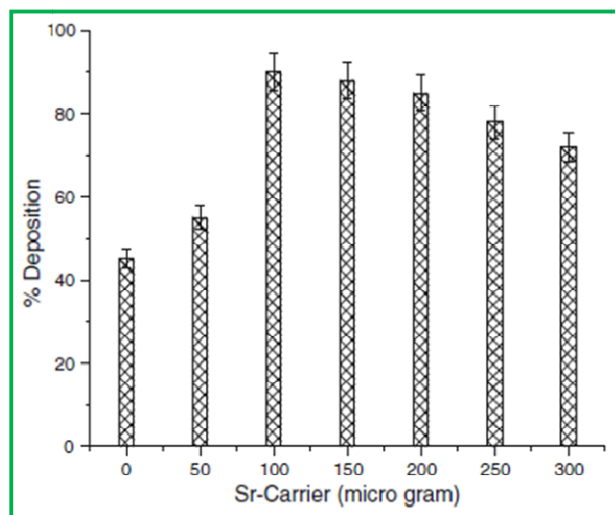


Fig. 3.12: Influence of strontium carrier on the deposition of ^{90}Sr

3.2.4.6. Influence of Deposition Time

In order to determine the time required to obtain optimum deposition of $^{90}\text{Sr}/^{90}\text{Y}$, experiments were conducted to determine the optimum time of electrodeposition and the results are depicted in Fig. 3.13. As expected, the percentage $^{90}\text{Sr}/^{90}\text{Y}$ deposition increased with increasing electrodeposition time and almost a quantitative deposition of activity was obtained after 4 h of electrolysis. As is known, electrodeposition of ^{90}Sr on the anodized titanium surface takes place owing to the formation of SrTiO_3 [121]. As the deposition time increases, more and more ^{90}Sr ions get deposited leading to the increase of the deposition rate. The maximum of deposition rate may be due to saturation of the surface sites.

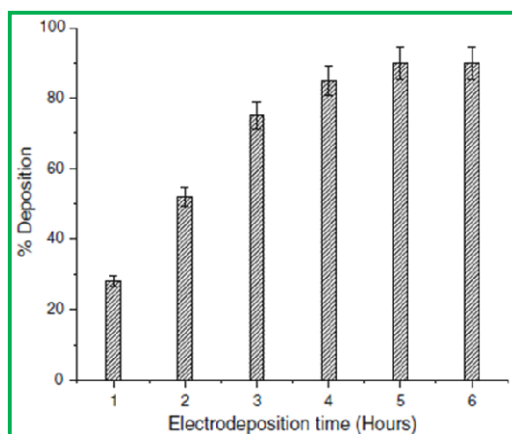


Fig. 3.13: Influence of deposition time

3.2.4.7. SEM Analysis

SEM images of anodized titanium substrate as well as the Sr deposited surface at different magnifications are shown. The surface morphology of the anodized titanium substrate is shown in Fig. 3.14. The SEM image showed the formation of porous TiO_2 structure well adherent to the Ti surface. Under the influence of an electric field, Sr^{2+} gets incorporated into the porous TiO_2 film owing to formation of SrTiO_3 . The SEM micrographs shown in Fig. 3.15 illustrate not only the formation of small granular crystals of SrTiO_3 layer but also indicate good adhesion with anodized titanium substrate. The SrTiO_3 layer seems to be distributed throughout the titanium substrate.

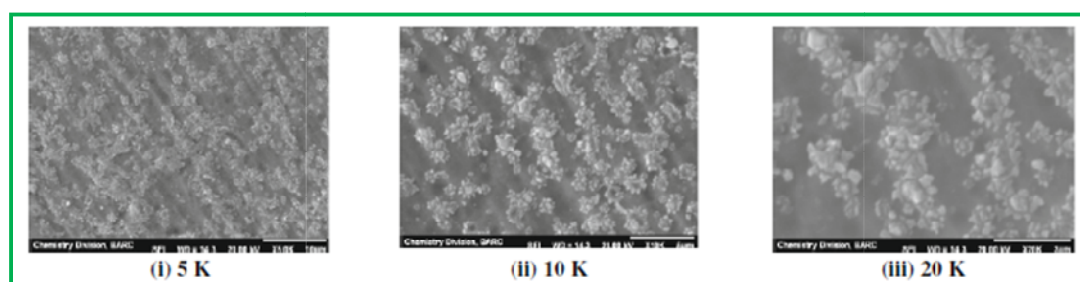


Fig. 3.14: Scanning electron microscopy (SEM) images anodized Ti substrate at different magnification

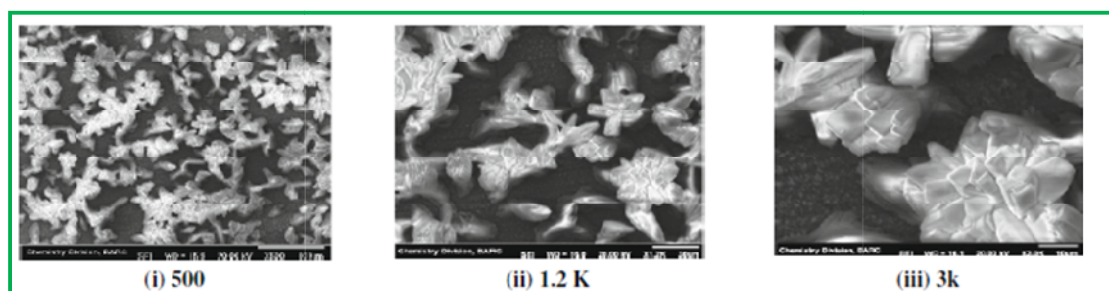


Fig. 3.15: Scanning electron microscopy (SEM) images of Sr deposited anodized Ti substrate at different magnification

3.2.4.8. EDS Characterization

Figure 3.16(a) depicts the EDS spectrum of anodized titanium substrate and Fig. 3.16(b) of the Sr deposited anodized Ti substrate. Figure 3.16(a) shows peaks pertaining to Ti and O only which not only indicates the formation of oxide films but also indicate that the substrate used is pure Ti and free from metallic impurities. Figure 3.16(b) shows peaks pertaining to Ti, Sr and O only which indicates coverage of Ti surface with Sr.

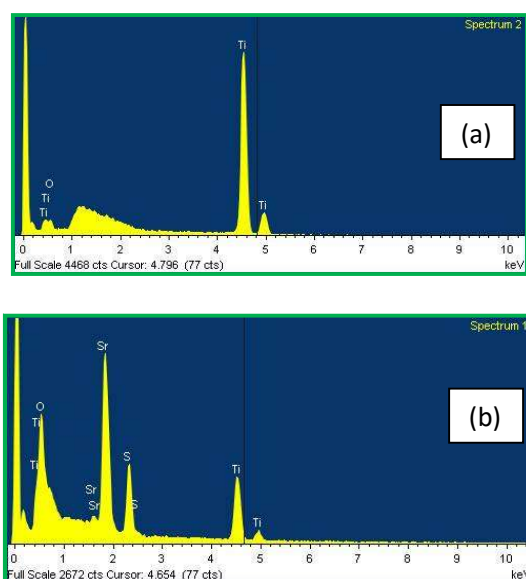


Fig. 3.16: EDS spectrum of (a) anodized Ti surface, (b) Sr deposited anodized Ti substrate

In order to ascertain the homogeneity of Sr deposited on the substrate surface, the EDS spectra were recorded at various locations and the quantification of the elemental composition as weight percentage is given in Table-3.4.

Table-3.5: Elemental composition of the Sr electrodeposited anodized Ti substrate

| Element | Weight (%) |
|---------|------------------|
| O | 44.25 ± 1.73 |
| Ti | 17.88 ± 0.81 |
| Sr | 37.88 ± 1.13 |

The results revealed that the substrate surface is covered with Sr and the variation in distribution of Sr along the surface of the substrate is within $\pm 4\%$. Several circular planar sources of different strengths were prepared under the optimum conditions of electrolysis, .results of deposition carried out from five different batches are presented in Table 3.5. It was observed that the efficiency of $^{90}\text{Sr}/^{90}\text{Y}$ electrodeposition did not differ markedly from batch to batch and was always $> 80\%$. The described procedure thus offers the scope of preparing $^{90}\text{Sr}/^{90}\text{Y}$ sources of different strengths simply by tailoring activity content of the electrolyte.

3.2.4.9. Measurement of Activity of the $^{90}\text{Sr}/^{90}\text{Y}$ Source

In order to monitor the progress of electrodeposition, indirect method of measurement of $^{90}\text{Sr}/^{90}\text{Y}$ activity by LSC was adopted. While the LSC measurement was effective in providing the fraction of $^{90}\text{Sr}/^{90}\text{Y}$ deposited on the anodized titanium substrate in the course of electrolysis, it did not necessarily give the fraction remaining on the substrate owing to loss during washing or attenuation of radioactivity after polymer coating. In order to mitigate such draw-backs, the measurement of ^{90}Sr activity deposited

on the anodized Ti surface was carried out using a dose calibrator which was used for quoting the activity of the source. The results show that the method was able to provide activity values with uncertainties less than 5%, which are far below the limit of 10 % required by AERB, India [63].

Table-3.6: Preparation of $^{90}\text{Sr}/^{90}\text{Y}$ sources of different strengths

| Sr. No. | ^{90}Sr activity of the feed MBq (μCi) | ^{90}Sr activity deposited on the substrate MBq (μCi) | Deposition efficiency (%) |
|---------|--|---|---------------------------------|
| 1 | 4.44(120) | 3.77(101.9) | 84.9 |
| 2 | 5.18(140) | 4.47(128.5) | 86.2 |
| 3 | 6.47(175) | 5.41(146.3) | 83.6 |
| 4 | 8.88(240) | 7.75(209.6) | 87.2 |
| 5 | 10.73(290) | 9.21(248.9) | 85.8 |

3.2.5. Quality Evaluation of $^{90}\text{Sr}/^{90}\text{Y}$ Source

In order to ensure the safety of the $^{90}\text{Sr}/^{90}\text{Y}$ sources during the conditions of normal use or under accidental conditions, a thorough quality assessment was considered essential.

3.2.5.1. Leachability

The results of leachability tests conducted on five randomly selected sources of different strengths are depicted in Table 3.6. It was seen that 1.93 ± 0.30 % of the original activity leached out in 48 h, which was significantly higher than the AERB prescribed norms [63]. In order to retard the leaching to an acceptable level, polystyrene coating of the source was carried out for arresting the leachability of $^{90}\text{Sr}/^{90}\text{Y}$ activity. However, it is

associated with the reduction in radiation output of the source owing to attenuation. With a view to evaluate the extent of radiation attenuation, the radiation outputs of the sources before and after polymer coating were determined using a dose calibrator. The results on attenuation effect conducted on five randomly selected $^{90}\text{Sr}/^{90}\text{Y}$ source cores before and after polystyrene coating indicated that 4.18 ± 1.25 % of the original activity attenuated. The activity deposited on the anodic titanium substrate was therefore kept 5 % more than the required activity based on the experimental results, in order to compensate the attenuation effects of the coating material. The concentration of polystyrene in benzene was kept at 150 mg.mL^{-1} based on the results obtained in the previous studies [68, 76-78, 116]. As can be seen from the results, polymer coating of the radioactive source was found to be effective in retarding the leachability to below detection limit, which is well within the limit prescribed by AERB, India [63].

Table-3.7: Leachability of ^{90}Sr from the electrodeposited surface

| Sr. No. | Activity of ^{90}Sr sources ($\mu\text{Ci/kBq}$) | (%) Leached before polymer coating | (%) Leached after polymer coating |
|---------------|---|------------------------------------|-----------------------------------|
| 1 | 3.77(101.9) | 1.68 | BDL |
| 2 | 4.47(128.5) | 1.76 | BDL |
| 3 | 5.41(146.3) | 1.82 | BDL |
| 4 | 7.75(209.6) | 1.97 | BDL |
| 5 | 9.21(248.9) | 2.45 | BDL |
| Mean \pm SD | | 1.93 ± 0.30 | |

3.2.5.2. Autoradiography Examination

In order to assess the distribution of deposited $^{90}\text{Sr}/^{90}\text{Y}$ on the surface of the substrate, autoradiography examination of three different sources of strength ~ 3.7 MBq (100 μCi) was carried out. Autoradiography image of the three sources are shown in Fig. 3.17. The images obtained were circular in shape without any visible breakage and deletion indicating that $^{90}\text{Sr}/^{90}\text{Y}$ was well covered on the circular planar surface of the substrate. The blackening of the images on the photographic film was measured in terms of optical density, which was taken as a measure of the local concentration of $^{90}\text{Sr}/^{90}\text{Y}$ on the surface. The optical density measured at five different positions of three different sources is shown in Table 4. It is seen from the results that the coefficient of variation as percentage (% CV) of optical density along the surface of the substrate was within ± 3 %, indicating reasonably good uniformity of radioactivity on the surface. As values less than ± 5 % are acceptable, the sources prepared by the reported method meet the specification for use [63].

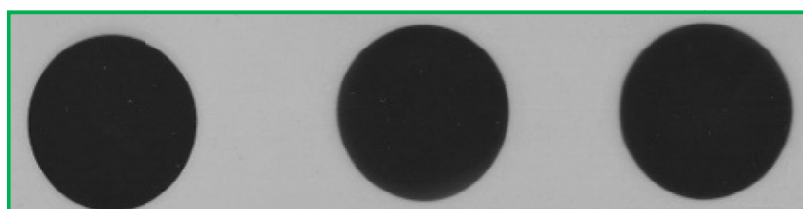


Fig. 3.17: Image of the exposed radiographic film

3.2.5.3. Swipe Test

Swipe test was performed on five randomly selected polymer coated sources. Five randomly selected sources of different strength showed that 82 ± 31 Bq were found in the swipe, which was well within the prescribed limit of 185 Bq [63].

3.2.5.4. Source Assembly in a Circular Holder

In order to ensure the safe handling of radioactive source during application, a source holder was designed which would retain the source firmly in a position amenable for the application. The design of the holder was configured appropriately to hold the source securely in position and at the same time able to provide desired radiation output during routine calibration of surface contamination monitors.

3.2.5.5. Preparation of $^{90}\text{Sr}/^{90}\text{Y}$ Sources

Following the described procedure, several $^{90}\text{Sr}/^{90}\text{Y}$ sources of activity ~ 3.7 MBq (~ 0.1 mCi) were prepared. The results show acceptable batch-to-batch reproducibility in terms of the radioactivity content. The sources that qualified all the Quality Control (QC) tests were finally encased in source holders. Each source was permanently marked indicating source number, date of preparation, radioisotope and activity content on the date of calibration.

3.2.6. Discussion

The primary endeavor of this investigation was to develop an indigenous technology for the preparation of circular planar $^{90}\text{Sr}/^{90}\text{Y}$ sources for routine calibration of surface contamination monitors. Titanium was chosen as the substrate for the electrodeposition of $^{90}\text{Sr}/^{90}\text{Y}$ owing to the attributes such as commercial availability in high purity, radiation stability, excellent corrosion resistance and adequate mechanical strength. In order to reduce radiation dose, attempt was made to utilize small quantity of ^{90}Sr activity during source fabrication. Hence, an electrochemical cell of special design that permits handling of limited activities was adopted. The major advantage of this electrochemical cell lies in the compactness and simplicity in the design that can be used for the routine production of circular planar $^{90}\text{Sr}/^{90}\text{Y}$ sources. In order to protect $^{90}\text{Sr}/^{90}\text{Y}$

deposit on the anodized titanium substrate from mechanical abrasion or damage during application as well as to reduce the leachability of deposited $^{90}\text{Sr}/^{90}\text{Y}$ to an acceptable level, the radioactive surface was coated with a thin layer of polymer. This work successfully addresses several issues such as preparation of anodized titanium substrate of defined geometry and size, electrochemical deposition of ^{90}Sr on to a planar substrate, coating the radioactive area with a thin layer of polymer, mounting the source in a holder and quality control of the source to comply with the regulatory norm. The convenience of depositing the required quantities of ^{90}Sr activity homogeneously on a planar substrate of defined geometry from an aqueous solution using electrochemical approach constitutes the novelty of the reported technique. In view of the long half-life of ^{90}Sr (~28 years), the shelf life of the source is quite long. Local availability of this type of radioactive source not only reduce user's dependence on imported radiation sources but also help in performing routine calibration of surface contamination monitors.

3.2.7. Conclusion and Scope of the Work

The objective of depositing the required quantity of ^{90}Sr activity on the designated area of a circular planar substrate using electrochemical technique has been successfully achieved. With a view to ensure their safety during application, the compliance of the prepared sources with the regulatory norms was evaluated and found to be satisfactory. The reported process can be implemented for the regular production of ^{90}Sr source.

CHAPTER-4

Preparation of $^{90}\text{Sr}/^{90}\text{Y}$ Sources towards Use in Hand Contamination Monitors Using Solvent Extraction and Polymerization Techniques

“Science is a beautiful gift to humanity; we should not distort it.”

-A. P. J. Abdul Kalam

4.1. Introduction

Hand contamination monitors are used to check the presence of radioactive contamination on the hands of the working personnel while leaving the radioactive laboratory. For carrying out the routine calibration of hand monitors for β^- radiation, an external radioactive source of large area containing the long lived β^- emitter ^{90}Sr ($t_{1/2}$ 28.8 years) is required. Hence, work towards the development of a simple method for the fabrication of large area ^{90}Sr sources for calibration of hand monitors was taken up. Preparation of such sources requires judicious selection of a technique, careful preparation of source to adhere to the specifications and evaluation of quality of the sources as per the regulatory requirements. There are two methods reported in the literature for the preparation of $^{90}\text{Sr}/^{90}\text{Y}$ sources [139,140]. The method reported by Sundara Rao et al is based on the deposition of a $^{90}\text{Sr}/^{90}\text{Y}$ solution on VYNS films followed by its slow evaporation. This method is suitable for the preparation of small area sources. The method reported by Tsoupko-Sitniko et al is based on the incorporation of the $^{90}\text{Sr}/^{90}\text{Y}$ activity in a thin conducting ion-exchanger polymeric film which is grown on a metal support. Although there is no technical impediment to adopt the latter method for the preparation of large area $^{90}\text{Sr}/^{90}\text{Y}$ sources, it requires intricate electrochemical polymerization process to prepare polymer film of desired attributes from the corresponding monomer, which is a major deterrent. A method based on the use of inkjet printers to print patterns on a material substrate such as a sheet of paper is also a promising technique for the preparation such sources [125,126,137,141]. However, the strategy involves many steps such as the formulation of radioactive ink of printing density, setting colored inks with different radioactive concentrations, adjustment function for obtaining the printing concentrations for each ink color, selection of nozzles

of printing head to deliver printable radioactivity, assessment of surface contouring and the absorption capacity of the printing medium. While methods based on inkjet printers are attractive for the preparation of such radioactive sources, extensive research efforts are required in order to realize its utility in the preparation of ^{90}Sr source. Nevertheless, each radioactive source preparation method has its own distinct advantages and disadvantages. In the pursuit of a facile approach for the preparation of large-area $^{90}\text{Sr}/^{90}\text{Y}$ sources, the utility of solvent extraction process to extract the required $^{90}\text{Sr}/^{90}\text{Y}$ activity into an organic phase followed by its immobilization with a polymer, thereby making a large area film of the radioactive polymer was considered. This method is similar to that reported earlier by our group for the preparation of ^{60}Co sources [80]. For the preparation of a radioactive polymer film of $^{90}\text{Sr}/^{90}\text{Y}$, quantitative extraction of $^{90}\text{Sr}/^{90}\text{Y}$ into an organic phase is desired which requires an effective extractant. There are several literature reports on the use of di-tertiary butyl cyclohexano 18-crown-6 (DCH18C6) for the selective extraction of ^{90}Sr from acidic solutions [127-130]. In this chapter, the development of a novel process for preparation of a large area $^{90}\text{Sr}/^{90}\text{Y}$ source is reported. The process consists of solvent extraction using DCH18C6 to extract the required quantity of $^{90}\text{Sr}/^{90}\text{Y}$ activity into an organic phase, addition of a soluble polymer to the organic solvent, spreading of the radioactive polymer solution on a suitable planar surface and evaporation of the solution to form a large area film. The factors that influence the extraction of $^{90}\text{Sr}/^{90}\text{Y}$ into the organic phase were identified and various experimental parameters were optimized to arrive at the conditions for optimum extraction. Quality of the radioactive film thus prepared was also evaluated to determine its suitability for the desired application as well as its compliance to the radiation safety aspects.

4.2. Materials

DCH18C6 (analytical grade) and methyl methacrylate polymer (PMMA) were purchased from M/s. Sigma-Aldrich, India. Unless otherwise stated, all other reagents used in this work were of analytical grade and were obtained from Merck (India) Limited, India. The radioactive isotopes $^{85+89}\text{Sr}$ and $^{90}\text{Sr}/^{90}\text{Y}$ were available in-house at the Radiopharmaceuticals Division, BARC. A shaker consisting of a stainless steel (SS) frame with an arm fitted with terry clips at equal distances for holding tubes was used for extraction experiments. A spirit level was used to level the surface of the metal platform. Viscosity of the composite solution containing the polymer and ^{90}Sr was measured using a Rheometer of Model MCR 101 (Antonpaar, Germany). Radioactivity measurement of ^{90}Sr solution was carried out in a liquid scintillation counter (Model No. Tricarb2100TR, Packard Instrument Co. USA). Counting of swipes containing ^{90}Sr was carried out in a GM counter (Electronics Corporation of India Ltd., India).

4.3. Experimental

4.3.1. Studies on the Extraction of ^{90}Sr into Organic Phase

Studies on the solvent extraction of Sr^{2+} ions from nitric acid solutions by DCH18C6 in chloroform were carried out using $^{85+89}\text{Sr}$ tracer. In order to study the extraction behavior of Sr^{2+} ions in chloroform, equal volumes (1.0 mL) of the aqueous phase spiked with $^{85+89}\text{Sr}$ (185 KBq or 5 μCi) and the organic phase (chloroform) were taken in cylindrical stoppered glass tubes of 5 mL capacity and were shaken in a shaker at room temperature ($25 \pm 0.1^\circ\text{C}$) for 10 min to ensure complete equilibration. Given the feasibility of producing $^{85+89}\text{Sr}$ by neutron irradiation of the natural SrCO_3 target and the convenient means for assaying the activity using a well-type NaI (TI) scintillation counter interfaced to a multi-channel analyzer, $^{85+89}\text{Sr}$ tracer was used as surrogate for ^{90}Sr

during the optimization experiments. The two phases were then centrifuged, separated and suitable aliquots of each phase were assayed for radioactivity using a NaI (TI) well-type counter by drawing suitable aliquots before and after extraction. The percent extraction (%) of $^{85+89}\text{Sr}$ into the organic phase was calculated using the following relationship:

$$\% \text{ Extraction} = \{(A_i - A_f)/A_i\} \times 100$$

Where A_i and A_f are the initial and final radioactivity of $^{85+89}\text{Sr}$ respectively in the aqueous phase. Each experiment was repeated three times and data are presented as the Mean \pm SD of three experiments.

4.3.2. Optimization of Solvent Extraction Parameters

4.3.2.1. Dependence of Extraction Yield of ^{90}Sr on the Acidity of the Aqueous Phase

The dependence of percentage extraction of $^{85+89}\text{Sr}^{2+}$ on nitric acid concentration (0.5-4 M) was studied at a fixed concentration of DCH18C6 (0.04 M solution of DCH18C6).

4.3.2.2. Dependence of Extraction Yield of ^{90}Sr on the Concentration of DCH18C6

Dependence of extraction yield of ^{90}Sr in the organic phase containing DCH18C6 was estimated by varying the concentration of DCH18C6 in chloroform (at the optimized aqueous phase acidity of 3 M HNO_3).

4.3.2.3. Dependence of Extraction Yield of ^{90}Sr on Equilibration Time

In order to determine the dependence of extraction equilibrium on time, percentage extraction was determined for extraction of $^{85+89}\text{Sr}^{2+}$ from 3 M HNO_3 solution using a 0.04 M solution of $\text{DCH}_{18}\text{C}_6$ in chloroform. The effect of concentration of the extractant on the distribution of Sr^{2+} was studied at 3 M HNO_3 using DCH18C6 in the concentration range of 0.02-0.1 M.

4.3.2.4. Selection of Polymer

Choice of a polymeric compound for making composite film depends on the ability to peel-off the source from the base (with which it remains in close contact) with ease and is the key step for successful technical realization of this approach. However, in order to achieve this objective, selection of a proper polymeric compound is required. A number of polymers such as poly(vinyl acetate), PMMA and polystyrene were evaluated for the purpose of preparation of composite films, their de-lamination characteristics were tested and the result obtained is depicted in Table-4.1. The de-lamination characteristics of PMMA and polystyrene polymers were nearly identical and hence both can be used for preparation of ^{90}Sr source. However, PMMA was chosen for the present work as the radioactive film is to be attached to the PMMA substrate. Our subsequent efforts were therefore concentrated towards the optimization of the concentration of the PMMA solution to prepare the composite film containing the ^{90}Sr activity.

Table-4.1: De-lamination characteristics of polymers for making radioactive film

| Polymer used for making radioactive film | Characteristics |
|--|---|
| Polyvinyl acetate (PVA) | Strongly attached to the substrate surface and therefore difficult to peel-off. During peeling, the film teared. |
| Poly-methyl methacrylate (PMMA) | Formed poor coating on the substrate surface and can be peel-off easily (spontaneously comes out on drying under IR lamp) |
| Polystyrene | Formed poor coating on the substrate surface and can be peeled off (spontaneously comes out on drying under IR lamp). |

4.3.2.5. Concentration of PMMA Solution for Preparation of Radioactive Film

As the ^{90}Sr -DCH18C6 complex is physically entrapped within the polymer, the possibility of leaching out of the ^{90}Sr activity can be effectively retarded by tailoring the concentration of PMMA in chloroform. Therefore optimization of the concentration of PMMA in chloroform was carried out to arrive at the conditions resulting in minimum leachability of ^{90}Sr activity upon keeping the film in water.

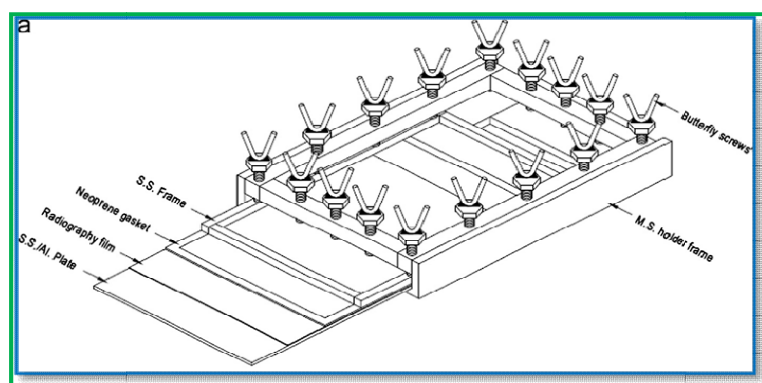
4.3.2.6. Viscosity of the Polymer Solution

Viscosity of the polymer should be ideal for spreading on the flat surface. An assessment of the viscosity (η) at different concentrations of PMMA in chloroform is essential for spreading on the flat surface to obtain a film of uniform thickness. Hence, study of the influence of the concentration of PMMA in chloroform on the viscosity of the resulting PMMA solution was studied.

4.3.3. Preparation of ^{90}Sr Source

After optimizing the experimental parameters for optimum solvent extraction of ^{90}Sr into an organic phase as well as the concentration of PMMA for obtaining the composite film, preparation of ^{90}Sr source was carried out. A device made of mild steel having rectangular cross section [174 mm (l) \times 125mm (b) \times 61.5mm (h)] was specially designed for the purpose. The device comprised of a base plate (150mm(l) \times 100mm (b) \times 20 mm (h)) a radiography film, a neoprene gasket cut in rectangular shape and a removable rectangular frame to be mounted back-to-back on the gasket. The device provided a “flexible platform” for mounting a flat rectangular bottom plate. The rectangular frame was placed along the outer perimeter of the surface of the flat rectangular base plate to form a rectangular cavity. The base plate and the rectangular frame were clamped together with butterfly screws and essentially formed a four-walled

rectangular structure with a sealed rectangular cavity. A radiography film of dimension similar to the base plate and a rectangular shaped neoprene gasket were sequentially placed just above the base plate and mounted on the frame using butterfly screws. This formed a rectangular cross-sectional leak-tight cavity with its seal ring. A schematic diagram and a photograph of the apparatus are shown in Fig. 4.1(a) and 4.1(b) respectively.



(a)



(b)

Fig. 4.1: (a) Schematic diagram of the gadget used for the preparation of large area rectangular $^{90}\text{Sr}/^{90}\text{Y}$ sources and (b) Actual photograph.

The ^{90}Sr solution was used for source preparation after separation of ^{90}Y using the procedure reported in literature [67]. Typically, in one batch, about 185 kBq (5 μCi) of ^{90}Sr activity was taken in 5 mL of 3 M HNO_3 in a 25 mL capacity separating funnel. To this, 5 mL of 0.06 M solution of DCH18C6 in chloroform was added. The mixture were shaken gently for 10 min and allowed to stand for 10 min. The organic chloroform layer containing ^{90}Sr activity was separated out into a beaker and diluted with required quantity of chloroform to obtain 170 Bq/mL solutions. The ^{90}Sr activity content in the organic solution was determined by measuring an aliquot using a liquid scintillation counter. 30 mL of this organic solution was taken and 750 mg of PMMA polymer was dissolved in it. The solution was mixed well and poured into the rectangular cross-sectional leak-tight cavity of the gadget (as described above) kept inside a fume hood. The upper portion of the rectangular cavity was kept open for 45 minutes to allow the chloroform to evaporate out. An acrylic sheet was used to cover the rectangular cavity for safety as well as to minimize disturbance of the film which was subjected to curing for 4–5 h at ambient temperature. After curing, the butterfly screws were loosened, the base plate containing the radioactive film on the surface of the radiography film was removed. The radioactive film was then peeled off from the surface of the radiography film gently from the outer edge pulling towards the center, taking care to avoid tearing of the film. The radiography film served as a buffer layer. It provided a smooth surface for uniform distribution of the polymeric solution and also facilitated release of cured radioactive thin film. The base plate can be used repeatedly without any radioactive contamination. The metal plate was cleaned and reassembled for preparation of the next batch. The radioactive film obtained was then fixed on an acrylic sheet of dimensions 150mm (l) \times 100mm (b) \times 20 mm (h) using chloroform.

4.3.4. SEM and EDS Analysis

The quality of the polymeric film was examined by SEM and EDS analysis of a dummy film prepared in an identical manner as of the active source using inactive Sr. EDS was used to identify the elemental constituents. SEM and EDS analyses were performed on specimens coated with thin (ca. 4nm) over layer of gold.

4.3.4. Assay of Activity of the Source Core

In order to measure the activity content of the prepared sources, a plastic scintillation detector with a 600 cm^2 working area having calibration factors for ^{90}Sr nuclides was used. The detector has a sensitivity of 0.4 Bq.cm^{-2} . It was calibrated with NIST calibrated ^{90}Sr sources. The reference position was chosen approximately 10 mm from the outer detector plane to obtain 2π geometry.

4.4. Quality Control Tests

4.4.1. Test for Leachability

Leachability test was carried out following the method prescribed by the AERB, India. In brief, one source was placed in a beaker containing 100 mL water at room temperature for 48 h. The source was removed at the end of the incubation period, the radioactivity in the water was concentrated to 0.1 mL by heating and radioactivity leached out of the source was determined by counting the water sample in a liquids scintillation counter.

4.4.2. Swipe Test

The prepared sources were tested for loose ^{90}Sr activity (surface contamination) by swiping the sources with a cotton wool immersed in alcohol and checking for radioactive contamination on the cotton wool by counting on a GM counter.

4.4.3. Autoradiography

Uniformity of activity distribution in the polymer sources was determined by autoradiography examination of randomly selected sources of size 150 mm \times 110 (l) \times 110 mm (b). A photographic film was wrapped on each of the radioactive polymeric film source and kept for 30 days to exposure. The uniformity of the ^{90}Sr deposition was monitored by measuring the optical density at different positions of the film. The optical density distribution of the exposed film was measured using a B/W transmission densitometer.

4.5. Results

In order to establish the optimum extraction conditions for transport of ^{90}Sr into organic phase prior to its incorporation in a polymer matrix, detailed study of the solvent extraction parameters were performed. The various parameters optimized were, acidity of the aqueous phase concentration of DCH18C6 in chloroform and determination of equilibration time

4.5.1. Studies on the Extraction of ^{90}Sr into Organic Phase

4.5.1.1. Dependence of Extraction Yield of ^{90}Sr on Acidity of the Aqueous Phase

The dependence of extraction yield of ^{90}Sr on the acidity of the aqueous phase (nitric acid concentration) at a uniform concentration of the extractant in the organic phase (0.04 M ligand) is shown in Fig. 4.2. As it is evident from result shown in fig.4.3, the extraction of Sr^{2+} into the organic phase is strongly dependant on the acidity of the aqueous solution. It is very evident that the percentage extraction of ^{90}Sr increases with increase in acidity and is nearly quantitative in the acidity range of 3–4 M HNO_3 and therefore 3 M HNO_3 was used as the aqueous phase for all subsequent experiments. Equilibration time should come last after other parameters.

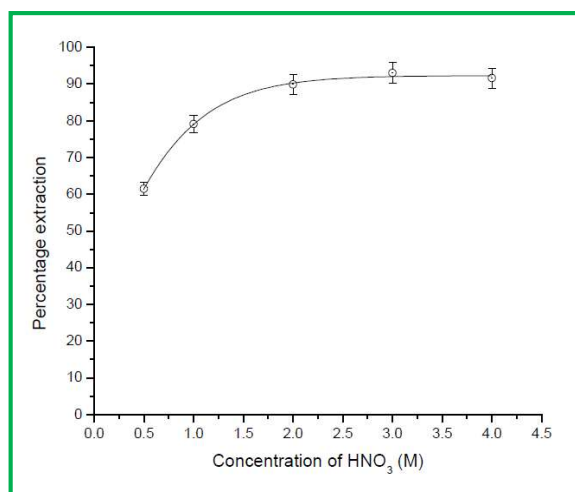


Fig. 4.2: Dependence of percentage extraction of ^{90}Sr on acidity of aqueous phase

4.5.1.2. Dependence of Extraction Yield of ^{90}Sr on the Concentration of DCH18C6

Influence of concentration of DCH18C6 in the organic phase on the extraction of ^{90}Sr from the aqueous phase is depicted in Fig. 4.3. The percentage extraction of ^{90}Sr from the aqueous phase (3M HNO_3) was observed to increase from 87 % to 96 % with increasing concentration of DCH18C6 and attained a maximum at 0.06 M concentration of DCH18C6 as shown in Fig.4.4. Hence, 0.06 M DCH18C6 solution in chloroform was used for extraction of ^{90}Sr in all the subsequent source preparation experiments.

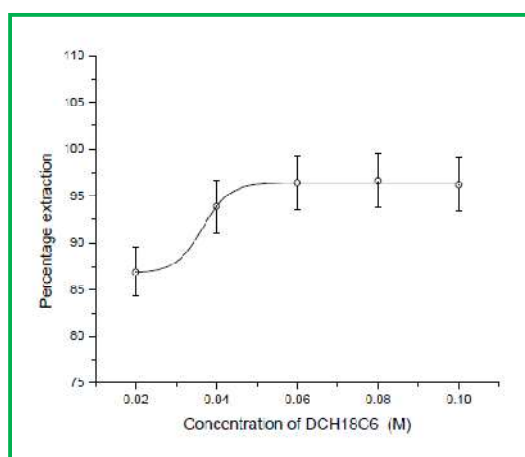


Fig. 4.3: Dependence of extraction yield of ^{90}Sr on concentration of DCH18C6 in organic phase

4.5.1.3. Dependence of Extraction Yield of ^{90}Sr on Equilibration Time

The influence of equilibration time on the extraction of Sr^{2+} with DCH18C6 in chloroform is depicted in Fig. 4.4. It is evident from the figure that the solvent extraction of ^{90}Sr is a very fast process because, equilibrium is achieved within 10 min. On the basis of the results of this experiment, a shaking time of 10 min was used for all of the subsequent experiments.

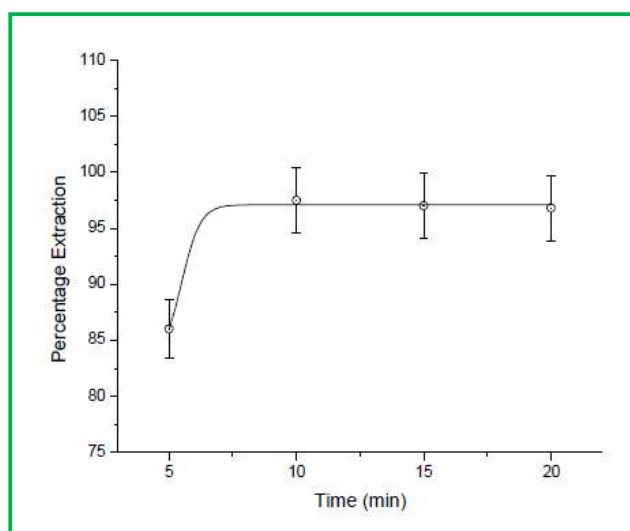


Fig.4.4: Variation of ^{90}Sr extraction yield with time

4.5.1.4. Concentration of PMMA Solution for Preparation of Radioactive Film

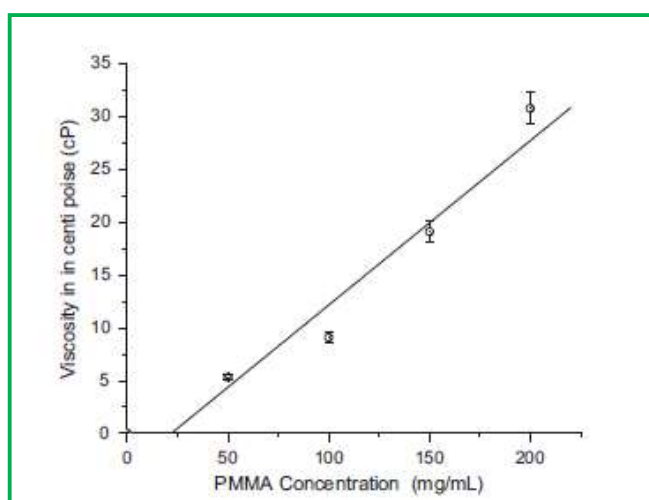
Optimization of the concentration of PMMA in chloroform was carried out to arrive at the conditions resulting in minimum leachability of ^{90}Sr activity upon contact of the film with water. Table-4.2 depicts the PMMA concentration used for making film and the corresponding ^{90}Sr activity released. Based on the optimization studies, it could be concluded that the PMMA polymer solution having a concentration of 150 mg.mL^{-1} is ideal for minimizing the release of ^{90}Sr activity to an acceptable limit.

Table-4.2: Optimization of the concentration of PMMA solution

| PMMA concentration (mg/mL) | % of ^{90}Sr released |
|----------------------------|--------------------------------|
| 50 | 5.06 |
| 100 | 1.30 |
| 150 | 0.07 |

4.5.1.5. Viscosity of the Polymer Solution

Experimentally, it has been observed that the polymer solution having a viscosity (η) in the range of 18–20 centipoise (cP) is ideal for spreading on the flat surface to obtain a film of uniform thickness. The variation of viscosity (η) with concentrations of PMMA in chloroform at 25 $^{\circ}\text{C}$ was studied and the result is depicted in Fig.4. 5.

**Fig.4.5: Variation of viscosity (η) with concentrations of PMMA in chloroform**

As expected, the viscosity of the solution increases linearly with increasing concentration of PMMA in chloroform. In order to obtain optimum viscosity of the polymer solution for spreading on a flat surface, the concentration of PMMA in chloroform was fixed at 150mg.mL $^{-1}$.

4.5.2. SEM and EDS Analysis

SEM micrographs of the PMMA film containing inactive Sr- DCH18C6 species at different magnifications are shown in Fig. 4.6.

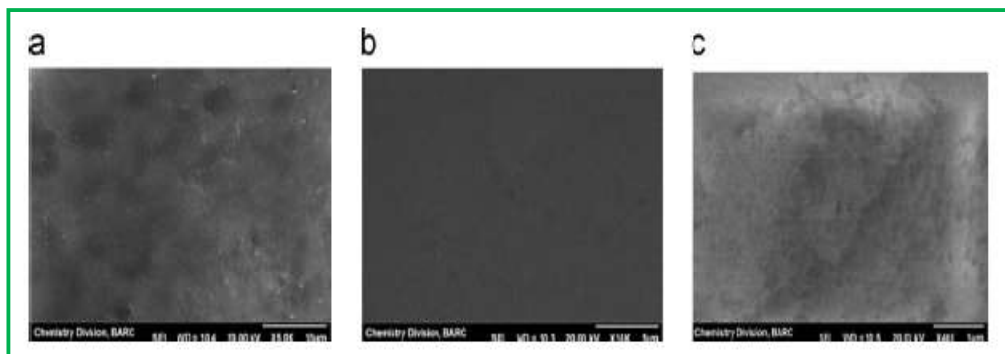


Fig. 4.6: SEM micrograph of the polymeric film at different magnifications (a) 5 K (b) 10K (c) 40K

The surface of the polymer film showed a smooth surface morphology. The film was found to have homogeneous appearance free from irregularities such as cracking, flaking or de-lamination. To verify the elemental composition of the film, an EDS profile was recorded which is shown in Fig. 4.7. The EDS of the polymer film confirm the presence of C, O, Cl and Sr ions in the prepared films. The presence of Au in the polymeric film is due to gold coating during the EDS analysis.

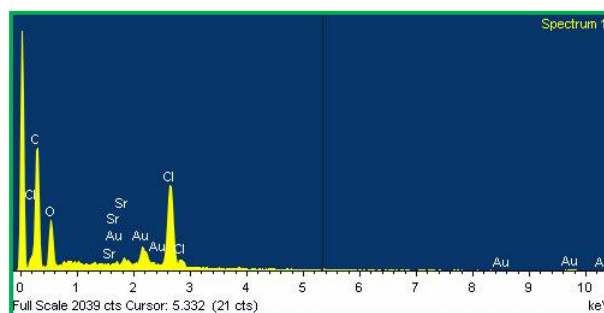


Fig. 4.7: EDS spectrum of the polymeric film containing inactive Sr

The chemical composition of the film surface was determined from the intensity of the peak pertaining to different elements and the quantification of results as weight

percentage is given in Table-4.3. In order to ascertain the homogeneity of Sr incorporated in the polymeric substrate, the EDS spectra were recorded at various locations and the quantification of results as weight percentage revealed that the variation in distribution of Sr along the surface of the polymer is within $\pm 4.8\%$.

Table 4.3: Elemental composition of the Sr PMMA film

| Element | Weight % |
|---------|----------|
| C | 61.72 |
| O | 27.98 |
| Cl | 6.23 |
| Sr | 0.78 |
| Au | 3.29 |

4.5.3. Extraction of ^{90}Sr into the Organic Phase

Results of the ^{90}Sr extraction studies carried out in 5 batches are presented in Table-4.4. It is well evident that the percentage of extraction of ^{90}Sr did not differ markedly from batch to batch. When a dilute solution of PMMA containing ^{90}Sr in chloroform solution was spread on a smooth surface platform and 45 minutes was allowed for complete evaporation of chloroform, large PMMA films containing $^{90}\text{Sr}/^{90}\text{Y}$ were formed.

Table-4.4: Extraction of $^{90}\text{Sr}/^{90}\text{Y}$ into the organic phase containing ligand

| Batch No | Activity taken in the aqueous phase (KBq) | Activity extracted in organic phase (KBq) | Percentage of extraction |
|----------|--|---|--------------------------|
| 1 | 185 | 168 | 90.1 |
| 2 | 202 | 187 | 92.5 |
| 3 | 188 | 171 | 90.9 |
| 4 | 195 | 181 | 92.8 |
| 5 | 208 | 190 | 91.3 |

Slow evaporation promotes the formation of thin film of uniform thickness and acceptable quality. Although the film thickness depends on the nature of solvent used [123,133,138], little is known about their effect on the film quality. The film formation mechanism is believed to occur through the evaporation of solvent at the interface between the film and air. The choice of the surface for making the film is very important. The surface should be smooth as the polymer will remain in intimate contact with the surface. Rough surfaces and grooved surfaces should be avoided as they will lead to non-uniformity in thickness. An exposed radiographic film is attached above the platform to get smooth surface which apparently forms a part of the platform. The use of exposed radiographic film not only promotes the formation of radioactive composite film of uniform thickness but also facilitates easy removal of the dry film. The rectangular frame ensures a conformal dimension and the exposed radiographic film surface facilitates peeling-off of the radioactive film without resulting in any damage. The measurement of ^{90}Sr activity of the final source by plastic scintillation detector was used for quoting the total amount of activity deposited on the dry film. Results of the measurement show that the $^{90}\text{Sr}/^{90}\text{Y}$ sources could be prepared with activity values having standard uncertainties less than 5%, which are far below the limit of required by AERB as well as ISO 8769 [63].

4.5.4. Autoradiography Examination

Special attention is warranted to achieve the reproducibility of the thickness of the active layer as well as uniformity of the β^- radiation flux over the flat rectangular surface of the source. The source required for this application should be mechanically rugged and the non-uniformity of the β^- radiation flux over the flat rectangular surface of the source must be less than 10 %. In order to evaluate the distribution of ^{90}Sr incorporated in the

polymer, the optical densities of the exposed radiographic film were measured at various locations. The results obtained with three different sources are depicted in Table-4.5. It was observed that the variation in distribution of ^{90}Sr along the surface of the film is within $\pm 5\text{-}6\%$ which corroborated the values obtained by EDS technique. As values with $\pm 10\%$ variation are acceptable, the source prepared by the above method meet the specifications. The uniformity of activity distribution is a consequence of large number of PMMA particles per unit volume of the polymer.

Table-4.5: Optical densities of the exposed radiographic films at different positions of the $^{90}\text{Sr}/^{90}\text{Y}$ sources

| Sr. No. | Optical Density | |
|-------------|------------------------------|------------------------------|
| | Source 1 | Source 2 |
| 1. | 3.53 | 3.4 |
| 2. | 3.15 | 3.75 |
| 3. | 3.58 | 3.76 |
| 4. | 3.7 | 3.76 |
| 5. | 3.43 | 3.37 |
| 6. | 3.45 | 3.53 |
| 7. | 3.60 | 3.53 |
| 8. | 3.38 | 3.18 |
| 9. | 3.50 | 3.74 |
| 10. | 3.61 | 3.77 |
| Mean | 3.47 | 3.57 |
| S. D | ± 0.16 | ± 0.21 |
| C.V. | 4.6% | 5.9% |

4.6. Discussion

In order to entrap the hydrophobic ^{90}Sr species within an organic polymer backbone, the prospect of using solvent extraction technique with DCH18C6 was pursued as it afforded the flexibility to fine-tune the activity in the organic phase while offering the convenience of extracting ^{90}Sr from a 3 M HNO_3 solution. In this work, $^{85+89}\text{Sr}$ tracer was used for optimization of the solvent extraction experiment instead of ^{90}Sr to preclude the contribution of ^{90}Y caused by the decay of ^{90}Sr as well as to avoid the direct handling of highly radiotoxic ^{90}Sr . The solvent used for the extraction of ^{90}Sr plays a vital role. The solvent used should preferably be of low boiling temperature so as to facilitate evaporation at room temperature. Although, a number of volatile organic solvents satisfy the above criteria, chloroform was the preferred solvent because of its ready availability, ease of separation from the aqueous phase and least solubility with water. While the addition of an appropriate polymer film on the surface of radionuclide entrapped polymer matrix has tangible benefits in diminishing the leaching of the radionuclide, but the entrapment of the radionuclide in an appropriate polymer matrix having negligible leaching is preferred. Equally important is the selection of an appropriate polymer matrix which should have the ability to entrap and retain the extracted ^{90}Sr species. The polymer film should also provide satisfactory immobilization performance in terms of resistance to leaching. Although several polymers are known and available, PMMA was chosen because it is hard, rigid and exhibits excellent solubility in chloroform due to strong polymer-solvent interactions [122]. The presence of ester groups in PMMA serve as anchors and promote spreading on smooth surface [134]. On comparison with commercially available sources of similar geometries, the characteristics of the prepared ^{90}Sr sources such as uniformity of activity distribution, activity content per source (1–5

kBq), particle emission rate (1270–6340/s) and removable surface contamination were similar. This reported method represents a facile large area source preparation procedure and the method afforded control of radioactivity in the film and permitted homogeneous distribution of ^{90}Sr throughout the surface. The method standardized herein could be adopted for preparation of ^{90}Sr polymer film sources of custom-size, as per the user's requirement. While DCH18C6 has been widely employed to extract ^{90}Sr for a variety of applications in separation science, its utility for making such radioactive polymeric film sources has never been reported so far, to the best of my knowledge. Using this solvent extraction cum polymer formation method 5 batches were prepared and > 95% efficiency was achieved.

4.7. Conclusion and Scope of the Work

In conclusion, the objective of making large-area ^{90}Sr sources commensurate with the specifications for use and compliant with the regulatory requirements has been accomplished. The reported process successfully exploits the capability of DCH18C6 to extract ^{90}Sr from an aqueous acid solution into a volatile organic solvent such as chloroform, versatility of PMMA to make a homogenous solution of appropriate concentration amenable to make large area radioactive polymeric film of defined size and the low boiling temperatures of chloroform (60°C) to facilitate drying at ambient temperature. The source preparation methodology described in this chapter represents a new method for preparing large area radioactive sources that obviate the need for sophisticated and expensive equipment. The reported method can be used for preparing large area sources of a wide variety of radionuclides for a broad range of applications.

CHAPTER-5

Preparation of ^{147}Pm Sources for Measurement of Dust in Environment Using Chemical Deposition on Ni Coated Copper Substrate

“Nothing in life is to be feared, it is only to be understood. Now is the time to understand more, so that we may fear less.”

-Marie Curie

5.1. Introduction

The technical and economic benefit of β^- gauge dust monitors towards the continuous monitoring of particulate concentration in air is well recognized [142-145]. The most important component of the dust monitors is a radioactive source which contains a low energy pure β^- emitting radioisotope. The beta emitter provides a steady β^- radiation flux to measure the concentration of suspended particles using β^- ray attenuation. In order to tap the potential of the β^- emitting radioactive sources for such applications, a rod type ^{147}Pm source was successfully developed previously by group which consisted of a cylindrical rod in which the activity was deposited on a small surface area at the tip of the rod [44, 72,145]. Although the basic principle of β^- particle attenuation remains unaltered in the current generation of dust monitors, over the years dust monitor technology has undergone an extensive design overhaul. Consequently, the radioactive source design has also changed and planar circular ^{147}Pm sources are replacing rod-type ^{147}Pm sources for these applications. Hence, an indigenous technology was adopted for the fabrication of such type of source. The radioactive source for this purpose consists of a circular planar ^{147}Pm source with an active area of 17 mm diameter containing 400 ± 20 kBq of ^{147}Pm activity homogeneously distributed on a Ni coated copper substrate on one face and housed in a 22 mm diameter cylindrical aluminum source holder. Among several methodologies available for preparation of radiation sources, in the present case, a two step process was considered appropriate to deposit the required amount of ^{147}Pm activity homogeneously on a planar substrate with good adherence owing to its proven effectiveness in making small area source [145]. In this chapter, utilization of chemical deposition technique for the deposition of ^{147}Pm activity on to Ni coated copper substrate (17 mm diameter) and quality control of the prepared ^{147}Pm source to ascertain

compliance with regulatory norms, is reported. The chapter describes in detail the process, experimental procedures and quality control of ^{147}Pm sources for use in dust monitors.

5.2. Experimental

5.2.1. Materials

^{147}Pm as promethium (III) chloride of specific activity $\sim 18.5\text{--}25.9\text{ GBq.g}^{-1}$ ($500\text{--}700\text{ Ci.g}^{-1}$) was procured from M/s. Tritec, Switzerland. Chemicals and reagents such as boric acid, nickel sulfate, sulfuric acid and ammonium hydroxide were of spectroscopic grade and were procured from BDH (India). Polystyrene granules used for coating were of analytical grade and were procured from BDH (India). Pure copper (99.99 %) and platinum plates of high purity with material testing certificates were procured from M/s. Hindustan Platinum Ltd., India. The circular copper substrates used in this work were machined from a sheet of copper metal. The electrolyte solutions were prepared from ultra pure water (Millipore Milli Qsystem).

5.2.2. Instrumentation

Regulated power supply in the range of 1-28 V, 0-2.5 A purchased from Aplab Limited (Model no. L1282), India was used for electrodeposition of Ni on the copper substrate. A beta radiation survey meter (PRM131A) purchased from PLA Electro Appliance Pvt Ltd., India was used to measure the radiation dose on the surface of the source. Liquid scintillation measurements were performed using a liquid scintillation counter (Model: Tricarb2100TR, Packard Instrument Co., USA) with Aqua safe 300 Plus scintillation cocktail (M/s Zinsser Analytic GmbH, Germany) and 10 mL scintillation vials (Meridian, UK). AGFA film grade-G-7 (AGFA India Pvt. Ltd.) was used for autoradiography. Optical density measurements were carried out using OPTTEL

Transmission densitometer (Model No.125.3 ENDT, LLC, USA). Cotton wool samples of swipe test and water samples of immersion test were counted in a G.M. counter (Model PNS-2, Electronic Enterprises (I) Pvt. Ltd., and India).

5.2.3. Preparation of Copper Electrode for Electrodeposition of Ni

A circular Cu strip of dimensions 18 mm (\varnothing) \times 0.5 mm (thickness) was used as the cathode. Prior to electrodeposition, the targeted circular area of the Cu strip was manually polished with emery paper and washed successively with acetone and deionized water. The back of cathode surface where Ni is not intended to be deposited was coated with a polymeric film, leaving the circular cross-sectional area available for Ni deposition. A Platinum plate having the same surface area was used as anode.

5.2.4. Preparation of Electrolyte for Ni Deposition

The required amount ($\sim 100\ \mu\text{g}$) of cold nickel as nickel sulphate was pipetted out into a 50 mL capacity glass beaker. 20 mL of 30 % w/vol boric acid in 0.01 M H_2SO_4 solution was added and the solution was transferred into the electro-deposition cell. The final pH of the solution was adjusted to 2-2.5 by the addition of 0.1 M ammonium hydroxide solution and dilute sulphuric acid.

5.2.5. Electrodeposition of Ni

A schematic diagram illustrating the electrochemical set-up used for the deposition nickel on a circular copper substrate is given in Fig. 5.1. One side of the circular substrate and the peripheral area not required for deposition of ^{147}Pm activity were blocked by coating with Araldite, an epoxy resin adhesive paste which is non-conductive. For enabling electrical connection, rods of the same material were welded at the top edge of the circular sheet and held by metallic vice. A circular platinum foil of equal area was used as the anode. The electrodes were positioned face to face, separated

10 mm apart and immersed in the electrolyte. Electrodeposition of Ni on one surface of the circular copper substrate was carried out galvanostatically using a modified Watt type bath following the reported procedure [67, 70]. After electrodeposition, the copper substrates were washed thoroughly with double distilled water and ethanol, and then dried in a current of dry air to a constant weight. These were stored in sealed containers until use.

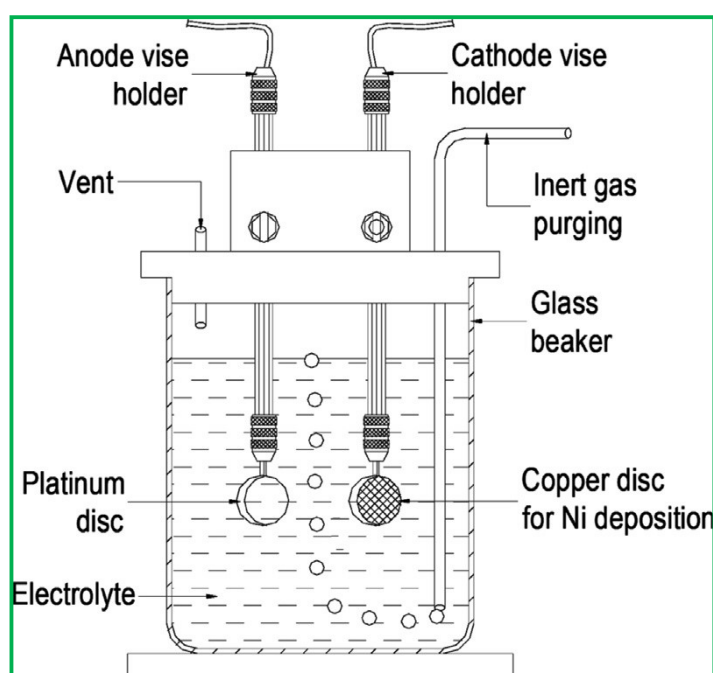


Fig. 5.1: Schematic set-up for electro-deposition of Ni on circular Cu substrate

5.2.6. Optimization of ^{147}Pm Deposition Parameters

The influence of pH on the deposition of ^{147}Pm was studied by varying the pH of the ^{147}Pm feed from 1 to 6, keeping the volume of the feed constant at 50 μL and time duration of 5 min. As ^{147}Pm is a carrier free radioisotope, the absolute content of Pm in the activity range used for preparation of the source is very less (~ 1 ng). Hence, addition of carrier may be preferable to obtain quantitative adsorption of Pm on the substrate. As there is no stable isotope of ^{147}Pm in nature, Sm was used as the inactive carrier owing to

their similar chemical properties [145]. The influence of Sm content was studied by varying its concentration from $100\text{ }\mu\text{g.mL}^{-1}$ to $400\text{ }\mu\text{g.mL}^{-1}$ keeping the pH constant at 6.0, The influence of reaction volume on ^{147}Pm deposition was investigated by varying the volume of the feed solution containing ^{147}Pm from $50\text{ }\mu\text{L}$ to $200\text{ }\mu\text{L}$ at pH 6 for 5 min. Further, the effect of time on the sorption of ^{147}Pm on the Ni electrodeposited Cu disc was studied by varying the sorption time from 1 to 10 min at pH 6 by keeping the volume of the feed constant at $50\text{ }\mu\text{L}$. Fresh aliquots of ^{147}Pm (3.7 KBq in $50\text{ }\mu\text{L}$) were used for each experiment. The activities of the solution before and after deposition were determined by counting the respective aliquots on a liquid scintillation counter (LSC).

5.2.7. Preparation of ^{147}Pm Source

Each Ni electrodeposited copper disc was kept in a beaker. The pH of the feed solution was maintained at 4-6 with the addition of dilute sodium hydroxide solution. About 1 mL of the ^{147}Pm feed solution containing $\sim 125\text{ kBq}$ of ^{147}Pm was pipetted out and added to a solution containing SmCl_3 at a concentration of $300\text{ }\mu\text{g}$ of Sm/mL in a 25 mL capacity beaker. The resulting solution was evaporated to dryness and reconstituted with dil. sulphuric acid and maintained at pH \sim 4. The Ni electrodeposited circular copper was kept in contact with the $^{147}\text{Pm}/\text{Sm}$ solution for 5 min after which it was taken out with the help of forceps, washed and dried under an IR lamp. The radioactivity content of the ^{147}Pm solution was measured before and after chemical deposition by liquid scintillation counting using suitable aliquot of the samples in order to determine the % activity adsorbed on the Cu disc. Subsequently, the active area of the sources was coated with polystyrene film by the dip-pull method [44].

5.2.8. Assay of Deposited ^{147}Pm Activity

The radioactivity assay procedure adopted for each ^{147}Pm source consisted of two stages for activity determination. In the first step, the total electrolyte activity strength was assayed by liquid scintillation counting by drawing suitable aliquots before and after the deposition. The amount of ^{147}Pm deposited on the matrix was calculated from the knowledge of the two activities. In the second step, dose rate of each source was individually measured and activity content was assessed from the relation between the activity and dose rate.

5.2.9. Source Assembly in a Circular Holder

Each circular holder consisted of an aluminum ‘cylinder’ with a flat bottom for nesting the circular source (Fig. 5.2). The flat bottom had a hole and a groove which nested the source. There was a machined depression at the bottom of the holder to mount the source in place. The holder was threaded on the inside edge to accommodate a matching cap. A circular cap threaded on the outside edge that matched the internal diameter of the holder was used to enclose the source. The cap could be used to turn in either direction. The cap could be rotated in a clockwise direction to screw in to the holder. The active area of the source was covered by an aluminum foil of 0.7 mg.cm^{-2} thickness to protect from mechanical abrasion during normal handling. It was placed with the help of tweezers to fit inside the base with its radioactive end facing down toward the open end and closed by winding the screwed cap tightly in position. This design secured the source in the holder during application. The cap could be removed by turning it in a counter clock-wise direction.

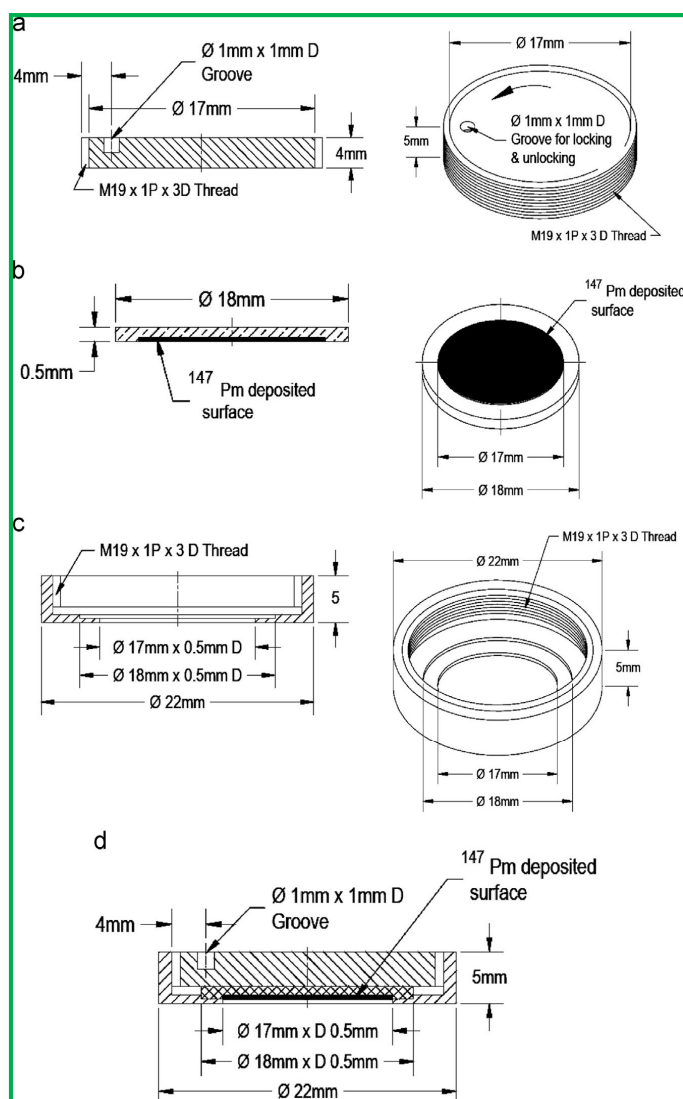


Fig. 5.2: Schematic diagram of (a) Circular threaded source holder cap, (b) Circular planar ^{147}Pm source, (c) Circular source holder base (d) Source assembly

5.2.10. X-ray, SEM, EDS and AFM Analysis

The quality of the Ni electrodeposited copper disc and the Sm deposited copper disc surfaces were examined by XRD, SEM, EDS and AFM of a dummy source prepared in an identical manner as that the active source. Since there is no stable isotope of ^{147}Pm in nature, Sm was used as the surrogate isotope in these experiments, owing to their very similar chemical properties. EDS microanalysis technique was used to identify the

elemental constituents of the electrodeposited samples. AFM technique was used to analyze surface roughness. The influence of Sm content in the feed solution on the surface morphology of Sm deposited source was studied to ensure homogeneous deposition of Sm or ^{147}Pm on the Ni electrodeposited Cu disc surface. Several optimization experiments were performed using different concentrations of the feed solution (100, 200, 300, 400 $\mu\text{g.mL}^{-1}$ of Sm) and the morphology of the Sm deposited surfaces was examined by SEM and EDS analyses.

5.2.11. Quality Control

(a) Swipe Test

A radioactive source should be free from loose contamination under normal conditions of use. Hence, in order to ascertain the integrity of the radioactive deposit, swipe test was performed by swiping the radioactive area using alcohol immersed cotton wool and the radioactive content of the swipe was checked in a G.M. counter.

(b) Leachability

The leachability of the ^{147}Pm source was tested following the technique prescribed by AERB [63]. In this procedure, each source was placed in beaker containing 100 mL water at room temperature for 48 h, at the end of which the sources were removed with the help of a tweezer. The water was concentrated to 0.1 mL by heating and radioactivity content was measured in a liquid scintillation counter.

5.3. Results

Owing to the no carrier-added (nca) nature of ^{147}Pm , the concentration of ^{147}Pm used for this purpose was extremely low and the effect of various experimental parameters such as pH of the chemical bath, amount of Sm carrier, volume of the feed

solution and time of deposition were optimized in order to arrive at the optimum deposition conditions.

5.3.1. Influence of pH of the Chemical Bath

The influence of pH on the percentage deposition of ^{147}Pm on the Ni electrodeposited Cu discs is presented in Figure-5.3.

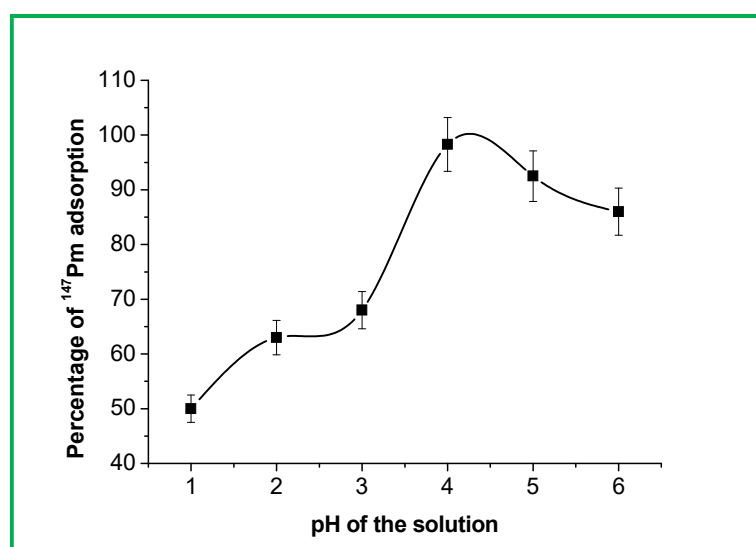


Fig. 5.3: Influence of pH of the feed solution on the chemical deposition of ^{147}Pm

From the above Figure, it can be inferred that, within the range of pH range investigated, optimum deposition of ^{147}Pm could be achieved when the pH was kept at 4 and thereafter any further increase of pH resulted in marginal decrease of the deposited activity. The deposition studies of ^{147}Pm were not pursued beyond pH 6 as ^{147}Pm would precipitate in alkaline solutions. The difference between the redox potential of the metals, (ΔE) is the driving force for deposition. It can be seen that with increase in pH, the potential shifts cathodically and the deposition of Pm increases and reaches a limiting value at pH 4. The marginal decrease of deposition rate beyond pH 4 may be attributed to the formation of a self-catalytic activity center in the bath, resulting in the decrease of the virtual deposition rate on the Ni deposited substrate.

5.3.2. Influence of Contact Time

The reaction time required to achieve nearly quantitative deposition of ^{147}Pm on the electrodeposited surface is another crucial parameter which needs to be optimized. In order to study the effect of contact time on the deposition of ^{147}Pm , deposition experiments were carried out at various time intervals and the results are depicted in Fig. 5.4. It is evident that the deposition of ^{147}Pm on the Ni electrodeposited Cu surface increased with increasing contact time and remained constant after 5 min of contact. This is a typical behavior of a chemical deposition process which is controlled both by the reaction kinetics and by mass transport. As is known, deposition of Pm at the electrodeposited Ni surface takes place by ion diffusion. As the contact time increases, more and more Pm ions gradually overcome the energy barrier for cathodic reaction (polarization resistance), diffusing on to the surface leading to the increase of the deposition rate. The maximum deposition rate maybe resulting from the complete diffusion of Pm ions.

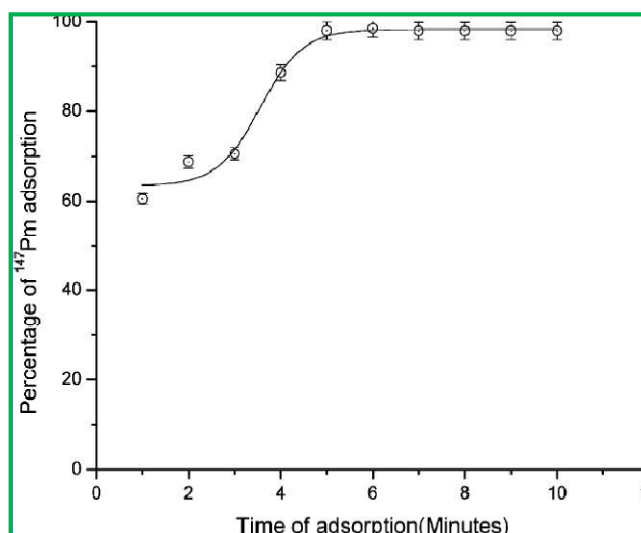


Fig.-5.4: Influence of contact time on the chemical deposition of ^{147}Pm

5.3.3. Effect of Reaction Volume

The feed volume of the chemical bath is another parameter which needed to be optimized. The dependence of the ^{147}Pm deposition efficiency on the reaction volume is shown in Fig. 5.5. Ignoring some fluctuation, the percentage deposition of ^{147}Pm activity on the substrate when the feed volume used is up to 50 μL was nearly quantitative, but after 50 μL decreases sharply and finally when the feed volume used was 200 μL , the retention was only 33 %. Hence, a reaction volume of 50 μL was used in subsequent experiments. With peculiar electronic structure and unique behavior of rare earths, ^{147}Pm will adsorb preferentially at the Ni deposited surface of the substrate. The adsorbed ^{147}Pm tends to give away electrons and part of ^{147}Pm becomes cationic due to the low electronegativity, which change the interface structure of the surface. With the increase of the reaction volume of bath, i.e., the decrease in the concentration of ^{147}Pm ions in bath, diffusion and deposition of the $^{147}\text{Pm}^{3+}$ ions are hindered, thus leading to the decrease in deposition.

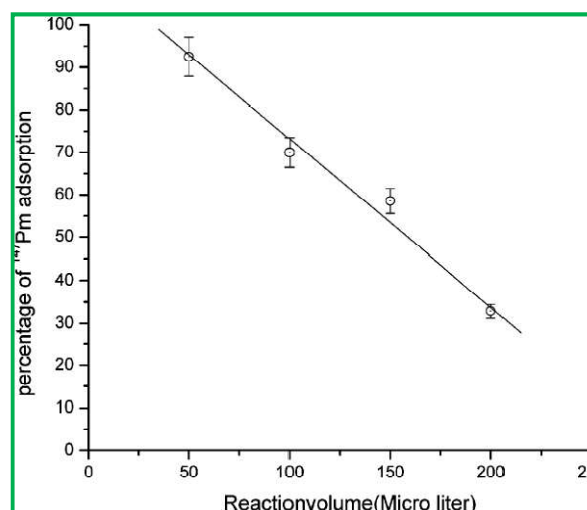


Fig. 5.5: Effect of reaction volume on the chemical deposition of ^{147}Pm

5.3.4. X-ray Diffraction Studies

Fig. 5.6 depicts the XRD pattern of the substrate, after Ni electrodeposition and after chemical deposition of Sm. Fig. 5.6(a) showed all the peaks of copper metal when compared with the standard PCPDF data (Card no- 04-0836). Fig. 5.6(b) showed peaks of Ni metal (card no- 04-0850) for the electrodeposited sample. However, we observed the presence of the copper also [Fig. 5.6(b)] even after the deposition of the nickel, possibly due to the very small thickness of the deposited Ni layers. Fig. 5.6(c) represents the XRD pattern of the chemical deposited surface. However, the XRD data did not show any peaks other than that of Cu substrate and Ni. Therefore, at this stage it is difficult to unequivocally characterize the nature of adsorbed Sm. There can be several possibilities namely (i) the Sm layer is amorphous, (ii) it is too thin to be seen by XRD, (iii) Sm deposition has not taken place. Therefore, this situation necessitated employing other techniques such as SEM and EDS.

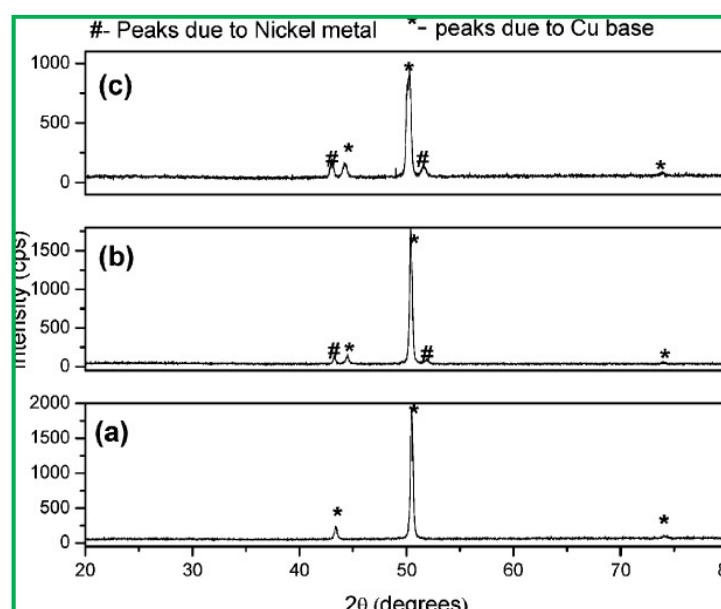


Fig. 5.6: XRD pattern of (a) Copper substrate (b) Electrodeposited Ni sample and (c) Chemical deposited Sm sample

5.3.5. Scanning Electron Microscopy (SEM) Analysis

The SEM micrographs of the copper substrate and electrodeposited Ni samples are shown in Fig. 5.7.

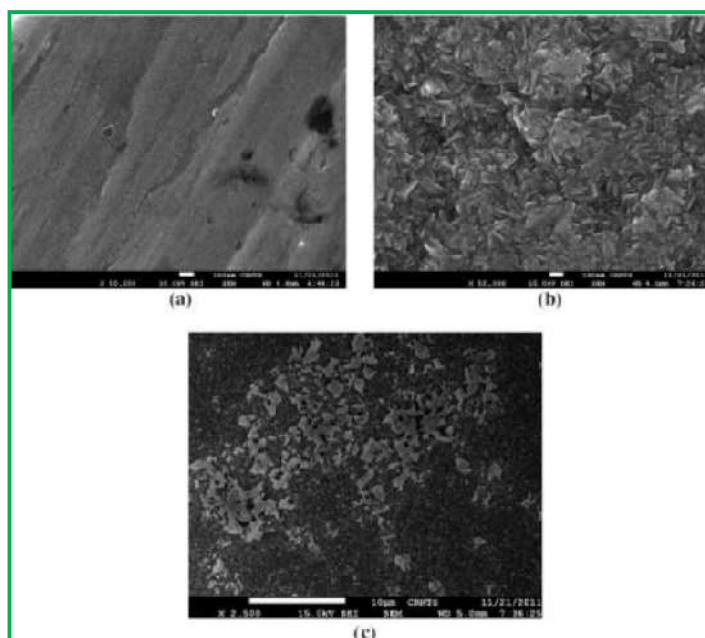


Fig. 5.7: SEM micrograph of (a) Copper substrate (b) Electrodeposited Ni surface (c) Chemically deposited Sm sample

It can be clearly seen that the electrodeposited sample [Fig. 5.7(b)] showed uniform deposition with small granular crystals of Ni metal on the surface of the Cu substrate indicating good adhesion with the copper backing. The SEM micrograph further indicated that the surface is very rough and flaky, which promotes the chemical deposition of Sm or Pm. The chemical deposited sample [Fig. 5.7(c)] showed various distinct areas, which could be due to Sm in agglomerated form. In a separate experimental run, the influence of Sm contents in the feed solution on the surface morphology of Sm deposited film were examined within the concentration range of $100\text{--}400\ \mu\text{g.mL}^{-1}$ of Sm. The surface morphology was studied by SEM analyses and determination of Sm content of the deposited film was carried out by EDS analyses. Fig. 5.8 shows the SEM images of

Sm deposited surface at different magnifications obtained for different concentrations of Sm in the feed solution (100, 200, 300, 400 $\mu\text{g.mL}^{-1}$). Several SEM images of the Sm deposited surface generated are shown in Fig. 8. Fig. 5.8 100a, 100b, 100c, depicts the SEM images obtained from using feed solution concentrations of 100 $\mu\text{g.mL}^{-1}$. Similarly, Fig. 5.8 200a, 200b, 200c were for 200 $\mu\text{g.mL}^{-1}$, Fig. 5.8 300a, 300b, 300c were for 300 $\mu\text{g.mL}^{-1}$, and Fig. 5.8 400a, 400b, 400c were for 400 $\mu\text{g.mL}^{-1}$. As can be seen, the four series of photomicrographs yielded interesting differences. Therefore, the concentration of the Sm solution has determinative effects on the morphologies of the deposited surface. When the concentration of Sm in the feed solution were 100 and 200 $\mu\text{g.mL}^{-1}$, agglomerated particles of irregular shapes and sizes were found to be randomly distributed over the surface of the substrate (Fig. 5.8 100a, 100b, 100c and Fig. 5.8 200a, 200b, 200c). On the other hand, by increasing the concentration of Sm in the feed solution to 300 $\mu\text{g.mL}^{-1}$, the microstructure, characterized by SEM, shows the development of a dense film with smooth surface (Fig. 5.8 300a, 300b, 300c). On further increasing the concentration of Sm to 400 $\mu\text{g.mL}^{-1}$, the deposit showed the presence of inter-grown aggregate crystals of heterogeneous size, distributed irregularly on the surface of the substrate (Fig. 5.8 400a, 400b, 400c).

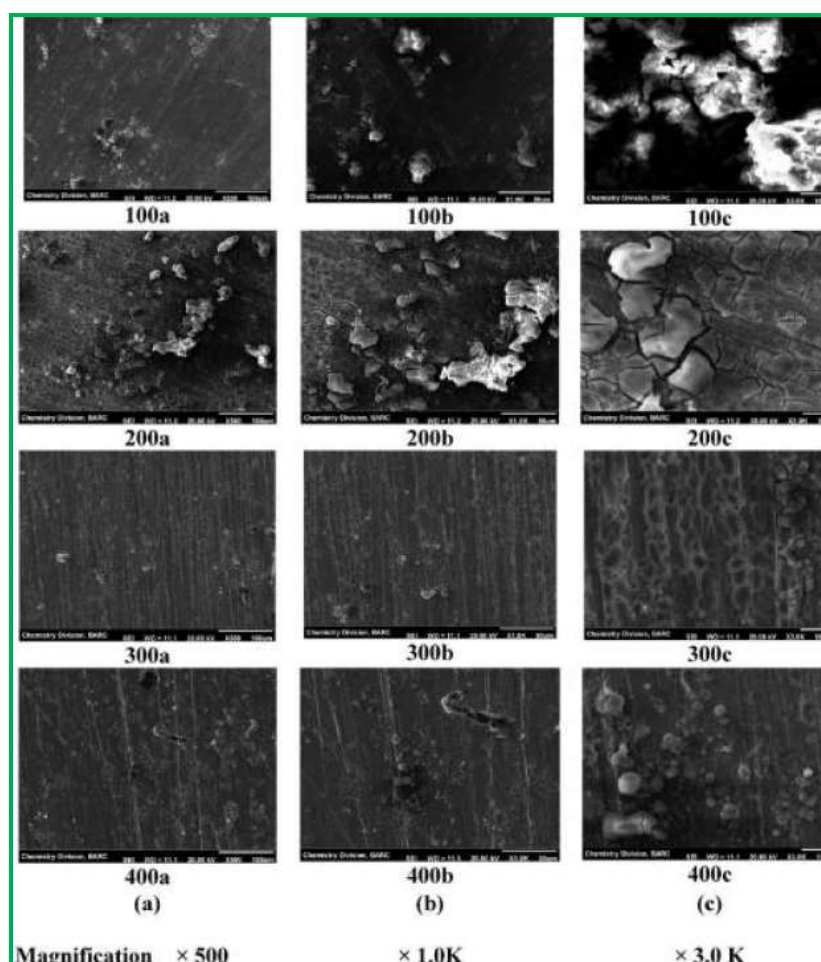


Fig. 5.8: SEM micrograph of chemical deposited Sm samples at different concentrations of Sm feed concentration (a) 500 \times magnification (b) 1K \times magnification (c) 3K \times magnification

5.3.6. EDS Characterization

Fig. 5.9(a) depicts the EDS spectrum of the electrodeposited Ni on the Cu substrate. It shows peaks pertaining to Ni only which indicates complete coverage of Cu substrate by Ni. The deposited surface is free from any other chemical impurities.

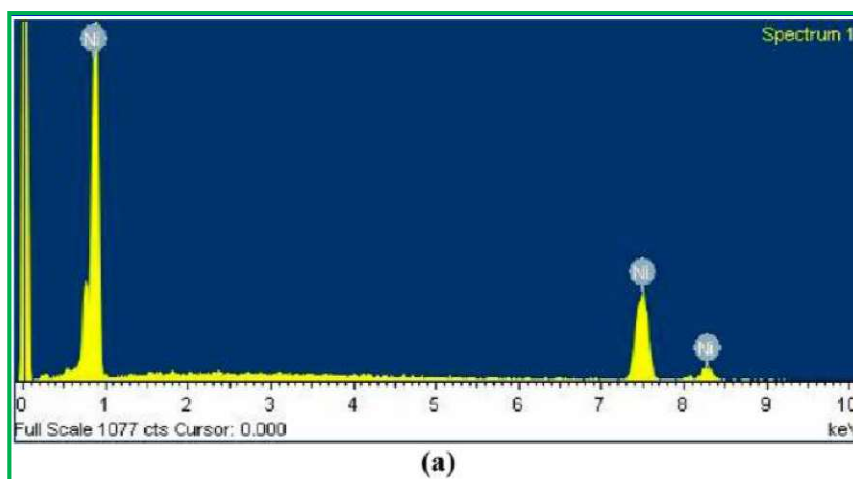


Fig. 5.9(a): Electrodeposited Ni surface

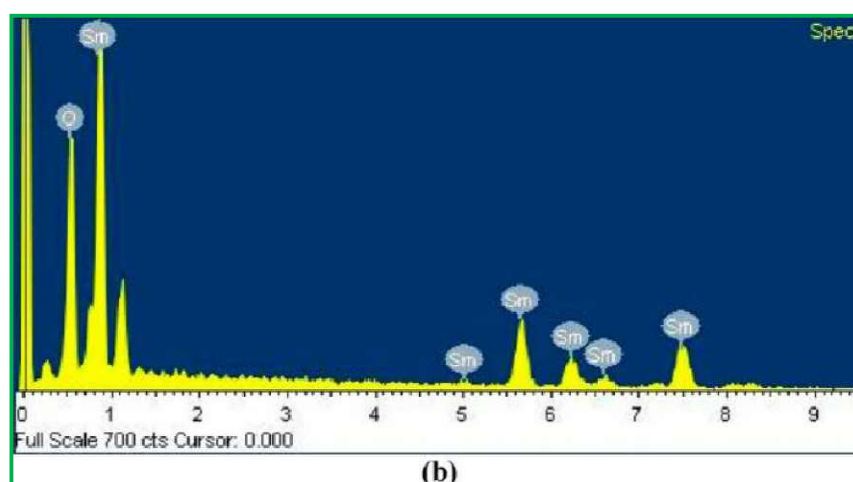


Figure-5.9(b): Chemically deposited Sm surface

EDS spectra of the chemical deposited surface as seen from Fig. 9b indicated the coverage of Ni surface with deposited Sm. From the EDS data, it appears that the deposited Sm is in the form of samarium oxide. Table-5.1 depicts the effect of concentration of Sm on the nature of the deposited surface.

Table-5.1: Effect of concentration of Sm in the feed solution on the Sm content of the deposited surface obtained from EDS Measurements

| Sr. No. | Feed concentration of Sm ($\mu\text{g/mL}$) | Concentration of Sm deposition at the surface (wt %) |
|---------|---|--|
| 1. | 100.0 | 3.87 |
| 2. | 200.0 | 4.02 |
| 3. | 300.0 | 4.06 |
| 4. | 400.0 | 8.14 |

The results in Table-5.1 indicate that increasing the concentration of Sm in the feed solution from 100 to 300 $\mu\text{g/mL}$ has only marginal effect. On further increasing the concentration of the Sm content in the feed solution to 400 $\mu\text{g/mL}$, Sm content on the deposited layer increases. On the basis of EDS elemental mapping of Sm at different position of deposited surface, homogeneity of deposition can be ascertained. The results of the EDS elemental mapping obtained with 100, 200, and 400 $\mu\text{g/mL}$ of Sm revealed non-uniformity of Sm deposition at the surface. On the other hand, when the concentration of Sm in the feed solution was maintained at 300 $\mu\text{g/mL}$, near uniform deposition of Sm was observed at the surface. From the above, it could be inferred that in order to obtain a homogeneous deposition of Sm or Pm on the Ni electrodeposited surface, the concentration of Sm in the feed needs to be maintained at 300 $\mu\text{g/mL}$. The concentration of carrier Sm in the feed solution plays a major role when large surface area target is to be prepared. For the envisaged application, it is important to deposit the required quantity of ^{147}Pm on the Ni electrodeposited Cu disc to obtain required the β^- output and fairly consistent deposition so as to attain uniform β^- radiation flux in all directions.

5.3.7. AFM analysis

In order to evaluate the influence of the surface properties of the Ni deposited surface on the chemical deposition of Pm, we carried out AFM analysis. AFM images of the Ni electrodeposited Cu disc and Sm adsorbed Cu disc are shown in images a and b of Fig. 5.10. The scanning area of AFM was $10\ \mu\text{m} \times 10\ \mu\text{m}$. The AFM images indicate that the Ni electrodeposited film surface as shown in Fig. 5.10(a) is homogeneous and rough with mean square roughness (rms) value of $\sim 93\ \text{nm} \pm 0.2\ \text{nm}$. AFM image of Sm adsorbed on the substrate as depicted in Fig. 5.10(b) demonstrated the rms value of $187\ \text{nm} \pm 0.2\ \text{nm}$. Further, it was found that the surface morphology was more uneven than that of Ni electrodeposited Cu disc. Thus, from the AFM images it could be concluded that after the adsorption of Sm on the surface of the electrodeposited Ni, the roughness of the surface increased.

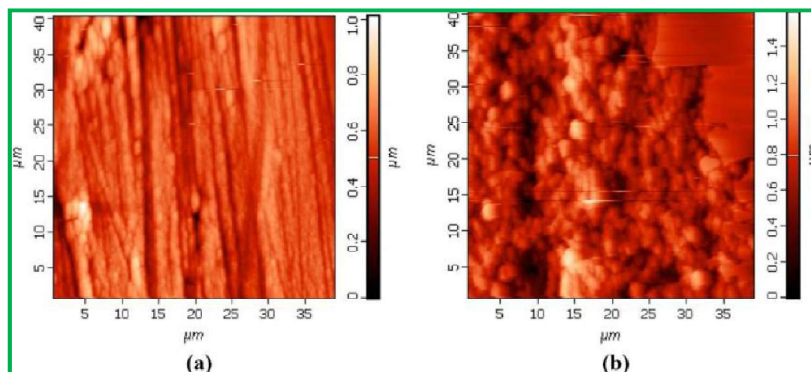


Fig.5.10: AFM images of the (a) Electrodeposited Ni surface (b) Chemical deposited Sm surface.

5.3.8. Source Preparation

In order to realize the chemical deposition of ^{147}Pm on a Ni coated planar Cu substrate, optimum values of experimental parameters such as pH of the feed solution, concentration of carrier Sm, reaction volume and deposition time were chosen. The need

to achieve homogeneous deposition of ^{147}Pm on the electro-deposited Ni surface necessitated the addition of inactive carrier such as Sm in the feed solution at a concentration of $300\ \mu\text{g.mL}^{-1}$ [145]. Results of deposition carried out from 4 batches at different activities of feed solution are presented in Table-5.2. It was observed that the percentage of ^{147}Pm deposited on the substrate remained practically unaltered irrespective of the activity in the feed solution and was always greater than 90 %. While the goal of the present investigation is to prepare sources of 400 kBq (10 μCi) of ^{147}Pm , the potential of the chemical deposition technique for preparation of sources using a wide range of ^{147}Pm activity (400–2003 kBq) was assessed. Results from Table-5.2 demonstrate that the method was found to be effective for the preparation of ^{147}Pm sources of strength ranging from 400 to 2003 kBq. Following the procedure described above, several ^{147}Pm sources were prepared with an aim to obtain ~ 400 kBq (10 μCi) of ^{147}Pm activity in each source. The results show acceptable batch-to-batch reproducibility. The need to protect the ^{147}Pm layer during use prompted us to coat the surface with polystyrene.

Table-5.2: Efficiency of the chemical deposition process

| Batch number | ^{147}Pm activity in the feed solution kBq (μCi) | Activity retained by the substrate kBq (μCi) | % of deposited activity |
|--------------|---|---|-------------------------|
| 1 | 400.7(10.8) | 381.1(10.3) | 95.6 |
| 2 | 801.4(21.7) | 729.4(19.71) | 91.0 |
| 3 | 1202.1(32.5) | 1118.3(30.2) | 93.1 |
| 4 | 1602.8(43.3) | 1468.2(39.68) | 91.6 |

5.3.9. Activity Assay of Deposited ^{147}Pm Source

In order to correlate the dose rate from the source to the activity of ^{147}Pm , simulated circular planar sources with known amount of activity were used. Fig. 5.11 displays the ^{147}Pm activity deposited as a function of the dose rate observed in the radiation monitor. The response is seen to be linear and therefore used for the measurement of ^{147}Pm activity of the final source. The activity content of individual ^{147}Pm sources were assayed following the liquid scintillation counting procedure as well as described dose rate vs. activity relationship data. The results show that there was no appreciable difference between the two methods and for the purpose of quoting activity of the source, an average of the two results was used.

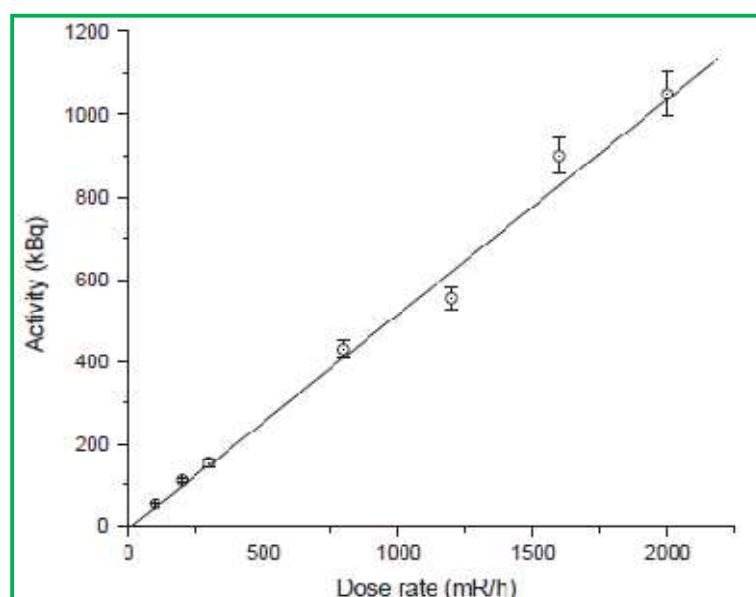


Fig. 5.11: Dose rate vs. activity relationship

5.3.10. Quality Control of the Sources

The prepared sources were subjected to quality control tests in order to ensure that they are in compliance with the requirements of AERB [63]. Results of quality control tests carried out using five sources of different activity contents prepared in different

batches are depicted in Table-5.3. Leaching studies conducted on 5 sources indicated that $< 0.01\%$ of the original activity leached out, which complied with the specifications laid by the AERB [63]. The results of the swipe test and immersion test as depicted in Table-5.3, indicate that the removable activities are lower than 185 Bq (5 nCi) in the solution as well as the swipe, which comply with the specifications laid down by AERB [63].

Table-5.3: Quality evaluation of ^{147}Pm sources

| Batch No. | Activity kBq (μCi) | Leachability (% total activity) | Immersion test (Total activity release in 4 h) Bq (nCi) | Surface contamination Bq (nCi) |
|-----------|------------------------------------|------------------------------------|---|-----------------------------------|
| 1 | 381.1(10.3) | 0.009 | 121(3.2) | 27(0.73) |
| 2 | 392.3(10.59) | 0.005 | 109(2.94) | 51(1.38) |
| 3 | 388.5(10.5) | 0.006 | 158(4.27) | 29(0.78) |
| 4 | 395.2(10.68) | 0.008 | 133(3.59) | 31(0.83) |
| 5 | 408.5(11.04) | 0.005 | 162(4.37) | 47(1.27) |

5.3.11. Source Assembly

Based on the procedure outlined, several ^{147}Pm sources of strength ~ 400 kBq (10.8 μCi) of activity were prepared. The source strengths were adequate for measurement of particulates in the $1\text{--}10\text{ mg.cm}^{-2}$ range. The use of holder to load the source is essential to make a mono-directional radiation source. We selected aluminum as holder material owing to its attributes such as ready availability in high purity, low cost, radiation stability, excellent corrosion resistance and adequate mechanical strength. The design of the holder was configured to provide adequate mechanical strength to secure the source in position during application as well as handling and at the same time provide

required radiation output without significant attenuation. The sources after the QC tests were supplied to the user.

5.4. Discussion

The aim of this investigation was to assess the potential of wet chemical deposition technique to realize homogeneous deposition of ^{147}Pm on one face of a circular planar Cu substrate which was previously electrodeposited with Ni. While the wet chemical deposition has been successful in the preparation of such sources with small surface area, its utility for the preparation of a source of large surface area has not been explored previously and was hence considered worth investigating. In order to achieve the objective of depositing ^{147}Pm within a geometrically well-designated area of a substrate utilizing chemical deposition technique, a two step process in which first Ni was electrodeposited on the circular copper substrate and in the second step the required activity of ^{147}Pm was chemically deposited on the target area using inactive Sm carrier was chosen. In order to realize homogeneous deposition of ^{147}Pm on a planar substrate, wet chemical deposition technique was considered. The results revealed that chemical deposition technique for large area substrate is as efficacious as small area substrate. The need to protect ^{147}Pm deposited from leaching of the activity and mechanical abrasion or damage during application is an issue, addressed adequately. Attenuation of radiation due to thin polymer coatings is negligible because it consists of material of low composite atomic number. Incorporation of an organic polymer barrier layer in contact with the ^{147}Pm deposited surface could result in achieving this aim in an efficient manner. In order to ensure safety of the source during normal use as well as under foreseeable accidental conditions, the need to perform the quality evaluation test is obligatory and thus pursued. Local availability of this type of radioactive source may not only reduce the user's

dependence on imported radiation sources but also may help in promoting the deployment of dust monitors in our country.

5.5. Conclusion and Scope of the Work

In conclusion, the utility of the chemical deposition technique to prepare circular planar ^{147}Pm sources commensurate with product specifications and regulatory requirements, has been successfully achieved. This process is advantageous, as it permits ‘all- radioactivity’ in situ approach and at the same time allows the control of radioactivity content in the source. The reported procedure is not only facile but also requires inexpensive simple equipment and can be scaled up to any production size.

CHAPTER-6

Summary, Conclusions and Future Directions

“Try not to become a man of success, but rather try to become a man of value.”

-Albert Einstein

6.1 Summary of the Thesis

In this thesis, preparation of custom-made radioactive sources using different source preparation techniques such as cathodic electrodeposition, electrodeposition-cum-adsorption, chemical displacement and solvent extraction followed by polymer film preparation for multifarious applications is described. Each of the chapters is focused on a particular source preparation technique and includes the use of non-destructive techniques such as XRD, SEM, EDS and autoradiography for complete characterization of the sources. The summary of the work reported in each chapter is given below.

Chapter-1 gives an overview of the types of sealed radiation sources, methods of preparation, quality control tests and their applications in various field including medicine and industries.

Chapter-2 describes the use of electro-deposition technique for the preparation of ^{55}Fe , ^{57}Co and ^{204}Tl sources. The sources prepared by this method complied with the standard safety requirements for radioactive sources laid down by AERB, India. While the Fe-55 sources were supplied to users for the calibration of low energy X ray detectors in space applications, the ^{57}Co sources prepared using the optimized technique were supplied to the customer for possible use in quality control of nuclear medicine imaging instruments.. The ^{204}Tl electrodeposited sources were found to be useful for calibration of detectors. This source preparation strategy based on electrochemical deposition will find applications in the preparation of solid sources of many other radioisotopes.

Chapter-3 describes the utilization of two-step electrodeposition technique for the preparation of electrodeposited sources of ^{133}Ba and $^{90}\text{Sr}/^{90}\text{Y}$ for the calibration dose calibrators and beta surface contamination monitors is described. The experimental

details from this investigation may be useful for institutions planning to pursue radioactive source preparation strategies to meet their domestic demands.

Extraction and radioactive polymer formation have been effectively utilized to prepare $^{90}\text{Sr}/^{90}\text{Y}$ sources for use in surface contamination monitors, as described in chapter-4. The source preparation methodology utilizing solvent extraction, described in this chapter represents a new paradigm for preparing large area radioactive sources that obviate the need for sophisticated and expensive equipment. The reported method can be used for preparing large area sources of wide variety of radionuclides for a broad range of applications.

Chapter-5 describes the utility of chemical deposition technique to prepare circular planar ^{147}Pm sources commensurate with product specifications and regulatory requirements. This process is advantageous as it permits ‘all- radioactivity’ in situ approach and at the same time allows the control of radioactivity content in the source. The reported procedure is not only facile but also requires inexpensive simple equipment and can be scaled up to any production size.

6.2 Future Scope of the Work

The different source preparation methodologies which are described in the thesis can be used for the fabrication of novel radiation sources for future applications. The experience gained in the preparation of custom-made radiation sources during the course of the thesis work would help in the preparation of custom-made radiation sources as per future requirements.

References

1. International Atomic Energy Agency, International catalogue of sealed radioactive sources, IcSRS.
2. Product catalogue of Board of Radiation & Isotope Technology (BRIT), 2013.
3. IAEA Safety Series No. 107: Radiation safety of gamma and electron irradiation facilities, 1992.
4. Technical information for radiation sources-IZOTOP.
5. Isotope Products-RITVERC.
6. Calibration standards and instruments product information-Eckert & Ziegler, 2007.
7. International Atomic Energy Agency, Categorization of radioactive sources, IAEA safety standards series No. RS-G-1.9, IAEA, Vienna, 2005.
8. International Atomic Energy agency, Regulatory control of radiation sources, IAEA safety standards series No. GS-G-1.5, IAEA, Vienna, 2004.
9. Kolb D M and Schneeweiss M A: Scanning Tunneling Microscopy for metal deposition studies, Electrochem. Soc. Interface, 8 , 26-30, 1999.
10. Andricacos P C: Copper on-chip interconnections, a breakthrough in electrodeposition to make better chips, Electrochem. Soc. Interface, 8, 32-37, 1999.
11. Schwarzacher W: Metal nanostructures, a new class of electronic devices, Electrochem. Soc. Interface, 8, 20-24, 1999.
12. Bartlett P N: Electrodeposition of nanostructured films using self-organizing templates, Electrochem. Soc. Interface, 3 , 28-33, 2004.

References

13. Puri and Sharma, Principles of Physical Chemistry, Vishal Publishing Co. 47th edition, 2017.
14. Pletcher D and Walsh F C, Industrial Electrochemistry, Springer; 2nd edition, 1990.
15. Bagotsky V S, Fundamentals of Electrochemistry, Wiley-Blackwell, 2nd Revised edition, 2005.
16. Pandey, Hand book of semiconductors electrodeposition, CRC Press, 1 edition, 1996.
17. Roberson Max: Substrate surface preparation handbook, Artech House Publishers, November 30, 2011.
18. Substrate surface preparation, Artech House Publishers, 2011.
19. Davis Joseph R: Copper and copper alloy, ASM International, 01-Jan-2001.
20. Josef Barthel, Heiner, J. Gores, Georg Schmeer, and Rudolf Wachter: Non-aqueous electrolyte solutions in chemistry and modern technology alloy, 2005.
21. Holliday A K, Massey A G, Robinson Robert, Irving H M N H and Staveley L A K: Inorganic chemistry in non aqueous solvents, 1965.
22. Zoski Cynthia G: Handbook of Electrochemistry, Elsevier Science; 1 edition February 21, 2007.
23. Electroplating, available online <http://www.flipchips.com/tutorial46.html>.
24. Strickland G R,: Introduction SUST repository, prod. Frinish, (condon), 1971.
25. Vanilburg G C: Modern electroplating book, plating surf. Finish, 1984.
26. Yoon S, Schwartz M and Nobe K: electrodeposition of Cu, Sn and Cu-Sn alloy, Plating Surf. Finish. 81, 65, 1994.
27. Yoon S, Schwartz M, and Nobe K, Plating Surf. Finish. 82, 64, 1995.

References

28. Farndon E E, Walsh F C, and Campbell S A: Effect of thiourea, benzotriazole and 4,5-dithiaoctane-1,8-disulphonic acid on the kinetics of copper deposition from dilute acid sulphate solutions, *J. Appl. Electrochem.*, 25, 574, 1995.
29. Armstrong M J and Muller R H: In situ Scanning Tunneling Microscopy of copper deposition with Benzotriazole, *J. Electrochem. Soc.*, 138, 2303, 1991.
30. Weil R and W J- Chang, *Plating Surf. Finish.* 75, 60, 1988.
31. Rashkov R and Nanev C: Effect of surface active agents on the initial formation of electrodeposited copper layers, *J. Appl. Electrochem.*, 25, 603, 1995.
32. Anoplate Industrial Metal Finishing Since 1960.
33. AERB Safety Standard No. AERB/SS/3 (Rev.1)/INDIA (based on ISO 2919).
34. Krishnaswami S, Lal D, Amin B S, Soutar A: Geochronological studies in Santa Barbara Basin: ^{55}Fe as a unique tracer for particulate settling *Limnol. Oceanogr.* 18, 763, 1973.
35. Denecke B, Sibbens G, Szabo T, Hult M, Persson L.: Improvements in quantitative source preparation. *Appl. Radiat. Isotopes* 52, 351, 2000.
36. Robinson P S: The production of radioactive sources by the electro spraying method. *Nucl. Instrum. Methods* 40, 136, 1966.
37. De Sanoit J, Leprince B, Bobin Ch and Bouchard J: Freezedrying applied to radioactive source preparation. *Appl. Radiat. Isot.* 6, 1391, 2004.
38. Power W H, Heyd J W: Modified joliot apparatus for study of electrodeposition of radioactive materials. *Anal. Chem.* 28, 523, 1956.
39. Steeb J, Josowicz M: Nickel-63 micro irradiators, *Anal. Chem.* 81, 1976 (2009).

References

40. Udhayakumar J, Pardeshi G S, Gandhi S S, Chakravarty R, Kumar M, Dash A, Venkatesh M: Development of technology for the large scale preparation of ^{60}Co polymer film source. *Appl. Radiat. Isotopes* 66, 1825, 2008.
41. Was B, Koval'ik A, Novgorodov A F, Rak J: A new technique for the preparation of small-size radioactive samples based on the Langmuir–Blodgett method. *Nucl. Instrum. Methods* 332, 334, 1993.
42. Zhang H, Häfeli U O: Preparation and characterization of radioactive $\text{Co}/^{188}\text{Re}$ stents intended for lung cancer treatment using an electrodeposition method. *J. Med. Eng. Technol.* 28, 197, 2004.
43. Tsoupko-Sitnikov V, Picolo J L, Carrier M, Peulon S, Moutard G.: A novel method for large-area sources preparation for the calibration of β - and α -contamination monitors. *Appl. Radiat. Isotopes* 56, 21, 2002.
44. Kumar M, Udhayakumar J, Gandhi S S, Satpati A K, Dash A, Venkatesh M: An electrochemical method for the preparation of ^{63}Ni source for the calibration of thermoluminescence dosimeter (TLD). *Appl. Radiat. Isotopes*. 67, 1042, 2009.
45. Longworth G, Window B: The preparation of narrow-line mossbauer sources of ^{57}Co in metallic matrices. *J. Phys. D Appl. Phys.* 4, 835, 1971.
46. D'iaz S L, Calder'on J A, Barcia O E, Mattos O R: Electrodeposition of iron in sulphate solutions. *Electrochim. Acta* 53, 7426, 2008.
47. Jartych E, Zurawicz J K, Maczka E, Borc J: Preparation of thin iron films by electrodeposition and characterization of their local magnetic properties. *Mater. Chem. Phys.* 72, 356, 2001.
48. Zarpellon J, Jurca H F, Klein J J, Schreiner W H, Mattoso N. Mosca D H:

- Electrodeposition of Fe thin films on Si (1 1 1) surfaces in the presence of sodium saccharin. *Electrochim. Acta* 53, 2002, 2007.
49. Renaux C S, Flandre V D: New experiments on the electrodeposition of iron in porous silicon. *Microelectron. Reliab.* 40, 877, 2000.
 50. Qaim S M, Black P J, Evans M J.: The preparation of narrow line ^{57}Fe Mössbauer sources and an investigation of some of the causes of their line broadening. *J. Phys. C Solid State Phys.* 1, 1388, 1968.
 51. Qaim S M: Mössbauer effect of ^{57}Fe in various hosts: isomer shifts of the 14.4 keV gamma line of ^{57}Fe in different metallic lattices. *Proc. Phys. Soc.* 90, 1065.1967.
 52. Qaim S M: Recoil-free fractions of the 14.4 keV Mössbauer gamma line of ^{57}Fe in various host lattices. *J. Phys. F Metal Phys.* 1, 320, 1971.
 53. Carmon B, Pasi M: Electrodeposition of a strongly adhesive iron-55 source for use in X-ray fluorescence analysis. *Int. J. Appl. Radiat. Isot.* 32, 600, 1981.
 54. Ammel Van, R Pomm'e, S., Sibbens, G.: Half-life measurement of ^{55}Fe . *Appl. Radiat. Isot.* 64, 1412, 2006.
 55. Labeyrie L D, Livingston H D, Gordon A G: Measurement of ^{55}Fe from nuclear fallout in marine sediments and seawater. *Nucl. Instrum. Methods* 128, 575 1975.
 56. Harwood J A, Taylor M R H: Measurements of iron-55 and iron-59 from blood samples using a cesium iodide crystal. *Phys. Med. Biol.* 11, 589, 1966.
 57. Layrisse M, Mart'inez-Torres C, Cook J D, Walker R, Finch C A: Iron fortification of food: its measurement by the extrinsic tag method. *Blood* 41, 333.1973.

References

58. Ganzoni A, Hillman R S, Finch C A: Maturation of the macroreticulocyte. Brit. J. Haematol. 16, 119, 1969.
59. Warner G T: The use of total-body counters for the study of iron metabolism and iron loss. Postgrad. Med. J. 49, 477, 1973.
60. Kumpulainen L H, Saukkonen H A: Blood sample $^{59}\text{Fe}/^{55}\text{Fe}$ activity ratio measurement using a semiconductor detector. Int. J. Appl. Radiat. Isot. 30, 407, 1979.
61. Skwarzec B: Procedure for radiochemical analysis of ^{55}Fe and ^{63}Ni in selected environmental samples. Ocean. Stud. 25, 15, 1996.
62. Kojima S, Furukawa M: Liquid scintillation counting of ^{55}Fe applied to air filter samples. Radioisotopes 34, 72, 1985.
63. AERB Safety standard no: AERB/SS/3 (Rev. 1), Class. of sealed sources, published by Atomic Energy Regulatory Board, Department of Atomic Energy, Mumbai, India, 2001.
64. Srimathi S N, Mayanna S M, Sheshadri B S: Electrodeposition of binary magnetic alloys. Surf. Techn. 16, 277, 1982.
65. Zanzonico P, Routine quality control of clinical nuclear medicine instrumentation: a brief review. J. Nucl. Med. 49, 1114–1131, 2008.
66. Dash A, Kumar M, Udhayakumar J, Gandhi S S, Satpati A K, Nuwad J, Shukla R, Pillai C G S, Venkatesh M, Venugopal: On the application of electrochemical techniques for the preparation of ^{57}Co source core, encapsulation and quality evaluation for radiometric assay of nuclear fuel rods. Radiochim. Acta. 99, 103–111, 2011.
67. Dash A, Udhayakumar J, Kumar M, Shukla R, Gandhi S S, Tyagi A K,

- Venkatesh M,. Development of a micro electrochemical cell for insitu deposition of ^{63}Ni for use in electron capture detector (ECD) in gas chromatography. *Radiochim. Acta* 99,733–741, 2011.
68. Gandhi S S, Kumar M, Chakravarty R, Nuwad J, dhayakumar J, Dash A. An electrochemical route to prepare planar ^{204}Tl sources for the calibration of beta surface contamination monitors. *Radiochim. Acta*. 2013.
69. Kumar M, Udhayakumar J, Gandhi S S, Satpati A K, Dash A, Venkatesh M: An electrochemical method for the preparation of ^{63}Ni source for the calibration of thermoluminescence dosimeter (TLD). *Appl. Radiat. Isotopes*. 67, 1042, 2009.
70. Kumar M, Udhayakumar J, Nuwad, J, Shukla R, Pillai C G S, Dash A, Venkatesh M,. Development of a ^{147}Pm source for beta-backscatter thickness gauge applications. *Appl. Radiat. Isot.* 69, 580–587, 2011.
71. Kumar M, Udhayakumar J, Dash A: A facile and novel process for the preparation of ^{147}Pm source. *J. Radioanal. Nucl. Chem.* 290, 53–58, 2011.
72. Kumar M, Shukla R, Gandhi S S, Udhayakumar J, Satpati A K, Tyagi A K and Dash A: Selective area chemical-deposition process an innovative and facile route to prepare ^{147}Pm sources for dust monitors. *Ind.Eng.Chem.Res.*51, 11147–11156, 2012.
73. Kumar M, Gandhi S S, Udhayakumar J, Satpati A K, Shukla R, Tyagi A K and Dash A: An electrochemical technique to prepare ^{55}Fe source for the calibration of the X-ray detectors. *Radiochim. Acta* .101, 185–194, 2013.
74. Kumar M, Gandhi S S, Nuwad J, Udhayakumar J, Dash A: b. A novel and facile approach for the preparation of Ba-133 source core, encapsulation and

- quality evaluation. *Radiochim. Acta.* 101, 195–204, 2013.
75. Mathew C, Majali M A, Balakrishnan S A: A novel approach for the adsorption of iodine-125 on silver wire as matrix for brachytherapy source for the treatment of eye and prostate cancer. *Appl. Radiat. Isot.* 57, 359–367, 2002.
 76. Saxena S K, Kumar Y, Pillai K T, Dash A: Development of a ^{125}I source for its application in bone densitometry. *Appl. Radiat. Isot.* 70, 470–477, 2012.
 77. Saxena S K, Pillai K T, Ram R, Dash A: Preparation of ^{137}Cs microspheres for their use in computer automated radioactive particle tracking (CARPT) studies. *Ind.Eng.Chem.Res.* 51, 4485–4492, 2012.
 78. Udhayakumar J, Kumar M, Gandhi S S, Tomar B S, Venkatesh M, Dash A: Preparation of spherical ^{57}Co source for the calibration of intra-operative gamma probe. *App. Radiat. Isot.* 70, 167–170, 2012.
 79. Schrader H, Activity Measurements with Ionization Chambers. Mono graphie BIPM- 4, Bureau International des Poids et Mesures, Sèvres, France, 1997.
 80. Udhayakumar J, Pardeshi G S, Gandhi S S, Chakravarty R, Kumar M, Dash A, Venkatesh M: Development of technology for the large-scale preparation of ^{60}Co polymer film source, *Appl. Radiat. Isot.* 66, 1825–1829, 2008.
 81. American National Standard Institute: Performance Testing of Extremity Dosimeters, ANSI/HPS N13.32-1995, Health Physics Society, McLean, VA, 8 1995.
 82. International Organization for Standardization, Nuclear energy, Reference beta-particle radiation – Part 3: Calibration of area and personal dose meters and the determination of their response as a function of beta radiation energy and angle of incidence ISO 6980-3, Geneva, 2006.

References

83. Lagoutine F, Coursol N, Legrand J: Table de Radionucléides. Commissariat à l'Energie Atomique, Bureau National de Metrologie, Laboratoire de Metrologie des Rayonnements Ionisants, Gif sur Yvette, France, 1985.
84. Lowenthal G C, Wyllie H A: Special methods of source preparation, Nucl. Instrum. Methods 112, 353, 1973.
85. El-Halim A M A, Khalil R M: Electrodeposition of catalytically active nickelthallium alloy powders from sulphate baths. J. Appl. Electrochem. 15, 217, 1985.
86. El-Halim A M A, Khalil R M: Electrodeposition of thallium powder from sulphate baths. Surf. Technol. 23, 215, 1984.
87. Switzer J A, Shane M J, Phillips R J: Electrodeposited ceramic super lattices. Science 247, 444, 1990.
88. Pettrii O A, Tsirlina G A, Rakova T V, Vassiliev S Yu: Anomalous features of thallium oxide electrodeposited layers and room temperature HTSC electro synthesis. J. Electroanal. Chem. 23, 583, 1993.
89. Liu J F, Wang S X, Yang K Z: Electrodeposition and characterization of thallium (III) oxide films. Thin Solid Films 298, 156, 1997.
90. Johal C P S, Gabe D R, Eastham D R: Electrodeposition of thallium from a sulphamate solution. Surf. Coat. Technol. 35, 181, 1988.
91. Bhattacharya R N, Blaugher R D, Natarajan A, Carlson C M, Parilla P A, Ginley D S, Paranthaman M, Goyal M, Kroeger A D: Thick-film processing for Tl-oxide wire and tape. J. Superconductivity 11, 173, 1998.
92. Bhattacharya R N, Blaugher R D, Ren Z F, Li W, Wang J H, Paranthaman M., Verebelyi D T, Christen D K: Superconducting thallium oxide films by the

- electrodeposition method. *Physica C* 304, 55, 1998.
93. Bhattacharya R N, Wu H L, Wang Y T, Blaugher R D, Yang S X, Wang D Z, Ren Z F, Tu Y, Verebelyi D T, Christen D K: Improved electrodeposition process for the preparation of superconducting thallium oxide films. *Physica C* 333, 59, 2000.
 94. Ferkel H, Mueller B, Riehemann W: Electrodeposition of particle-strengthened nickel films. *Mater. Sci. Eng. A* 234-236, 474, 1997.
 95. Hoare J P: On the role of boric acid in the Watts bath. *J. Electrochem. Soc.* 133, 2491, 1986.
 96. Franklyn J A: The management of hyperthyroidism. *N. Engl. J. Med.* 330, 1731, 1994.
 97. Ross D S: Radioiodine therapy for hyperthyroidism. *N. Engl. J. Med.* 364, 542, 2011.
 98. Farrar J J, Toft A D: Iodine-131 treatment of hyperthyroidism: current issues. *Clin. Endocrinol.* 3, 207, 1991.
 99. Dantas B M, Dantas A L A, Santos D S, Cruz-Suárez R: IAEA regional intercomparison of *in vivo* measurements of ¹³¹I in the thyroid the Latin American and Caribbean experience. *Radiat. Prot. Dosim.* 144, 291, 2011.
 100. De Bessa A C M, da Costa A M, Caldas L V E: Survey on quality control of radiopharmaceutical dose calibrators in nuclear medicine units in the city of São Paulo, SP, Brazil. *Radiol. Bras.* 41, 115, 2008.
 101. Dantas B M, Lucena E A, Dantas A L A, Araújo F, Rebelo A M O, Terán M, Paolino A, Hermida J C, Rojo A M, Puerta J A, Morales J, Bejerano G M L, Alfaro M, Ruiz M A, Videla R, Piñones O, González S, Navarro T, Melo D,

- Cruz-Su'arez R: A protocol for the calibration of gamma cameras to estimate internal contamination in emergency situations. *Radiat. Prot. Dosim.* 127, 253, 2007.
102. Zanzonico P: Routine quality control of clinical nuclear medicine instrumentation: a brief review. *J. Nucl. Med.* 49, 1114, 2008.
103. Nagai M, Yamashita K, Umegaki T, Takuma Y: Electrophoretic deposition of ferroelectric barium titanate thick films and their dielectric properties. *J. Am. Ceram. Soc.* 76, 253, 1993.
104. Hosokura T, Shindo S, Kuwabara M: Preparation of barium titanate patterned microstructures by a novel sol-electrodeposition method using a highly concentrated alkoxide solution. *Key. Eng. Mater.* 248, 69, 2003.
105. Tamaki J, Goh G K L, Lange F F: Novel epitaxial growth of barium titanate thin films by electrodeposition. *J. Mater. Res.* 15, 2583, 2000.
106. Hosokura T, Ando A, Sakabe Y: Fabrication and electrical characterization of epitaxially grown (Ba,Sr)TiO₃ thin films prepared by sol-gel method. *Key. Eng. Mater.* 320, 81, 2006.
107. Tan C K, Goh G K L: Growth and dielectric properties of solvothermal BaTiO₃ polycrystalline thin films. *Thin. Solid. Films.* 515, 6572, 2007.
108. Wang Y, Tao J, Wang L, He P E, Wang T: HA coating on titanium with nanotubular anodized TiO₂ intermediate layer *via* electrochemical deposition. *Trans. Nonferrous. Met. Soc. China* 18, 631, 2008.
109. Park J H, Lee Y K, Kim K M, Kim K N: Bioactive calcium phosphate coating prepared on H₂O₂-treated titanium substrate by electrodeposition. *Surf. Coat. Tech.* 195, 252, 2005.

References

110. Raja K S, Misra M, Paramguru K: Deposition of calcium phosphate coating on nanotubular anodized titanium. *Mater. Lett.* 59, 2137, 2005.
111. Schrader H: Activity measurements with ionization chambers Monographie BIPM4 Bureau International des Poids et Mesures. Sèvres, France, 1997.
112. American National Standard Institute: Performance testing of extremity dosimeters, Health Physics Society, McLean, VA, 8 ANSI/HPS N13.32-1995.
113. International Organization for Standardization, Nuclear energy, Reference beta-particle radiation—Part 3: calibration of area and personal dose meters and the determination of their response as a function of beta radiation energy and angle of incidence ISO 6980-3 Geneva, 2006.
114. Woods M J and Hedley R P: IRMF Inter comparison of calibration of large area reference sources and portable alpha and beta surface contamination monitors 1993/94—Part 1, NPL Report CIRA (EXT) 002, 1996.
115. Kumar M, Gandhi SS, Nuwad J, Udhayakumar J, Dash A: A novel and facile approach for the preparation of ^{133}Ba source core, encapsulation and quality evaluation. *Radiochim. Acta* 101:195–204, 2013.
116. Saxena SK, Kumar, Kumar Y, Udhayakumar J, Pandey U, Dash A: Preparation of ^{57}Co point sources for the performance evaluation of nuclear imaging instruments. *Appl Radiat Isot* 79:12–17, 2013.
117. Udhayakumar J, Gandhi SS, Kumar M, Dash A: A chemical deposition method to prepare circular planar ^{147}Pm sources for the measurement of particulate emission in air. *Appl. Radiat. Isot.* 79:80–84, 2013
118. Kumar M, Gandhi SS, Chakravarty R, Nuwad J, Udhayakumar J, Dash A: A novel method for the preparation of large-area $^{90}\text{Sr}/^{90}\text{Y}$ sources for the

- calibration of hand contamination monitors. *Appl. Radiat. Isot.* 79:5–11, 2013.
119. Saxena SK, Kumar Y, Pandey U, Shinde SN, Muthe KP, Venkatesh M, Dash A: A facile and viable approach towards the preparation of ^{32}P -patches for the treatment of skin cancer. *Cancer Biother Radiopharm* 26, 665–670, 2011.
 120. Dash A, Varma RN, Ram R, Saxena SK, Mathakar AR, Avhad BG, Sastry KVS, Sangurdekar PR, Venkatesh M: Fabrication of cesium-137 brachytherapy sources using vitrification technology. *Cancer Biother Radiopharm* 24, 489–502, 2009.
 121. Kang J, Ryu J, Ko E, Tak Y: Electrochemical fabrication of SrTiO_3 nano wires with nano porous alumina template. *J Nanosci Nanotechnol* 7, 4194–4197, 2007.
 122. Bobiak J P, Koeng J L, Fourier transforms infrared imaging of stereo regular poly (methylmethacrylate) dissolution. *Appl. Spectrosc.* 58, 1141–1146, 2004.
 123. Bornside D E, Macosco C W, Scriven L E: Spin coating: one-dimensional model. *J. Appl. Phys.* 66, 5185–5193, 1989.
 124. Bornside D E, Brown R A, Ackmann P W, Frank J R, Tryba A A, Geyling F T: The effects of gas phase convection on mass transfer in spin coating. *J. Appl. Phys.* 73, 585–600, 1993.
 125. El-Ali H, Ljungberg M, Strand S-E, Palmer J, Malmgren L, Nilsson J: Calibration of a radioactive ink-based stack phantom and its applications in nuclear medicine. *Cancer Biother. Radiopharm.* 18, 201–207, 2003.
 126. Hino Y, Sato Y, Yamada T, Matsumoto M: Fabrication of weak area sources and their applications for imaging-plate system. In: *Proceedings of Autumn Conference, I waki City, Atomic Energy Society of Japan*, p.167, 2002.

References

127. Horwitz E P, Dietz M L, Fisher D E: Correlation of the extraction of strontium nitrate by crown ether with the water content of the organic phase. *Solvent Extr. Ion Exch.* 8, 199–208. 1990.
128. Horwitz E P, Dietz M L, Fisher D E: Extraction of strontium from nitric acid solutions using dicyclohexano-18-Crown-6 and Its derivatives. *Solvent Extr. Ion Exch.* 8, 557–572, 1990.
129. Horwitz E P, Dietz M L, Fisher, D E., SREX: a new process for the extraction and recovery of strontium from acidic nuclear waste streams. *Solvent Extr. Ion Exch.* 9, 1–25, 1991.
130. Horwitz E P, Schulz W W, In Bond A H, Dietz M L, Rogers R M (Eds.): *Solvent extraction in the treatment of acidic high-level liquid waste where do we stand? Metal-Ion separation and pre-concentration progress and opportunities,*. American Chemical Society, Washington, D.C., vol.716, pp.20–50, 1999.
131. International Organization for Standardization, Reference sources for the calibration of surface contamination monitors: Beta-Emitters (Maximum Beta Energy Greater Than 0.15 MeV) and Alpha -emitters. ISO 8769, Geneva, 1988.
132. Law J D, Wood D J, Olson L G, Todd T A, Demonstration of a SREX flow sheet for the partitioning of strontium and lead from actual ICPP sodium-bearing waste. INEEL/EXT-97-00832, 1997.
133. Idaho National Engineering Laboratory, Idaho Falls, ID. Oztekin A, Bornside D E, Brown R A, Seidel P K: The connection between hydrodynamics stability of gas flow in spin coating and coated film uniformity. *J. Appl. Phys* 77, 2297–2308, 1995.

References

134. Saraswat H C, Kalyanasundaram A: Spreading properties of high polymers. J. Polym. Sci. 7, 325–331, 1951.
135. Sato Y, Hino Y, Yamada T, Matsumoto M: The new fabrication method of standard surface sources. Appl. Radiat. Isot. 60, 543–546, 2004.
136. Scafè R, Auer P, Bennati P, LaPorta L, Pisacane F, Cinti M N, Pellegrini R, De Vincentis G, Conte G, Pani, R: Production of radioactive phantoms using a standard inkjet printer and the public domain multi-printing code GENIA. Phys. Med. 27, 209–223, 2011.
137. Sossi V, Buckley K R, Piccioni P, Rahmim A, Camborde M L, Strome E M, Lapi S, Ruth T J: Printed sources for positron emission tomography (PET). IEEE. Trans. Nucl. Sci. 52, 114–118, 2005.
138. Spangler L L, Torkelson J M, Royal J S: Influence of solvent and molecular weight on thickness and surface topography of spin-coated polymer films. Polym. Eng. Sci. 30, 644–653, 1990.
139. Sundara Rao I S, Vadiwala R, Ram N: Preparation and standardization of β -surface sources for calibration of contamination monitors. Int. J. Appl. Radiat. Isot. 34, 1398–1399, 1983.
140. Tsoupko-Sitniko V, Picolo J L, Carrier M, Peulon S, Moutard G, A novel method for large-area sources preparation for the calibration of beta-and alpha-contamination monitors. Appl. Radiat. Isot. 56, 21–29, 2002.
141. Van Staden J A, duRaai H, Lötter M G, van Aswegen A, Herbst C P: Production of radioactive quality assurance phantoms using a standard inkjet printer. Phys. Med. Biol. 52, N329–N337, 2007.
142. Courtney W J, Shaw R W, Dzubay T G: Precision and accuracy of a β -gauge

References

- for aerosol mass determinations. Environ. Sci. Technol. 16, 236–239, 1982.
143. Dresia H, Spohr F: Experience with the radiometric dust measuring unit ‘beta staubmeter’. Staub 31, 12–27, 1971.
144. Gotoh T: Application of digital image-processing to a beta gauge for determining mass concentration of suspending particulate matter in atmosphere. Appl.Radiat.Isot. 43, 659–662, 1992.
145. Jaklevic J M, Gatti R C, Golding F S, Loo B W A: β -gauge method applied to aerosol samples. Environ. Sci. Technol. 15, 680–686, 1980.

-----*****-----